Model-Based Mechanical Ventilation for the Critically Ill

Chiew Yeong Shiong

A thesis submitted for the degree of

Doctor of Philosophy in

Mechanical Engineering

at the

University of Canterbury

Christchurch, New Zealand

June 2013

MODEL-BASED MECHANICAL VENTILATION FOR THE CRITICALLY ILL

A thesis submitted in partial fulfilment of the requirements for the Degree

of Doctor of Philosophy in Mechanical Engineering

in the University of Canterbury

by Y. S. Chiew

University of Canterbury

2013

Acknowledgement

I would like to thank a number of people who supported me throughout the course of completing this thesis.

To my supervisors, Professor Dr. J. Geoffrey Chase, Dr. Geoffrey M. Shaw and Dr. Thomas Desaive for their invaluable advice and guidance throughout this research. Their encouragement and dynamic ideas enabled the research to be carried out successfully.

I would also like to thank the members of the Centre of BioEngineering in University of Canterbury, GIGA Cardiovascular Science in University of Liege, and Institute of Technical Medicine in Furtwangen University who have unselfishly shared their time and knowledge with me.

Last but not least, to my family and friends for their caring and support during the many trying moments. Thank you for being there.

Table of Contents:

List of Figures:

List of Tables:

Abstract

Mechanical ventilation (MV) is the primary form of therapeutic support for patients with acute respiratory failure (ARF) or acute respiratory distress syndrome (ARDS) until the underlying disease is resolved. However, as patient disease state and response to MV are highly variable, clinicians often rely on experience to set MV. The result is more variable care, as there are currently no standard approaches to MV settings. As a result of the common occurrence of MV and variability in care, MV is one of the most expensive treatments in critical care. Thus, an approach capable of guiding patient-specific MV is required and this approach could potentially save significant cost.

This research focuses on developing models and model-based approaches to analyse and guide patient-specific MV care. Four models and metrics are developed, and each model is tested in experimental or clinical trials developed for the purpose. Each builds the understanding and methods necessary for an overall approach to guide MV in a wide range of patients.

The first model, a minimal recruitment model, captures the recruitment of an injured lung and its response to positive end expiratory pressure (PEEP). However, the model was only previously validated in diagnosed ARDS patients, and was not proven to capture behaviours seen in healthy patients. This deficiency could potentially negate its ability to track disease state, which is crucial in providing rapid diagnosis and patient-specific MV in response to changes in patient condition. Hence, the lack of validation in disease state progression monitoring from ARDS to healthy, or vice-

versa, severely limits its application in real-time monitoring and decision support. To address this issue, an experimental ARDS animal model is developed to validate the model across the transition between healthy and diseased states.

The second model, a single compartment linear lung model, models the lung as a conducting airway connected to an elastic compartment. This model is used to estimate the respiratory mechanics (Elastance and Resistance) of an ARDS animal model during disease progression and recruitment manoeuvres. This model is later extended to capture high resolution, patient-specific time-varying respiratory mechanics during each breathing cycle. This extended model is tested in ARDS patients, and was used to titrate patient-specific PEEP using a minimum elastance metric that balances recruitment and the risk of lung overdistension and ventilation-induced injury.

Studies have revealed that promoting patients to breathe spontaneously during MV can improve patient outcomes. Thus, there is significant clinical trend towards using partially assisted ventilation modes, rather than fully supported ventilation modes. In this study, the patient-ventilator interaction of a state of the art partially assisted ventilation mode, known as neurally adjusted ventilatory assist (NAVA), is investigated and compared with pressure support ventilation (PS). The matching of patient-specific inspiratory demand and ventilator supplied tidal volume for these two ventilation modes is assessed using a novel Range90 metric. NAVA consistently showed better matching than PS, indicating that NAVA has better ability to provide patient-specific ventilator tidal volume to match variable patient-specific demand.

Hence, this new analysis highlights a critical benefit of partially assisted ventilation and thus the need to extend model-based methods to this patient group.

NAVA ventilation has been shown to improve patient-ventilator interaction compared to conventional PS. However, the patient-specific, optimal NAVA level remains unknown, and the best described method to set NAVA is complicated and clinically impractical. The Range90 metric is thus extended to analyse the matching ability of different NAVA levels, where it is found that response to different NAVA levels is highly patient-specific. Similar to the fully sedated MV case, and thus requiring models and metrics to help titrate care. More importantly, Range90 is shown to provide an alternative metric to help titrate patient-specific optimal NAVA level and this analysis further highlights the need for extended model-based methods to better guide these emerging partially assisted MV modes.

Traditionally, the respiratory mechanics of the spontaneously breathing (SB) patient cannot be estimated without significant additional invasive equipment and tests that interrupt normal care and are clinically intensive to carry out. Thus, respiratory mechanics and model-based methods are rarely used to guide partially assisted MV. Thus, there is significant clinical interest to use respiratory mechanics to guide MV in SB patients. The single compartment model is extended to effectively capture the trajectory of time-varying elastance for SB patients. Results show that without additional invasive equipment, the model was able estimate unique and clinically useful respiratory mechanics in SB patients. Hence, the extended single compartment model can be used as ‘a one model fits all’ means to guide patient-specific MV

continuously and consistently, for all types of patient and ventilation modes, without interrupting care.

Overall, the model-based approaches presented in this thesis are capable of capturing physiologically relevant patient-specific parameters, and thus, characterise patient disease state and response to MV. With additional, larger scale clinical trials to test the performance and the impact of model-based methods on clinical outcome, the models can aid clinicians to guide MV decision making in the heterogeneous ICU population. Hence, this thesis develops, extends and validates several fundamental model-based metrics, models and methods to enable standardized patient-specific MV to improve outcome and reduce the variability and cost of care.

Abbreviations:

ΔP	- Change of pressure
ΔV	- Change of volume
∫Eadi	- Patient total inspiratory demand
$\int E_{drs}$	- E_{drs} Area
ADTF	- The ARDS definition task force
AIDS	- Acquired immune deficiency syndrome
ALI	- Acute lung injury
APE	- Absolute percentage error
APRV	- Airway pressure release ventilation
ARDS	- Acute respiratory distress syndrome
ARF	- Acute respiratory failure
Bi-PAP	- Biphasic positive airway pressure
BMI	- Body mass index
CDF	- Cumulative distribution function
CO_2	- Carbon dioxide
COPD	- Chronic obstruct pulmonary disease
CT	- Computer tomography
CV	- Coefficient of variation
CVR	- Robust coefficient of variation
dFRC	- Dynamic functional residual capacity
DSG	- Disease state grouping
Eadi	- Electrical activity of the diaphragm/ inspiratory demand
E_{cage}	- Cage Elastance
E_{cw}	- Chest wall elastance
E_{demand}	- Demand elastance
E_{drs}	- Time-varying/ dynamic respiratory system elastance/
EIP	- End of inspiratory pause
EIT	- Electric impedance tomography
E_{lung}	- Lung elastance
E_{rs}	- Respiratory system elastanc
E_{rsIB}	- Model-based estimated respiratory system elastance
E_{rsVent}	- Ventilator measured elastance
E_{Static}	- Static ventilation elastance
ETS	- Expiratory trigger sensitivity
ETT	- Endotracheal tube
FiO_2	- Fraction of inspired oxygen
FRC	- Functional residual capacity
H1N1	- Swine flu
ICU	- Intensive Care Unit
IQR	- Interquartile range
IV	- Invasive ventilation
LIP	- Lower inflection point
MV	- Mechanical ventilation
NAVA	- Neurally adjusted ventilatory assist
NIV	- Non-invasive ventilation
nTi	- New/ normalized inspiratory time frame

O_2	- Oxygen
P Slope	- Pressurization slope
P0	- Offset pressure
PaO_2	- Partial pressure of arterial oxygen
P_{aw}	- Airway pressure
P_{cage}	- Pressure in the cage
P_{demand}	- Pressure change due to demand
PEEP	- Positive end-expiratory pressure
P_{oe}	- Oesophageal pressure
PF ratio	- PaO_2/FiO_2
PIP	- Peak airway pressure / peak airway inspiratory pressure
P_{lung}	- Pressure build-up in the lung compartment
P_{pl}	- Pleural pressure
P_{plat}	- Plateau pressure
prct	- percentile
P_{rs}	- Pressure drop due to airway resistance and endotracheal tube
PS level	- Pressure support level
PS/ PSV	- Pressure support
P_{tp}	- Transpulmonary pressure
PV	- Pressure volume
Q	- Air flow
R_{cw}	- Chest wall resistance
R_{lung}	- Lung resistance
RM	- Recruitment Manoeuvre
R_{rs}	- Airway resistance
R_{rsIB}	- Model-based estimated airway resistance
R_{Static}	- Static ventilation resistance
SAPSII	- Simplified acute physiology score
SB	- Spontaneous breathing
SD	- Standard deviation
SIMV	- Synchronized intermittent mandatory ventilation
SIRS	- Systematic inflammation response syndrome
SpO_2	- Oxygen saturation
t	- Sample time
TCP	- Threshold closing pressure
Ti	- Inspiratory time
$Ti_{\_Neural}$	- Neural inspiratory time
TOP	- Threshold opening pressure
Ttot	- Total time for inspiratory and expiratory
UIP	- Upper inflection point
V	- Lung volume
VILI	- Ventilator induced lung injury
Vt	- Tidal volume
Vt/∫Eadi ratio	- Neuroventilatory efficiency
WOB	- Work of breathing
WOB_E	- Work of breathing required to overcome elastance
WOB_R	- Work of breathing required to overcome airway resistance

Chapter 1

Introduction

1.1 The Human Lung

The primary function of the human lung is ventilation-perfusion matching, such that gas exchange between alveolar air and alveolar capillary blood is efficient. Oxygen (O_2) is delivered from surrounding air into the body tissues through inspiration. Carbon dioxide (CO_2) is transferred out from the body tissues via the blood and to the air through expiration (Levitzky, 2007, Robert J. Mason et al., 2010). Thus, incoming oxygen is efficiently exchanged for outgoing CO_2.

During inspiration in normal breathing, the diaphragm moves down and the intercostal muscle moves the rib cage outwards and upwards. This combined movement expands the chest cavity and creates a negative pressure gradient in the lung with respect to atmospheric pressure. The negative pressure draws air into the lung through the airway passage allowing the pressure inside the lung to equilibrate. The process of transporting air into the lung is known as ventilation. Oxygen in the inspired air is absorbed into the blood at the alveolar level via gas exchange with the blood at the alveolar capillaries. Known as perfusion, this exchange process provides the human body a constant supply of air (oxygen, O_2) to enable conversion of glucose in the cells to energy, and, at the same time, the exchange of CO_2 and the other

metabolism end products back to the air during expiration. (Levitzky, 2007, Robert J. Mason et al., 2010). Figure 1.1 shows the mechanism of inspiration and expiration.

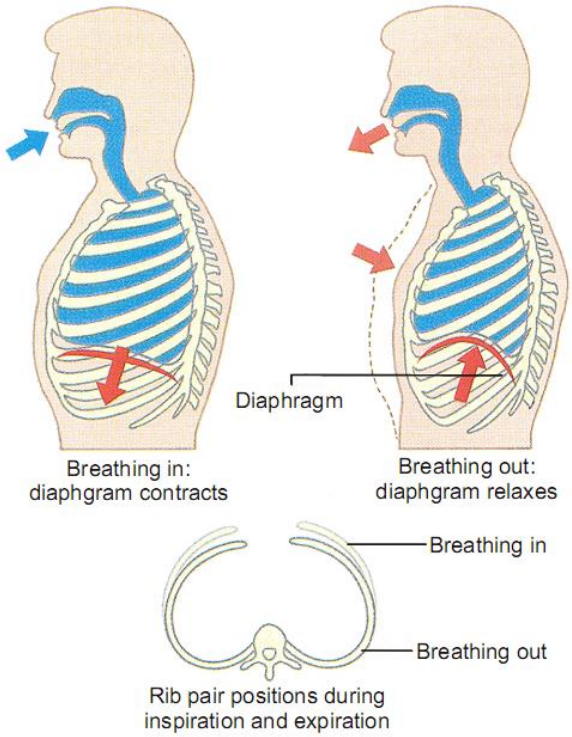

Figure 1.1: Diaphragm and rib cage movement during inspiration and expiration (Sebel, 1985). (Left) When breathing in, the diaphragm contracts and intercostal muscle moves upward creating negative pressure gradient in the lung. (Right) When breathing out, the diaphragm relaxes and intercostal muscle moves down pushing the air out from the lung.

1.2 Acute Respiratory Distress Syndrome

Patients admitted to the intensive care unit (ICU) often experience difficulties in breathing denoted as acute respiratory failure (ARF) which affects lung ventilation and perfusion matching (Pappert et al., 1994). Loss of ventilation perfusion matching reduced O_2 supply and CO_2 removal, affecting other organs and tissues, and thus creating significant physiological stress (Ferring and Vincent, 1997, Slutsky and Tremblay, 1998, Ranieri et al., 2000a). Acute respiratory distress syndrome (ARDS) is a form of severe ARF, which occurs due to severe inflammatory response of the

lung, resulting in direct alveolar injury, pulmonary oedema and alveolar collapse (Ashbaugh et al., 1967, Bernard et al., 1994b, Kollef and Schuster, 1995). This dynamic response further reduces ventilation and perfusion matching, and lung function. The clinical disorders associated with the development of ARDS are shown in Table 1.1 (Ware and Matthay, 2000). Overall, these lung injuries greatly impair the breathing process, reducing alveolar gas exchange and resulting in increased risk of organ failure and mortality if not treated (Slutsky and Tremblay, 1998, Ranieri et al., 2000a, Mortelliti and Manning, 2002, Rouby et al., 2004, Ferguson et al., 2005, Girard and Bernard, 2007).

Table 1.1: Clinical disorders associated with the development of the acute respiratory distress syndrome (Ware and Matthay, 2000)

Direct Lung Injury	**Indirect Lung Injury**
Common Causes • Pneumonia • Aspiration of gastric contents	Common Causes • Sepsis • Severe Trauma with shock and multiple transfusions
Less common causes • Pulmonary contusion • Fat emboli • Near-drowning • Inhalational injury • Reperfusion pulmonary oedema after lung transplantation or pulmonary embolectomy	Less common causes • Cardiopulmonary bypass • Drug Overdose • Acute pancreatitis • Transfusions of blood products

ARDS was first described by Ashbaugh et al. (Ashbaugh et al., 1967, Petty and Ashbaugh, 1971) in 1967 and its definition has changed in several ways over the years due to the lack of specification (Ware and Matthay, 2000). The definition was redefined in 1994 as:

- A syndrome of acute onset of respiratory failure with findings of bilateral infiltrates on chest radiograph, the absence of elevated left heart filling pressure determined either diagnostically with a pulmonary artery catheter (pulmonary artery occlusion pressure of < 18 *mmHg*) or clinically (absence of evidence of left arterial hypertension) (Bernard et al., 1994b, Burleson and Maki, 2005).
- If partial pressure of arterial oxygen to fraction of inspired oxygen ratio (PaO_2/FiO_2) is less than 300 *mmHg*, the patients is diagnosed with acute lung injury (ALI), and if PaO_2/FiO_2 ratio is less than 200 *mmHg*, the patients is diagnosed with acute respiratory distress syndrome (ARDS).

ARDS was again redefined in 2012 by the acute respiratory distress syndrome task force (ADTF), with added additional clinical implications (The ARDS Definition Task Force, 2012). The use of ALI was removed and ARDS was graded based on the arterial blood gases information into 3 severities:

- Mild ARDS ($200 < PaO_2/FiO_2 \leq 300$ *mmHg*),
- Moderate ARDS ($100 < PaO_2/FiO_2 \leq 200$ *mmHg*), or
- Severe ARDS ($PaO_2/FiO_2 \leq 100$ *mmHg*).

The acute time frame is also specified to be within 1 week. Overall, it is clear that ARDS defines respiratory failure, and, in particular, failure to achieve adequate gas exchange.

As might be expected, ARDS and respiratory failure patients have associated high morbidity and mortality. ARF or ARDS are also relatively common, affecting 33% of the ICU patients (Dasta et al., 2005). It is estimated that in U.S., the mortality of the ARDS patients is higher than patients with acquired immune deficiency syndrome (AIDS) (Goss et al., 2003), and mortality can range from 30% up to 60% (Montgomery et al., 1985, Lewandowski et al., 1995, Reynolds et al., 1998, Luhr et al., 1999, Zambon and Vincent, 2008, Phua et al., 2009). They entail significant medical cost of almost double that of a non-mechanically ventilated patient without ARDS (Valta et al., 1999, Dasta et al., 2005, Zilberberg et al., 2008). In particular, the estimated cost of ARDS survivor was USD 73,000 (Valta et al., 1999, Dasta et al., 2005). Therefore, giving the proper treatment to the ARDS patient is an important clinical and economic challenge.

1.3 Mechanical Ventilation

Over the years, various treatments have been suggested for patients with respiratory failure. These treatments can be divided into 2 categories; 1) pharmacological treatments and 2) non-pharmacological treatments. While some pharmacological treatments were able to show improvement for ARDS patients (Ware and Matthay, 2000, Günther et al., 2002), mechanical ventilation (MV), a non-pharmacological treatment, remains as the dominant therapeutic approach for these patients (Rouby et al., 2004, Hasan, 2010). In particular, MV has evolved from a supporting therapy to a therapy that is actively directed and can influence the progression of the lung disease and patient outcome (Esteban et al., 1999, Esteban et al., 2002, Desai and Deep, 2006, Girard and Bernard, 2007, Gama de Abreu et al., 2009).

MV is fundamentally about delivering a supply of oxygen to a patient for breathing support through the use of a mechanical ventilator (Hasan, 2010). The ventilator can either partially assist or fully replace the patient's breathing effort depending on the patient's condition (Ranieri et al., 2000a, Hasan, 2010, Marini, 2011). The breathing support provided by the ventilator reduces the patient's work of breathing, and increases the lung's ability to recruit and retain lung units (alveoli), thus improving gas exchange (ventilation-perfusion matching) while also allowing a better chance for the lung to recover (Cabello and Mancebo, 2006).

Various MV modes and strategies have been introduced for the support of patients with ARDS (Stock et al., 1987, Younes, 1992, The Acute Respiratory Distress Syndrome Network, 2000, Sinderby, 2002, Putensen and Wrigge, 2004, Brower et al., 2004, Mireles-Cabodevila et al., 2009). Several methods are applied separately, but combined methods also exist in an attempt to improve patient condition (Amato et al., 1998, Marini and Gattinoni, 2004). Some specific approaches: include low tidal volume ventilation (The Acute Respiratory Distress Syndrome Network, 2000), control of positive end-expiratory pressure (PEEP) (Suter et al., 1975, Sundaresan and Chase, 2011, Slutsky and Hudson, 2006, Brower et al., 2004), monitoring lung recruitment using lung imaging method and several others (Gattinoni and Caironi, 2008). Each mode offers different potential advantages (Mireles-Cabodevila et al., 2009). However, different modes and approaches for MV treatment further complicate clinical decision making and introduce significant variability in care within and between patients. An important complicating factor is that it is not clinically practical to assess internal lung status regularly to optimise therapy. Thus,

clinicians often “drive” the therapy partly blind, which is another course of variability in care and outcome. Hence, there is a significant clinical, social and economic need to standardise MV treatment based on measurable, directly quantified patient-specific needs.

1.4 Research Focus

This research focuses on model-based MV research for mechanically ventilated patients. Model-based method offer the ability to uniquely capture patient-specific condition and their response to different MV and treatment approaches from typically measured clinical data (Chase et al., 2011). In particular, model-based approaches provide the opportunity to individualise MV therapy based on patient-specific needs quantified in real-time from that date (Sundaresan and Chase, 2011). Several models are developed and studied in this research for their ability to provide useful clinical and patient-specific information at the bedside, and in real-time to monitor condition, as well as to subsequently guide and optimise care. The thesis can be divided into 5 sections as follows:

a) Section 1 - Introduction and Literature Review

The first section of the thesis is composed of introductory chapters and literature reviews including:

- Chapter 1 (Introduction): This Chapter gives an overview of the thesis outline with the focus of this research.

- Chapter 2 (Mechanical Ventilation Management): Chapter 2 covers existing mechanical ventilation management in treating ARDS patients.

b) Section 2 - Sedated Patients - Fully dependant on MV

In the second section, three model-based methods to optimise MV treatment are presented. More specifically, three models are developed for ICU patients who are anesthetised and fully dependent on MV for breathing support.

- Chapter 3 (Application of a Minimal Recruitment Model): The performance of a minimal lung recruitment model is investigated. An experimental ARDS animal model is developed for this purpose. Materials included in Chapter 3 are published in (Chiew et al., 2012a, Chiew et al., 2012c).
- Chapter 4 (Respiratory Mechanics Monitoring: Single Compartment Linear Lung Model): A single compartment linear lung model and patient-specific identification method are used to capture respiratory mechanics of experimental ARDS animal models during disease progression.
- Chapter 5 (Proof of Concept Study using Respiratory Mechanics Monitoring): The single compartment model is further modified to capture patient-specific dynamic response (Time-varying elastance, E_{drs}) during standard clinical care to optimise MV settings. The materials used in this chapter has been published (Chiew et al., 2011, Chiew et al., 2012b).

c) Section 3 - Spontaneous Breathing Patients- Partially Dependant on MV

The model-based methods in Section 2 are developed and validated for sedated patients. However, only 20–40% of all ventilated ICU patients are fully sedated, and other patients breathe, at least in part, spontaneously with their own work of breathing (Putensen et al., 1999, Kuhlen and Putensen, 1999, Putensen et al., 2001). Hence, a different metric to account for spontaneously breathing patients is required to provide useful information for clinical decision making. Section 3 focuses on the development and study of these metrics.

- Chapter 6 (Spontaneous Breathing and Assisted Ventilation: Pressure Support (PS) and Neurally Adjusted Ventilatory Assist (NAVA)): The performance of a new MV mode, dubbed NAVA is investigated and compared with commonly used pressure support ventilation mode (PSV or PS) . A new metric (Range90) to quantify the matching of patients ventilatory supply and demand is introduced. This metric is used to assess the supply and demand matching between PS and NAVA ventilation (Moorhead et al., 2012).
- Chapter 7 (Application of NAVA for the Noninvasively Ventilated Patients): In this Chapter, the performance of NAVA compared to PS is investigated in non-invasively ventilated patients. The effect of various NAVA levels is also investigated, and an optimal NAVA setting can be obtained using the Range90 metric. Materials used in this chapter has been published (Piquilloud et al., 2011a, Chiew et al., 2012d)

d) Section 4 - Combine MV

4 different models and metrics are presented in Section 2 and Section 3. More specifically, these models and metrics are only fully applicable in either fully sedated patients or spontaneously breathing patients. Thus, there is a need to have a model that is applicable across both patient groups. In this section, a proof of concept study is presented. This study provides a platform to extend a model in previous section to account for both spontaneous breathing patients and fully sedated patients.

- Chapter 8 (Respiratory Mechanics Estimation for Spontaneously Breathing Patient): The model used in Section 2 is extended to estimate respiratory mechanics of the spontaneously breathing patients. This model investigates the time-varying elastance (E_{drs}) of patients ventilated during pressure support and NAVA as presented in Chapter 6 and Chapter 7. A metric which investigates average E_{drs} of a spontaneous breathing patient is developed. This metric allows comparison of ventilation mode in spontaneous breathing patients, revealing potential to titrate care in spontaneously breathing patient without interrupting treatment.

e) Section 5 - Conclusions and Future Works

In Section 5, the conclusion and potential future works are presented.

- Chapter 9 (Conclusions): This chapter concludes the finding of the research.

- Chapter 10 (Future Work): The future works that are required to improve the performance, validity and clinical feasibility of the models and methods are presented.

1.5 Summary

This chapter presented the fundamental background on human respiratory function, respiratory failure and the use of mechanical ventilation as the primary form of treating these ICU patients. The thesis outline is also presented to show the overall content of this research. In the next chapter, the existing and state of the art in mechanical ventilation management strategies for ICU patients is presented to provide a more comprehensive understanding on MV and the challenges it presents.

Chapter 2

Mechanical Ventilation Management

Mechanical ventilation (MV) is a form of therapeutic support, supporting breathing work and function for ICU patients until the underlying disease processes are resolved. The primary goal is to support breathing by applying positive pressure during respiration to retain lung volume for gas exchange and to provide flow to reduce or replace the work of breathing. Thus, MV assists the breathing process, and seeks to maintain ventilation-perfusion matching rather than being a curative treatment.

Patients treated with suboptimal ventilation are exposed to the risk of ventilator associated lung injuries (Slutsky, 1999, Ricard et al., 2003, Carney et al., 2005, Garcia et al., 2006, Pavone et al., 2007), such as barotrauma and volutrauma due to excessive pressure or volume being applied (Dreyfuss and Saumon, 1992, Rouby et al., 1993, Chao and Scheinhorn, 1996, Cooper et al., 1999). These lung injuries further complicate patient disease state and prolong the length of ventilation required, with any resulting further injuries repeating this injurious cycle. Hence, it is important to have optimal MV management to support patient recovery and improve outcome (Weinacker and Vaszar, 2001, Marini and Gattinoni, 2004, Esteban et al., 2005, Desai and Deep, 2006, Girard and Bernard, 2007).

In this chapter, several fundamental concepts on MV management and recent developments on ventilation strategy are presented to give a comprehensive overview and understanding of the clinical and physiological problem. The field of MV is extremely large in clinical research with literally thousands of articles. Hence, this overview focuses on providing a definition of the clinical problem, the measurements metrics and main issues that define it.

2.1 Tidal Volume (*Vt*)

MV supports patient breathing through delivering a fixed or variable amount of air supply (Marini, 1992, Hasan, 2010). This air supply, also known as tidal volume (*Vt*), can have different oxygen concentration depending on the fraction of inspired oxygen (FiO_2) set in the ventilator (Allardet-Servent et al., 2009). Gas exchange only occurs in the alveoli sacs. Thus, it is important to provide patients with sufficient tidal volume and oxygen concentration, after accounting for physiological dead space (Aboab et al., 2006, Robert J. Mason et al., 2010).

Physiological dead space is the sum of the anatomical dead space and alveolar dead space where no gas exchange occurs. Anatomical dead space is the conducting airways (tracheal, bronchus, bronchiole), as shown in Figure 2.1. The alveolar dead space is formed when there is little or no blood flow to the capillaries surrounding the alveoli for gas exchange. Thus, alveolar dead space is the sum of the alveoli, that are ventilated, but not perfused, and is normally found in diseased lung regions.

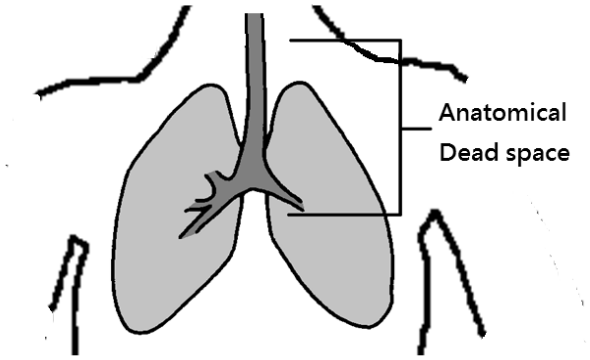

Figure 2.1: Example of dead space in a human lung. The area shaded dark grey is the anatomical dead space where there is no gas exchange. The lighter grey area is the lung region with alveoli and potential gas exchange. Alveolar dead space is normally found in the light grey area for a diseased lung.

The optimal tidal volume settings have been widely debated over the years (Schultz et al., 2007). High tidal volume is often associated with ventilator induced lung injury or VILI (Slutsky, 1999, Gajic et al., 2004, Bonetto et al., 2005). Equally, several reports and randomised controlled trials (RCT) have shown patients ventilated with low tidal volume (6~8 *ml/kg*) have lower mortality rate compared to higher tidal volume (10~12 *ml/kg*) (Brochard et al., 1998, The Acute Respiratory Distress Syndrome Network, 2000, Malhotra, 2007, Meade et al., 2008, Putensen et al., 2009). However, not all such studies have shown the same trend of outcome, with some relatively little effect (Stewart et al., 1998). A recent debate on low tidal volume ventilation by Dr. Gattinoni and Dr. Hubmayr concluded that while low tidal volume ventilation has shown better patient outcome, this ventilation is not a 'one size fit all' for all patients, and tidal volume management should be patient-specific based on lung size (Hubmayr, 2011a, Gattinoni, 2011a, Hubmayr, 2011b, Gattinoni, 2011b). However, there are currently no metrics or methods for guiding or achieving this patient-specific *Vt* without additional invasive procedures that can be done regularly or in real-time.

2.2 Positive End-Expiratory Pressure (PEEP)

Positive end-expiratory pressure (PEEP) is the additional pressure applied at the end of expiration in each breath during mechanical ventilation (Falke Konrad, 2003). The goal of using PEEP is to recruit alveoli and retain these alveoli at expiration by preventing their collapse between breaths, which damages them further (Slutsky and Hudson, 2006, Grasso et al., 2007, Albert et al., 2009, Gattinoni et al., 2010). There is equally no gold standard for setting the optimal PEEP (Lichtwarck-Aschoff et al., 1999, Levy, 2002, Suh et al., 2003, Brower et al., 2004, Kallet and Branson, 2007, Mercat et al., 2008, Markhorst et al., 2008, Meade et al., 2008, Spieth and Gama de Abreu, 2012).

In particular, several studies have revealed that higher PEEP can be beneficial for ARDS patients (Villar et al., 2006, Mercat et al., 2008, Briel M and et al., 2010). Higher PEEP allows the recruitment of collapsed alveoli in the ARDS patient, improving gas exchange and minimising damage due to collapse (Mercat et al., 2008, Putensen et al., 2009). Similarly, while high PEEP is beneficial for recruiting diseased alveoli, it is also possible that high PEEP has detrimental effects on healthy and mildly injured alveoli, causing barotrauma (Chao and Scheinhorn, 1996, Slutsky, 1999, Lucangelo et al., 2008). Such damage negates positive effects and further complicates the patient condition (Cooper et al., 1999). Thus, setting optimal PEEP during MV must balance risk and reward (Sundaresan and Chase, 2011, Chiew et al., 2011), and is an important task for clinicians. Since every patient and disease states are different, it is clear that a patient- and time-specific solution is required, especially as patient condition and response to therapy evolves.

2.2.1 Setting PEEP - Lower and Upper Inflection Point

One of the earliest methods for setting PEEP is through the use of the patient's static compliance curve, also known as the static pressure volume (PV) curve (Maggiore et al., 2003, Cagido and Zin, 2007). Each patient's PV and compliance curve is uniquely shaped (Venegas et al., 1998, Albaiceta et al., 2007), and can thus be used to characterise patient-specific lung condition (Harris et al., 2000) and their response to specific treatment choice. It is suggested that PEEP can be set above the lower inflection point (LIP) and below upper inflection point (UIP) (Jonson et al., 1999, Mergoni et al., 2001, Ward et al., 2002, Takeuchi et al., 2002, Markhorst et al., 2004, Albaiceta et al., 2004, Albaiceta et al., 2005, Pestaña et al., 2005, Rossi et al., 2008) in the patient-specific static compliance curve, as shown in Figure 2.2. LIP is defined as the point where lung volume begins to increase rapidly with increasing pressure. UIP is detected in the upper part of the PV curve, when the overall lung begins to over-inflate, and increasing pressure only obtains a relatively small amount of increased volume. In consideration of units and sign convention, while these are collected PV curves, the plot has volume (V) on the y-axis; the slope is thus compliance, not stiffness. Thus, setting PEEP above LIP will theoretically maximise recruitment and below UIP will theoretically avoid over-distension.

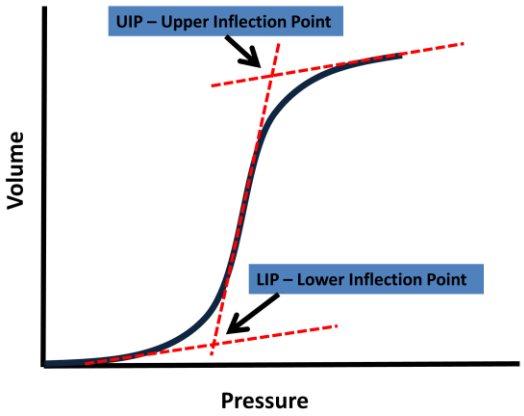

Figure 2.2: Example of LIP and UIP location in a static compliance curve. The curve defines 3 average compliances in a tri-linear approximation used to find these points. The intersections for the tri-linear approximation are the location for LIP and UIP.

The concept of LIP and UIP provides a guideline for clinicians to set PEEP (Albaiceta et al., 2008). However, the patient's static compliance curve is highly variable between patients and over time, as well as disease state dependant. In addition, the location of the LIP and UIP are normally not identifiable during normal tidal ventilation, requiring a separate manoeuvre to obtain them that interrupts therapy (Lichtwarck-Aschoff et al., 2000, NÈVE et al., 2000).

Furthermore, as seen in Figure 2.2, it is clear that how one defines the centre compliance line will significantly offset the identified LIP and UIP, creating a further source of variability (Servillo et al., 2002). Finally, the methods to obtain patient-specific static compliance curves, such as the super-syringe method (Janney, 1959, Lee et al., 2002), inspiration occlusion (Ranieri et al., 1994, Servillo et al., 1997), and quasi-static low-flow ventilation, are invasive (Servillo et al., 1997, Lu and Rouby, 2000), interrupt treatment, time consuming, clinically intensive, and not normally performed for ICU patients (Servillo et al., 1997, Karason et al., 2000b, Kondili et al.,

2000, Karason et al., 2001, Oostveen et al., 2003). Thus, the application of setting PEEP based on LIP and UIP is limited by clinical practicality.

More importantly, the application of LIP and UIP in ICU patients has not been shown to affect clinical outcome (Jonson and Svantesson, 1999, Kondili et al., 2000, Hickling, 2002, Nieszkowska et al., 2004, Victorino et al., 2004). Hence, this approach is risky, not clinically practical in some cases, and not proven to affect outcomes. There is thus a need to improve the approach to care.

2.2.2 Setting PEEP - Maximum Compliance

Several studies suggested that PEEP should be selected at maximum lung compliance or minimal lung elastance (Elastance = 1/compliance) (Suarez-Sipmann et al., 2007, Carvalho et al., 2007, Lambermont et al., 2008). In particular, these authors have studied this concept on ARDS animal models and all resulted in similar findings. These studies showed that after a recruitment manoeuvre, PEEP can be titrated to subject specific minimal elastance (or maximum compliance) (Suarez-Sipmann and Bohm, 2009, Huh et al., 2009). The PEEP selection at maximum compliance revealed that ventilation at maximum compliance (minimal elastance) potentially benefits mechanically ventilated subjects in lung recruitment, improve gas exchange and avoid over-distension (Ward et al., 2002, Suarez-Sipmann et al., 2007, Carvalho et al., 2007, Lambermont et al., 2008).

Figure 2.3 shows the ARDS animal model response to PEEP titration in Suarez-Sipmann's et al.'s study (Suarez-Sipmann et al., 2007). It was found that when

ventilated at PEEP 10~15 cmH_2O, most subjects had the highest compliance, higher PaO_2/FiO_2 ratio (PF ratio) and lower pulmonary shunt. Pulmonary shunt is the opposite condition of alveolar dead space. Pulmonary shunt occurs during regional lung collapse when there is blood flow in the capillaries of the alveoli, but there is no ventilation (air supply) in the perfused region. Lambermont et al. (2008) showed that highest compliance occurred during PEEP of 15 and 20 cmH_2O during a similar PEEP titration. In addition, these PEEP levels are associated with significant improvement in PaO_2 and higher functional residual capacity (FRC), which may be contributed by alveolar recruitment at these PEEP levels (Lambermont et al., 2008).

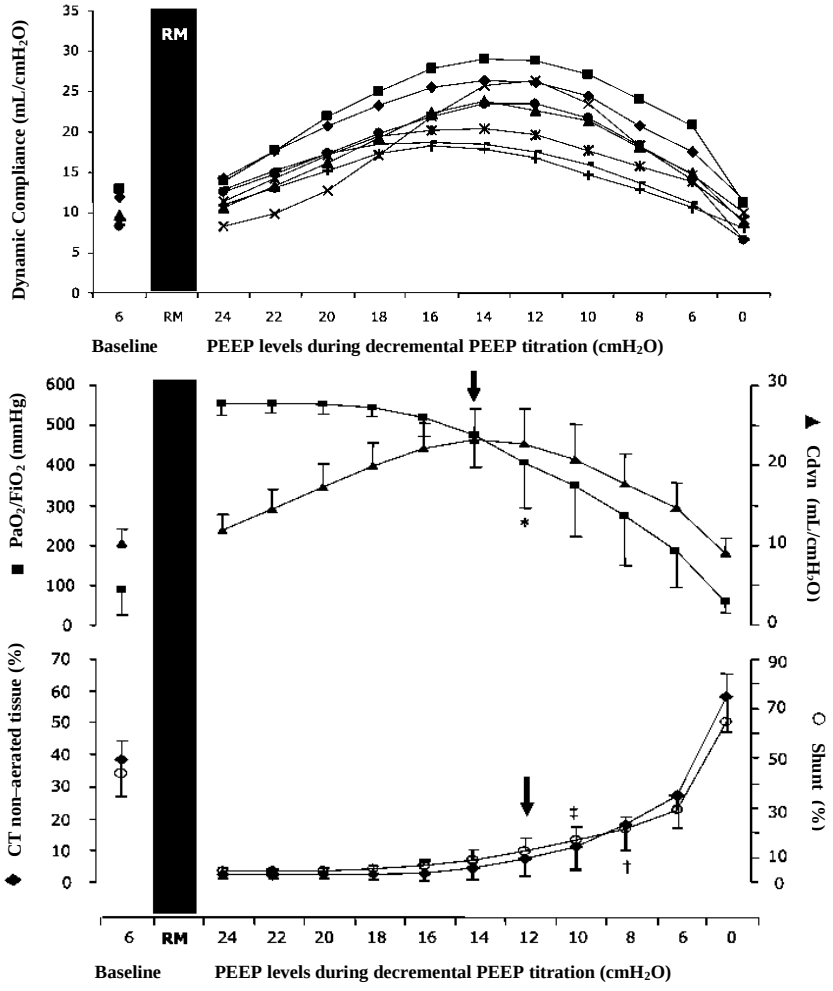

Figure 2.3: Findings by Suarez-sipmann (Suarez-Sipmann et al., 2007). (Top) Change of dynamic compliance with PEEP. (Bottom) Amount of aerated tissue and arterial blood gas at different PEEP settings.

Overall, it should be noted that maximum compliance is preferred because it implies that volume is opening for minimal pressure increase. If compliance is rising (or elastance is falling) in a breath, it implies that lung volume is opening faster than pressure is being delivered. Hence, this method seeks the best point of recruiting with minimal chance of over-distension or excess pressure.

Equally, the LIP and UIP methods described earlier also define a potential range of compliance at which to set PEEP. However, what is missing is the dynamic aspect where compliance changes over time and potentially within a breath. Hence, LIP and UIP are hindered by their inability to assess the true dynamic patient-specific response.

These studies were performed on experimental ARDS animal models, where ARDS formation was controlled and these models only capture specific ARDS physiology and mechanics (Rosenthal et al., 1998, Matute-Bello et al., 2008, Ballard-Croft et al., 2012). Hence, the result may not generalise well. Importantly, this approach to PEEP selection is yet to be tested in an ICU setting, where the course, impact and response to ARDS and MV therapy are patient-specific, variable and time-varying.

2.3 Imaging Guided Therapy

2.3.1 Computer Tomography (CT)

Computer Tomography (CT) is considered as a gold standard in lung condition monitoring. Sections of lung CT images allow the clinicians to assess patient condition, response to different PEEP levels, alveoli recruitment/ distension and gas distributions (Schlesinger et al., 1995, Vieira et al., 1998, Malbouisson et al., 2001,

Gattinoni et al., 2001, Caironi and Gattinoni, 2007, Caironi et al., 2010). However, performing CT imaging for ICU patients is largely impractical. It is a costly and over-demanded hospital resource and exposes the patient to the risk involved when transferring them to a radiology unit (Pesenti et al., 2001). The risk of radiation exposure is another important factor that deters regular CT application for MV optimisation (Brunet et al., 1995, Lu et al., 2001, Brenner and Hall, 2007, Tubiana et al., 2008). Nevertheless, while CT to guide bedside MV therapy is limited, it has provided a research platform for better understanding on disease state and lung physiology of the ARDS patient (Luecke et al., 2012).

2.3.2 Electric Impedance Tomography (EIT)

Another emerging form of lung imaging is Electrical Impedance Tomography (EIT). EIT has been introduced as a potential bedside tool for real-time monitoring of patients ventilation aside from CT imaging (Holder et al., 1996, Rao et al., 1997, Adler et al., 1998, Kunst et al., 2000a, Kunst et al., 2000b, Frerichs, 2000, Bodenstein et al., 2009, Fagerberg et al., 2009, Zhao et al., 2009, Denai et al., 2010, Luecke et al., 2012). During EIT, a high frequency, low amplitude electrical currents is injected around subject's thorax, to obtain images of the lung during ventilation. The resulting electrical potential during ventilation is then measured and the ventilation process can be monitored using a reconstruction algorithm (Dong et al., 2003, Costa et al., 2009, Zhao et al., 2010a). EIT has demonstrated good correlation with CT findings, such that it has been proposed to guide ventilation therapy, (Zhao et al., 2010b, Muders et al., 2010). However, the complex algorithm required for image reconstruction (Lionheart, 2004) and limited availability of the EIT technology along with cost and

lack of trained personnel remain issues against its widespread application, despite the advantages it may provide.

2.4 Safe Plateau Pressure and Maximum Recruitment Strategy

Several studies (Marini and Gattinoni, 2004, Hager et al., 2005, Shiu and Rosen, 2006) have suggested that the peak ventilation plateau pressure should not exceed 30~35 cmH_2O. This pressure can be measured by performing an end inspiratory breathing hold for 1~5 seconds, and this capability is normally available in most ventilators. This range of plateau pressures has been considered as the safe range (Slutsky, 1993, Bernard et al., 1994a, Barberis et al., 2003, Gattinoni et al., 2003) and a threshold to prevent injury caused by excessive pressure (Slutsky, 1993, Bernard et al., 1994a, Barberis et al., 2003, Gattinoni et al., 2003). Hence, it provides an upper bound for applied pressure during MV, which can further help guide treatment.

In a related approach, Borges et al. (Borges et al., 2006) and de Matos et al. (de Matos et al., 2012) have conducted maximum recruitment manoeuvres (RM) on patients during the early stage of ARDS. This manoeuvre requires patients to be ventilated to a PEEP setting up to 45 cmH_2O with a resulting peak airway pressure as high as 60 cmH_2O. The studies found that this maximum recruitment approach, when applied early, was able to reverse ARDS lung collapse and improve patient outcome. However, the approach was questionable based on previous studies and was criticized by the medical community for its risk, as it may also cause barotrauma and have long term negative effects (Borges Sobrinho et al., 2006, Gattinoni et al., 2006a, Guerin,

2008). Thus, it is clear that there is little consensus on pressure limits, both minimum and maximum, that can provide best MV treatment and outcome.

One limitation of these methods that they only monitor pressure and they do not consider volume, *Vt*. Hence, only a part of the problem has been addressed. Any pressure that does not recruit volume will cause damage. Similarly, high pressure that recruits a lot of volume may be beneficial. Thus, all these pressure based approaches neglect patient-specific aspect of the problem in attempting to find a "one size fits all" solution, with the result that these in no clear consensus approach or limit.

2.5 Partial Assist Ventilation

Traditionally, acute respiratory failure patients on MV require an adequate amount of sedation to enable the patient to breathe with the ventilator (Kress et al., 2002). But recent studies have shown that patients who more actively participate in the breathing process, have a greater chance of recovery and a higher success rate in weaning (Kuhlen and Putensen, 1999, Putensen et al., 1999, Slutsky et al., 2005b, Kogler, 2009, Marini, 2011). Thus, assisted ventilation modes, such as partial ventilator support using pressure support (PS) (MacIntyre, 1986, Brochard et al., 1991, Jaber et al., 2005, Spieth et al., 2009a), biphasic positive airway pressure (Bi-PAP) or airway pressure release ventilation (APRV) (Frawley and Habashi, 2001, Varpula et al., 2004, Putensen and Wrigge, 2004, Rose and Hawkins, 2008, Modrykamien et al., 2011), and neurally adjusted ventilatory assist (NAVA) (Sinderby, 2002, Slutsky et al., 2005a, Terzi et al., 2010, Branson and Johannigman, 2009, Schmidt et al., 2010), all of which promote the patient's spontaneous breathing effort, have captured significant

clinical attention (Esteban et al., 2000, Rose et al., 2009). The management of spontaneous breathing patients is also highly variable and patient-specific, if not more so, and there are various investigations on-going to optimise spontaneous breathing therapy (Gama de Abreu et al., 2008, Barwing et al., 2011, Carvalho et al., 2011). However, like the prior discussion, there are several conflicting results, and no clear consensus, and the impact on patient outcome is similar.

2.6 Model-based Approaches

Modelling respiratory mechanics in conjunction with clinical data enables patient-specific understanding of lung mechanics in a real-time basis, breath to breath. An in-depth understanding of patient condition would allow clinicians to select MV therapy based on a patient's exact-current condition and needs (Sundaresan and Chase, 2011, Chase et al., 2011), which could then balance the risk of lung injury and benefit of optimal ventilator support (MacIntyre, 2008). Respiratory system modelling has been carried out extensively over the years, ranging from simple lumped parameter models to highly complex finite element models (Burrowes et al., 2005, Ben-Tal, 2006, Schranz et al., 2011). The following section outlines several models and metrics that have been developed in recent years.

2.6.1 Recruitment Models

Recruitment explains the lung expansion theory through opening or closing of the alveoli. This model is first introduced by Hickling (Hickling, 1998) and has been incorporated into models to capture patient-specific parameters that can be used to

guide therapy (Sundaresan et al., 2009, Schranz et al., 2012). However, the use of these models is yet to be validated in a clinical setting.

2.6.2 Model-based LIP and UIP

The use of static PV curves, more specifically, LIP and UIP have provided the first guideline to select PEEP. It has been extensively studied in characterising patient-specific condition (Suter et al., 1975, Amato et al., 1998, Murray et al., 1988, Venegas et al., 1998, Pelosi et al., 2001, Heller et al., 2002, Henzler et al., 2003, Albaiceta et al., 2004). More specifically, these studies use different sigmoid equations to characterise the shape of the static PV curve. They were able to mathematically define the location of the LIP and UIP. However, the location of the LIPs and UIPs were found to deviate depending on the sigmoid equation (Albaiceta et al., 2007). This problem has resulted in inconsistency of setting PEEP and thus, the application of model based LIP and UIP in setting PEEP remains limited.

2.6.3 Non-invasive Static PV Curve Estimation

One of the major problems of patient-specific static PV curves is that it is not normally available without additional invasive and burdensome protocols. Karason et al. proposed an algorithm to estimate a alveoli pressure-volume curve similar to the static PV, known as the dynostatic algorithm (Karason et al., 1999, Karason et al., 2000b, Karason et al., 2000a, Karason et al., 2001, Sondergaard et al., 2003). This algorithm assumes the flow resistance at iso-lung volume during inspiration and expiration are the same. With this assumption, a surrogate of the alveolar pressure, dubbed the dynostatic pressure, can be estimated during tidal ventilation. This

dynostatic pressure at iso-lung volume curve can be used as an alternative for the static PV curve. However, as stated earlier; LIP and UIP may not be present during tidal ventilation (Lichtwarck-Aschoff et al., 2000, NÈVE et al., 2000).

2.6.4 Complex and Finite Element Models

Complex and finite element models of the respiratory system have been developed based on specific patient airway dimensions (Donovan, 2011, Tawhai et al., 2004, Tawhai and Bates, 2011). These models were able to simulate realistic description of disease formation, ventilation flow profile in the airway and gas distribution (Burrowes et al., 2008, Burrowes et al., 2011, Xia et al., 2010, Swan et al., 2012, Clark et al., 2011, Werner et al., 2009). However, these models are computationally intense and are thus not suitable for bedside monitoring to guide patient-specific care.

2.6.5 Detailed Perfusion and Ventilation Models

Models of perfusion and ventilation are comparatively simpler compared to the finite element models (Sharan et al., 1988, Busso and Robbins, 1997, Mogensen et al., 2011, Steimle et al., 2011, Rees et al., 2002, Richard et al., 2005, Hardman and Aitkenhead, 2003). They have shown capability in simulating pulmonary capillary perfusion and alveolar ventilation of a healthy human lung based on clinically available measurement. These models were able to provide comprehensive understanding of ventilation and perfusion. However, they require assumptions and unknown parameters. Thus, they are yet to be applied to guide clinical MV and tested in clinical settings.

2.6.6 Other Model-based Methods

The growth in computational technology has opened a wide range of possible options to improve mechanical ventilation support. Each model-based method and monitoring tool offers different theoretical advantages for patient-centred care. A summary of several other model-based methods are listed in Table 2.

Nevertheless, there is still no consensus in a 'standard' model or method to guide MV therapy due to large patient heterogeneity, combined with the limited human and economic available resources to add to clinical care. While modelling approaches are capable of providing unique and physiological insight to patient-specific disease state, to date, only a few have been tested (Quaglini et al., 2001, Carvalho et al., 2007, Sundaresan et al., 2011a) and their potential in critical care is not yet validated, either technologically or clinically.

Table 2.1: List of model-based methods in their respected categories

No.	Categories and Functions	References
1.	Compartment Models	(Lucangelo et al., 2007, Bates, 2009a, Abboud et al., 1995, Ma and Bates, 2010, Massa et al., 2008)
2.	SLICE Methods	(Guttmann et al., 1994, Zhao et al., 2012a, Zhao et al., 2012b)
3.	Stress Index	(Ranieri et al., 2000b, Grasso et al., 2007)
4.	Stress Strain Approaches	(Sundaresan et al., 2011b, Chiumello et al., 2008)
5.	Alveolar and Surface tension Models	(Reddy et al., 2011, Kitaoka et al., 2007, de Ryk et al., 2007, Schirrmann et al., 2010)
6	Spontaneous Breathing Models	(Schuessler et al., 1997, Khirani et al., 2010)
7.	Mechanical Lung Models	(DiCarlo, 2008, Chase et al., 2006, Kuebler et al., 2007)

2.7 Summary

There remains a huge area of research interest in developing a patient-specific models or methods to optimise MV management. Importantly, the model and metrics should be patient-specific, physiologically relevant and computationally simple. They should also avoid interrupting care, or requiring significant added input or cost. This thesis addresses these issues through the development and validating of several model-based methods that are capable of guiding patient-specific MV in a heterogeneous patient population.

In the next chapter, a model-based approach derived by Sundaresan et al. (Sundaresan et al., 2009), which is capable of capturing alveolar recruitment during MV, is further investigated. More specifically, the model is tested in an experimental setting, investigating its performance and ability to capture physiological relevant condition of ARDS, and thus, validating its clinical and technological applicability.

Chapter 3

Application of Minimal Recruitment Model

3.1 The Concept of Recruitment

Conventional lung mechanics described alveolar expansion as isotropic and balloon like (Chevalier et al., 1978, Hickling, 2002, Albaiceta et al., 2007). These models assume all alveoli are engaged and expand with increasing inspiratory pressure and flow. The most well-known model is the Venegas Model that defines a sigmoid equation for patient static PV curve (Venegas et al., 1998). These models fit overall static pressure volume (PV) curves well, but show no further insight into the proven heterogeneous nature of the ARDS lung (Gattinoni et al., 2001, Gattinoni et al., 2006b, Caironi and Gattinoni, 2007, Mertens et al., 2009, Fagerberg et al., 2009, Grant et al., 2009), where it is clear that the model is not applicable, even though it captures overall PV curves data.

Several in-*vivo* studies and measurements have suggested a different alveolar expansion theory. This theory, known as recruitment (Cheng et al., 1995, Hickling, 1998, Schiller et al., 2003, Albert et al., 2009), describes the alveoli state as either opened or collapsed. During respiration, after a certain threshold pressure is reached, the alveolar will open and assume an alveolar volume (Crotti et al., 2001, Pelosi et al., 2001). Once the alveoli are opened, they do not have significant volume change (Carney et al., 1999, Schiller et al., 2003). Hence, this approach can capture the

internal heterogeneity observed in the ARDS lung. The difference between traditional theory and the recruitment theory is shown in Figure 3.1.

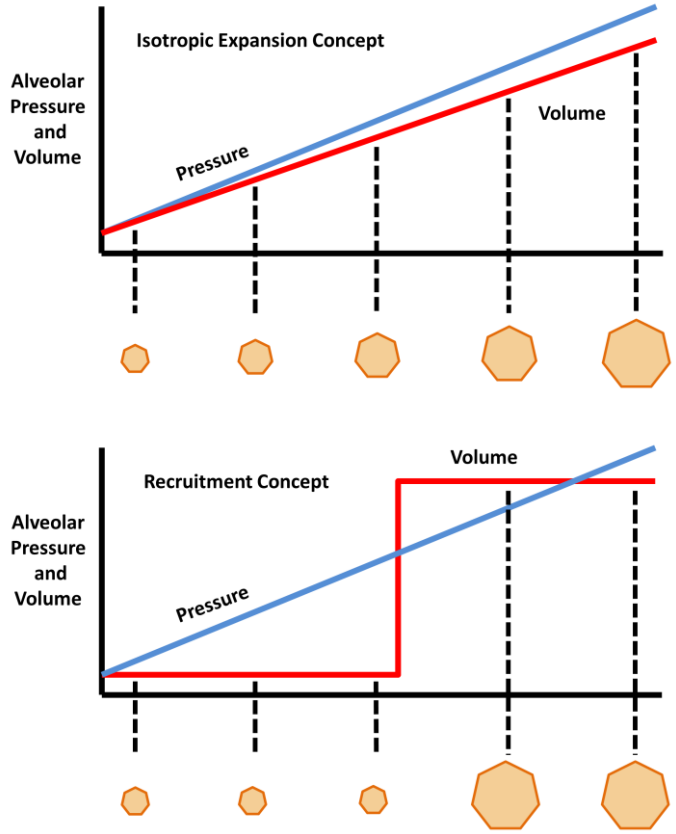

Figure 3.1: Different alveolar expansion theories during pressure increase. (Top) Traditional Theory describes the alveolar expansion as isotropic balloon like. (Bottom) Recruitment Theory shows that the alveolus is either open or closed.

The concept of recruitment provides new insight to lung physiology and thus, opportunity for new modelling approaches to guide clinical therapy. Hickling (Hickling, 1998) had proposed a mathematical model to characterise ARDS lung physiology based on this concept of recruitment. This model describes the lung as a collection of lung units, distributed in layers subjected to a superimposed pressure, as shown in Figure 3.2, where the lung units at each layer had a distribution of opening pressure.

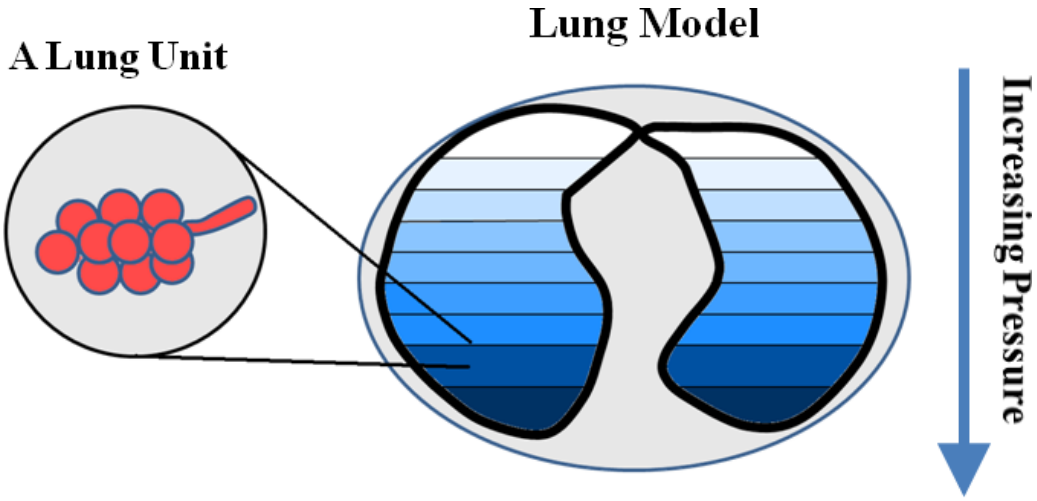

Figure 3.2: Human lung is described as a collection of lung units with the effect of superimposed pressure (Hickling, 1998, Sundaresan et al., 2009).

During inspiration, the lung units are normally closed and can be opened (Recruited) with positive pressure through mechanical ventilation. To open a lung unit, the MV pressure has to overcome an effective threshold opening pressure (TOP). Once the lung units are recruited, they will assume a unit volume that forms the pressure volume curve. It is important to note that the healthy, non-diseased lungs are typically recruited at all times (Schiller et al., 2003).

3.2 A Model of Recruitment (Minimal Model)

Sundaresan et al. have developed a minimal model to capture ARDS lung physiology using similar recruitment concept (Sundaresan et al., 2009). In this model, the lung is modelled as a collection of healthy and injured lung units. The healthy lung units are normally open and assumed a unit volume at zero added pressure. Injured lung units are collapsed and have relatively no residual volume. Similar to the Hickling's model (Hickling, 1998), the collapsed lung units can be opened with positive pressure overcoming the effective threshold pressure. Once the alveoli are opened, they

assume a unit volume similar to healthy lung units. The opening and closing of collapsed lung units are governed by a distribution of effective threshold opening pressure (TOP) and threshold closing pressure (TCP) at each superimposed level (Crotti et al., 2001, Pelosi et al., 2001). The discretisation in number of layers and distribution is up to the modeller.

During inflation, if airway pressure exceeds a lung unit's effective TOP, the lung unit will assume a lung unit volume. Each opened unit volume is added to form the inflation PV curve. Similarly, if the airway pressure during deflation drops below the effective closing pressure, the lung unit collapses and loses the unit volume, which forms the deflation curve. Each lung unit has different effective opening pressure and closing pressure, and they are assumed normally distributed (Pelosi et al., 2001, Crotti et al., 2001, Pulletz et al., 2012), and saturated at zero pressure to capture open healthy lung units.

The minimal model calculates the mean and standard deviation of the TOP and TCP distribution of the estimated static pressure volume curve from measured patient-specific dynamic pressure volume curves, as shown in Figure 3.3. These parameters provides unique insight to patient-specific physiological condition, response to different MV settings, and thus the opportunity to optimise patient-specific MV settings (Sundaresan et al., 2011a).

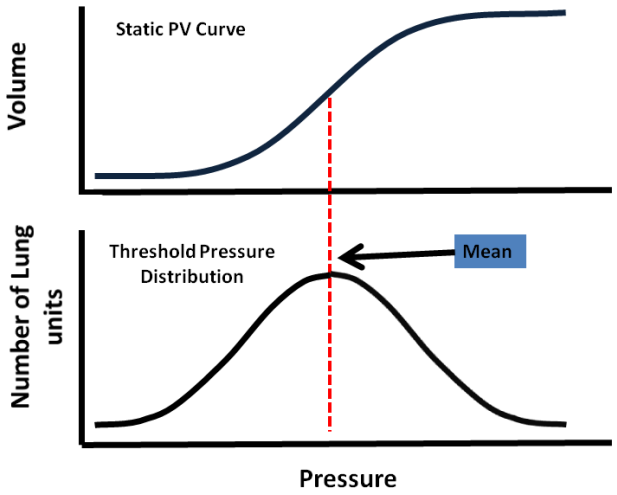

Figure 3.3: Patient-specific pressure volume curve and relation to normal distribution curve.

In a TOP distribution, the mean of the distribution is the pressure when the maximum rate of recruitment occurs. The mean TOP also indicates the mean of recruitable lung units when ventilated at that pressure. Equally, the mean of TCP distribution indicates the maximum rate of derecruitment during deflation and, the mean lung units that will remain recruited during deflation. The standard deviation (SD) describes the shape of the TOP or TCP distribution, and it is an indication of lung heterogeneity. The combination of mean TOP and SD thus reflect the lung condition.

Figure 3.4 shows examples of different lung conditions affect the shape (SD) and location of the mean TOP distribution. The upper figures are the PV curves and the lower figures are the corresponding TOP distribution. Compared to a normal lung, a collapsed lung requires higher pressure to open and recruit the lung units. Mean TOP for a collapsed lung is higher than normal lung, as shown in Figure 3.4 (Left) and reflect in the clinical need to add PEEP. The SD is the "spread" of the TOP distribution and thus, a heterogeneous lung will result in higher SD, as shown in

Figure 3.4 (Right). Combination of TOP and SD thus give the information on the overall lung compliance at that time, and can be tracked to monitor disease state and response to therapy in a patient-specific fashion.

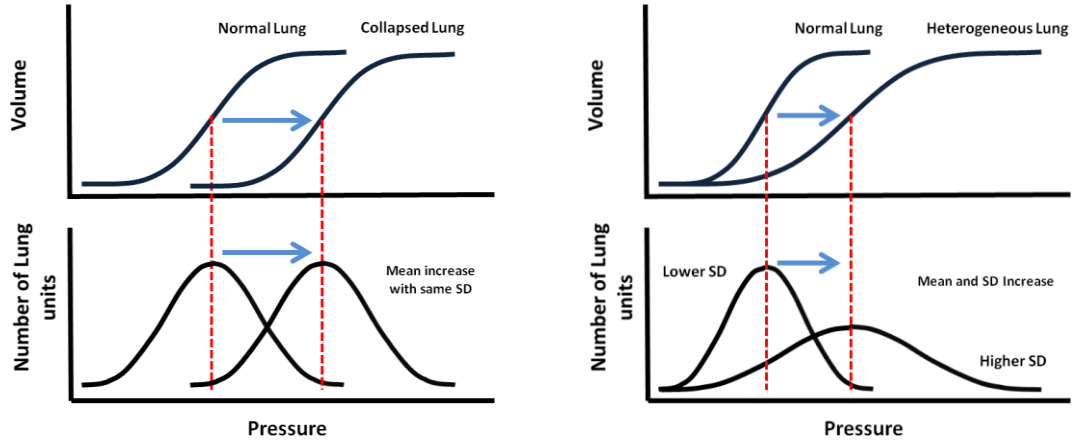

Figure 3.4: Effect of TOP and SD towards a PV curve (Top - PV curve during inflation, Bottom - TOP distribution based on PV curves). (Left) From a normal lung to collapse Lung. (Right) From a normal lung to heterogeneous lung.

Similar concepts apply to the TCP distribution. An increase of mean TCP means that there are more lung units that are prone to collapse. During mechanical ventilation, the collapsed lung units can be recruited with additional PEEP. These newly recruited lung units are likely to be unstable and prone to collapse, resulting in the increase of mean TCP. Thus, the minimal model captures the patient-specific lung condition, recruitment status and response to different PEEP. This information can be used to set PEEP to recruit collapsed lung units and, equally, a PEEP to prevent these newly recruited lung units from collapsing (Sundaresan et al., 2011a).

The minimal model was retrospectively tested in the ICU and has shown the capability of monitoring the patient-disease state, predicting recruitment for changes in PEEP, and to guide MV therapy in the ICU (Sundaresan et al., 2009, Sundaresan et

al., 2011a). However, the model was only tested in ARDS patients, and not for healthier patients' disease tracking. A healthy lung normally has no collapsed alveoli (Schiller et al., 2003). Thus, recruitment models are only considered applicable to characterise lung mechanics in ARDS patient or similar conditions that resulted in lung collapse. The lack of validation in disease state progression monitoring from ARDS to healthy or vice-versa limits its application in real-time monitoring, as well as leaving the model not fully validated. Validation for generality across healthy and diseased state would significantly strengthen and extend the model potential.

3.3 ARDS Animal Models for the Study of Lung Mechanics

In this study, animal trials are carried out to test the minimal model's physiological relevance and performance in both healthy and ARDS lungs. An animal model is used for ethical reasons as intubating and sedating healthy individuals is not possible. We hypothesise that the minimal model is able to represent both diseased and healthy lungs, as well as being able to monitor the progression of the disease state from the healthy case in a physiologically and clinically expected fashion.

More specifically, it is assumed that the open alveoli in a healthy lung will have lower overall threshold opening pressures (lower mean TOP) compared to ARDS lungs, and that the difference between healthy and ARDS states will be evident in lowered compliance and greater variability in threshold opening pressures (Higher standard deviation, SD) for the ARDS lung. Satisfying these hypotheses would assist in validating the model's generality and thus its application in MV patients.

3.4 Methodology

3.4.1 Subject Preparation

Pure pietrain piglets weighing 20~30 *kg* were used in this experiment conducted at the hemodynamics laboratory of GIGA-Cardiovascular Research in Centre Hospital University of Liege. The experimental piglets were first premedicated with tiletamin zolazepam 5 *mg/kg* and subsequently anaesthetised by a continuous infusion of sufentanil 0.5 $\mu g/kg/h$, pentobarbital 5 *mg/kg/h* and cisatracurium 2 *mg/kg/h*.

The piglets were then ventilated through a tracheotomy intubation using Engström CareStation ventilator (Datex, General Electric Healthcare, Finland). The mechanical ventilator was set in volume control mode, with tidal volume, Vt = 10~12 *ml/kg*, inspired oxygen fraction (FiO_2) 0.5, and at PEEP of 5 cmH_2O. Throughout the trial, subject airway pressure, flow and volume profile were recorded using the Eview module (Datex, General Electric Healthcare, Finland) provided with the ventilator.

3.4.2 Protocol-based Recruitment Manoeuvre

Each piglet underwent 3 phase protocol. Each phase will provide unique information of the piglet's condition and specific response to PEEP.

- Phase 1 - Healthy state staircase recruitment manoeuvre (RM)
- Phase 2 - Progression to ARDS state
- Phase 3 - Disease state RM during ARDS

a) Phase 1 - Healthy State Recruitment Manoeuvre

At the start of the trial, the subject underwent a step-wise PEEP increase manoeuvre, also known as staircase recruitment manoeuvre (RM) (Hodgson et al., 2011a). During the RM, PEEP was increased with a 5 cmH_2O step from baseline 5 cmH_2O until 20 cmH_2O. Other ventilator settings were maintained constant throughout the RM. Each PEEP level was maintained for 10~15 breaths before increasing to a higher PEEP level. After reaching 20 cmH_2O, PEEP was decreased by steps of 5 cmH_2O to the baseline PEEP. An example of the recorded pressure flow and volume profile during the PEEP increasing phase of RM is shown in Figure 3.5.

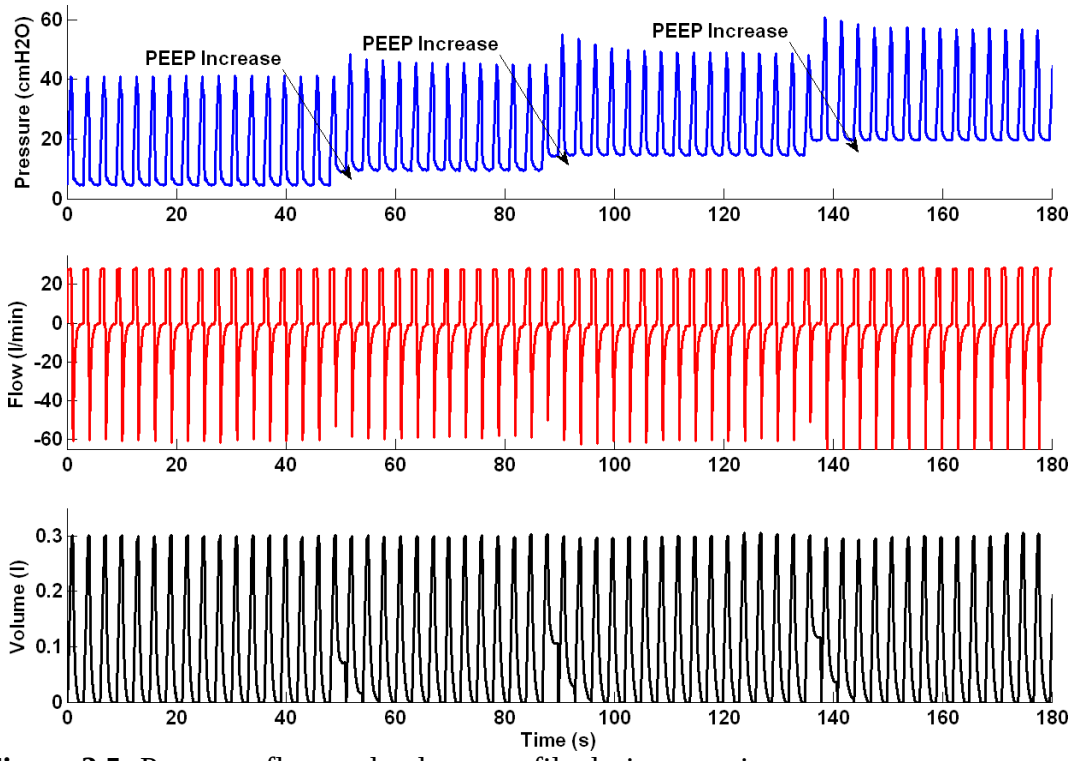

Figure 3.5: Pressure, flow and volume profile during recruitment manoeuvre.

b. Phase 2 - Progression State - Oleic Acid injections

The piglets were then injected with oleic acid to induce ARDS. Oleic acid was administrated slowly at 0.1*ml*/10 minutes until 0.1 *ml/kg* of the subject's weight.

Arterial blood gases were monitored half hourly using a RAPIDPoint 500 (Siemens Healthcare Diagnostics, Tarrytown, NY). All blood samples were taken at baseline PEEP of 5 cmH_2O.

c) Phase 3 - Disease State Recruitment Manoeuvre

In this study, the animal model ARDS criterion is defined as hypoxemia when subjects' arterial blood gas, PaO_2/FiO_2 (PF ratio) is less than 200 *mmHg* (The ARDS Definition Task Force, 2012). Once the piglet is diagnosed with ARDS, a second RM similar to Phase 1 was performed.

All experimental procedure, protocols and the use of data in this study were reviewed and approved by the Ethics Committee of the University of Liege Medical Faculty (Comité d'éthique du centre hospitalier universitaire de Liège, Faculté de Médecine).

3.4.3 Data Processing for the Minimal Model

To examine the subject-specific response to PEEP, a representative breath is selected from the last 2 breaths at each PEEP level during Phase 1 and Phase 3. When PEEP increases from a lower to higher level, recruitment occurs and the deflation/unloading of the lung is not complete, with additional air "trapped" in lung. This recruitment and "trapped" volume is the estimated lung volume increase for the PEEP increment. Figure 3.6 shows an example of the estimated lung volume increase, and the associated post-processed pressure volume curve (PV) is shown in Figure 3.7.

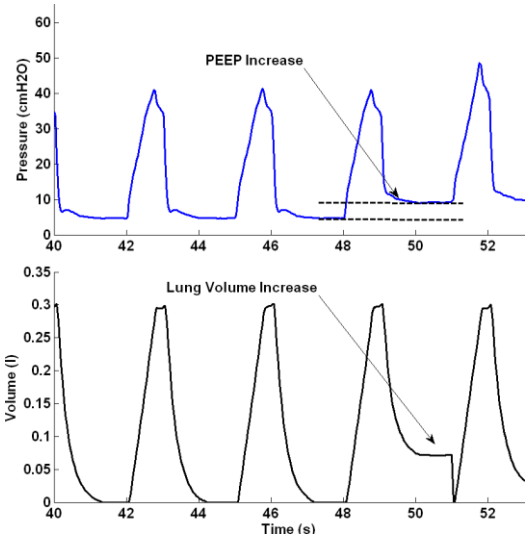

Figure 3.6: Estimation of volume increase during PEEP increment.

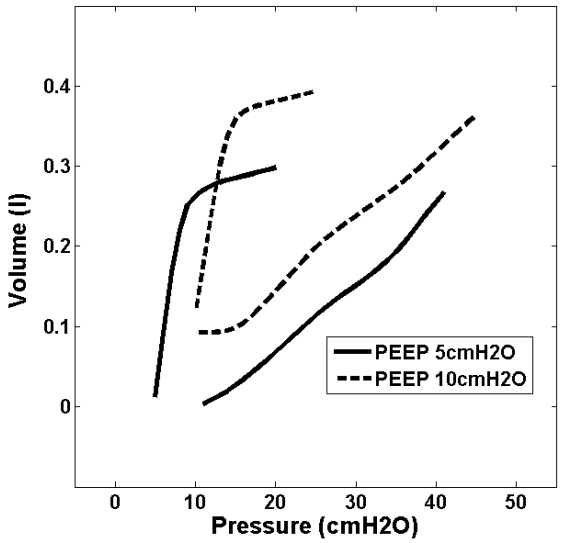

Figure 3.7: Example of pressure volume curves with volume increase with PEEP.

3.4.4 Model Fitting and Data Analysis

The processed PV curves were fitted to the minimal model (Sundaresan et al., 2009) to identify model-based mean TOP, mean TCP, and the standard deviations (SD) of both TOP and TCP distributions. Fitting errors are presented as mean absolute percentage error. Model-based mean TOP, TCP and SD in both healthy and ARDS states are compared to examine the effect of ARDS on model parameters, and their physiological and clinical relevance.

3.4.5 Disease State Grouping (DSG)

The estimated patient-specific parameters (mean TOP and SD) can be used to group patients based on their disease state using the 4 panel disease state grouping metric (DSG) shown in Figure 3.8. In general, patients grouped in Panel B (low SD and TOP) are healthier compared to other panels. A decrease of SD or mean TOP indicate a less heterogeneous lung and/or an overall decrease in collapsed lung units. This change is illustrated in Figure 3.9 (Left) and show improvement in lung condition. Conversely, an increase of either of these parameters indicates that lung condition is worsening over time as shown in Figure 3.9 (Right). Hard boundaries are deliberately not shown as specific because it may be patient- or group-specific. However, the overall diagram of Figure 3.8 can be used to clarify and monitor changes in patient condition, which is a main goal that must be validated for any model proposed for clinical use; as illustrated in Figure 3.9.

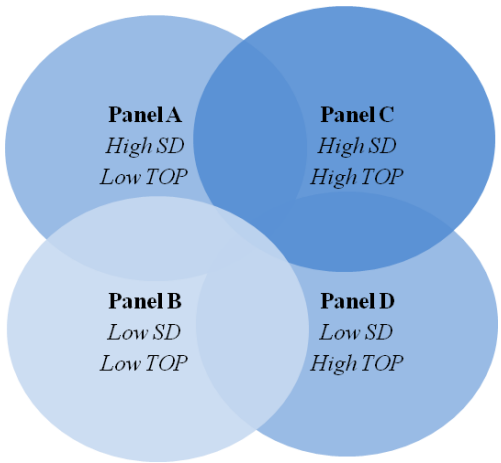

Figure 3.8: Patients-specific disease state grouping.

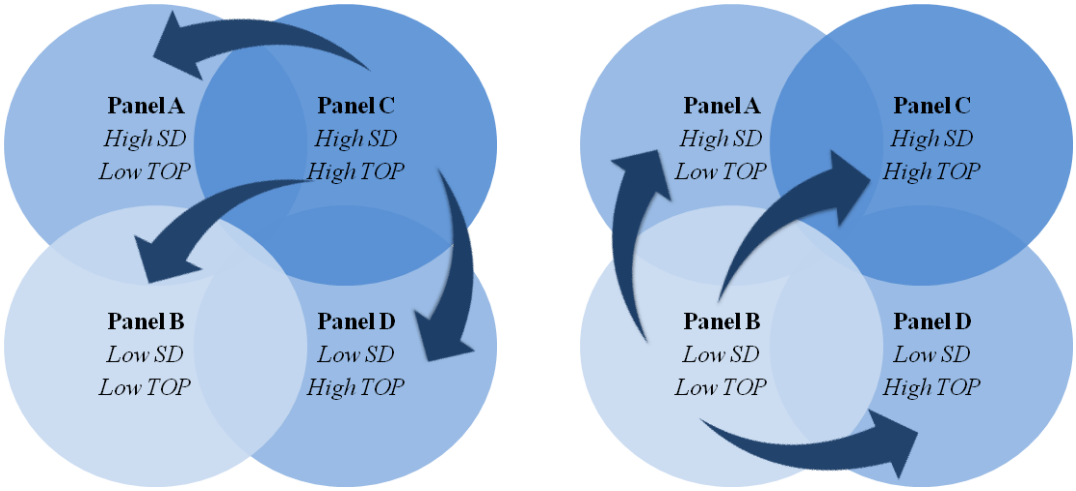

Figure 3.9: A metric for disease state tracking. (Left) Lung is recovering over time. (Right) Lung condition worsening.

3.5 Results and Discussion

9 piglets weighing median [Interquartile range (IQR)] 24.0 *kg* [IQR: 21.0-29.6] were included in the study. 3 of 9 subjects reached an ARDS state (Subjects 5, 6 and 9) after oleic acid injection. The mean TOPs, mean TCPs and SD of these 3 piglets that reached ARDS state are compared between the healthy and ARDS state.

3.5.1 Model Fitting

The minimal model fitting during inflation and deflation for healthy and ARDS subjects are shown in Tables 3.1-3.3. An example of model fit to measured PV curves of a healthy subject, and the resulting TOP and TCP distributions at PEEP of 10 cmH_2O and 15 cmH_2O are shown in Figure 3.10.

Table 3.1: Model fitting error during inflation at different PEEP levels for healthy subjects

Subject	Mean Absolute Percentage Fitting Error (%), Inflation				Median [IQR]
	PEEP 5	PEEP 10	PEEP 15	PEEP 20	
1	6.46	5.97	2.66	0.84	4.31 [2.20-6.09]
2	12.45	9.56	2.25	0.31	5.91 [1.77-10.28]
3	27.46	4.81	3.11	0.86	3.96 [2.55-10.47]
4	9.96	3.36	2.49	0.53	2.92 [2.00-5.01]
5	32.48	2.19	1.56	0.72	1.88 [1.35-9.76]
6	24.94	2.08	2.25	1.71	2.17 [1.98-7.93]
7	15.46	3.36	2.74	1.09	3.05 [2.33-6.38]
8	10.93	5.25	2.75	0.36	4.00 [2.15-6.67]
9	24.62	7.43	3.05	2.63	5.24 [2.95-11.73]
Median [IQR]	15.45 [10.93-24.94]	4.81 [3.36-5.97]	2.66 [2.25-2.75]	0.84 [0.53-1.09]	2.90 [1.98-7.97]

Table 3.2: Model fitting error during deflation at different PEEP levels for healthy subjects

Subject	Mean Absolute Percentage Fitting Error (%), Deflation				Median [IQR]
	PEEP 5	PEEP 10	PEEP 15	PEEP 20	
1	13.84	4.07	2.89	1.48	3.48 [2.53-6.51]
2	13.35	7.48	3.21	1.00	5.35 [2.66-8.95]
3	9.48	2.41	0.92	0.98	1.70 [0.96-4.18]
4	9.93	1.77	1.00	0.167	1.39 [0.79-3.81]
5	8.94	1.77	1.91	0.66	1.84 [1.49-3.67]
6	4.54	1.12	1.01	0.76	1.07 [0.95-1.97]
7	10.09	2.49	0.84	0.50	1.67 [0.75-4.39]
8	12.05	5.46	3.34	2.05	4.40 [3.01-7.11]
9	12.06	11.40	10.01	4.52	10.70 [8.63-11.56]
Median [IQR]	10.09 [9.48-12.06]	2.49 [1.77-5.46]	1.91 [1.00-3.21]	0.98 [0.66-1.48]	2.69 [1.00-9.07]

Table 3.3: Model fitting error for subjects with ARDS

Subject	Mean Absolute Percentage Fitting Error (%)				Median [IQR]
	Inflation				
	PEEP 5	PEEP 10	PEEP 15	PEEP 20	
5	5.81	7.27	3.08	1.08	4.45 [2.58-6.18]
6	2.85	5.64	4.13	0.69	3.49 [2.31-4.51]
9	41.44	9.62	2.17	3.63	6.62 [3.27-17.57]
	Deflation				
	PEEP 5	PEEP 10	PEEP 15	PEEP 20	
5	9.98	3.66	0.90	1.46	2.56 [1.32-5.24]
6	9.64	1.19	3.63	0.37	2.40 [0.99-5.13]
9	6.34	3.92	1.80	1.91	2.91 [1.88-4.52]

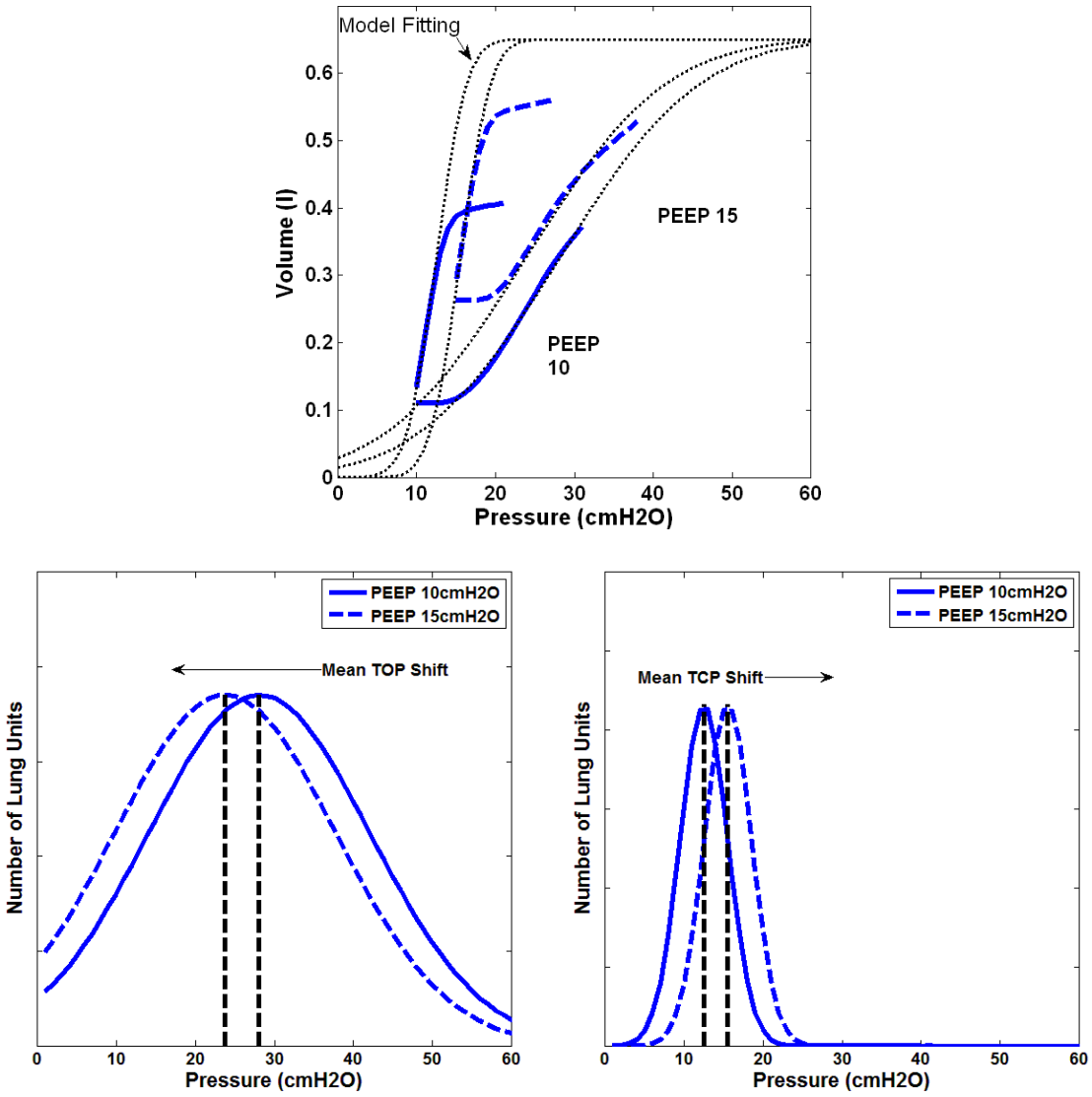

Figure 3.10: Model Fitting with TOP and TCP distribution shift for healthy Subject 2. (Upper) Model Fitting for PV curve in PEEP 10 and 15cmH_2O. (Bottom) TOP shifts left and TCP shifts right with PEEP increase.

Median [IQR] fitting errors in healthy subjects during inflation is 2.90% [IQR: 1.98-7.97] and 2.69% [IQR: 1.00-9.07] during deflation. Similar to healthy subjects, the model fits well for ARDS subjects with median absolute percentage error less than 7% during inflation and less than 3% during deflation (Table 3.3). There is a noticeable high fitting error for ARDS subject 9 at PEEP 5 cmH_2O, at 41.44% during inflation. The model was not able to capture these specific physiological conditions at

low PEEP. In particular, this case can be associated with the effect of Auto-PEEP distorting the actual lung condition (Sundaresan et al., 2009). The recruitment model fits better when Subject 9 is ventilated at higher PEEP ($p < 0.005$) compared to lower PEEP. However, the relatively low median error overall subjects indicates the model is capable of capturing fundamental mechanics of both healthy and ARDS lungs.

3.5.2 TOP, TCP and SD Response to PEEP

Table 3.4 shows the model estimated mean TOP and TCP at different PEEP for healthy subjects, and Table 3.5 for the ARDS subjects (5, 6 and 9). Table 3.6 shows the SD of the TOP and TCP distribution for the subjects that developed ARDS in both healthy and ARDS state.

Table 3.4: Mean TOP and TCP for healthy subjects

Subject	Threshold Opening Pressure (TOP, cmH_2O)				Threshold Closing Pressure (TCP, cmH_2O)			
	PEEP 5	**PEEP 10**	**PEEP 15**	**PEEP 20**	**PEEP 5**	**PEEP 10**	**PEEP 15**	**PEEP 20**
1	42.4	39.2	32.9	27.2	9.6	13.4	16.6	19.8
2	36.3	40.0	33.8	29.3	8.2	13.5	16.8	20.4
3	44.6	37.4	32.2	25.1	10.2	13.2	16.4	19.7
4	39.0	33.9	29.0	19.2	10.4	13.7	16.6	19.0
5	42.6	32.7	24.8	19.2	10.2	13.2	15.7	18.4
6	31.3	28.1	23.8	21.5	9.03	12.5	15.5	18.8
7	47.7	40.8	34.1	27.0	11.1	14.6	17.2	19.6
8	46.0	40.2	33.4	27.9	10.6	13.4	16.6	19.5
9	38.2	33.9	29.4	22.8	8.7	12.3	15.8	19.3
Median [IQR]	42.4 [38.2-44.6]	37.4 [33.9-40.0]	32.2 [29.0-33.3]	25.0 [21.5-27.1]	10.2 [9.0-10.4]	13.3 [13.2-13.5]	16.6 [15.8-16.6]	19.5 [19.0-19.7]

Table 3.5: Mean TOP and TCP for ARDS subjects

Subject	Threshold Opening Pressure (TOP, cmH_2O)				Threshold Closing Pressure (TCP, cmH_2O)			
	PEEP 5	PEEP 10	PEEP 15	PEEP 20	PEEP 5	PEEP 10	PEEP 15	PEEP 20
5	48.1	44.1	33.3	22.7	10.2	14.0	16.7	19.0
6	49.5	41.6	31.1	19.1	10.2	13.7	16.7	18.9
9	68.1	64.7	58.7	49.4	9.6	14.1	18.2	21.8
Average	55.2	50.1	41.0	30.4	10.0	13.9	17.2	19.9

Table 3.6: SD in healthy and ARDS lung

Subject	Healthy		ARDS	
	Inflation	Deflation	Inflation	Deflation
5	23	4	25	4
6	14	3	25	4
9	21	3	23	3
Average	19.3	3.3	24.3	3.7

In healthy subjects, the overall mean TOP is decreased with increasing PEEP, from 42.4 cmH_2O [IQR: 38.2-44.9] to 25.0 cmH_2O [IQR: 21.5-27.1]. Mean TCP increases from 10.2 cmH_2O [IQR: 9.0-10.4] to 19.5 cmH_2O [IQR: 19.0-19.7] with increasing PEEP. The TOP and TCP distribution shift of a subject during PEEP increase is observed in Figure 3.10 (Bottom), and are capturing the recruitment as expected.

Similar mean TOP and TCP trends are also observed in ARDS subjects. However, an overall higher TOP is observed compared to healthy subjects, which is also expected for an ARDS lung. The overall higher mean TOP indicates that the ARDS lung consists of relatively more collapsed alveoli and higher pressure is needed to recruit the collapsed alveoli.

An example of the PV curve shift from a healthy state to an ARDS state is shown in Figure 3.11 (Upper). The change in TOP and TCP distributions between healthy and ARDS state for the 3 subjects in Tables 3.5-3.6 is shown in Figure 3.11 (bottom).

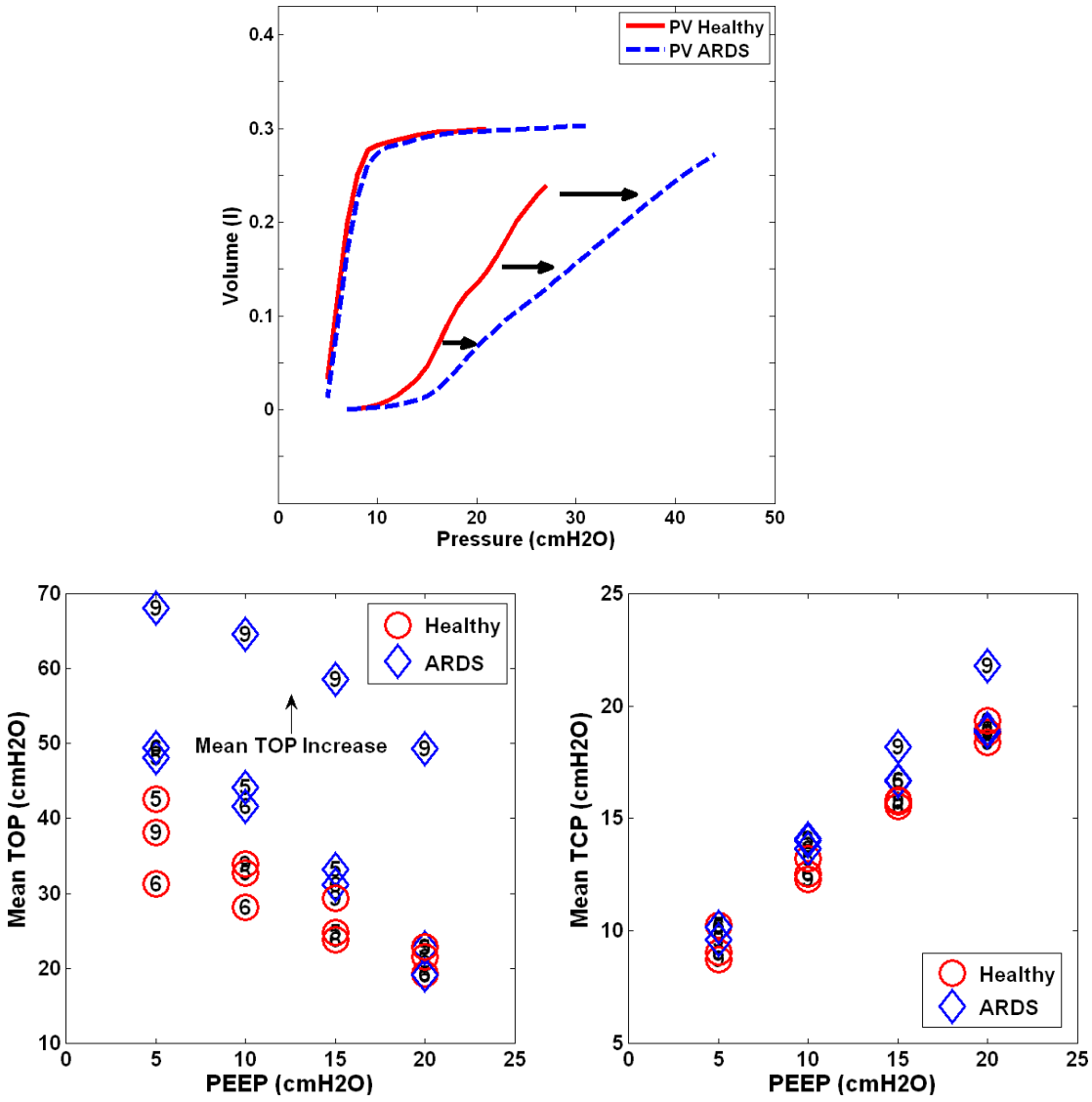

Figure 3.11: Pressure-volume curve of Subject 5 and overall TOP and TCP comparison between healthy and ARDS. (Top) Inflation curve right shift from healthy to ARDS. (Bottom) TOP in healthy lung is lower than in ARDS. Relatively little change in TCP during healthy and ARDS state.

Healthy lungs normally consist of only opened or recruited lung units, and a model based on the concept of recruitment may not be applicable. However, in a healthy

anesthetised and sedated subject, pulmonary atelectasis can be observed, but it is less severe compared to an ARDS lung and can be easily recruited (Tusman et al., 1999, Rusca et al., 2003, Tusman et al., 2012). Thus, during inflation, relatively lower pressure is needed to ventilate the healthy "collapsed" lung compared to ARDS lung. Therefore, for a given tidal volume, the area within the PV curve for a healthy lung should be smaller than ARDS lung. Equally, the healthy lung is less heterogeneous and the lower SD will keep the PV loop area smaller. Figure 3.11 shows a clear comparison of a healthy and ARDS PV curve, in which the ARDS PV curve has greater area than the healthy PV curve and correspondingly higher SD for this Subject 5 in Table 3.6. The change thus shows the expected higher work of breathing in the heterogeneous ARDS lung.

Comparing the healthy and ARDS state, mean TOP for healthy lungs are lower when compared to ARDS lungs in Figure 3.11 (Bottom). A healthy lung is a less heterogeneous lung and the effect of superimposed pressure to alveoli is less detrimental. As suggested earlier, a healthy lung is normally open, which results in a lower mean TOP. Thus, the model captures the fact that, for the same subject at a healthy and ARDS state, higher pressure is required to recruit and open the lung. The inter-subject variability in this behaviour is evident in Figure 3.12. Overall, these model results match clinical observation and expectation, which further validates the model.

The deflation curve remains unchanged in ARDS compared to healthy subjects, as shown in Figure 3.11 (Upper), which results in relatively no change in TCP, as seen in

Figure 3.11 (Lower Right) and Table 3.3. Hypothetically, mean TCP should be higher in the ARDS state compared to the healthy state (Sundaresan et al., 2009, Pulletz et al., 2012). ARDS lung units are more unstable and vulnerable to collapse. Thus, higher pressure is required to retain recruitment. However, this hypothesis was neither observed nor apparent in these results. Only a small increase in TCP is observed during ARDS state compared to healthy state as shown in Figure 3.11.

3.5.3 Application of DSG Metric

The DSG for the ARDS subjects are shown in Figure 3.12. It is observed that all 3 subjects experienced different SD and TOP increase when transitioning from healthy to ARDS state. In particular, Subject 5 has a relatively small increase in both SD and TOP between healthy and ARDS state. Subject 6 had very large increase in SD (heterogeneity) but less change in TOP (Collapsed lung units). Subject 9 had a very high TOP change (Lung collapse) but minimal changes in SD (Heterogeneity). These results show the diversity in the impact of the ARDS induced and thus the overall difficulty of the clinical problem in general. Clearly, patient-specific solutions will be required.

It is known that ARDS induced in animal model using oleic acid are highly variable (Schuster, 1994). A small variation in ventilation and hemodynamic management during preparation, time and dosage may alter the severity or extensiveness of the lung injury, resulting in different pathophysiological consequences (Schuster, 1994, Rosenthal et al., 1998, Ware, 2008, Bastarache and Blackwell, 2009, Ballard-Croft et al., 2012). That behaviour is clearly evident in these results.

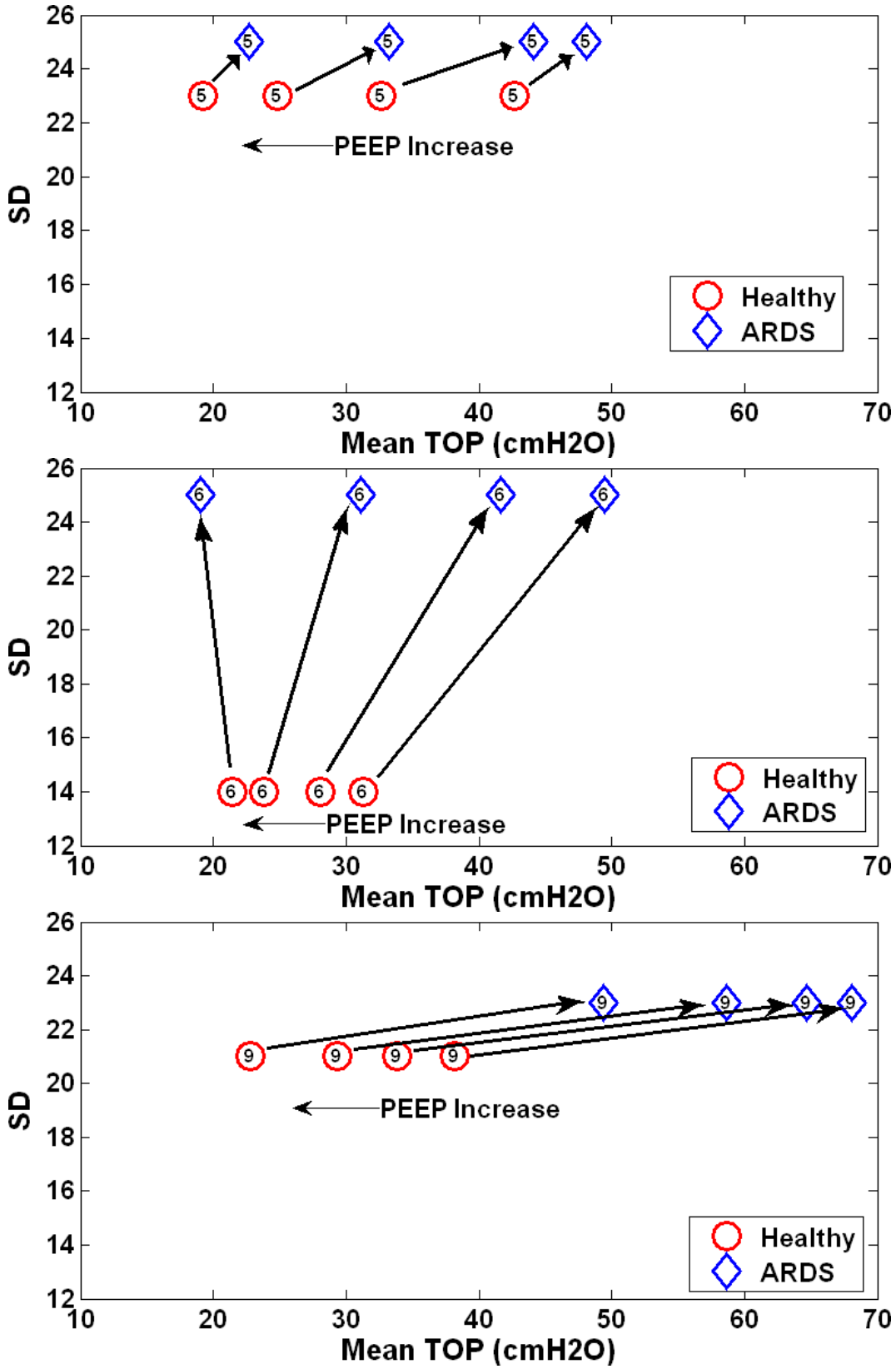

Figure 3.12: Change of TOP and SD for healthy subject which later develop ARDS. (Top) Subject 5, with slight increase of SD and TOP. (Middle) Subject 6, large increase of SD. (Bottom) Subject 9, slight increase of SD with high TOP change.

Importantly, this research focuses on minimal model performance in healthy and ARDS lungs. Combining the DSG for all 3 subjects, as shown in Figure 3.13, the healthy subjects have overall lower TOP and SD than in the ARDS state. This finding suggests that the DSG application is not limited to patient-specific disease state tracking, but can be expanded into population monitoring. Capturing 3 different ARDS respiratory mechanics or pathophysiological consequences, thus encourages the model's application in clinical setting, where the presentation of ARDS and its evolution over time and treatment can be variable.

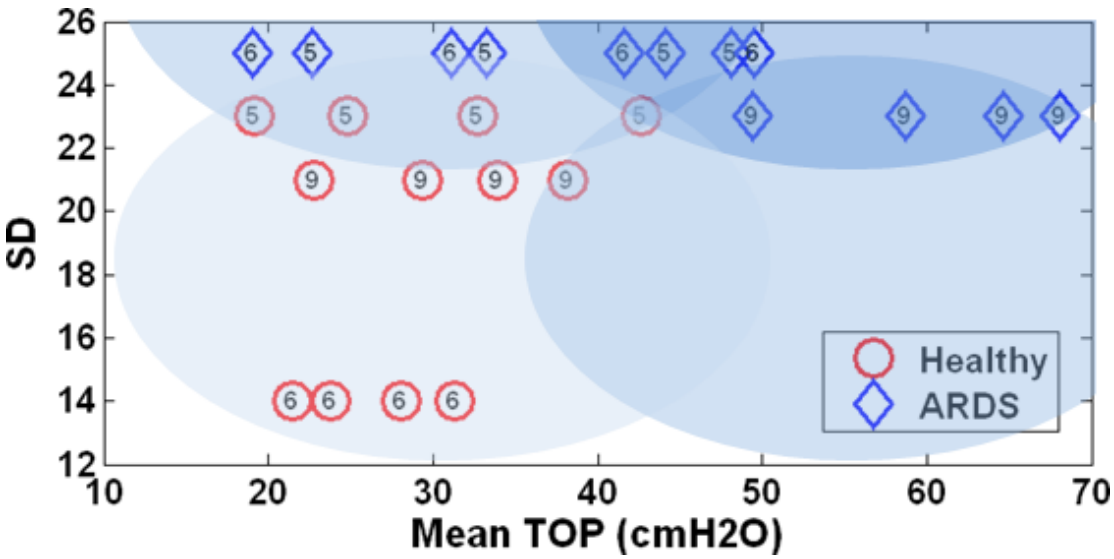

Figure 3.13: The 4 panel DSG and the mean TOP and SD changes with PEEP for the 3 ARDS subjects.

This DSG application is unique and observing DSG shifts should provide useful information for clinical decision support. For example, patients who are grouped in Panel D (High TOP, low SD), have a less heterogeneous lung, but with overall higher lung unit opening pressure. For example, it is hypothesised that a high PEEP can be used in MV to recruit overall collapsed lung units and improve gas exchange

(Takeuchi et al., 2005, Spieth and Gama de Abreu, 2012). For patients who are grouped in Panel A (Low TOP, high SD), ventilation modes with 2 PEEP levels (Bi-Level PEEP ventilation, airway pressure release ventilation (APRV)) can reduce cyclic opening and collapse of lung units and improve patient outcome (Varpula et al., 2004, Brower et al., 2004, Barbas et al., 2005). Tracking patient DSG with time will also show the effect and patient's response to specific treatment. In this research, the effect of oleic acid can be seen in increase of TOP and SD. However, the exact limits of these groupings remain to be determined, although it does not affect the ability to track patient condition and response to therapy as in Figure 3.12 or compared as in Figure 3.13.

Overall, the difference of mean TOP and SD between the healthy and ARDS state can be identified using the minimal model. The application of minimal model is not limited to the diseased lung, and allows comparison between healthy and ARDS lungs, and thus encourages its application and future investigation in the ICU to monitor patients-specific condition to guide MV therapy. An overall down shift of mean TOP and/or lowered SD will indicate that the lung recovering for injurious state. In contrast, an up-shift of TOP and/or SD, will show that the lung is more injured. This unique pair of metric thus provides the ability to track the disease state from healthy to injured state and vice-versa. However, mean TCP appears to have little change between healthy and ARDS state, indicating that the TCP parameter was less significant in this clinical use.

3.6 Limitations

3.6.1 Repeatability of ARDS Piglets

After oleic acid injections, only 3 of 9 subjects successfully developed ARDS. Others experienced hemodynamic failure before ARDS could develop fully or detected. This result shows that oleic acid induced ARDS animals are less reproducible and the subject preparation method should be re-examined (Julien et al., 1986, Schuster, 1994, Grotjohan et al., 1996, Rosenthal et al., 1998). The estimation and comparison of TOP, TCP and SD during healthy and ARDS state is thus, not conclusive with statistical significance given low subject numbers. However, individual data revealed that subjects that developed ARDS had overall higher TOP compared to subject in a healthy state. This physiologically relevant result is supported by past literature that examines similar clinical conditions (Lu et al., 2001, Crotti et al., 2001, Pelosi et al., 2001). In addition, all other results follow clinically expected trends.

3.6.2 Ventilation Tidal Volume

In this study, tidal volume is set to 10~12 *ml/kg* to ventilate the experimental piglets. It is known that such a high tidal volume is injurious with higher mortality (The Acute Respiratory Distress Syndrome Network, 2000). However, the focus of the study is the investigation of the model's performance in healthy and ARDS states. During a healthy state, the recruitment manoeuvre with airway pressure and flow measurements were performed at the very beginning of the trial. This time frame is relatively short and thus, the effect of high tidal volume ventilation was minimal and likely did minimal or no damage. Moreover, a more injurious ventilation strategy

would indirectly benefit the overall study goals comparing healthy and damaged lung state.

3.6.3 Estimation of the Volume Change

The measurement of volume change was estimated during RM PEEP increase. The calculation method assumes that deflation of the lung is not fully complete and the air remained in the lung due to PEEP. This estimation based on Figure 3.6 may not be entirely true. However, direct measurement of the lung volume during short PEEP increases is not available at the bedside. In particular, FRC estimation using nitrogen washout requires several breathing cycles and a long stabilisation period and thus, was not suitable in this trial or for regular clinical use (1-4 times per day). The volume change estimation is this study is thus a surrogate of the actual lung volume increase. This estimation method can be validated in future studies using nitrogen or oxygen washin/washout method (Weismann et al., 2006, Maisch et al., 2007, Olegard et al., 2010, Dellamonica et al., 2011). However, all trends remain valid, and it is these changes that are critical here. Equally, low fitting errors indicate it did not appear to affect the model.

3.6.4 Minimal Model and Patient DSG

The minimal model is a model that estimates TOP, TCP and SD during PEEP titration of the mechanically ventilated. It is unable to predict the alveolar over-distension directly. However, the use of TOP mean shift as proposed by Sundaresan et al (Sundaresan et al., 2011a), it is possible to monitor the recruitability of the lung and thus, indirectly reveal potential over-distension that may cause lung injury.

The DSG provides a unique metric to monitor patient's condition and potentially be used to guide ventilator settings. However, there are currently insufficient samples to validate this metric, or to prove the patients outcome for different TOP and SD. In particular, questions such as: "what is the actual physiological findings in patients with particular SD/ TOP value", "what SD or TOP values are considered as high or low" need to be addressed. Figure 3.13 is an example of the metric application, but there is insufficient information to determine which specific TOP/SD is high/low. In addition, the estimated TOP and SD in animals may be different if compared with human subjects. Future clinical trials or clinical PV data from other trials are required to validate this proof of concept.

3.7 Summary

The minimal model fits well in both healthy and ARDS lungs, and is capable of capturing the fundamental lung mechanics of the healthy and ARDS lung. The application of minimal model is thus not limited to diseased lung cases, but can be even used for healthy lungs. The model was able to estimate clinically and physiological relevant parameters for healthy and ARDS piglets thus allowing disease state tracking (DSG), which in turn illustrates the difficult problem and need for patient-specific solution, as well as showing the potential to use this model to assist in clinical decision making.

In the next chapter, a compartment model that describes the respiratory mechanics during mechanical ventilation is presented. This model estimates the respiratory elastance and the airway resistance of the experimental piglets. Hence, it captures

metrics that cannot be obtained with simple clinical metrics or static approaches, as it identifies underlying patient-specific parameters with clinical relevance to the problem. Therefore, similar to the minimal model presented here, the compartment model can provide clinically useful information in setting MV.

Chapter 4

Respiratory Mechanics Monitoring:

Single Compartment Linear Lung Model

Modelling the respiratory mechanics of mechanically ventilated (MV) patients is an emerging clinical research area. These models can potentially provide clinically and physiological useful information to guide MV therapy (Lauzon and Bates, 1991, Sundaresan et al., 2009, Ma and Bates, 2010, Sundaresan and Chase, 2011). Complex modelling of respiratory mechanics can be developed, to describe patient-specific condition (Tawhai et al., 2004, Burrowes et al., 2008, Tawhai et al., 2009, Choi et al., 2010). However, these complex models are computationally intense and cannot be customised to a specific patient in clinically relevant time frames to guide decision making. Thus, their real time clinical application to guide MV is limited (Bates, 2009b, Schranz et al., 2010). Furthermore, specific protocols are required to define patient-specific complex respiratory system models (Farre et al., 1998). These protocols may be invasive and not clinically feasible due to the heterogeneity and severity of the patient's conditions.

4.1 Single Compartment Linear Lung Model

Recent studies revealed that simple respiratory models have the potential to guide MV (Lucangelo et al., 2007). Studies that dynamically monitored a model-based or

clinically derived elastance component dynamically during breathing cycle (Guttmann et al., 1994, Chiew et al., 2011, Zhao et al., 2012a, Chiew et al., 2012b) revealed similar outcomes with the benefit of minimising work of breathing. In particular, the most commonly used model in clinical practice is the lumped parameter model (single compartment linear lung model) (Mead and Whittenberger, 1953). The respiratory system is modelled as a combination of an elastic/compliance component with a resistance component. The elastic or compliance component represents the physical lung, whereas the resistive component models the airway. The schematic representation of the single compartment lung model is shown in Figure 4.1.

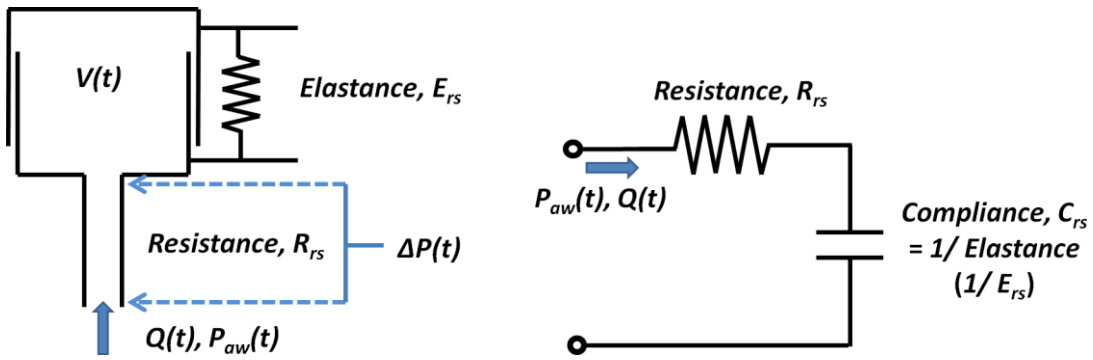

Figure 4.1: Schematic drawing for single compartment linear lung model. (Left) Mechanical system. (Right) Electric circuit representation of the respiratory model.

When the air enters the lung through the endotracheal tube (ETT) and patient's airway, there is a pressure drop due to the resistance component (R_{rs}) of the combined conducting airway as shown in Equation 4.1. The lung is modelled as an expandable compartment connected by a spring with elastic property (E_{rs}) as shown in Equation 4.2).

$$\Delta P(t) = R_{rs} \times Q(t) \tag{4.1}$$

$$P_{lung}(t) = E_{rs} \times V(t) \quad (4.2)$$

Where ΔP is the pressure drop, t is time, R_{rs} is the conducting airway resistance, Q is the air flow, P_{lung} is the pressure build-up in the lung compartment, E_{rs} is the elastic property of the lung and V is the lung volume. Thus, the equation of motion of the respiratory system can be derived by combining both Equations 4.1 and 4.2 to yield:

$$P_{aw}(t) = \Delta P(t) + P_{lung}(t) \quad (4.3)$$

$$P_{aw}(t) = R_{rs} \times Q(t) + E_{rs} \times V(t) \quad (4.4)$$

Where P_{aw} is the airway pressure. Equation 4.4 is augmented with an offset pressure, *P0* to account for pressure equilibrium. *P0* is normally zero at atmospheric pressure and will only change when PEEP is applied and accounts for Auto-PEEP (Bates, 2009a). Thus, the respiratory system may be simply modelled as in this form using a model defined:

$$P_{aw}(t) = R_{rs} \times Q(t) + E_{rs} \times V(t) + P0 \quad (4.5)$$

4.2 Application of Compartment Model in Respiratory Mechanics Monitoring

As briefly discussed in Chapter 2, monitoring respiratory mechanics in ARDS patients has been shown to be beneficial in clinical decision making, as the respiratory mechanics represents the patient-specific and condition-specific response to MV settings (Carvalho et al., 2007, Lucangelo et al., 2007, Suarez-Sipmann et al., 2007,

Lambermont et al., 2008). However, its application is limited and it is yet to be used continuously in regular clinical practice to guide therapy (Rousselot et al., 1992, Baconnier et al., 1995, Bersten, 1998, Muramatsu et al., 2001, Eberhard et al., 2003, Lucangelo et al., 2007, Brochard et al., 2012).

In this chapter, the feasibility of continuously monitoring respiratory mechanics using single compartment respiratory model is studied extensively in experimental ARDS animal model. The respiratory mechanics in Equation 4.5 (E_{rs} and R_{rs}) of the mechanically ventilated animal are estimated and monitored using model-based methods (Rousselot et al., 1992, Muramatsu et al., 2001). These estimated values are compared with conventional clinically derived respiratory mechanics. It is hypothesised that monitoring the model-based respiratory mechanics for ARDS animal, or patient, in real-time will provide unique descriptions of the subject's disease progression, and response to MV different settings. Such data can provide guidelines to guide MV therapy and decision making in real-time.

4.3 Methodology

4.3.1 Experimental Data

The recorded pressure, flow and volume profile from the experiment described in Chapter 3 were used to examine the hypothesis. Unlike the minimal model (Chiew et al., 2012a), where it can only compare 2 distinct state; the healthy state and ARDS state, the single compartment model can be used to monitor respiratory mechanics throughout the trial, including Phase 2 (Disease progression). An example of the

pressure profile during all 3 phases, as described in the methodologies presented in Chapter 3 is shown in Figure 4.2.

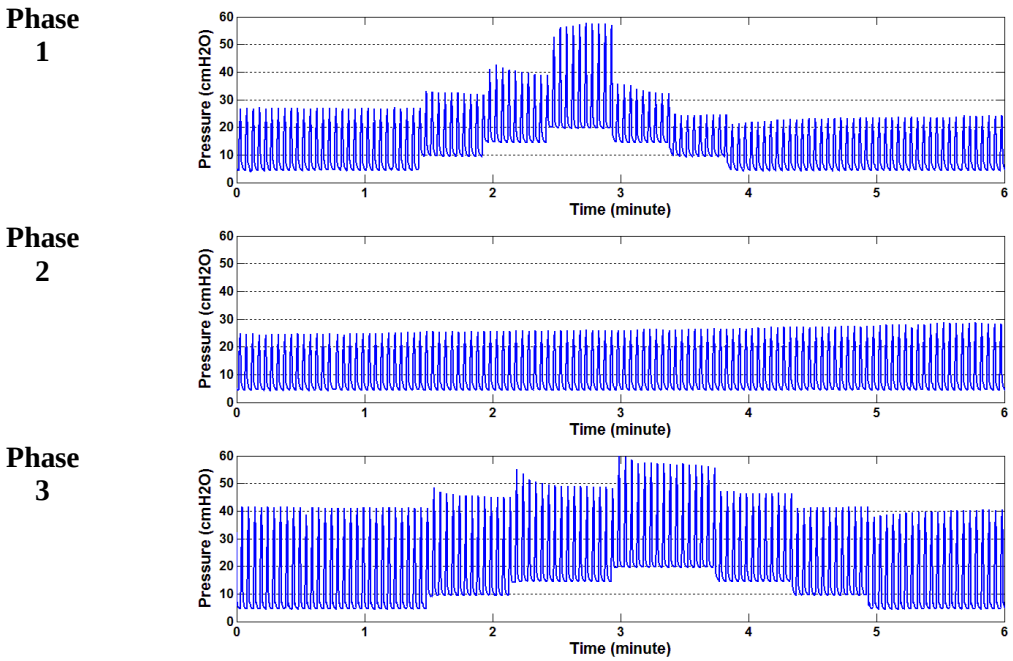

Figure 4.2: Pressure profile during the 3 phase clinical trial. (Top) Phase 1 - Healthy state staircase RM, (Middle) Phase 2 - Progression to ARDS State and, (Bottom) Phase 3 - Disease State RM during ARDS. The single compartment model is used to estimate the respiratory mechanics continuously for all 3 phases.

4.3.2 Respiratory Mechanics Estimation

Respiratory mechanics of every breathing cycle from the 3 piglets that reached an ARDS state were estimated using 3 different methods: 1) model-based method using Equation 4.6; 2) a conventional method and 3) Automated end of inspiratory pause (EIP).

a) Model-based Method

The model-based method uses integral-based method (Hann et al., 2005) to estimate E_{rsIB} (Elastance) and R_{rsIB} (Resistance) value that best fit Equation 4.5. Integral-based

parameter identification is similar to multiple linear regression, where using integrals significantly increases robustness to noise. Equation 4.6 defines the overall approach that yields a set of the expressions in terms of elastance and resistance when integrating 2 or more time frames within a breath (Chiew et al., 2011).

$$\int P_{aw}(t) = R_{rsIB} \times \int Q(t) + E_{rsIB} \times \int V(t) + \int P0 \qquad (4.6)$$

b) Conventional Method

The conventional method (2-point calculation) calculates of respiratory elastance using the difference between clinically observed peak airway inspiratory pressure (*PIP*) and PEEP, divided by inspiratory tidal volume (V_t). This conventional elastance (E_{rsVent}) is defined:

$$E_{rsVent} = (PIP - PEEP)/ V_t \qquad (4.7)$$

The conventional method is comparatively simpler than the model-based method. However, E_{rsVent} is often overestimated in this approach as the term E_{rsVent} includes information of the airway resistance (Storstein et al., 1959, Barberis et al., 2003, Lucangelo et al., 2007). Thus, E_{rsVent} can be associated with dynamic elastance (1/ dynamic compliance). Airway resistance is not normally measured without an end inspiratory pause (EIP) (Storstein et al., 1959, Barberis et al., 2003, Lucangelo et al., 2007). Thus, model-based methods should provide better resolution and identification of clinically relevant respiratory mechanics without additional clinical protocol.

c) Automated End of Inspiratory Pause (EIP)

In this study, the experimental piglets were ventilated using Engström CareStation ventilator (Datex, General Electric Healthcare, Finland), volume control, square flow profile. The ventilation mode was set with an automated short end inspiratory pause (EIP) (Ingelstedt et al., 1972, Fuleihan et al., 1976, Pillet et al., 1993). The zero-flow phase during EIP omits the resistance component in Equation 4.3. The resulting end of inspiratory pressure after EIP (plateau pressure, P_{plat}) can be used to estimate the static ventilation elastance as shown in Equation 4.8 (Shiu and Rosen, 2006). Equally, the pressure difference between peak pressure (PIP) and P_{plat} can be used to calculate the airway resistance as shown in Equation 4.9.

$$E_{Static} = (P_{plat} - PEEP)/ V_t \quad (4.8)$$

$$R_{Static} = (PIP - P_{plat})/ Q \quad (4.9)$$

Both E_{Static} and R_{Static} can be derived directly from the modern ventilators with automated EIP feature. This feature allows the model-based estimated E_{rsIB} and R_{rsIB} to be compared with E_{Static} and R_{Static}, validating the model-based method.

4.4 Results and Discussion

4.4.1 Model Fitting

The model-based method estimates the E_{rsIB} and R_{rsIB} values using the integral based method as fitted to the measured airway pressure. Median absolute percentage fitting errors of the model of Equation (4.6) to measured airway pressure are reported in Table 4.1. Overall, the median absolute percentage fitting error to the model is 2.42%

[IQR: 1.95-2.77] in every subject over all three phases. This result indicates that the single compartment lung model was able to identify the fundamental, subject-specific and clinically relevant respiratory mechanics (Marini, 1992, Lucangelo et al., 2007, Brochard et al., 2012).

Table 4.1: Model fitting errors using E_{rsIB}, R_{rsIB}, median [IQR] using integral based method of (Hann et al., 2005)

Subject	Absolute Percentage Fitting Error (%)			Overall
	Phase 1	Phase 2	Phase 3	
1	1.73 [0.98-3.17]	2.42 [1.83-3.06]	3.41 [2.58-4.44]	
2	2.22 [1.60-2.72]	2.01 [1.53-2.51]	2.55 [2.21-3.04]	
3	1.77 [1.32-2.17]	2.48 [1.49-4.26]	5.93 [3.48-7.70]	
				2.42 [1.95-2.77]

4.4.2 Clinically Derived and Model-based Respiratory Mechanics

Tables 4.2-4.4 reported and compared the identified respiratory mechanics during the healthy state (Phase 1) and during the ARDS state (Phase 3). Figures 4.3-4.5 show all respiratory mechanics estimated throughout the clinical trial in different subjects at every breathing cycle. Note that only the integral based method can also identify resistance (R_{rsIB}) in Table 4.4, which the conventional method ignores.

As expected, the elastance calculation in the conventional method is higher than model-based method due to the effect of respiratory system resistance (as noted in Equation 4.5). The linear definition of ventilator elastance (E_{rsVent}) also means that it cannot capture any non-linearity compared to the physiologically realistic Equation (4.5), and this nonlinearity difference can vary within a subject.

Table 4.2: E_{rsVent} for all 3 subjects in Phase 1 and Phase 3 (ARDS) using the conventional method of Equation of 4.7

Subject	E_{rsVent} (cmH_2O/l), Median [IQR]			
	PEEP 5	**PEEP 10**	**PEEP 15**	**PEEP 20**
5	73.61 [71.54-75.75]	77.55 [74.12-79.15]	90.14 [84.63-96.11]	131.26 [126.73-133.01]
6	73.11 [72.43-73.81]	75.19 [73.44-75.95]	84.56 [81.34-88.71]	126.24 [125.93-127.22]
9	90.94 [90.21-91.49]	91.11 [88.10-94.84]	88.57 [84.85-93.12]	104.71 [100.44-106.89]
	E_{rsVent} (cmH_2O/l), Median [IQR]			
	PEEP 5	**PEEP 10**	**PEEP 15**	**PEEP 20**
ARDS5	127.50 [126.60-127.73]	142.71 [133.29-152.59]	129.25 [121.23-150.26]	146.11 [142.47-154.94]
ARDS6	121.16 [120.86-121.40]	121.11 [117.50-123.40]	114.57 [112.57-118.11]	124.15 [121.20-126.88]
ARDS9	180.85 [179.16-181.82]	168.34 [167.48-171.25]	156.59 [155.64-160.63]	152.37 [149.78-156.62]

Table 4.3: E_{rsIB} for all 3 subjects in Phase 1 and Phase 3 (ARDS) using the integral-based method of (Hann et al., 2005)

	E_{rsIB} (cmH_2O/l), Median [IQR]			
	PEEP 5	**PEEP 10**	**PEEP 15**	**PEEP 20**
5	58.72 [56.43-60.23]	62.06 [59.50-63.91]	75.52 [71.07-84.70]	106.89 [104.61-113.49]
6	52.50 [52.16-53.15]	58.57 [56.35-60.25]	68.78 [66.18-74.68]	109.26 [108.10-111.35]
9	71.86 [71.42-72.12]	67.47 [65.68-70.53]	69.27 [66.27-74.49]	84.97 [81.36-88.76]
	E_{rsIB} (cmH_2O/l), Median [IQR]			
	PEEP 5	**PEEP 10**	**PEEP 15**	**PEEP 20**
ARDS5	108.85 [106.92-111.34]	123.40 [117.70-130.76]	109.87 [105.80-130.40]	128.36 [123.04-141.69]
ARDS6	113.46 [112.26-114.57]	114.71 [113.85-116.69]	112.95 [109.38-117.03]	119.71 [117.17-122.98]
ARDS9	122.25 [119.74-126.14]	134.29 [132.00-136.58]	132.88 [131.13-137.13]	131.83 [128.85-136.59]

Table 4.4: R_{rsIB} for all 3 subjects in Phase 1 and Phase 3 (ARDS) using the integral-based method of (Hann et al., 2005)

	R_{rsIB} (cmH_2Os/l) Median [IQR]			
	PEEP 5	**PEEP 10**	**PEEP 15**	**PEEP 20**
5	10.99 [10.71-12.64]	8.17 [7.20-9.97]	5.73 [4.59-7.52]	7.88 [5.53-8.85]
6	18.17 [17.87-18.52]	13.30 [12.71-13.53]	9.54 [9.26-9.67]	6.33 [6.29-6.55]
9	16.89 [16.71-17.04]	14.96 [14.83-16.67]	12.53 [12.38-12.81]	10.21 [10.13-10.52]
	R_{rsIB} (cmH_2Os/l) Median [IQR]			
	PEEP 5	**PEEP 10**	**PEEP 15**	**PEEP 20**
ARDS5	13.64 [12.60-14.47]	7.24 [6.31-8.44]	6.30 [5.51-7.18]	6.13 [5.48-7.43]
ARDS6	15.29 [14.13-15.95]	8.77 [6.81-10.56]	4.69 [2.92-4.99]	4.45 [2.18-4.66]
ARDS9	53.11 [51.55-54.32]	36.88 [36.18-37.96]	27.02 [25.45-28.05]	19.92 [18.42-20.95]

In this study, the highest airway pressure (70 cmH_2O) was observed at PEEP 20 cmH_2O. Theoretically, airway pressure that exceeds 45 cmH_2O, potentially causes alveolar overdistension and ventilator induced lung injury (VILI) (Chiumello et al., 2008, Caironi et al., 2010). However, recent studies by Borges et al using recruitment manoeuvres with airway pressures up to 60 cmH_2O reversed ARDS lung collapse, without inducing lung injury (Borges et al., 2006, de Matos et al., 2012). This finding confirms that the airway pressure alone does not necessarily represent the alveolar pressure well, given high airway resistance.

In this study, airway resistance (R_{rsIB}) was subject-specific and high. Therefore, monitoring model-based respiratory mechanics which identifies a subject-specific airway resistance (R_{rsIB}) can provide a better indication of alveolar condition, and thus better protection in overdistension. In contrast, the conventional approach of identifying E_{rsVent} alone does not segregate this effect, resulting in potentially misleading results and less insight.

4.4.3 Recruitment Manoeuvre - Phase 1 and Phase 3

Figure 4.3 show the RM results in Phase 1. Increased respiratory elastance was observed at the start of every increase in PEEP. As the breathing pattern stabilises, respiratory elastance slowly decreases to a specific minimum at that PEEP level. Decrease of elastance over time can be described by the lung's viscoelastic properties, which causes hysteresis (Ganzert et al., 2009, Andreassen et al., 2010). Equally, PEEP induced recruitment is time dependant, and will contribute to prolonging the stabilisation period (Albert et al., 2009).

In this animal trial, it was also found that decreasing PEEP titration resulted in lower overall respiratory elastance compared to increasing PEEP titration, as shown in Figures 4.3 and 4.4. When PEEP is increased to a higher level, recruitment, as well as potential lung overstretching, occurs. However, after PEEP is decreased from a higher PEEP value, the lung remained compliant. This observation is supported by several studies that showed PEEP titration should be performed after recruitment manoeuvres to keep the lung open (Lachmann, 1992, Halter et al., 2003, Huh et al., 2009, Suarez-Sipmann and Bohm, 2009, Hodgson et al., 2011b, Hodgson et al., 2011a). Hence, the model is capturing clinically observed and relevant behaviours.

During PEEP titration in Phase 3, subject-specific respiratory elastance drops to an overall minimum at specific PEEP (PEEP = 15 cmH_2O for Subjects 5 and 6, and PEEP = 5 cmH_2O for Subject 9). Setting PEEP at minimum elastance theoretically benefits ventilation by maximising recruitment, reducing work of breathing and avoiding overdistension, as shown in previous works (Carvalho et al., 2007, Suarez-Sipmann et al., 2007, Lambermont et al., 2008, Zhao et al., 2010a). It should also be noted that, the methods for PEEP titration between these works are different. Studies by Lambermont, Carvalho and Suarez-Sipmann (Lambermont et al., 2008, Carvalho et al., 2007, Suarez-Sipmann et al., 2007) used decreasing PEEP titration after a recruitment manoeuvre, whereas Zhao (Zhao et al., 2010a) used increasing PEEP titration to monitor respiratory elastance with shorter stabilisation period. However, the overall result and trends were consistent, and are captured by this model in these experiments.

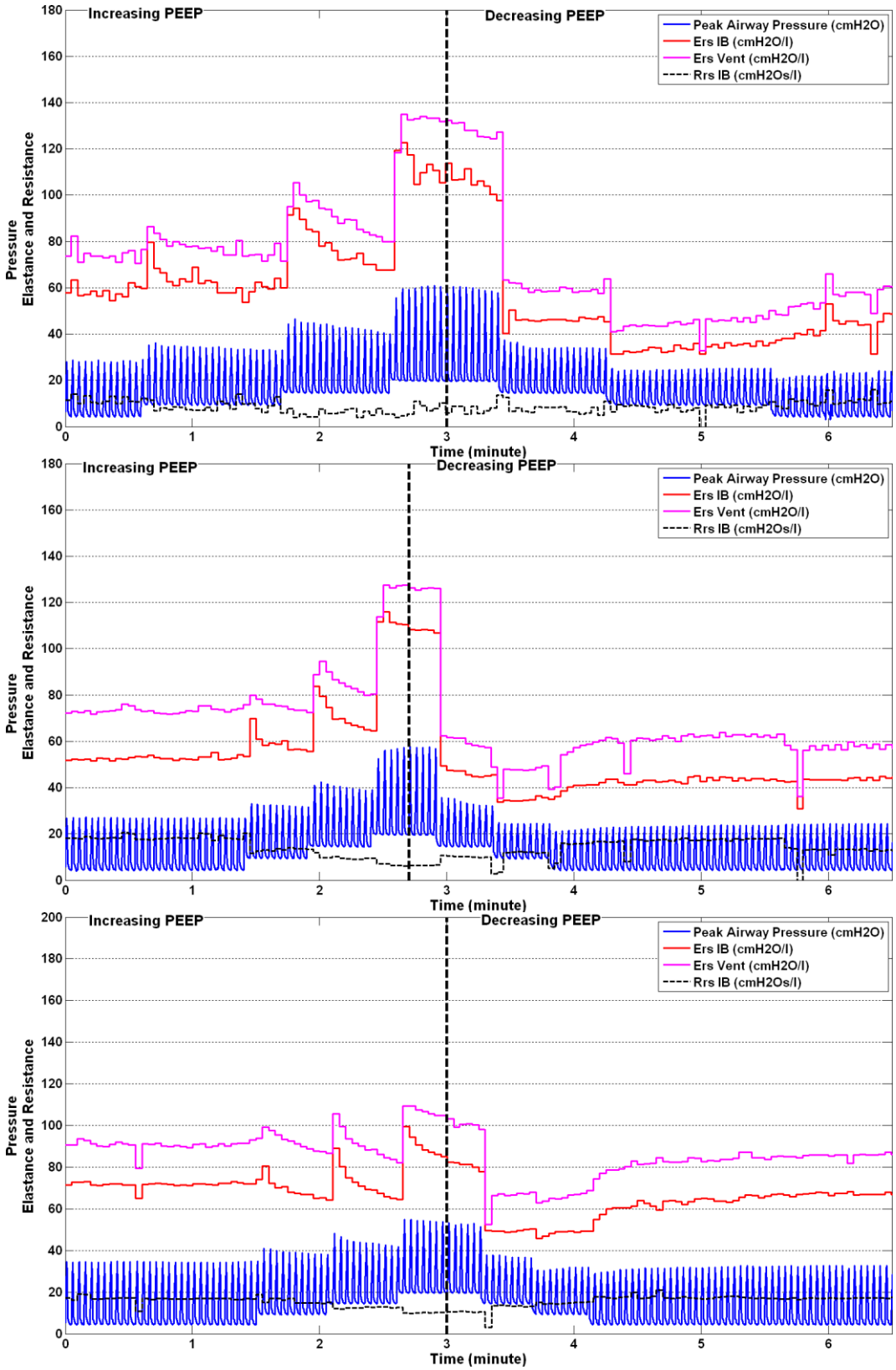

Figure 4.3: Respiratory system mechanics monitoring of during Phase 1, healthy state recruitment manoeuvre. The recruitment manoeuvre is separated by increasing PEEP and decreasing PEEP changes. (Top) Subject 5, (Middle) Subject 6 and (Bottom) Subject 9.

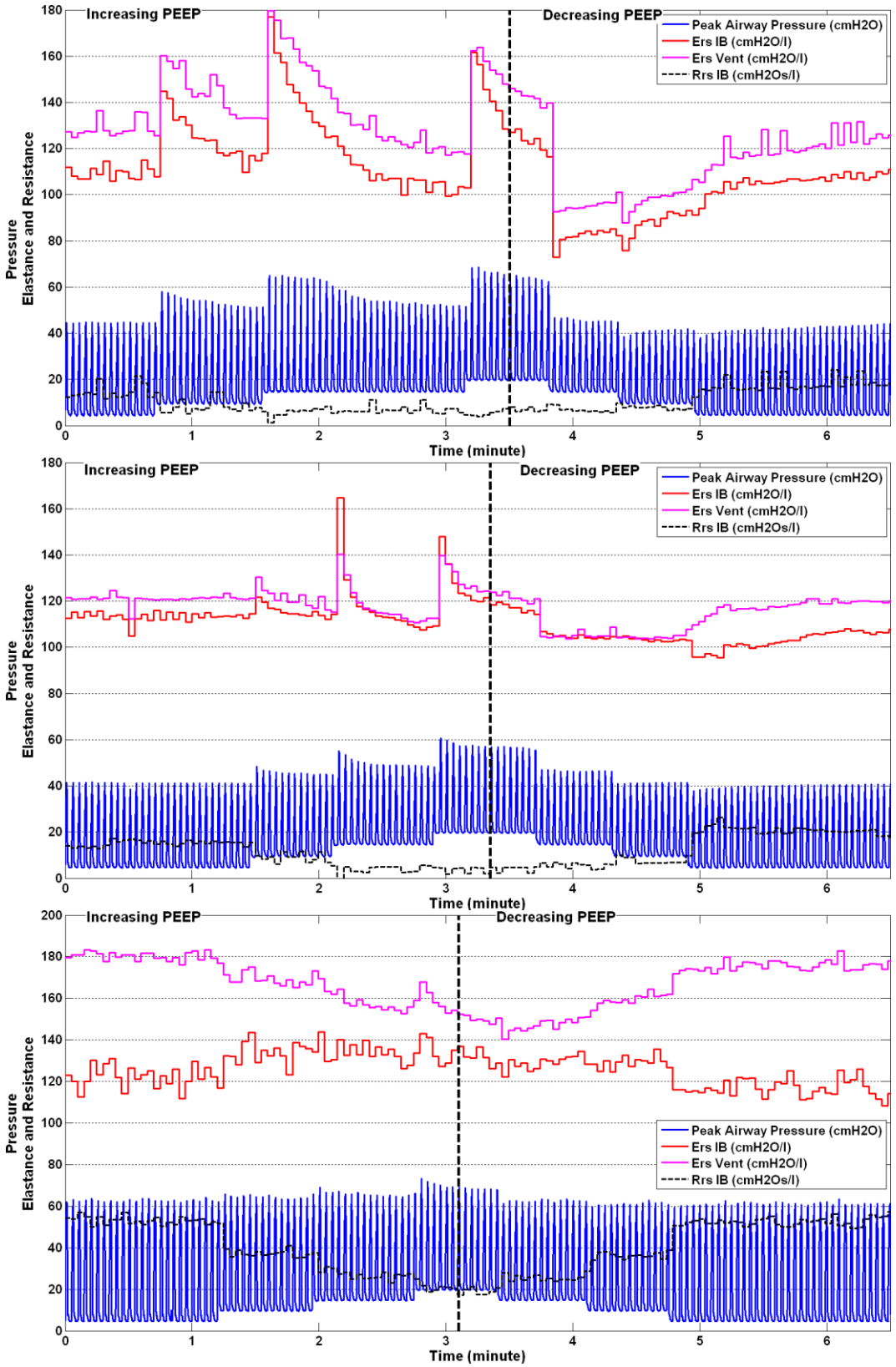

Figure 4.4: Respiratory system mechanics monitoring of during Phase 3, ARDS recruitment manoeuvre. The recruitment manoeuvre is separated by increasing PEEP and decreasing PEEP changes. (Top) Subject 5, (Middle) Subject 6 and (Bottom) Subject 9.

Recruitment is a function of PEEP and time (Barbas et al., 2005, Albert et al., 2009), and, equally, the ARDS affected lung is prone to collapse due to the instability of ARDS affected lung units (Pelosi et al., 2001, Halter et al., 2003). That said, respiratory elastance during increasing PEEP titrations is expected to reduce as time progress to achieve stability and in contrast, elastance will increase with time during decreased PEEP to achieve stability, assuming that the severity of ARDS does not change during the process. However, this study found that minimum elastance occurs at a similar PEEP in both increasing and decreasing PEEP titration. Thus, the authors hypothesise that PEEP can be titrated to a minimum elastance either way, provided a stabilisation period is given at each PEEP level to obtain the true minimal elastance. Hence, these results provide first insight into how the model can be used to capture relevant dynamics and subsequently guide decision making.

Identified airway resistance decreases were seen consistently in Subjects 5 and 6 with varying PEEP (Mols et al., 2001). However, in Subject 9 the airway resistance was lowest at higher PEEP, suggesting that increasing PEEP was opening up the respiratory system airways in this subject resulting in airway resistance drop. This finding coincides with several studies reporting lower airway resistance at high PEEP (Suarez-Sipmann et al., 2007, Mols et al., 2001, Carvalho et al., 2007). The results highlight both the patient/ subject-specificity of the model, as well as the significant inter-subject variability that defines MV patient in general. The change of airway resistance in Subject 9, Phase 3 indirectly affects the estimated model-based estimated elastance, resulting in different trend than ventilator calculated elastance.

4.4.4 Disease Progression - Phase 2

The comparison for the model-based estimated respiratory mechanics and conventional method is presented in Figure 4.5. It was found that Subjects 6 and 9 were diagnosed with ARDS after 60 ~70 minutes, whereas Subject 5 took more than 2 hours to develop ARDS. The difference in ARDS progression over time indicates the inter-subject variability response to oleic acid, as well as variability to MV (Schuster, 1994, Ware, 2008, Bastarache and Blackwell, 2009, Ballard-Croft et al., 2012). Disease progression was captured in this study by tracking the parameter of the single compartment model.

After oleic acid injection, it was found that the respiratory elastance gradually increases in 2 basic steps in Figure 4.5 as ARDS develops. After being diagnosed with ARDS (with PF ratio < 200), the respiratory elastance is as high as two times (2X) the initial elastance. These two steps shows a slow and then rapid change. Hence, the ability to capture this subject-specific progression at this resolution indicates the ability of the model to track progression with high resolution and thus to potentially intervene in the process.

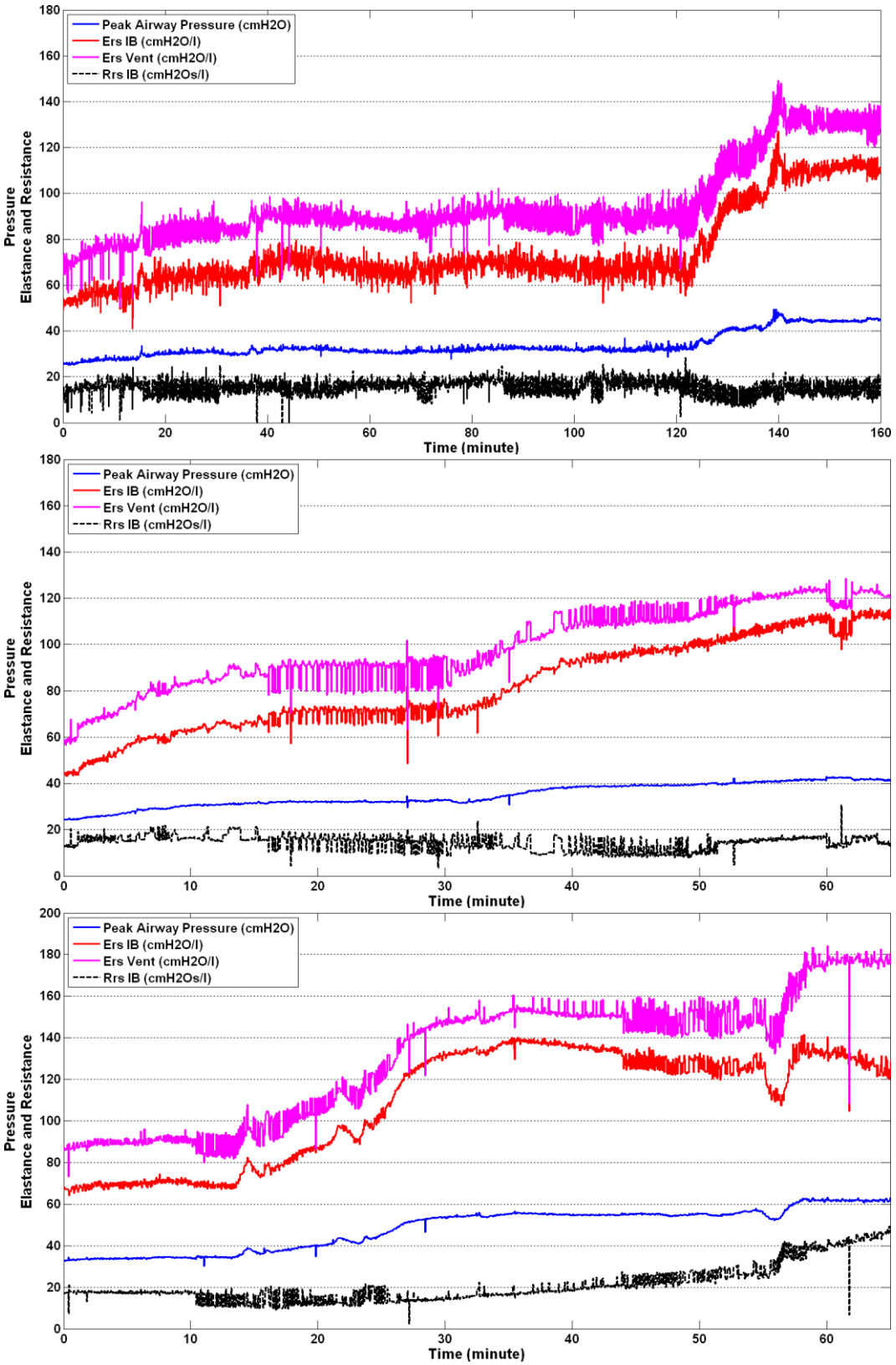

Figure 4.5: Respiratory system mechanics monitoring of during Phase 2, ARDS progression. (Top) Subject 5, (Middle) Subject 6 and (Bottom) Subject 9.

The single compartment lung model has demonstrated its robustness in monitoring subject's respiratory mechanics continuously with fitting error less than 10%. The model is less descriptive compared to highly complex models (Tawhai et al., 2004, Tawhai et al., 2009, Bates, 2009b, Schranz et al., 2010), unable to determine the intra-lung ventilation inhomogeneity, alveolar opening pressure (Sundaresan et al., 2009) or the viscoelastic properties of the lung (Schranz et al., 2011). However, comparing the trends of model-based elastance and examining identified airway resistances, it was able to provide sufficient and, importantly, clinically relevant physiological insight not readily available at the bedside to guide MV therapy in ICU. The model-based method was also able to better define the observed dynamics than the conventional method (E_{rsVent}), particularly in capturing the nonlinear effect of the respiratory mechanics. All these results show its potential to augment and aid clinical decision making.

4.4.5 Validation of Model-Based Methods using Automated End of Inspiratory Pause

The Engström CareStation ventilator (Datex, General Electric Healthcare, Finland) automates short end inspiratory pause (EIP) in MV patients (Ingelstedt et al., 1972, Fuleihan et al., 1976, Pillet et al., 1993). This finite pause at the end of inspiratory enables a zero-flow phase that prolongs inspiration, retaining the inspired tidal volume in the lung for a longer period. The prolonged inspiration time allows the inspired tidal volume to distribute evenly in the lung and have resulted in improved alveolar ventilation (Fuleihan et al., 1976, Lindahl, 1979, Baehrendtz, 1985, Pillet et al., 1993, Devaquet et al., 2008).

Table 4.5 and 4.6 show E_{Static} and R_{Static} derived directly from the ventilator using automated EIP. It was found that both elastance and resistance are different between model-based methods and measured ventilators values. The overall E_{Static} is higher than E_{rsIB} whereas the ventilator R_{Static} is lower than R_{rsIB}. However, E_{rsIB} has similar trend to E_{Static}, and R_{rsIB} showed similar trend to R_{Static}. An example of the trend comparison between E_{Static} and E_{rsIB}, R_{Static} and R_{rsIB} for Subject 6 Phase 1 is shown in Figure 4.6. The trend comparison in E_{Static} and E_{rsIB}, R_{Static} and R_{rsIB} for all other cases are included in Appendix 01 for further reference.

Table 4.5: E_{Static} for all 3 subjects in Phase 1 and Phase 3 (ARDS) using automated EIP in modern ventilators

Subject	E_{Static} (cmH_2O/l), Median [IQR]			
	PEEP 5	**PEEP 10**	**PEEP 15**	**PEEP 20**
5	59.50 [57.90-59.84]	65.25 [61.77-66.55]	77.39 [73.43-82.69]	122.27 [118.59-123.28]
6	58.57 [57.99-59.28]	63.12 [61.37-63.69]	72.28 [70.92-75.44]	117.21 [116.86-118.19]
9	70.33 [48.86-70.96]	74.94 [72.35-78.25]	74.64 [71.17-78.68]	91.42 [87.99-93.00]
	E_{Static}(cmH_2O/l), Median [IQR]			
	PEEP 5	**PEEP 10**	**PEEP 15**	**PEEP 20**
ARDS5	111.64 [110.75-113.35]	128.10 [120.12-138.25]	111.13 [105.72-122.94]	132.86 [128.38-140.28]
ARDS6	108.37 [107.70-109.27]	110.35 [107.20-113.16]	105.56 [103.80-108.28]	117.19 [114.99-119.86]
ARDS9	157.08 [155.43-158.40]	147.37 [147.12-148.91]	138.62 [136.58-142.21]	138.49 [134.65-141.48]

Table 4.6: R_{Static} for all 3 subjects in Phase 1 and Phase 3 (ARDS) using modern ventilators

	R_{Static} (cmH_2Os/l) Median [IQR]			
	PEEP 5	**PEEP 10**	**PEEP 15**	**PEEP 20**
5	11.38 [10.16-12.43]	9.51 [9.35-9.81]	9.22 [8.17-10.20]	6.42 [5.90-7.24]
6	11.19 [11.10-11.67]	9.32 [9.04-9.59]	8.61 [8.46-9.32]	6.34 [5.83-6.83]
9	20.12 [19.27-42.49]	13.19 [12.30-13.66]	10.84 [10.47-11.05]	9.53 [8.98-10.05]
	R_{Static}(cmH_2Os/l) Median [IQR]			
	PEEP 5	**PEEP 10**	**PEEP 15**	**PEEP 20**
ARDS5	11.42 [10.80-11.77]	10.31 [9.61-10.63]	10.23 [9.56-13.69]	9.57 [8.82-10.23]
ARDS6	9.35 [9.08-9.59]	7.91 [7.68-8.44]	6.67 [6.29-7.07]	4.91 [4.40-5.15]
ARDS9	16.02 [15.47-17.52]	14.79 [14.05-15.81]	12.64 [12.41-13.72]	10.55 [10.32-11.31]

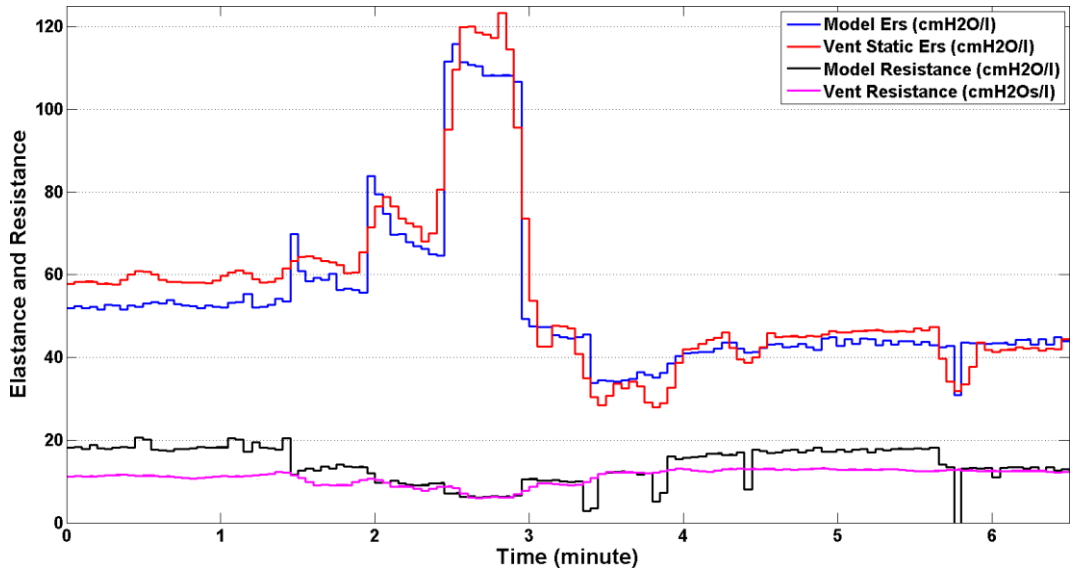

Figure 4.6: Comparison between ventilator measured E_{Static} and R_{Static} with model-based E_{rsIB} and R_{rsIB} for Subject 6, Phase 1. The elastance and resistance between two methods are different but have showed similar trend.

While the automated EIP feature in ventilator provides a simpler way to measure 'static' elastance and resistance, this mode of ventilation is not normally available in other ventilators. In addition, this method may be erroness in some cases because the automated end inspiratory pause is too short and does not allow peak pressure to drop to the true plateau pressure (Barberis et al., 2003). Figure 4.7 shows an example of further drop in plateau pressure to a true plateau pressure if a longer EIP is performed on an experimental subject (Barberis et al., 2003). The true plateau pressure will decrease E_{Static} and increase R_{Static} resulting in more similar values to model-based E_{rsIB} and R_{rsIB}. Nevertheless, the automated *EIP* method is comparatively less invasive which allows a surrogate of airway resistance and static elastance to be estimated. In summary, the model-based method was able to capture respiratory mechanics similar to the modern ventilators, thus further validates the model-based findings.

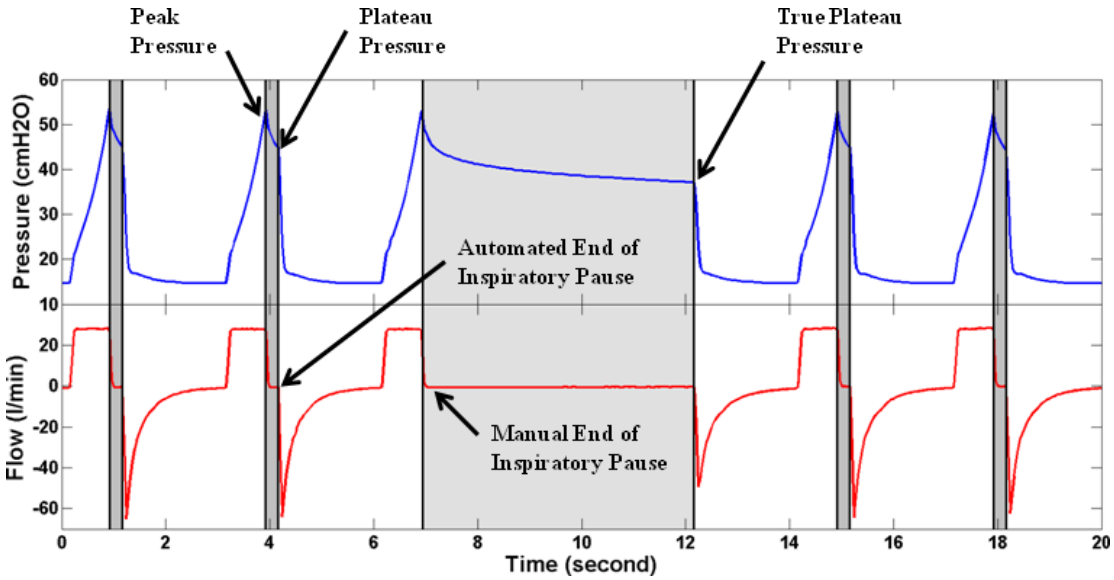

Figure 4.7: Pressure and flow profile with automated short end inspiratory pause (Area shaded grey). During end of inspiration pause, the airway pressure decreases from peak pressure to plateau pressure. This pressure difference is due to the airway resistance. A longer end of inspiratory pause enables true plateau pressure to be found.

4.5 Study Limitations

4.5.1 Variable ARDS

In this study, it was found that 2 of 3 subjects showed similar respiratory mechanics trends. Subject 9 in particular, given a similar preparation method and similar protocol, resulted in different observed respiratory mechanics. The overall peak airway pressure of Subject 9 during ARDS state at baseline PEEP is much higher than in Subjects 5 and 6. The PEEP titration carried out in this work also does not show significant change in overall respiratory mechanics compared to Subject 5 and 6. Thus, we are unable to conclude the findings with statistical significance. However, the findings showed subject's variable response to protocol and MV settings, and further encourages patient-specific MV treatment in ICU to optimise outcome.

4.5.2 Respiratory Mechanics Monitoring for Sedated Patients

The application of single compartment lung model is limited to patients who are fully sedated and dependant on mechanical ventilation (Brochard et al., 2012). When a patients' breathing effort is taken over by the ventilator, the mechanics of the patients breathing is similar to mechanics of the ventilator support, allowing the respiratory mechanics to be determined. However, this is not the case for spontaneously breathing patients. Spontaneous breathing patients have individual breathing efforts aside from ventilator support (Grinnan and Truwit, 2005), altering the respiratory mechanics. Hence additional equipment (e.g. oesophageal balloon catheters) may be required to best measure patient-specific mechanics and this overall approach thus requires further study to be extended to this cohort (Mead and Whittenberger, 1953, Benditt, 2005, Talmor et al., 2006, Khirani et al., 2010). However, the methods presented are still viable for a large portion of the most ill and costly MV patients.

4.6 Summary

Respiratory system mechanics vary due to inter-subject variability in disease state development and in response to MV settings. A single compartment lung model with integral-based parameter identification was effective in capturing fundamental respiratory mechanics in all patients' conditions (Healthy, Progression and ARDS). The trends match clinical expectation and provide better resolution commonly, clinically derived linear metrics, demonstrating the method's robustness and potential to guide MV therapy. Overall, the results show the importance and potential of including continuous monitoring of respiratory mechanics in clinical practice to optimise mechanical ventilation.

ARDS animal models are more consistent where the methods of developing ARDS are known and controlled. ICU patients, on the other hand, are comparatively more variable as the causes of disease are different and patients may be more inter-patient variable to treatment. Thus, the use of respiratory mechanics monitoring in actual patients needs to be tested in humans. In the next chapter, the investigation of the performance model-based method is further extended in clinical settings. It is a proof of concept study for the model's applicability in actual ICU setting. A different clinical protocol which is used to examine patient's respiratory mechanics is also developed to account for patient safety, feasibility and practicability.

Chapter 5

Proof of Concept Study using Respiratory Mechanics Monitoring

5.1 Implementation of Model-based Methods

The fundamental of MV for ARDS patients remains in selecting an optimal positive end-expiratory pressure (PEEP) to maximise patient-specific lung recruitment, prevent alveoli collapse and avoid ventilator induced lung injury (VILI) (Slutsky, 1999, Esteban et al., 2002, Gajic et al., 2004, Gullo et al., 2006, Desai and Deep, 2006, Girard and Bernard, 2007, Gattinoni et al., 2010). Several attempts have been made to standardize MV, and in particular, PEEP selection (Levy, 2002, Meade et al., 2008, Mercat et al., 2008, Briel M and et al., 2010). However, due to inter-patient variability and intra-patient heterogeneity of ARDS, most have failed to deliver conclusive results on PEEP selection as discussed earlier in Chapter 2 (Ware and Matthay, 2000, Stenqvist, 2003, Suh et al., 2003, Esteban et al., 2005, Sundaresan and Chase, 2011). Thus, without a gold standard method for setting PEEP, clinicians rely on intuition and experience, leading to more variable care and outcomes.

Model-based and patient-specific approaches offer the ability to identify intra- and inter-patient variability in real-time (breath-to-breath) and thus, potentially to guide MV therapy based on patient-specific conditions and needs (Sundaresan and Chase,

2011, Chase et al., 2011). This approach provides the opportunity to balance risk of lung injury and lung function support, and to reduce the work of breathing during MV (MacIntyre, 2008). However, to date, only a few such methods have been tested (Quaglini et al., 2001, Carvalho et al., 2007, Badet et al., 2009, Sundaresan et al., 2011a, Kostic et al., 2011, Zannin et al., 2012) and their potential in critical care is not yet validated.

This chapter further extends the studies of model-based approaches to identify patient-specific disease state and patient-specific response to MV therapy using patient-specific constant lung elastance (E_{rs} = 1/ Compliance) as presented in Chapter 4 (Suarez-Sipmann et al., 2007, Carvalho et al., 2007, Lambermont et al., 2008). In addition, the Equation 4.5 is further modified to calculate dynamic (sample-to-sample) lung elastance (E_{drs}) in ARDS within a breathing cycle. The dynamic lung elastance (E_{drs}) is a time-variant lung elastance at each breath during MV. A metric that compares E_{rs} and E_{drs} during PEEP change are thus proposed for guiding PEEP selection. By monitoring both the identified parameters (Elastance = 1/ Compliance) through limited PEEP titration, it is possible to identify PEEP settings that safely maximize recruitment, minimize elastance, and thus minimize the work of breathing without inducing lung injury.

5.2 Study Design in Christchurch Hospital

5.2.1 Patients

Patients in the Intensive Care Unit (ICU), Christchurch Hospital, New Zealand, diagnosed with ARDS (Acute onset, findings of bilateral infiltrates on chest

radiograph, absence of left side heart failure and PaO_2/FiO_2 (PF ratio) between 150-300 *mmHg*), are eligible for the study. The exclusion criteria for the study are: 1) Patients who were likely to be discontinued from MV in 24 hours; 2) Age < 16 years old; 3) Moribund and/ or not expected to survive for greater than 72 hours; and 4) Patient who are minimally sedated. 10 patients who were eligible for study underwent a modified recruitment manoeuvre (RM).

Prior to the study, written informed consent was obtained from the patient, immediate family members or relatives. These trials and the use of the data were approved by the New Zealand, South Island Regional Ethics Committee (U1111-1125-7363). The trial is registered with Australian New Zealand Clinical Trials Registry (ACTRN 12611001179921).

5.2.2 Mechanical Ventilation and Data Acquisition

All patients recruited for the study were intubated and ventilated using Puritan Bennett, PB840 ventilator (Covidien, Boulder, CO, USA). They are ventilated with volume control (tidal volume, Vt = 6~8 *ml/kg*), synchronized intermittent mandatory ventilation (SIMV) mode, throughout the trial. Patients were sedated and paralyzed with muscle relaxants to prevent spontaneous breathing efforts. Arterial blood gas (PaO_2) was recorded at each clinically selected PEEP. This PEEP was selected by the attending doctor as they see fit. One arterial blood gas was taken before the RM and a second arterial blood gas sample is taken 30 minutes after the RM for comparison.

A pneumotachometer with Hamilton Medical flow sensor (Hamilton Medical, Switzerland) connected to the ventilator circuit Y-piece is used to record patient's airway pressure and flow data. A Dell^{TM} (Dell, Austin, TX, USA) laptop was used in conjunction with National Instruments USB6009 and Labview Signal Express (National Instruments, Austin, TX, USA) to obtain measurements at a sampling rate of 100Hz. Analysis was performed using MATLAB (The Mathworks, Natick, Massachusetts, USA).

5.2.3 Clinical Protocol - Modified Recruitment Manoeuvre (RM)

At the start of the RM, the clinically selected PEEP is decreased to zero PEEP for 5 breathing cycles. The clinically selected PEEP is determined by the attending clinicians as they see fit. At the end of the 5th breath, an end expiratory hold is performed to obtain the alveolar intrinsic PEEP (Auto-PEEP) (Rossi et al., 1995). An end inspiratory pause is also performed to obtain plateau pressure for resistance calculations (Barberis et al., 2003). PEEP is then increased with increments of 5 cmH_2O from PEEP = 0 cmH_2O (ZEEP) until peak airway pressure (PIP) reaches a limit of 45 cmH_2O (Gattinoni et al., 2006a). Every subsequent PEEP level was maintained for 5 breathing cycle before increasing to a higher PEEP. PIP of 45 cmH_2O is set as a threshold safety to avoid any possible overdistension. After reaching PIP 45 cmH_2O, PEEP is reduced by steps of 5 cmH_2O to the clinically selected PEEP. Throughout the trial, other ventilator settings were not changed.

Through continuous monitoring of airway pressure and flow data, the volume of air entering the lung can be calculated by integrating flow with time. Thus, the patient-

specific lung volume increase corresponding to PEEP increase can be calculated. The minimum lung volume at the beginning of a breathing cycle at different PEEP level with reference to atmospheric pressure is denoted as dynamic functional residual capacity (dFRC) (Desaive et al., 2009, Sundaresan et al., 2011b).

5.2.4 Single Compartment Model

The model-based approach presented in Chapter 4 in Equations 4.4-4.5 is used to estimate patient-specific respiratory elastance and resistance. These two equations are renumbered as Equation 5.1 and 5.2. Patient-specific respiratory elastance denoted E_{rs} reflects the lung stiffness (1/Compliance). Therefore, a lower E_{rs} indicates a more compliant lung. Airway resistance is denoted as R_{rs}.

$$P_{aw}(t) = R_{rs} \times Q(t) + E_{rs} \times V(t) \quad (5.1)$$

$$P_{aw}(t) = R_{rs} \times Q(t) + E_{rs} \times V(t) + P0 \quad (5.2)$$

Next, E_{rs} in Equation 5.2 can be replaced with time-variant dynamic respiratory elastance, $E_{drs}(t)$. Thus, Equation 5.2 can be modified into:

$$P_{aw}(t) = R_{rs} \times Q(t) + E_{drs}(t) \times V(t) + P0 \quad (5.3)$$

Compared to a single, constant E_{rs} value at each PEEP, identifying time-variant E_{drs} allows this change to be seen dynamically within each breath as pressure increases. This approach enables a more detailed view of patient-specific lung physiological condition and response to MV. To ensure that the identified parameters of constant E_{rs}

and time-variant E_{drs} are valid, the absolute percentage error (APE) between the identified model and measured clinical pressure data is reported.

5.2.5 PEEP Selection Metric

During each breathing cycle, as PEEP rises, lung elastance (E_{rs}) falls as new lung volume is recruited faster than the pressure build-ups in the lung. If little or no recruitment occurs, E_{rs} rises with PEEP, indicating that pressure above that PEEP level was unable to recruit significant new lung volume and is, instead, beginning to stretch already recruited lung units (Vieira et al., 1998). Hence, recruitment and potential lung injury can be balanced by selecting PEEP at minimum E_{rs} or E_{drs} (Carvalho et al., 2007). Three model-based approaches based on patient-specific E_{rs} and E_{drs} trajectory in a patient's breath at different PEEP levels are used to optimize PEEP selection.

a) Minimum E_{drs} and E_{rs} - Locates the point where minimum time-varying E_{drs} or constant E_{rs} occurs over all PEEP values (and pressure for E_{drs}) during the recruitment manoeuvre.

b) Minimum E_{drs} Area - E_{drs} Area is obtained by integrating time-varying E_{drs} over time during the patient's breathing cycle at each PEEP. E_{drs} Area is more clinically relevant than median or mean E_{drs} throughout each breath and can be shown to be proportional to patient-specific work of breathing.

c) Inflection Method - This method detects the inflection in the E_{drs} Area-PEEP and E_{rs}-PEEP curves. Inflection is defined here at the PEEP value with E_{drs} value 5-10%

above (before) minimum E_{drs} Area or E_{rs} (105~110% of minimum E_{drs} Area or E_{rs}). PEEP is selected where inflection occurs, as a point of diminishing returns.

The overall approach implies that as long as E_{rs} or E_{drs} falls during each breath, as PEEP level increases, that recruitment of new volume outweighs lung stretching as flow and volume follow a path of lesser or least resistance. These methods are thus attempts to maximize recruitment (Minimum E_{drs} and Minimum E_{drs} Area) and also ensure safety from excessive pressure (Inflection Method). These metrics are three of many possibilities which can be defined here to demonstrate the concept in a clinically relevant fashion. The PEEP selected is compared to the clinically selected PEEP value to assess the opportunity for improvement in this non-intervention trial.

5.2.6 E_{drs} Area and Work of Breathing

These approaches were also compared with selecting PEEP using the identified minimum or inflection of constant E_{rs}, for comparison to other similar work (Carvalho et al., 2007). Patient-specific E_{rs} and E_{drs} are only analyzed during inspiration and not during the expiratory cycle. This choice was made because increases in pressure induce both recruitment and lung damage as it passes a limit, and thus expiration (decreasing pressure) should not be used to guide PEEP selection in respect.

A higher resolution of the trend changes in E_{drs} can be observed using E_{drs} Area. E_{drs} Area is obtained through integration of E_{drs} with time. It is also known that the work of breathing (*WOB*) (Otis et al., 1950, Marini et al., 1985) for a patient is proportional

to lung elastance. In general, more work is required to fill a given lung volume with higher elastance. *WOB* is defined:

$$WOB = P_{aw} \times V \tag{5.4}$$

Substituting P_{aw} from Equation (5.3) into Equation (5.4) and using $P0 = 0$, (atmospheric). The work of breathing can be defined as:

$$WOB = (E_{rs}V + R_{rs}Q) \times V = E_{rs}V^2 + R_{rs}Q\,V \tag{5.5}$$

From Equation (5.5), work of breathing can be divided into work to overcome lung elastance ($WOB_E = E_{rs}V^2$) (Grinnan and Truwit, 2005, Kallet et al., 2007) and work to overcome airway resistance ($WOB_R = R_{rs}QV$). Substitution of dynamic lung elastance, E_{drs}, for constant E_{rs} enables a derivation for WOB_E:

$$E_{drs} = WOB_E(t) / V(t)^2 \tag{5.6}$$

E_{drs} Area in Equation 5.7 is the integral of Equation 5.6, yielding the relation of E_{drs} to *WOB* required to overcome lung elastance at a given level of PEEP and mode of MV.

$$E_{drs}\,Area = \int E_{drs}(t)\,dt \tag{5.7}$$

Equation 5.7 clearly relates WOB_E and E_{drs}, thus showing the relation of E_{drs} to a clinically relevant metric that is commonly used.

5.2.7 Analysis and Comparisons

E_{rs} and median E_{drs} are compared using Pearson's linear correlation coefficients to relate these metrics. E_{rs} and E_{drs} Area ($\int E_{drs}$) are also compared to median E_{drs} and WOB_E to ensure there was no loss of information for each patient at different PEEP values, and to show the validity of Equation 5.6 and using E_{drs} Area. Finally, clinically selected PEEP is compared to the value determined by proposed model-based metrics.

5.3 Results and Discussion

5.3.1 PaO_2 Before and After RM

The patient demography with their clinical diagnosis, including PaO_2 before and after the RM are shown in Table 5.1. It was found that PaO_2 for 7 out of 10 patient decreased from 84.0 *mmHg* [IQR: 73.0-114.0] to 77.5 *mmHg* [IQR: 68.0-86.0], 30 minutes after recruitment manoeuvre ($p > 0.005$). While not statistically significant, this result contradicts other reports (Tusman et al., 1999, Gattinoni et al., 2006a, Hodgson et al., 2011a) that showed significant increase in PaO_2 after RM. It is hypothesised that 30 minutes after the RM were insufficient for perfusion to occur fully. Similarly, this result can be an indication of the level of lung injury, in which some patients are not responsive to RM (Gattinoni et al., 2006a, Caironi et al., 2010). This issue should be considered in future clinical trials when monitoring arterial blood gas information. In particular, arterial blood gas should be monitored over a longer period with additional time steps (15, 30, 45, 60, 90, 120 minutes after a RM (Tusman et al., 1999)), to verify and confirm the hypothesis.

Table 5.1: Patient demography

Patient	*Sex*	*Age (year)*	*Clinical Diagnostic*	*PF Ratio (mmHg)*	*FiO_2*	*PaO_2 Before RM (mmHg)*	*PaO_2, 30 minutes After RM*
1	F	61	Peritonitis, COPD*	209	0.35	73	60
2	M	22	Trauma	170	0.50	85	73
3	M	55	Aspiration	223	0.35	78	76
4	M	88	Pneumonia, COPD*	165	0.40	66	56
5	M	59	Pneumonia, COPD*	285	0.40	114	79
6	M	69	Trauma (Abdominal Sepsis)	280	0.35	98	118
7	M	56	Legionnaires	265	0.55	146	68
8	F	54	Aspiration	303	0.40	121	106
9	M	37	H1N1, COPD*	183	0.40	73	86
10	M	56	Legionnaires, COPD*	237	0.35	83	83
Median [IQR]						84.0 [73.0-114.0]	77.5 [68.0-86.0]

*COPD - Chronic obstructive pulmonary disease; *PF* Ratio - Partial pressure of oxygen in arterial blood/ fraction of inspired oxygen; *FiO_2* - Fraction of inspired oxygen; *PaO_2* - Partial pressure of oxygen in arterial blood; RM - Recruitment manoeuvre, H1N1 - Swine flu

5.3.2 Model Fitting

Table 5.2-5.4 shows the median [Inter-quartile Range (IQR)] E_{drs}, E_{rs} and E_{drs} Area for each patient and PEEP, and absolute percentage fitting error (APE). Median absolute percentage fitting error ($APE_{Edrs(t)}$) across all patients and PEEP is 0.9% [IQR: 0.5-2.4]. Median fitting error for time-variant E_{drs} is less than 1%, showing that a single compartment lung model can be used for time-varying E_{drs} estimation. Compared to the estimation of E_{rs} in Table 5.3, median fitting error is 5.6% [IQR: 1.8-11.3] and in specific cases, fitting error can be as high as 15.7-17.7% (Patients 4 and 5). This latter result indicates that a first order model can be used to estimate most patient-specific constant E_{rs}, but, in several cases, the model may not accurately represent patients' physiological dynamic and condition. Time-varying E_{drs} provides a better model fit across all patients and also provides a clearer insight into the patient's physiological condition, and is thus the better model-based metric.

Table 5.2: Patient-specific dynamic lung elastance (E_{drs}) at each PEEP level

Patient	Dynamic Lung Elastance, E_{drs} (cmH_2O/l) Median [IQR] PEEP (cmH_2O)							E_{drs} (cmH_2O/l) Median [IQR]	APE+ (%) Median [IQR]
	0	5	10	15	20	25	30		
1	63.1 [46.9-114.9]	53.8 [43.0-80.2]	43.6 [38.4-54.5]	35.0 [33.3-39.4]	33.4 [32.0-34.2]	31.1 [32.0-32.4]	PEEP 27 32.2 [31.9-32.6]	35.0 [32.5-51.2]	1.1 [0.5-4.1]
2	30.8 [26.3-45.1]	26.4 [23.7-31.4]	23.1 [22.0-24.3]	22.1 [22.0-22.6]	22.5 [22.4-22.6]	PEEP 22 23.1 [22.9-23.2]		23.1 [22.5-26.4]	0.7 [0.6-2.4]
3	26.9 [22.6-36.9]	22.1 [20.2-25.6]	18.3 [18.0-19.0]	17.3 [17.2-17.4]	17.5 [17.1-17.5]	17.8 [17.4-18.7]	PEEP 28 19.2 [17.9-19.7]	18.3 [17.6-21.4]	0.6 [0.5-1.3]
4	73.2 [50.4-144.4]	70.4 [49.9-126.9]	54.5 [41.7-82.3]	36.8 [30.6-43.9]	28.5 [25.6-31.4]	25.9 [21.6-28.4]	23.1 [19.4-25.5]	36.8 [26.6-66.4]	3.4 [0.9-5.4]
5	105.7 [80.6-199.8]	97.8 [77.5-166.8]	89.3 [74.3-143.4]	79.4 [68.6-107.3]	67.3 [61.4-79.4]	52.3 [52.0-55.8]		84.4 [67.3-97.8]	3.2 [0.9-6.0]
6	30.4 [25.9-39.1]	26.2 [25.5-27.2]	23.3 [22.4-23.5]	21.6 [21.5-21.8]	21.8 [21.3-22.5]	23.3 [22.6-23.9]		23.3 [21.8-26.2]	0.8 [0.6-1.2]
7	49.3 [46.1-62.4]	42.2 [41.5-43.1]	44.3 [41.8-47.7]	53.6 [48.8-59.7]	PEEP 16 52.4 [50.3-57.6]			49.3 [43.8-52.7]	1.6 [1.3-2.0]
8	45.7 [37.9-67.8]	37.2 [32.9-43.0]	31.8 [29.9-33.5]	28.8 [28.0-29.8]	27.4 [27.1-27.9]	26.8 [26.3-27.0]	27.0 [26.8-27.5]	28.8 [27.1-35.9]	0.8 [0.5-2.2]
9	58.1 [47.1-100.8]	40.5 [36.4-52.8]	39.9 [35.8-48.7]	31.2 [30.2-33.6]	28.3 [27.9-29.0]	26.3 [26.3-26.5]	26.2 [25.8-26.5]	31.2 [26.8-40.4]	0.8 [0.4-2.1]
10	54.4 [48.1-76.2]	45.2 [41.9-51.8]	39.4 [38.4-41.7]	35.9 [35.7-36.0]	33.9 [33.7-34.1]	33.9 [33.4-34.6]	PEEP 27 33.9 [33.2-34.8]	35.9 [33.9-43.8]	0.4 [0.4-0.9]
Median [IQR]	51.9 [30.8-63.1]	41.4 [26.4-53.8]	39.7 [23.3-44.3]	33.1 [22.1-36.8]	28.4* [22.5-33.9]	26.3* [23.1-32.2]	26.6* [23.1-32.2]	32.2 [26.1-46.6]	0.9 [0.5-2.4]

+APE - Absolute percentage fitting error, *Values presented include value from different PEEP. Eg. PEEP 16 is included in PEEP 20 Median [IQR]

Table 5.3: Patient-specific constant lung elastance (E_{rs}) at different PEEP

Patient	Constant Lung Elastance, E_{rs} (cmH_2O/l)							E_{rs} (cmH_2O/l) Median [IQR]	APE (%) Median [IQR]
	PEEP (cmH_2O)								
	0	5	10	15	20	25	30		
1	53.8	47.0	41.2	32.8	32.8	32.1	PEEP 27 32.2	34.7 [32.4-45.5]	7.2 [1.7-19.0]
2	27.7	25.3	22.8	22.3	22.6	PEEP 22 23.1		23.0 [22.6-25.3]	2.5 [1.1-7.7]
3	24.0	21.6	18.3	17.3	17.4	18.1	PEEP 28 19.1	18.3 [17.6-20.9]	4.2 [1.6-6.6]
4	60.2	59.7	50.1	35.1	27.8	25.3	22.5	35.1 [25.9-57.3]	17.7 [15.4-32.1]
5	87.4	84.0	81.2	74.3	65.7	53.1		77.8 [65.7-84.0]	15.7 [9.2-19.8]
6	27.1	25.5	22.8	21.6	21.8	23.4		23.1 [21.8-25.5]	2.7 [2.2-4.2]
7	47.7	42.5	45.5	55.7	PEEP 16 55.3			47.7 [44.8-55.4]	6.2 [5.0-7.7]
8	41.7	35.5	31.2	28.7	27.5	26.6	27.0	28.7 [27.2-34.4]	2.9 [1.3-8.7]
9	51.3	39.1	38.2	31.1	28.2	26.2	26.1	29.7 [26.2-38.7]	3.1 [1.0-10.8]
10	51.0	44.1	39.2	35.8	33.9	34.0	PEEP 27 34.2	35.8 [34.1-42.9]	2.0 [1.0-5.6]
Median [IQR]	49.4 [27.7-53.8]	40.8 [25.5-47.0]	38.7 [22.8-45.5]	31.9 [22.3-35.5]	28.0* [22.6-33.9]	26.2* [23.3-32.6]	26.6* [22.5-32.2]	32.2 [25.0-45.9]	5.6 [1.8-11.3]

*Values presented include value from different PEEP. Eg. PEEP 16 is included in PEEP 20 Median [IQR]

Table 5.4: Patient-specific E_{drs} Area at different PEEP

Patient	E_{drs} Area (cmH_2Os/l) PEEP (cmH_2O)							E_{drs} Area (cmH_2Os/l) Median [IQR]
	0	**5**	**10**	**15**	**20**	**25**	**30**	
1	84.6	49.5	37.1	28.9	26.6	25.7	PEEP 27 25.7	28.9 [25.9-46.4]
2	34.0	24.8	21.0	20.2	20.3	PEEP 22 20.7		20.9 [20.3-24.8]
3	37.7	27.6	22.2	20.8	19.1	19.7	PEEP 28 18.9	20.8 [19.3-26.3]
4	102.2	91.2	61.7	37.9	31.7	48.1	47.5	48.1 [40.3-83.8]
5	118.7	99.9	89.1	70.6	75.7	42.9		82.4 [70.6-99.9]
6	29.4	23.8	20.8	21.6	19.5	20.8		21.2 [20.8-23.8]
7	37.6	33.8	31.3	37.9	PEEP 16 32.1			33.8 [31.9-37.7]
8	55.1	38.5	32.0	29.0	27.5	24.1	24.3	29.0 [25.1-36.9]
9	106.5	55.2	51.3	38.3	34.1	31.6	31.3	38.4 [32.2-54.2]
10	74.7	52.6	44.0	39.5	37.3	37.2	PEEP 27 37.3	39.5 [37.3-50.5]
Median [IQR]	64.9 [37.6-102.2]	44.0 [27.6-55.2]	34.6 [22.2-51.3]	33.5 [21.6-38.4]	29.6* [20.3-34.1]	25.7* [20.8-38.6]	28.5* [24.3-37.3]	34.0 [24.7-48.5]

*Values presented include value from different PEEP. Eg. PEEP 16 is included in PEEP 20 Median [IQR]

5.3.3 Model-based Estimated E_{rs} and E_{drs}

The median E_{drs} is 32.2 cmH_2O/l [IQR: 26.1-46.6]. Patients who suffer from COPD (Patients 1, 4, 5, 9 and 10) have significantly higher E_{drs} than others ($p < 0.005$), as expected clinically. Similar to E_{drs} trend the constant E_{rs} at each PEEP is 32.2 cmH_2O/l [IQR: 25.0-45.9] and E_{drs} Area at each PEEP is 34.0 cmH_2Os/l [IQR: 24.7-48.5]. The wide range of patient-specific E_{drs} across all patients and PEEP shown in Table 5.2 reflects the heterogeneity of ARDS patient condition and response to PEEP that makes standardising and PEEP selection difficult (Mercat et al., 2008).

5.3.4 Effect of PEEP towards Patient-Specific E_{rs}, E_{drs} and dFRC

5.3.4.1 Overall

Figure 5.1 shows the changes of E_{rs} comparing to peak inspiratory pressure, dynamic functional residual capacity (dFRC) with PEEP increase. In the beginning of the recruitment manoeuvre, Figure 5.1 (Top), at ZEEP, E_{rs} is relatively very high for all patients. As PEEP rises, it is observed that E_{rs} drops, but at patient-specific rates. This E_{rs} drop with PEEP increase trend coincides with previous PEEP titration studies in animal subjects (Carvalho et al., 2007, Suarez-Sipmann et al., 2007, Lambermont et al., 2008). It is observed that PIP did not increase significantly with PEEP increase. Both E_{rs} and PIP trends suggest recruitment, with increase of lung volume, and thus relatively little peak pressure increase. The dFRC shown in Figure 5.1 (Bottom) increases with PEEP and follows a sigmoidal curve that is similar to the static compliance curve (Venegas et al., 1998). dFRC is the lung volume at PEEP where zero flow occurs, and thus, it is a surrogate for patient-specific static compliance. The dFRC trends in this study suggested overstretching of the lung at high PEEP. This

result is similar to the results presented by Lambermont et al, where the changes in functional residual capacity decreased after a certain PEEP level is reached (Lambermont et al., 2008).

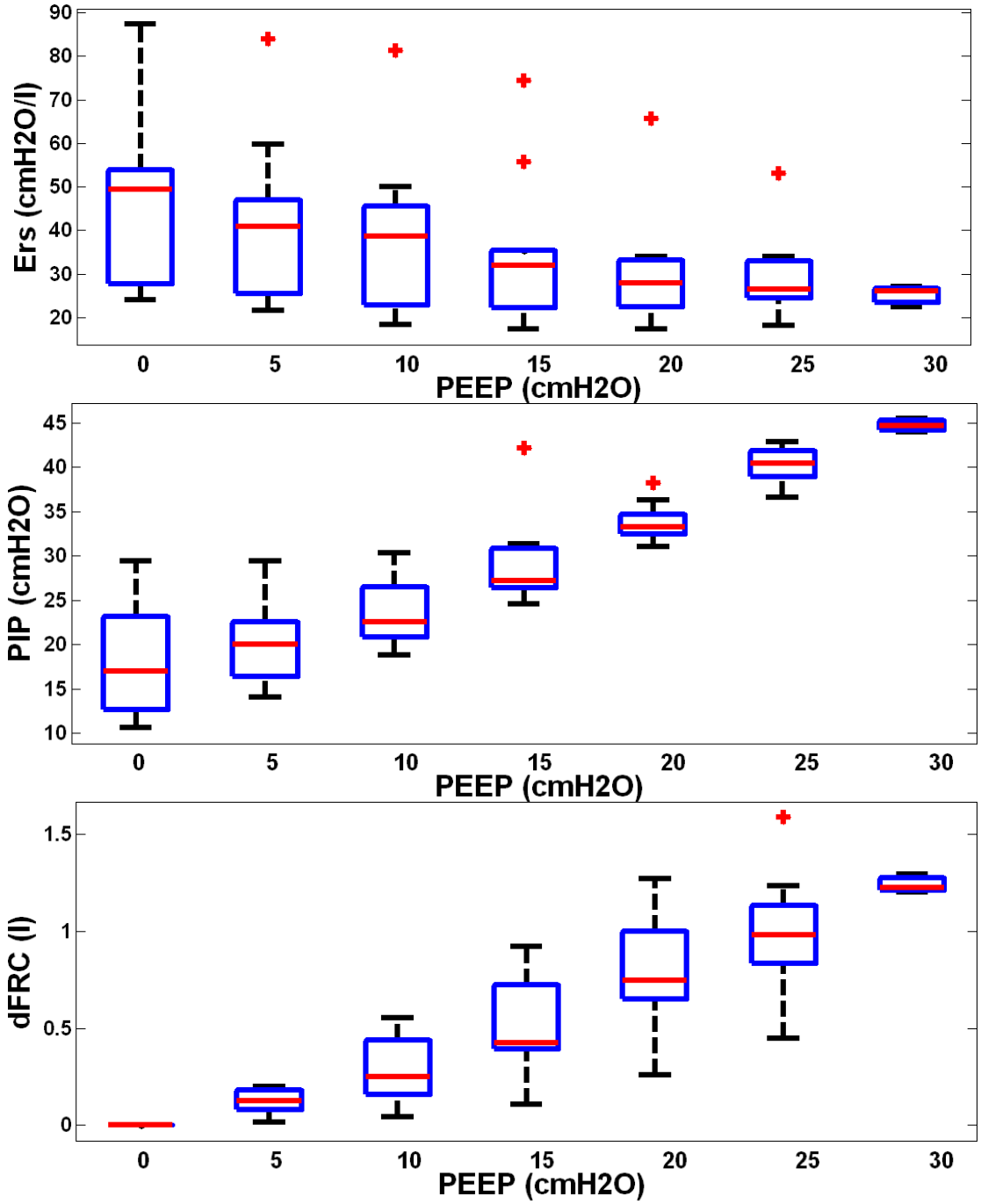

Figure 5.1: E_{rs}-PEEP, PIP-PEEP and dFRC-PEEP plot. (Top) E_{rs} range for the 10 patients with PEEP increase. (Middle) PIP range for the 10 patients with PEEP increase. (Bottom) dFRC range for the 10 patients with PEEP increase.

Table 5.2 shows median [IQR] E_{drs} for every patient and PEEP. The IQR range drops significantly for every patient as PEEP increases. This range is an indication of the lung response to pressure. A small IQR range indicates that the lung is ventilated at a PEEP level where maximal lung recruitment occurs over a narrow pressure range as tidal volume, V_t is fixed in the MV mode used. A high IQR range shows the opposite, indicating a more variable change in overall lung recruitment within a breath.

5.3.4.2 Patient-Specific Finding

Figure 5.2 shows patient-specific time-varying E_{drs} at each PEEP level for Patients 2, 6, 8 and 10. E_{drs} decreases as pressure increases at each PEEP. However, at higher PEEP, this trend can reverse, indicating stretching exceeding recruitment of new lung volume. The optimal PEEP derived by minimum E_{drs} is indicated. Similar to Figure 5.2, Figure 5.3-5.4 shows patient-specific E_{drs} Area and E_{rs} for Patients 2, 6, 8 and 10 with PEEP. The optimal PEEP is derived using minimum E_{drs} Area or minimum E_{rs} and Inflection method with the band of 5-10% above minimum E_{drs} Area or minimum E_{rs} shown by the dashed-lines.

E_{drs}-Pressure-PEEP curves and E_{drs} Area decrease with increasing PEEP, lung pressure, and volume over each breath. In the beginning of the recruitment manoeuvre, at zero end-expiratory pressure (ZEEP), E_{drs} is relatively very high for all patients with median 51.9 cmH_2O/l [IQR: 30.8-63.1]. In particular, chronic obstructive pulmonary disease (COPD) patients or patients with similar clinical features (Hoare and Lim, 2006) (Patients 1, 4, 5, 9 and 10) have initially the highest E_{drs} median, as

expected, from 63.1 cmH_2O/l [IQR: 57.2-81.3] versus 30.8 cmH_2O/l [IQR: 29.5-46.6] for the other patients ($p < 0.005$).

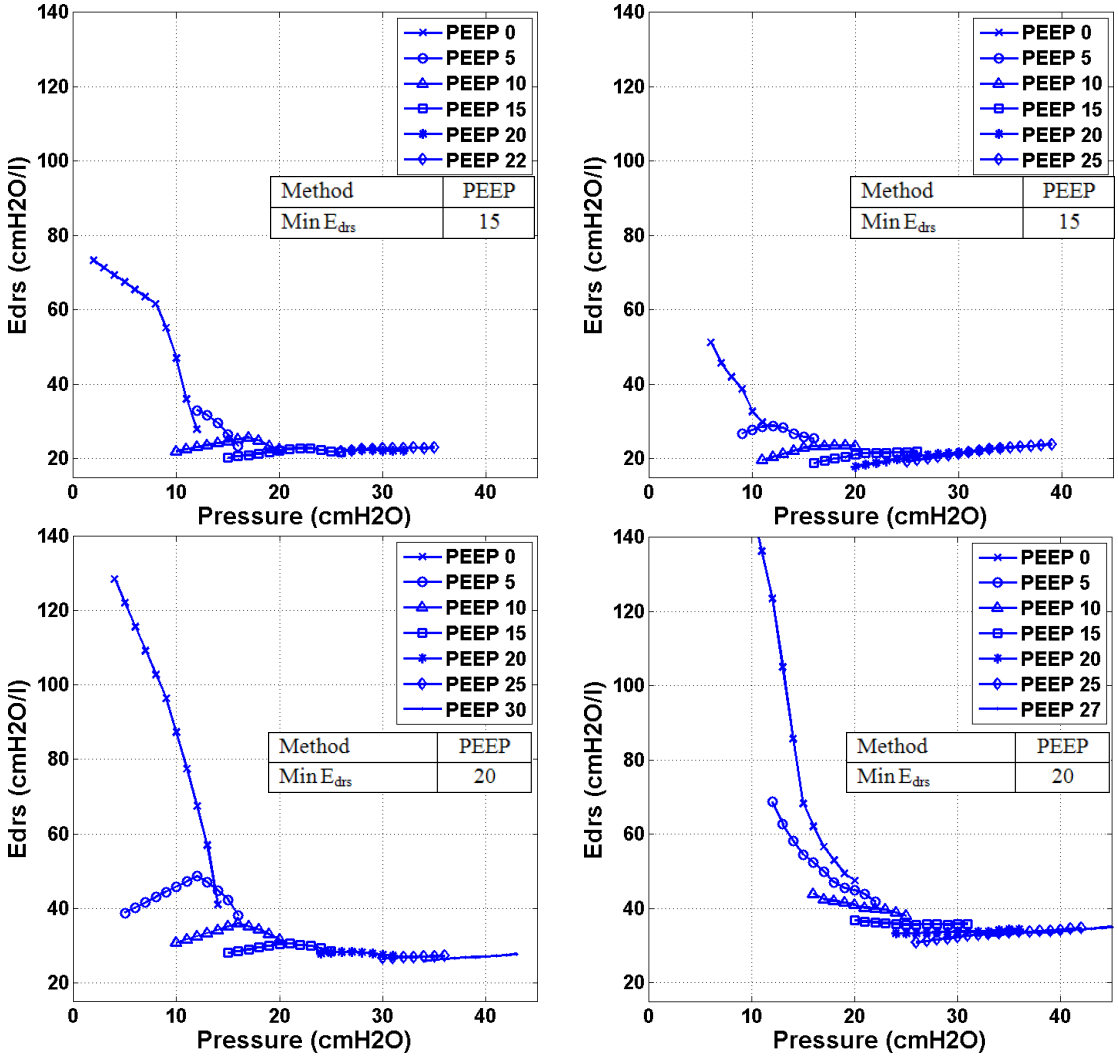

Figure 5.2: Dynamic lung elastance (E_{drs})-Pressure-PEEP plot. (Top Left) Patient 2, (Top Right) Patient 6. Both patients show significant E_{drs} drop from lower zero PEEP to PEEP 15 cmH_2O. Further increase of PEEP to 20 cmH_2O shows increase of overall E_{drs}. (Bottom Left) Patient 8, (Bottom Right) Patient 10. Both patients show a consistent drop in overall E_{drs} with increasing of PEEP and overall E_{drs} did not rise with PEEP for the entire ranged considered.

As PEEP rises, it is observed that E_{drs} curves drop at patient-specific rates. High constant lung elastance, E_{rs} at ZEEP and decreasing elastance as PEEP increments are

also observed in Figure 5.4 for Patient 10. COPD patient show the greatest drop as PEEP exceeds the pressure that opens their obstruction. Thus, the model detects this dynamic and can diagnose a suitable PEEP to reduce the obstruction effect.

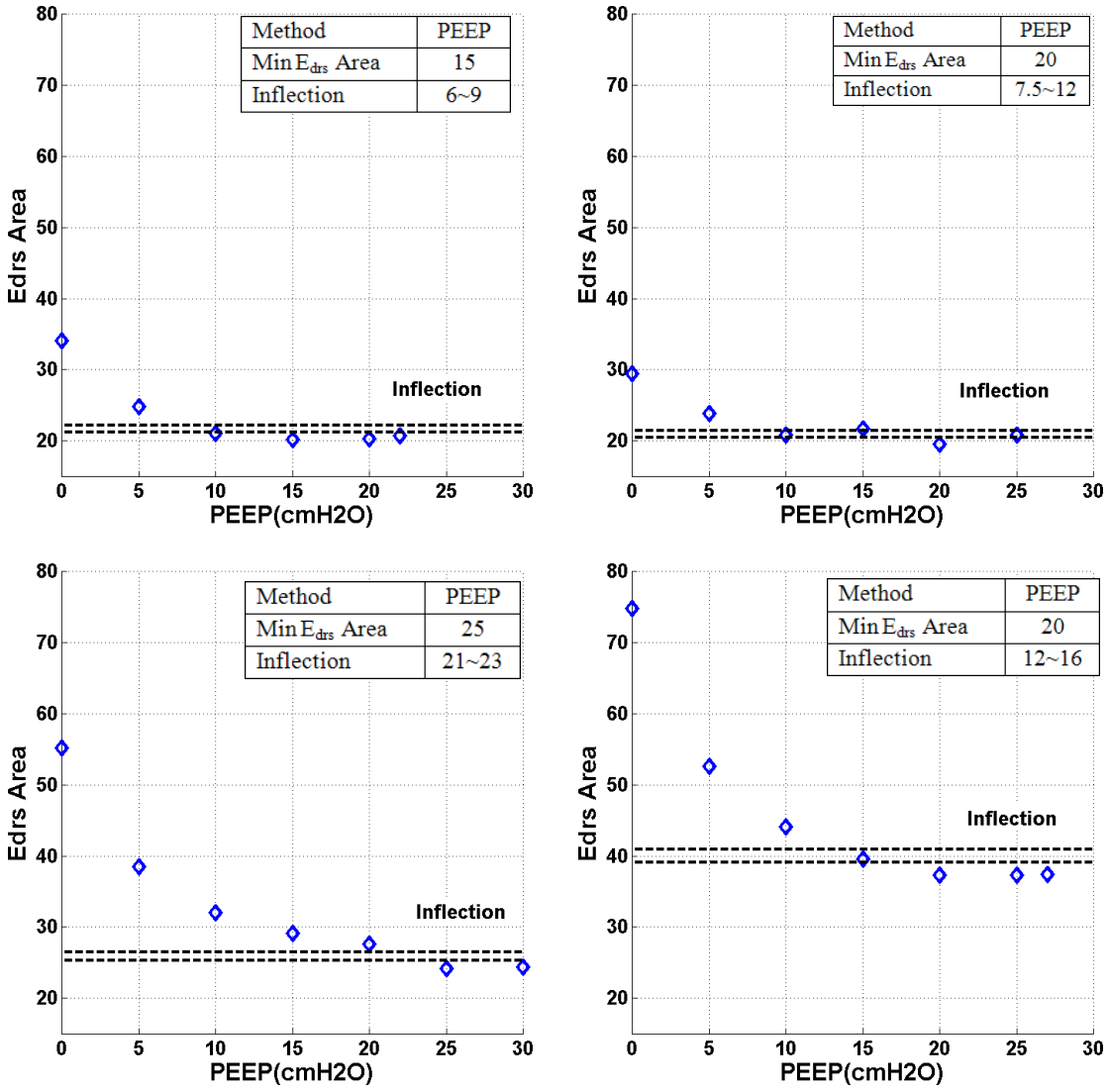

Figure 5.3: E_{drs} Area-PEEP plot. (Top Left) Patient 2, (Top Right) Patient 6. (Bottom Left) Patient 8, (Bottom Right) Patient 10. Severe COPD or patients with similar clinical features (e.g. Patient 10) showed significantly higher E_{drs} Area compared to other patients. PEEP selection is based on minimum E_{drs}-Area and the inflection method with PEEP increase.

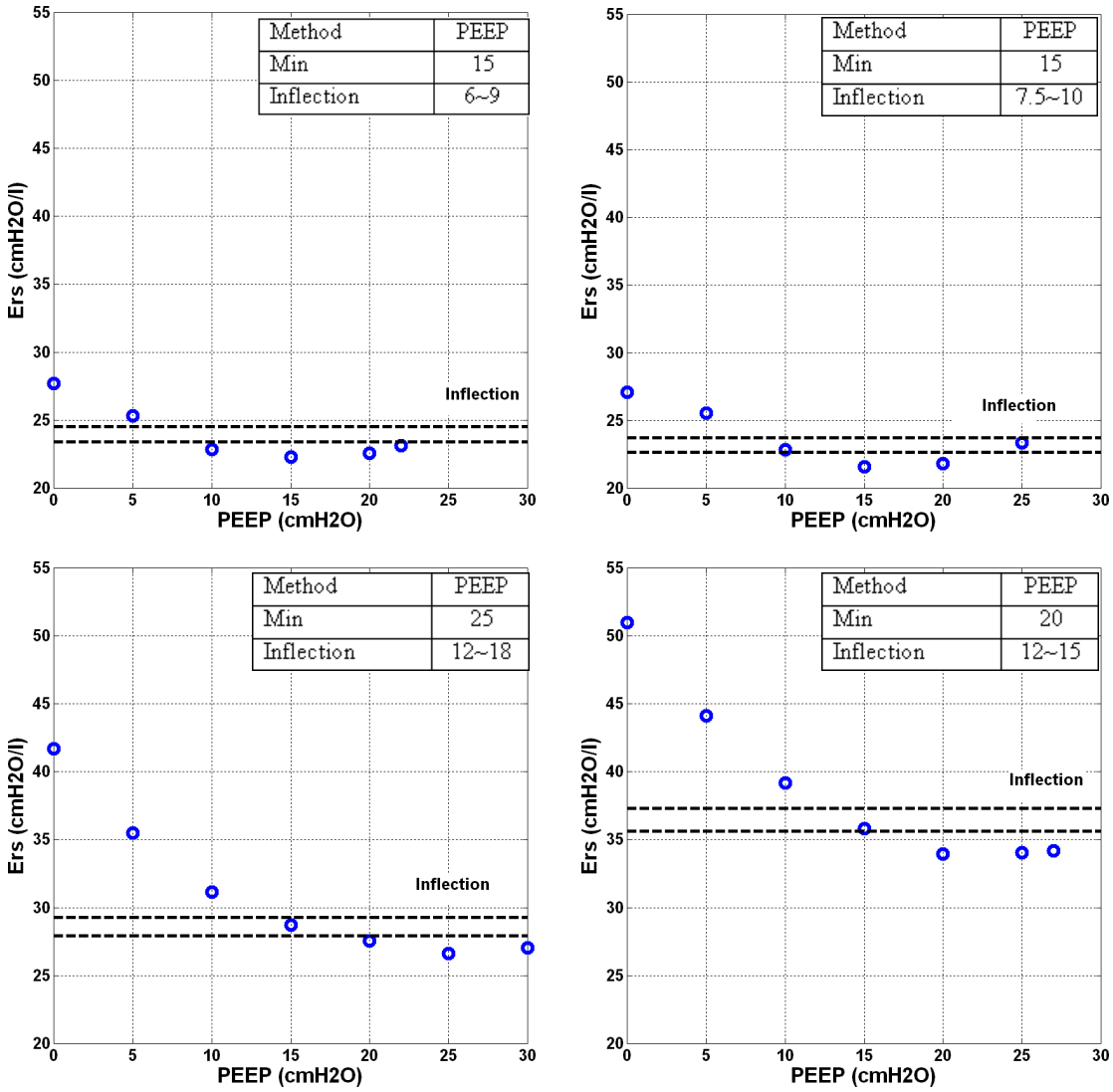

Figure 5.4: E_{rs}-PEEP plot. (Top Left) Patient 2, (Top Right) Patient 6. (Bottom Left) Patient 8, (Bottom Right) Patient 10. PEEP derived from Minimum E_{rs} and Inflection method are as indicated.

In all cases, patient-specific E_{drs} and E_{rs} decrease to a patient-specific minimum before increasing at higher PEEP. Minimum E_{drs} and E_{rs} suggest the point where the lung is most compliant, if ventilated at that PEEP level. Further increases in PEEP and pressure thus lead to increased E_{rs} or E_{drs}, and thus increase detrimental effects. In particular, increases in E_{rs} or E_{drs} can be associated with overstretching of the patient's lung (Carvalho et al., 2006, Carvalho et al., 2007). However, the heterogeneity of ARDS means there is a possibility of overstretching of healthy lung

units even at low PEEP and airway pressures (Stenqvist, 2003). Thus, Minimum or, perhaps preferably, Inflection E_{drs} and E_{rs} can provide a potentially higher resolution metric.

Patients 2 and 6 (Figure 5.2-5.4: Top panels) are examples where patient-specific E_{drs}, E_{drs} Area and E_{rs} increase after descending to a minimum. Results suggest that further increases of PEEP and inflation pressures will stretch lung units causing possible damage, as seen by increasing E_{drs} at higher PEEP. The rise of E_{drs} occurs at relatively low PEEP and pressure 15-20 cmH_2O in these two patients.

In contrast, Patients 8 and 10 (Figure 5.2-5.4: Bottom panels) never see E_{drs} or E_{rs} rising even at the maximum PEEP used in this study. However, the E_{drs} range at higher PEEP for Patients 8 and 10 (PEEP 15~30 cmH_2O) is relatively small with median E_{drs} = 31.3 cmH_2O/l, [IQR = 27.2-33.9]. This outcome indicates that further increases of PEEP from 15 to 30 cmH_2O has no added advantage in reducing E_{drs}, suggesting PEEP selection should be made at using the Inflection method.

5.3.5 Relation of Patient-Specific E_{drs} Area, E_{drs} and Work of Breathing

Across all 10 patients, patient-specific constant lung elastance (E_{rs}) can be represented by the median of dynamic lung elastance (E_{drs}) with correlation R = 0.987. Correlation of E_{rs} and WOB_E is R = 0.815. E_{drs} Area and median E_{drs} are also closely correlated with R = 0.896. Hence, E_{drs} can be represented with E_{drs} Area, where E_{drs} Area captures all E_{drs} values in a given breath and thus, is a more physiologically representative metric. Finally, validating Equation (2), E_{drs} Area is correlated to the

work to overcome lung elastance, WOB_E, as expected, with R = 0.936. The correlations are shown in Figure 5.5.

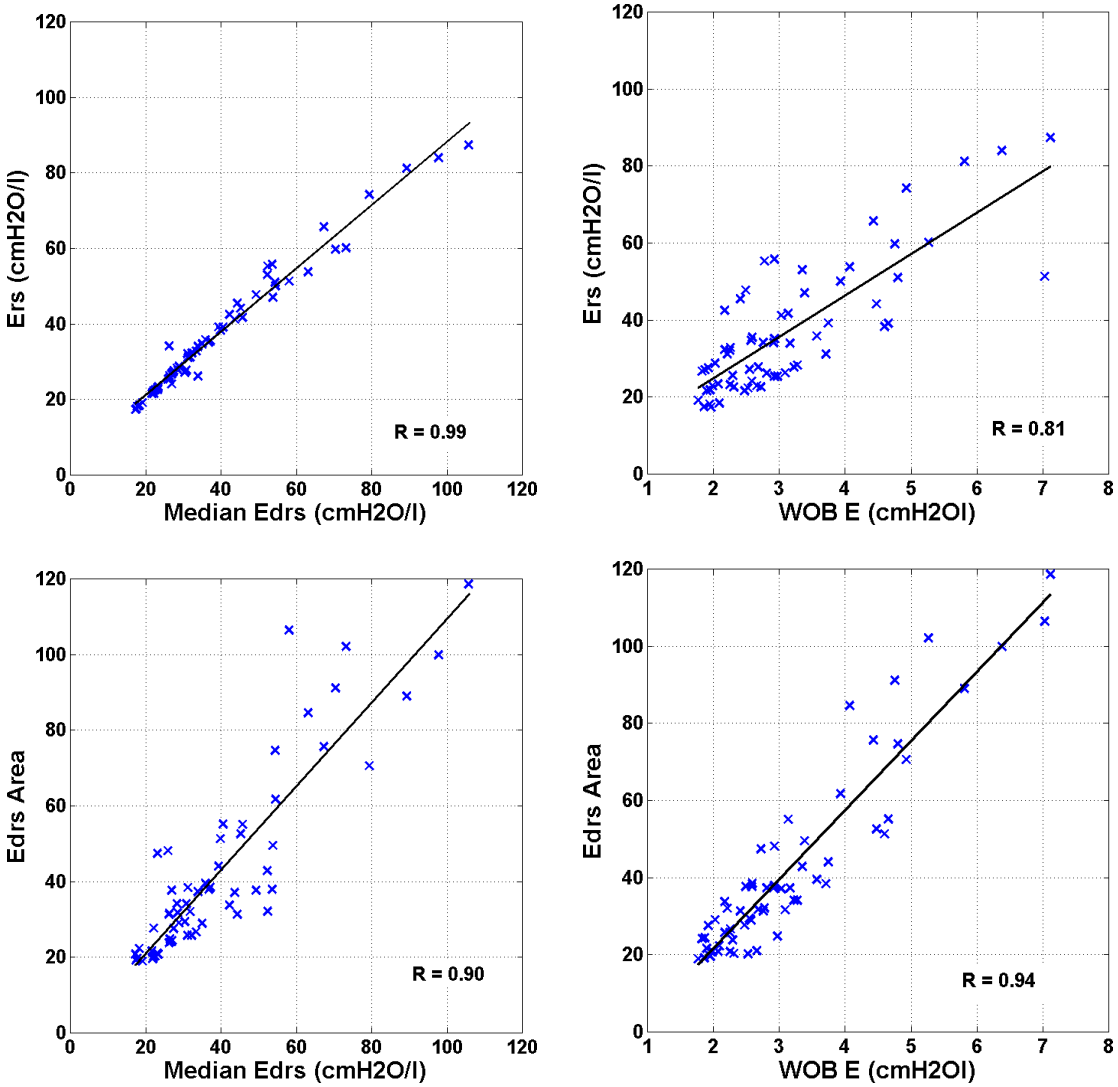

Figure 5.5: Pearson's Correlation. (Top Left) E_{rs}-Median E_{drs}, R = 0.987. (Top Right) E_{rs}-WOB_E, R = 0.815. (Bottom Left) E_{drs} Area-Median E_{drs}, R = 0.896. (Bottom Right) E_{drs} Area-WOB_E, R = 0.936.

It is found that E_{drs} Area is closely related to median E_{drs}, as shown in Figure 5.5. E_{drs} Area at lower PEEP with median 64.9 cmH_2Os/l [IQR: 37.6-102.2] is observed and as PEEP increases, E_{drs} Area decreases. Upon reaching minimum E_{drs} Area, patient-specific E_{drs} Area increase with PEEP (Patients 2, 4, 6, 7 and 10). This trend is similar

to the trend observed in patient-specific time-variant E_{drs} (Table 5.2) and constant E_{rs} (Table 5.3). Optimal PEEP derived using minimum or inflection method in E_{drs} Area is similar to minimum patient-specific E_{drs} but different as E_{drs} Area considers the whole inspiration and the effect of WOB_E. It is also found that E_{drs} Area is closely correlated to work in overcoming the lung elastic properties (WOB_E). This means that E_{drs} Area provides combined information of patients-specific lung physiological conditions as well as work of breathing, In this study, Patient 10 who is diagnosed with legionnaires and COPD, had significant E_{drs} Area drop when PEEP increases from 0 to 10 cmH_2O (Figure 5.3 Bottom right). Patient with COPD requires higher work of breathing to ventilate the lung, and this information is clearly shown in Patient 10's E_{drs} Area-PEEP curve, and thus E_{drs} Area is a better metric for decision making.

5.3.6 Clinically Selected PEEP vs Model-based PEEP Selection.

Table 5.5 compares clinically selected PEEP during MV therapy with PEEP selected using Minimum E_{drs}, and Minimum E_{drs} Area and the Inflection method. The clinical values are set over a much narrower range, both higher and lower than those selected using model-based methods. Minimum E_{drs} Area always selects a higher PEEP, by definition, than the Inflection method. However, Minimum E_{drs} Area selects PEEP similar to or higher than Minimum E_{drs}, where it also adds in the consideration of the reduction in overall WOB_E in selecting PEEP. PEEP derived from minimum E_{rs} and Inflection E_{rs} are also indicated.

Table 5.5: PEEP (cmH_2O) selection in clinical and model-based approach

Selection Method	Patients									
	1	**2**	**3**	**4**	**5**	**6**	**7**	**8**	**9**	**10**
Clinical	10	12	10	10	12	11	7.5	12	10	10
Minimum E_{drs}	20	15	15	25	25	15	5	20	15	20
Minimum E_{drs} Area	25	15	20	20	25	20	10	25	25	20
Inflection E_{drs} Area	14~16	6~9	15~17	16~18	22~24	7.5~12	5~7.5	21~23	20~23	12~16
Minimum E_{rs}	25	15	15	30	25	15	5	25	30	20
Inflection E_{rs}	13~17	6~9	8~10	26~27	21~24	7.5~10	5	12~18	19~22	12~15

For 9 of 10 patients, the PEEP selected using Minimum E_{drs} and E_{drs} Area results in a value higher than the clinically selected PEEP. This latter result suggests that these patients could be treated at PEEP levels higher than clinically selected PEEP. When Minimum E_{drs} or E_{drs} Area metrics are compared with Minimum E_{rs} (Carvalho et al., 2007), they result in selecting similar PEEP. However, selecting PEEP is a trade off in minimizing lung pressure and potential damage, versus maximizing recruitment. Hence, the Inflection method offers similar recruitment at a lower PEEP and may be a safer choice, although its selected values are still higher than clinically selected values in 7 of 10 cases. Overall, these results reflect the heterogeneity of the ARDS lung and the need for patient-specific approaches to select PEEP, perhaps allowing also for more regular changes over time to optimize care.

5.3.7 Individual Case Finding

Patient 9 is an interesting case that illustrates the model's potential to capture unique patient-specific lung recruitment and condition as it occurs in a clinically and physiologically relevant manner. When the patient is ventilated from PEEP of 5 to 10 cmH_2O, E_{rs} only decreases by less than 1.0 cmH_2O/l. However, when PEEP is

increased to 15 cmH_2O, the E_{rs} drops significantly, as shown in Figure 5.6 (Left). This E_{rs} drop suggests that only minimal lung volume is recruited from PEEP of 5 to 10 cmH_2O. The significant drop in E_{rs} at PEEP 15cmH_2O indicates that PEEP *15* cmH_2O has overcome recruitment resistance and additional new lung volume is recruited. The recruitment that causes the significant drop in E_{rs} is shown the rapid increase of lung volume in Figure 5.6 (Right). Patient 9 was diagnosed with H1N1 and high PEEP for lung recruitment has proven to be beneficial for these patients (Ramsey et al., 2010, Peris et al., 2010, Briel M and et al., 2010). Similar trends can be observed with the E_{drs} and E_{drs} Area as shown in Table 5.2 and 5.4.

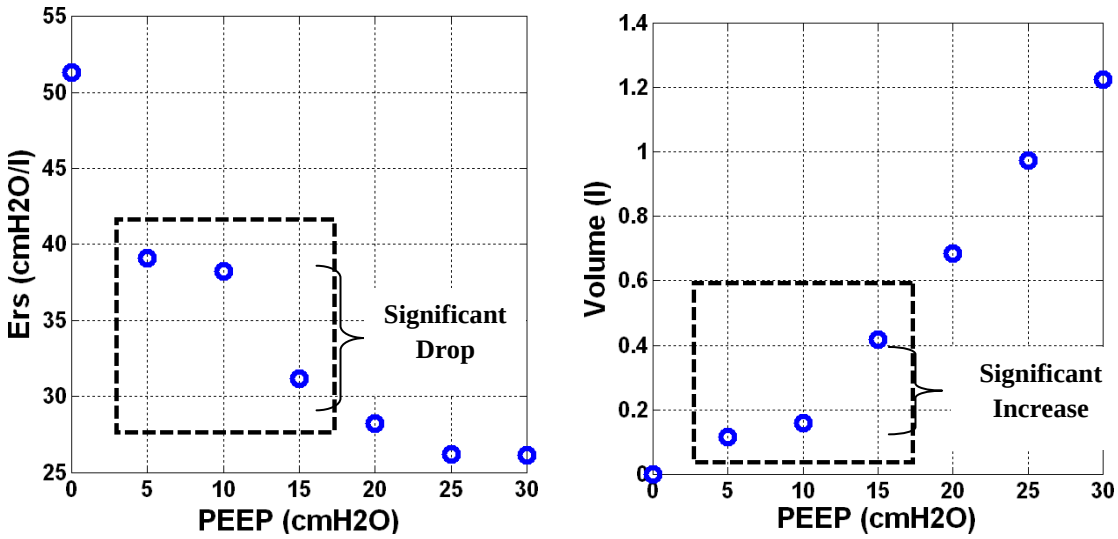

Figure 5.6: Patient 9's E_{rs}-PEEP (Left) and dFRC-PEEP (Right) curve. The significant increase in dFRC result in E_{rs} drop when PEEP is increased from 10 to 15 cmH_2O.

5.4 Study Limitations

5.4.1 Simple Compartment Model and Offset Pressure

In this research, the lung model used to identify patient-specific E_{drs} comprised a single compartment lung model. It was initially proposed for simple computational

analysis and neglects the effect of nonlinear flow (Bates, 2009a). However, this analysis is based predominantly on trend comparisons, where the patient is their own reference. In addition, the model is simple and capable of capturing the fundamental lung mechanics, which varies intra- and inter- patients. Hence, this limitation should be minimal in this case, but should be confirmed with direct prospective clinical studies.

Compared to Equation 5.1, Equation 5.2 is extended with an offset pressure (*P0*) to equilibrate Equation 5.2 because the total lung volume is not known (Bates, 2009a). In this study, the pneumotachometer allows the air entering the lung to be calculated continuously without interruption. Thus, the *V(t)* term used in Equation 5.1 is the change of total lung volume instead of change of tidal volume. Equally, using the information on the change of total lung volume takes into account of Auto-PEEP and external PEEP, allowing easier implementation of the model-based method in this study. Equation 5.1 can be replaced with Equation 5.2, if information on the change of total lung volume is not available.

5.4.2 Sedation and Patient Effort

During the clinical trials, the patients were sedated and paralyzed using muscle relaxants. It is assumed that after sedation, the patient will be fully dependant on mechanical ventilation and not have spontaneous breathing effort. This assumption thus assumes the patient's pleural pressure (P_{pl}) after sedation is zero or constant allowing P_{pl} to be omitted from Equation 5.1, and 5.2, which may not be entirely valid (Fernandes, 2006, Bates, 2009a) . However, this assumption is made for the first step

study to prove the concept within a simpler situation. Given the low fitting errors observed, this issue should have little impact in this research.

5.4.3 Is Airway Resistance Constant?

During the course of estimating patient-specific E_{rs} or E_{drs}, respiratory system resistance, R, is assumed overall constant within a physiological range (Mols et al., 2001) as PEEP increases. This assumption may not be entirely valid in some cases (Mols et al., 2001, Guérin et al., 2001). The airway resistance decreases with PEEP increase (Also shown in Chapter 4.0, Subject 9, Phase 3 - airway resistance decrease with PEEP). This can be explained by higher PEEP opened up the airway, resulting and overall drop in resistance. Continuous measurements of respiratory resistance are not typically available without additional invasive protocols, for example, using end inspiratory hold, that takes time, interrupt care and are thus not practical in regular care. In this clinical trial, the effect of this resistive term is limited mathematically in its impact. Equally, trend comparison, as used here, across PEEP values will reduce the impact.

5.4.4 Validity of PEEP Selection Metric

The identification of E_{rs}, E_{drs} and E_{drs} Area during MV is presented as a method to select PEEP, but there is currently no conclusive, optimum overall E_{drs} or E_{drs} Area in patients. E_{drs} range varies depending on patient disease state and thus will also change over time. However, this trial includes only 10 patients, and there is not yet enough clinical data to indicate an optimum E_{rs}, E_{drs} or E_{drs} Area value for a specific patient or group. On-going, prospective trials with more specific patient groups should

develop more conclusive outcomes, relating specific set values of E_{drs} metrics to effective patient-specific treatments and clinical outcome.

In particular, the time-varying E_{drs} value and its changes over a given breathing cycle, provides additional insight to guide ventilation that is not investigated here. For example, changes in ventilator pattern or mode to modify the E_{drs} trajectory could also be used with this data to guide therapy choice. However, this study does not have the numbers or design to provide that advice, or specific E_{drs} values associated with specific decrease state or lung damage.

5.5 Summary

This study presents the first clinical trial carried out in ARDS patients that monitors patient-specific respiratory system elastance for PEEP selection. The patient-specific elastance was shown to be correlated with clinically significant work of breathing and lung volume metrics, and further validating its relevance and potential.

The model-based approach is capable of providing patient-specific, physiological insight not directly measurable without additional invasive, disruptive and clinically intensive test manoeuvres. This method can be directly implemented using modern ventilators with minimal, limited PEEP titrations, and thus without significant interruption to ongoing therapy. In particular, the full manoeuvres used here would not be required for clinical use, and only modest PEEP changes (3-8 cmH_2O) would be required to determine if E_{drs} was decreasing at a different PEEP. E_{drs} offers higher resolution in patients' response to change of pressure and PEEP, which is potentially,

a better metric compared to existing constant lung elastance estimation. Thus, the overall method is readily generalisable and clinical practicable. It is able to capture patient-specific condition, responsiveness to PEEP and recruitment accurately as clinically expected. Hence, the approach presented offers significant potential to improve clinical insight and delivery of mechanical ventilation, and should be prospectively tested.

In the next chapter, mechanical ventilation of spontaneously breathing patients is presented. The patients' fundamental breathing pattern is greatly altered by patient-specific breathing effort and thus, Equation 5.1 and 5.2 is not suitable for respiratory mechanics monitoring without additional information or invasive measurements. Thus, different decision metrics are needed and their performance is tested.

Chapter 6

Spontaneous Breathing and Assisted Ventilation: Pressure Support (PS) and Neurally Adjusted Ventilatory Assist (NAVA)

6.1 Background

Assisted ventilation modes were initially designed for spontaneously breathing patients with the aim to facilitate the weaning process of mechanically ventilated patients. Weaning is the discontinuation process from mechanical ventilation and is a critical phase in respiratory therapy. In addition, studies by Kuhlen et al., Putensen et al. and Slutsky et al. have indicated that promoting patients to breathe spontaneously with the ventilator during the course of treatment will result in better outcome (Kuhlen and Putensen, 1999, Putensen et al., 1999, Putensen et al., 2001, Slutsky et al., 2005b).

In particular, spontaneous breathing patients benefit from improving arterial oxygenation, recruitment, increase of cardiac output, ventilation-perfusion matching, reduction of the use of analgesia and sedation, prevention of respiratory muscle

dysfunction, indirectly reduced length of MV, improved weaning and recovery (Burchardi, 2004, Wrigge et al., 2005, Brander and Slutsky, 2006, Kogler, 2009). Thus, there is increasing interest in providing optimal MV therapy through spontaneous breathing ventilation, and promoting patients who are sedated in MV to spontaneous breathing MV modes as rapidly as possible.

6.2 Pressure Support (PS) and Neurally Adjusted Ventilatory Assist (NAVA)

One of the most used partial assist ventilation modes is the pressure support ventilation (PS or PSV) (Esteban et al., 2000, Rose et al., 2009). In PS, each supported ventilation cycle is initiated by a pneumatic signal (flow or pressure), detected at the airway as produced by the patient's inspiratory effort (Tutuncu et al., 1997, Goulet et al., 1997, Correa et al., 2007). The ventilator sensor detects a drop in airway pressure signalling the start of a breath and adds pressure, like PEEP, to assist breathing. The amount of pressure support delivered to the patient is set by the clinician, and the transition of the breath from inspiration to expiration occurs when the inspiratory flow decreases to a predetermined level (MacIntyre et al., 1990, Tassaux et al., 2004, Tassaux et al., 2005). However, under PS, a constant pressure is delivered by the ventilator regardless of the patient's relative inspiratory effort. As this constant pressure produces the majority of resulting tidal volume (*Vt*) supply, PS is expected to reduce *Vt* variability.

Neurally Adjusted Ventilatory Assist (NAVA) is an assisted ventilation mode that uses electrical activity of the diaphragm (*Eadi*), an expression of the patient's inspiratory demand, to trigger and cycle the ventilator (Sinderby et al., 1999,

Sinderby, 2002, Slutsky et al., 2005a). The amount of pressure support delivered is in direct proportion to the patient's *Eadi* (Sinderby et al., 1999, Terzi et al., 2012). A description on the difference between the triggering of NAVA ventilation and to other assisted ventilation modes (In this study, Pressure Support) is shown in Figure 6.1.

Compared to PS, NAVA was found to improve patient-ventilator interaction by reducing trigger delay, improving expiratory cycling and reducing the number of asynchrony events (Colombo et al., 2008, Piquilloud et al., 2011b, Spahija et al., 2010, Piquilloud et al., 2012). NAVA also increases respiratory variability in *Vt* and flow compared to PS (Colombo et al., 2008, Schmidt et al., 2010). Improved variability has been associated with improved ventilation perfusion and oxygenation (Boker et al., 2004, Gama de Abreu et al., 2008, Spieth et al., 2009a, Spieth et al., 2009b).

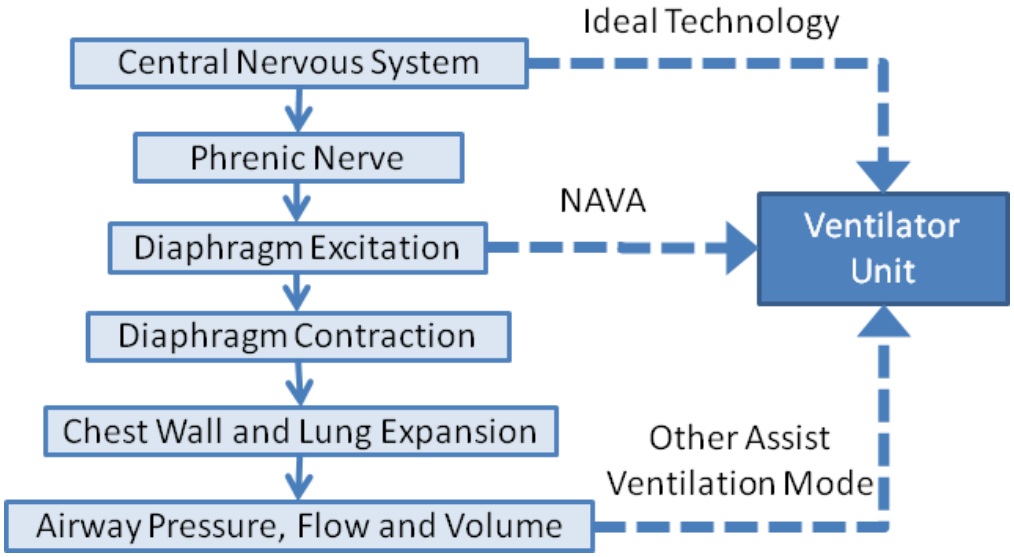

Figure 6.1: Difference between NAVA ventilation and other conventional assisted ventilation mode (Sinderby et al., 1999). NAVA triggers ventilation cycle using neural signal from diaphragm excitation whereas conventional assist ventilation modes triggers the ventilator using pneumatic signal from the airway.

However, no studies make these comparisons in relative to the inspiratory demand (*Eadi*), which may vary between modes and patients. Thus, to determine the true impact of NAVA on *Vt* variability, *Eadi* must be accounted for in the analysis. Such an analysis would validate whether these improvements associated with NAVA are real.

It is hypothesized that the magnitude of *Vt* under NAVA mode would show better correlation with the magnitude of *Eadi*, better matching between *Vt* with *Eadi* and greater variability, compared to PS. This chapter presents the study and data used to confirm these hypotheses by analysing the flow and *Eadi*-time curves for PS and NAVA using a simple, new metric (Range90), that quantifies the matching of patient's demand (*Eadi*) and ventilator supply (*Vt*). The result will clearly shows which mode provided better matching for each patient.

6.3 Methodology

This study analyses recorded *Eadi*-time and flow-time curves, as well as derived parameters, from a study exploring patient-ventilator synchrony on clinically based criteria (Piquilloud et al., 2011b). The data were obtained at the University Hospital of Geneva (Switzerland) and Cliniques Universitaires St-Luc (Brussels, Belgium). The study protocol was approved by the Ethics Committee of the University Hospital of Geneva (Commission centrale d'éthique hôpitaux universitaires de Genève) and the Ethics Committee at Cliniques Universitaires Saint-Luc (Commission d'Ethique biomédicale hospitalo-facultaire, université catholique de Louvain, faculté de médecine).

6.3.1 Patients and Ventilator Settings

22 patients admitted to the ICU, intubated because of acute respiratory failure, and ventilated with PS mode were included for the study. The exclusion criteria are: 1) severe hypoxemia requiring $FiO_2 \geq 50\%$; 2) Hemodynamic instability; 3) Known oesophageal problem (hiatal hernia, oesophageal varicosities); 4) Active upper gastro-intestinal bleeding or any other contraindication to the insertion of a naso-gastric tube; 5) Age ≤ 16 years old; 6) Poor short term prognosis (defined as a high risk of death in the next seven days); or 7) Neuromuscular disease. All included patients were ventilated with a Servo-I ventilator (Maquet, Solna, Sweden) equipped with the commercially available NAVA module and software, which delivers both PS and NAVA. The patients' clinical characteristic and ventilator settings are summarised in Table 6.1.

6.3.2 Clinical Protocol

After written informed consent was obtained, the patient's standard nasogastric tube was replaced with NAVA tube to measure *Eadi* signal and perform NAVA ventilation. Airway suctioning was performed before the beginning of the protocol. A 20 minute continuous recording of patients airway pressure, *Eadi* and flow profile (~300-500 breaths) was first carried out during PS mode with the clinician predetermined ventilator settings. PS mode was then changed to NAVA mode with the NAVA gain (or NAVA level) (the proportionality factor between recorded *Eadi* and ventilator delivered pressure), set to obtain similar peak airway pressure during PS for that patient using a previsualisation system provided with the ventilator. During NAVA ventilation, further 20 minutes of recording is taken.

Table 6.1: Patients main clinical characteristics for both PS and NAVA and their main ventilator settings in each mode

Patients		
Age (years)	66 ± 12 years	
Body Mass Index (BMI)	23.4 ± 3.1 kg/m^2	
PaO_2/FiO_2	194.8 ± 58.1 *mmHg*	
Pulmonary restrictive disease	1 of 22 patient	
Pulmonary obstructive disease	8 of 22 patients	
Ventilator Settings	**PS**	**NAVA**
FiO_2	0.43 ± 0.17	0.43 ± 0.17
PEEP	7 ± 2 cmH_2O	7 ± 2 cmH_2O
Inspiratory Trigger	Flow Trigger: 1.2 *l/min* (20/22 patients) Pressure Trigger: -4 to -5 cmH_2O (2/22 patients)	0.5 *uV*
Expiratory Trigger Sensitivity (ETS)	25-30%	-
PS Level	13 ± 3 cmH_2O	-
Pressurization Slope	100-150 *ms*	-
NAVA Gain Level	-	2.2 ± 1.8 $cmH_2O/\mu V$

Airway pressure, *Eadi* and flow profile were acquired from the Servo-I ventilator and recorded at a frequency of 100 *Hz* by Servo-tracker V 4.0 (Maquet, Solna, Sweden). During the entire period, the pressure support level in PS and NAVA gain in NAVA were kept constant. Equally, other ventilator settings such as positive end expiratory pressure (PEEP), FiO_2, inspiratory trigger, and cycling off settings were maintained at the same level.

6.3.3 Data Processing and Analysis

Flow and *Eadi*-time signal obtained from the Servo-tracker were used to perform the analysis using MATLAB software (The Mathworks, Natick, Massachusetts, USA). An inspiratory breath was determined by the flow signal, and was defined to commence when the flow signal became positive, and terminate when the flow signal

became negative. The flow-time signal was integrated to obtain tidal volume, *Vt.* Breaths with *Vt* < 50 *ml* were discarded from analysis as being very small and potentially artefacts.

The *Eadi* signal was integrated between the same two time points to obtain the corresponding integrated *Eadi* value (∫*Eadi*), to represent total inspiratory demand (Schmidt et al., 2010). Peak *Eadi* value was captured and compared with the corresponding ∫*Eadi* to ensure that there is no loss of information. ∫*Eadi* is the time integral of *Eadi* signal and this parameter carries the information on the change of *Eadi* with time, while retaining information on peak *Eadi*. Thus, ∫*Eadi* is used to represent patient inspiratory demand rather than the Peak *Eadi* value. Finally, the inspiratory time, *Ti*, is defined as the time when flow becomes positive until the time when flow became negative; and neural inspiratory time $Ti_{\_Neural}$, is defined as the time when flow became positive until the time when peak *Eadi* occurs. Figure 6.2 shows the location of ∫*Eadi*, *Vt*, *Ti* and $Ti_{\_Neural}$ in a patient flow and *Eadi*-time curve.

6.3.3.1 Correlation Analysis

Pearson's linear correlation coefficients were calculated for each patient between peak *Eadi* value and ∫*Eadi*, and also between *Vt* and ∫*Eadi*. Two-sample non parametric Kolmogorov-Smirnov hypothesis tests were then used to compare variability (Coefficient of variation, CV) at each variable between the PS and NAVA groups.

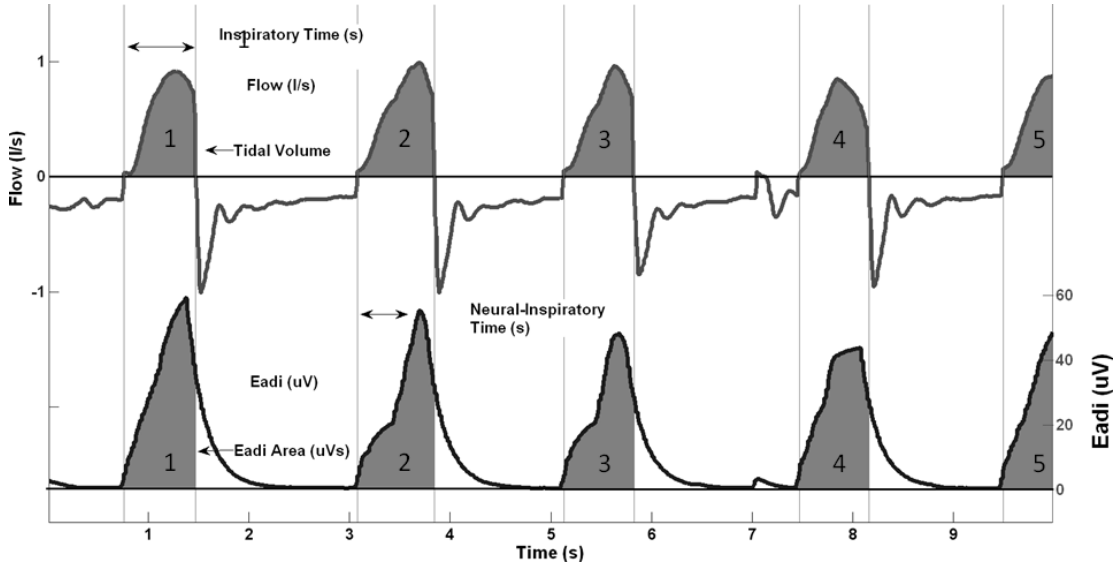

Figure 6.2: Example of a patient's flow and *Eadi* curve. Inspiratory time *Ti* is the time when flow becomes positive until the time when flow became negative. Tidal volume, *Vt* is the area under the flow curve. ∫*Eadi* is the corresponding area under *Eadi* curve. Neural inspiratory time, $Ti_{\_Neural}$ is the time when flow became positive until the time when peak *Eadi* occurs.

6.3.3.2 Variation Analysis - Robust Coefficient of Variation

Coefficient of variation (CV = standard deviation/mean) were calculated for *Vt*, ∫*Eadi* and *Ti* over all breaths for each patient in each ventilator mode for variation analysis (MacIntyre et al., 1990, Schmidt et al., 2010). A lower CV value indicates lower variability (Wysocki et al., 2006). However, normality was assessed using a one-sample Kolmogorov-Smirnov goodness to fit test, which showed that some parameters were not normally distributed. Hence, a non-normal alternative variation test is used (Robust Coefficient of Variation, CVR = median absolute deviation/ median). CVRs for the PS and NAVA group are compared using a two-sample non parametric Kolmogorov-Smirnov hypothesis test.

6.3.3.3 A Metric for Matching Analysis – Range90 Supply over Demand

Vt and ∫*Eadi* were determined, and the ratio *Vt*/∫*Eadi* was assessed for each breath in both ventilation mode. *Vt* is the tidal volume supply given to patient and ∫*Eadi* is defined as an expression for patient's ventilatory demand. The ratio of *Vt*/∫*Eadi* represents an output over input ratio and it is also defined as the Neuroventilatory efficiency (Passath et al., 2010). This ratio thus carries the information of the matching of ventilator supply over patient demand, which thus captures a form or a level of patients-ventilator interaction.

To calculate Range90 for a patient, the empirical cumulative distribution function (CDF) of *Vt*/∫*Eadi* ratio for each breath in each ventilation mode was plotted. Range90 is calculated as the 5^{th} to 95^{th} range of *Vt*/∫*Eadi* ratio as shown in Equation 6.1.

$$\text{Range90} = 95^{th}\ Vt/\int Eadi - 5^{th}\ Vt/\int Eadi \qquad (6.1)$$

A smaller Range90 indicates better matching of the response *Vt* to the variable inspiratory ∫*Eadi* demand resulting in a more constant ratio. A larger Range90 indicates a lesser ability to match *Vt* and ∫*Eadi* for each breath regardless of the underlying patient-specific variability in ∫*Eadi*. Thus, if *Vt* variability were equally matched to variability in ∫*Eadi*, then the ratio would be more consistent and Range90 would be smaller. Equally, a larger Range90 thus indicates an inability to consistently match *Vt* to ∫*Eadi* demand. Detailed description of Range90 and several case

examples beyond these presented in this chapter can be found in Appendix 02 at the end of the thesis.

The Range90 metric normalizes differences in *Eadi* demand within and between patients and-or ventilatory modes in analysing the resulting *Vt* variability. The ratio of $Vt/\int Eadi$ for each breath and the analysis of its variability (Range90) over a given mode thus allows fair comparison between modes (for a patient) and between patients, where *Eadi* demand may vary significantly.

In this study, the range of 5^{th}-95^{th} percentile of $Vt/\int Eadi$ is used for matching analysis rather than other ranges, for example, the interquartile range, 25^{th}-75^{th} percentile of $Vt/\int Eadi$ (Range50). Range90 captures 90% of the patients breathing pattern whereas, a smaller range such as Range50 only capture the central tendency and spread of the patients breathing pattern.

6.4 Results and Discussion

For the 22 patients, the median [IQR)] for $\int Eadi$ were not different between PS and NAVA: 4.10 μVs [IQR: 2.55-5.99] vs 3.97 μVs [IQR: 2.59-6.64]. *Ti* was 0.97 *s* [IQR: 0.70-1.15] in PS and 0.80 *s* [IQR: 0.65-0.92] in NAVA. Median *Vt* was 468 *ml* [IQR: 418-514] in PS and 431 *ml* [IQR: 378-472] in NAVA. Peak inspiratory pressure (*PIP*) was 21.44 cmH_2O [IQR: 18.57-24.11] in PS and 21.63 cmH_2O [IQR: 19.61-24.56] in NAVA. No significant difference ($p > 0.005$ using Wilcoxon ranksum test) was found between these median values for PS and NAVA. Table 6.2 shows the details and median [IQR] values for $\int Eadi$, *Vt*, *Ti_Neural*, *Ti* and *PIP* for all 22 patients for PS

and NAVA. The summary of Table 6.2 is shown in Table 6.3 and as a box-whisker in Figure 6.3.

Table 6.2: *∫Eadi*, *Vt*, *Ti_Neural*, *Ti* and *PIP* of the 22 patients

Patients		*∫Eadi (μVs)*	*Vt (ml)*	*Ti_Neural (s)*	*Ti (s)*	*PIP (cmH_2O)*
1	**PS**	3.01 [2.71-3.36]	671 [653-687]	0.94 [0.90-1.02]	1.20 [1.18-1.23]	20.40 [20.33-20.46]
	NAVA	3.80 [3.37-4.46]	626 [584-671]	1.02 [0.95-1.09]	1.20 [1.14-1.29]	21.89 [20.56-23.43]
2	**PS**	1.02 [0.71-1.96]	449 [394-517]	0.79 [0.63-0.92]	1.05 [0.99-1.13]	15.25 [14.99-15.64]
	NAVA	2.06 [1.21-4.13]	303 [180-529]	0.76 [0.55-0.93]	0.92 [0.76-1.06]	12.26 [9.85-17.97]
3	**PS**	1.90 [1.42-2.64]	463 [454-472]	0.86 [0.79-0.94]	1.00 [0.97-1.03]	24.56 [24.50-24.69]
	NAVA	1.71 [1.39-1.97]	472 [382-520]	0.86 [0.68-0.98]	1.05 [0.89-1.14]	31.33 [27.62-35.37]
4	**PS**	12.28 [10.67-13.90]	418 [400-435]	0.50 [0.45-0.54]	0.65 [0.63-0.68]	21.57 [21.50-21.63]
	NAVA	13.08 [11.39-15.05]	412 [387-442]	0.53 [0.49-0.59]	0.71 [0.67-0.77]	21.89 [20.59-23.36]
5	**PS**	4.35 [3.81-5.03]	510 [495-525]	0.57 [0.52-0.62]	0.80 [0.76-0.82]	25.21 [25.08-25.41]
	NAVA	3.11 [2.68-3.74]	423 [384-475]	0.54 [0.49-0.60]	0.65 [0.61-0.71]	24.56 [22.46-27.06]
6	**PS**	7.33 [4.88-9.59]	336 [318-353]	0.47 [0.39-0.55]	0.81 [0.77-0.84]	19.42 [19.29-19.48]
	NAVA	6.64 [5.62-7.63]	293 [257-325]	0.56 [0.52-0.65]	0.79 [0.70-0.87]	18.12 [16.23-19.48]
7	**PS**	3.18 [1.70-4.17]	528 [486-555]	0.43 [0.36-0.49]	0.68 [0.61-0.71]	25.54 [25.47-25.60]
	NAVA	4.20 [2.73-4.83]	476 [434-513]	0.44 [0.38-0.49]	0.56 [0.51-0.60]	24.43 [21.76-26.06]
8	**PS**	3.94 [2.68-4.98]	460 [432-479]	0.51 [0.46-0.57]	0.57 [0.55-0.61]	20.46 [20.40-20.53]
	NAVA	2.10 [1.81-2.43]	462 [429-498]	0.70 [0.61-0.77]	0.81 [0.74-0.87]	21.37 [19.09-23.85]
9	**PS**	5.27 [4.72-5.96]	411 [396-423]	0.60 [0.57-0.63]	0.70 [0.68-0.72]	21.50 [21.44-21.57]
	NAVA	5.97 [5.36-6.86]	393 [361-426]	0.60 [0.57-0.64]	0.72 [0.69-0.75]	23.91 [21.78-25.91]
10	**PS**	2.46 [2.06-2.87]	382 [352-407]	1.07 [0.96-1.20]	1.45 [1.39-1.52]	14.15 [14.02-14.34]
	NAVA	2.88 [2.41-3.38]	319 [282-342]	1.02 [0.82-1.14]	1.24 [1.10-1.34]	10.76 [10.05-11.54]
11	**PS**	7.31 [6.53-8.16]	397 [389-406]	0.48 [0.44-0.52]	0.54 [0.53-0.55]	28.79 [28.66-29.12]
	NAVA	7.75 [6.60-9.17]	378 [350-408]	0.44 [0.40-0.49]	0.59 [0.55-0.64]	31.98 [29.77-35.47]
12	**PS**	11.97 [8.14-17.64]	474 [437-501]	0.69 [0.61-0.76]	0.93 [0.89-0.99]	14.73 [14.60-14.86]
	NAVA	12.00 [9.91-14.90]	456 [418-486]	0.66 [0.60-0.75]	0.84 [0.78-0.91]	13.50 [12.06-15.32]
13	**PS**	2.90 [1.71-5.59]	345 [317-384]	0.45 [0.28-0.67]	1.14 [1.05-1.27]	17.21 [17.08-17.53]
	NAVA	3.14 [1.66-5.94]	220 [124-397]	0.54 [0.36-0.69]	0.70 [0.54-0.83]	16.98 [13.01-25.57]
14	**PS**	1.86 [1.25-2.38]	473 [417-516]	0.62 [0.47-0.72]	0.73 [0.68-0.80]	23.07 [22.87-23.20]
	NAVA	3.13 [0.96-5.32]	394 [108-560]	0.58 [0.38-0.71]	0.79 [0.60-0.89]	19.78 [10.89-24.17]
15	**PS**	5.66 [4.67-8.41]	507 [459-538]	0.61 [0.53-0.69]	1.15 [0.96-1.26]	24.11 [23.98-24.24]
	NAVA	5.91 [4.90-6.91]	544 [475-613]	0.74 [0.65-0.82]	0.92 [0.84-0.99]	32.63 [28.17-38.82]
16	**PS**	5.99 [5.25-6.97]	622 [608-634]	0.79 [0.73-0.85]	0.93 [0.90-0.96]	18.77 [18.70-18.90]
	NAVA	6.77 [6.04-7.68]	615 [583-644]	0.84 [0.75-0.87]	0.96 [0.90-1.03]	20.53 [18.90-22.67]
17	**PS**	4.42 [3.24-5.61]	633 [579-727]	0.32 [0.18-0.44]	1.19 [1.07-1.35]	21.37 [21.31-21.50]
	NAVA	5.79 [3.83-7.77]	453 [341-568]	0.44 [0.34-0.54]	0.64 [0.51-0.79]	19.68 [16.84-22.94]
18	**PS**	4.26 [3.51-5.09]	476 [465-489]	0.63 [0.53-0.77]	1.05 [1.01-1.10]	23.52 [23.39-23.59]
	NAVA	4.13 [3.11-5.40]	429 [326-514]	0.65 [0.50-0.78]	0.87 [0.73-0.96]	24.63 [21.11-28.39]
19	**PS**	2.74 [1.46-4.56]	514 [406-586]	0.32 [0.20-0.48]	1.15 [0.80-1.43]	22.64 [22.41-23.33]
	NAVA	1.83 [1.49-2.24]	292 [241-336]	0.40 [0.32-0.47]	0.54 [0.48-0.61]	24.11 [21.57-27.75]
20	**PS**	1.73 [1.50-1.97]	445 [430-462]	0.54 [0.42-0.64]	1.03 [0.99-1.06]	18.57 [18.51-18.64]
	NAVA	2.31 [2.01-2.73]	432 [380-488]	0.67[0.58-0.75]	0.87 [0.79-0.98]	20.04 [18.12-21.96]
21	**PS**	2.55 [2.21-2.96]	836 [800-854]	0.87 [0.73-1.08]	1.16 [1.06-1.32]	14.99 [14.86-15.06]
	NAVA	2.59 [1.56-3.29]	758 [586-848]	0.71 [0.55-0.84]	0.92 [0.69-1.04]	19.61 [15.79-23.41]
22	**PS**	22.51 [17.90-25.43]	431 [399-460]	0.38 [0.32-0.45]	0.58 [0.53-0.62]	26.84 [26.78-26.91]
	NAVA	19.96 [17.25-22.44]	440 [394-478]	0.46 [0.40-0.52]	0.60 [0.54-0.63]	35.50 [33.09-37.84]

Table 6.3: Summary of ∫*Eadi*, *Vt*, $Ti_{\_Neural}$, *Ti* and *PIP* median [IQR]

		∫*Eadi* (μ*Vs*)	*Vt* (*ml*)	$Ti_{\_Neural}$ (*s*)	*Ti* (*s*)	*PIP* (cmH_2O)
Summary Median [IQR]	**PS**	4.10 [2.55 - 5.99]	468 [418 - 514]	0.97 [0.70 - 1.15]	0.97 [0.70 - 1.15]	21.44 [18.57 - 24.11]
	NAVA	3.97 [2.59 - 6.64]	431 [378 - 472]	0.80 [0.65 - 0.92]	0.80 [0.65 - 0.92]	21.63 [19.61 - 24.56]
p-value		>0.005	>0.005	>0.005	>0.005	>0.005

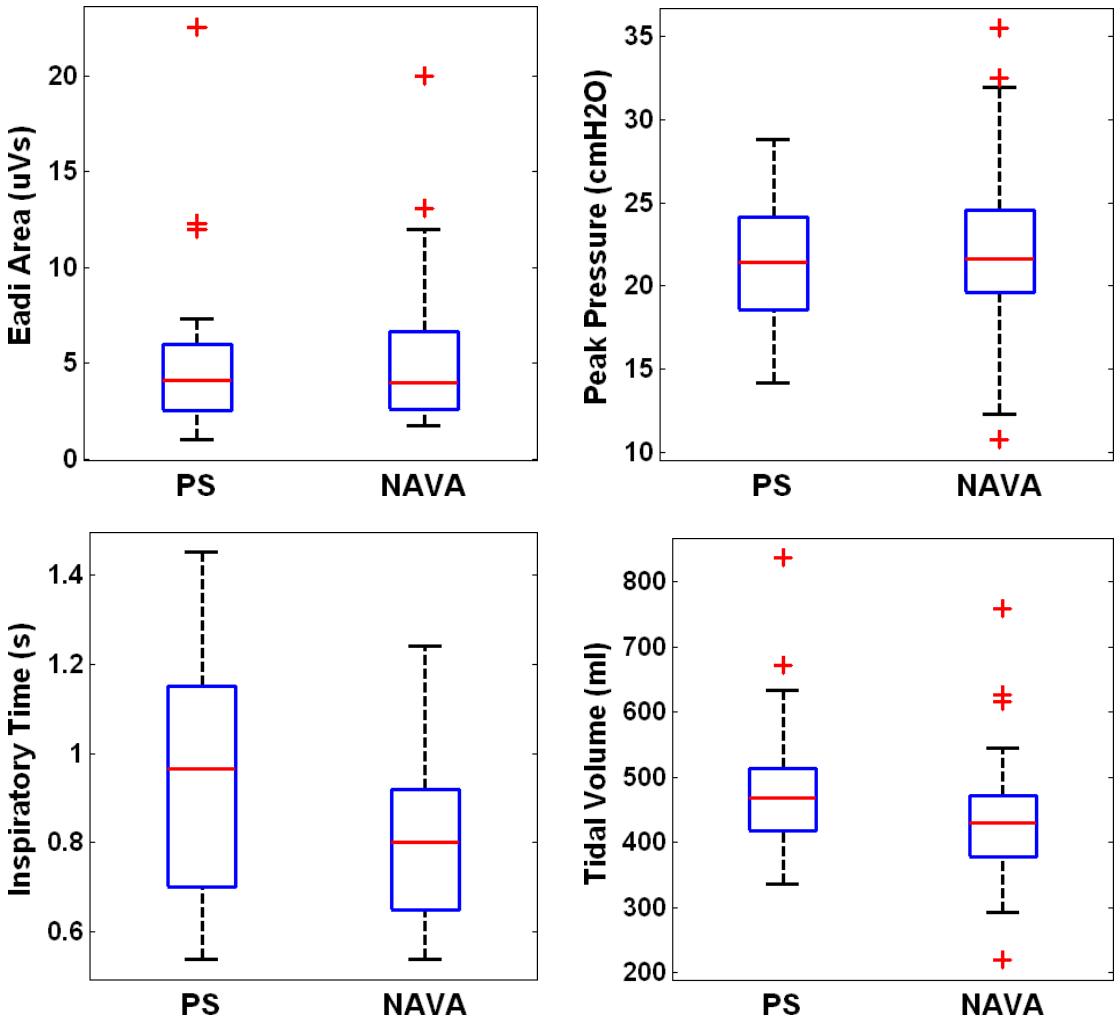

Figure 6.3: Summary of ∫*Eadi*, *Vt*, *Ti* and *PIP* for all 22 patients in PS and NAVA.

6.4.1 Correlation Analysis

Across all 22 patients, peak *Eadi* and ∫*Eadi* are correlated (median [IQR]) with R = 0.93 [IQR: 0.88-0.96] for PS and R = 0.87 [IQR: 0.78-0.90] for NAVA. The

correlation of ∫*Eadi* and *Vt* (median [IQR]) for PS is R = 0.50 [IQR: 0.05-0.65]. For NAVA, R = 0.85 [IQR: 0.78-0.90]. Peak *Eadi* and ∫*Eadi* were well correlated under both PS and NAVA ventilation modes. Hence, peak *Eadi* and ∫*Eadi* are essentially identical and could be used to characterize *Eadi* in future studies. ∫*Eadi* is used in this study instead of *Eadi* value in this study as it is more physiologically relevant as total inspiratory demand and readily calculated. Similarly, ∫*Eadi* and *Vt* were only moderately correlated for PS, whereas these parameters were strongly correlated under NAVA mode.

A two sample Kolmogorov-Smirnov hypothesis test shows that the NAVA and PS correlation datasets for ∫*Eadi* and *Vt* are significantly different ($p < 0.005$), illustrating the much better correlation seen for NAVA, which thus better matches these two variables than PS. Significantly better correlation between *Vt* and ∫*Eadi* under NAVA than PS, suggested that the delivered ventilation is possibly more physiological to the patient under NAVA than PS by better matching the patient's demand and its variability.

6.4.2 Variability Analysis

The non-parametric coefficients of variation (CVRs) in *Vt*, ∫*Eadi*, *Ti*, $Ti_{\_Neural}$ and *PIP* for the 22 patients are shown in Table 6.4. The PS and NAVA CVR in *Vt*, *Ti* and *PIP* are significantly different ($p < 0.005$), with the NAVA being more variable. Conversely, no significant difference was observed between ∫*Eadi* or $Ti_{\_Neural}$ CVR, with $p = 0.563$ and $p = 0.332$, respectively. More importantly, it should be noted that

these results are reported for the whole population of 22 patients. Individual patients could exhibit a very different variability between PS and NAVA, and the specific variables reported.

Table 6.4: Robust Coefficient of Variation (CVR) in *Vt*, *∫Eadi*, *Ti_Neural*, *Ti* and *PIP* (Median [IQR])

	Median [IQR]	
	PS	**NAVA**
∫Eadi	0.211 [0.140 - 0.326]	0.167 [0.153 - 0.272]
Vt	0.050 [0.029 - 0.077]*	0.111 [0.076 - 0.163]*
Ti_Neural	0.135 [0.093 - 0.203]	0.126 [0.094 - 0.200]
Ti	0.046 [0.031 - 0.082]*	0.093 [0.074 - 0.138]*
PIP	0.006 [0.003 - 0.008]*	0.103 [0.083 - 0.156]*

***** p-value < 0.005

As increased in variability has previously been associated with improved ventilation-perfusion ratio and improved oxygenation both in animal models (Gama de Abreu et al., 2008, Spieth et al., 2009a, Spieth et al., 2009b) and humans (Boker et al., 2004), the ability of NAVA in maintaining higher variability in tidal volume compared to PS could be of potential clinical interest and will require further investigation. Moreover, overall, it is hypothesized that greater variability in breathing pattern is a healthier patient condition. Thus, it is thought that better patient outcomes could be expected for those patients with a higher variability in *∫Eadi* when it is equally matched by a high variability in *Vt.* The results presented show that such a result is significantly more likely under NAVA than PS.

6.4.3 Patient Range90 Matching Analysis

For NAVA, the median [IQR; 5^{th}-95^{th} percentile] Range90 = 71.0 *ml/µVs* [IQR: 36.5-153.6; 15.0-531.3]. For PS, Range90 = 129.9 *ml/µVs* [IQR: 64.0-341.5; 19.2-645.2].

These results indicate significant variability in the matching of *Vt* and *∫Eadi* for both modes, but a consistently lower range for NAVA. The Range90 for both PS and NAVA in all patients are shown in Table 6.5.

Table 6.5: PS and NAVA Range90 (*ml*/*μVs*) for all patients

Patients	PS	NAVA	Range90 Ratio for PS/NAVA
1	111.3	76.0	1.47
2	644.4	153.6	4.20
3	330.6	219.0	1.51
4	21.2	17.1	1.24
5	78.2	55.6	1.41
6	64.0	19.9	3.22
7	593.3	515.5	1.16
8	285.2	183.9	1.56
9	42.1	23.2	1.82
10	124.9	103.1	1.22
11	36.0	26.4	1.37
12	62.5	36.5	1.72
13	323.2	50.9	6.35
14	523.1	154.8	3.38
15	125.4	55.8	2.25
16	77.5	44.4	1.75
17	341.5	108.8	3.14
18	134.1	78.4	1.72
19	646.0	76.8	8.42
20	187.8	66.0	2.85
21	375.7	554.9	0.68
22	16.4	11.8	1.39
Median [IQR]	129.8 [64.0 - 341.5]	71.0 [36.5 - 153.6]	1.72 [1.39 - 3.14]
5^{th}-95^{th}	[19.2 - 645.2]	[15.0 - 531.3]	[0.97 - 7.18]

The CDFs for the *Vt*/*∫Eadi* ratio for 3 specific patients, along with dashed lines indicating the Range90 value (5^{th} and 95^{th} percentile of *Vt*/*∫Eadi*) are shown in Figure 6.4. These three patients show a typical case where NAVA better matches *Vt* and *∫Eadi* than PS, the one case where PS better matches these variables than NAVA, and one case where they are similar showing the patient with ratio of Range90 values (PS/NAVA = 1.24) that is close to 1.0.

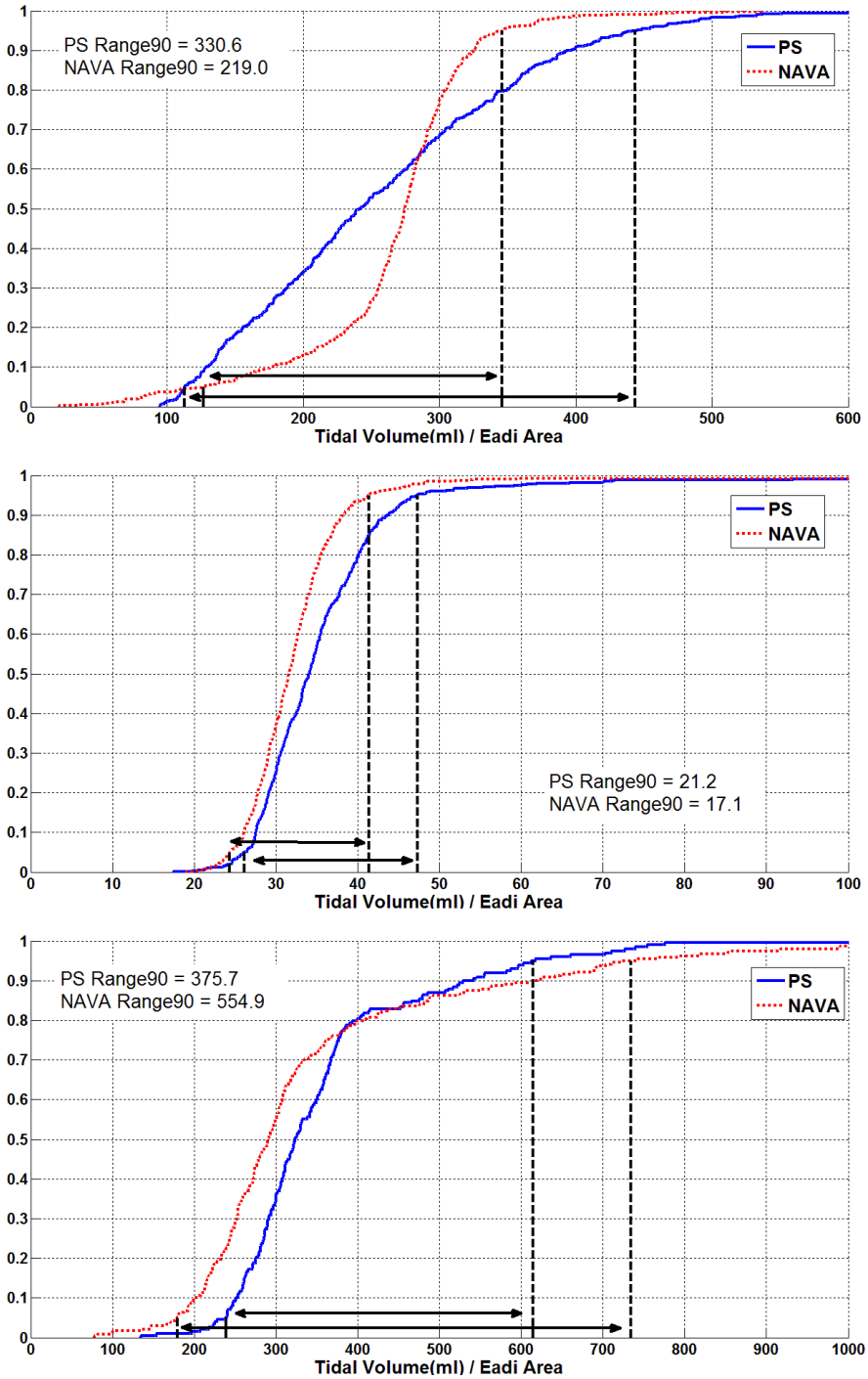

Figure 6.4: Cumulative distribution function (CDF) plots of $Vt/\int Eadi$ for both NAVA and PS for three patients. The CDFs show the ~300-500 such values per patient and mode. The dashed lines show the variability (along x-axis) in this ratio or matching, where a narrower band is a smaller Range90 value and thus better matching of Vt and $\int Eadi$. Panels: (Top) Patient 3: NAVA is better than PS; (Middle) Patient 4: NAVA and PS are similar; (Bottom) Patient 21: PS is better than NAVA.

Figure 6.5 shows the *Vt*-∫*Eadi* scatter plot for two patients, who are also shown in Figure 6.4. The results from these two patients highlight the differences in ability to match *Vt* to ∫*Eadi.* In particular, the figure plots ∫*Eadi* and *Vt* for each breath for both modes and each patient. Figure 6.5 (Top) shows a much higher *Vt* variability compared to PS. Patient 4 in Figure 6.5 (Bottom) had similar *Vt* variability when PS to NAVA. In these figures, it is clear that PS provides a far more constant range of *Vt* (Supply) despite similar variation in ∫*Eadi* for both ventilatory modes.

Range90 is a novel method of determining the matching using Neuroventilatory efficiency (*Vt*/∫*Eadi* ratio) for each breath in a patient. The resulting 90% range (Range90) value for each mode shows how well outcome *Vt* was matched by the ventilatory mode to inspiratory demand, ∫*Eadi.* A smaller Range90 indicates better matching and thus better response to variable demand with equally variable *Vt*. Thus, this approach thus provides a patient-specific comparison of which mode better matched *Vt* and ∫*Eadi.* Equally, the comparison of Range90 values for a given patient enable one to quantify how much better one mode matched inspiratory demand and resulting tidal volume.

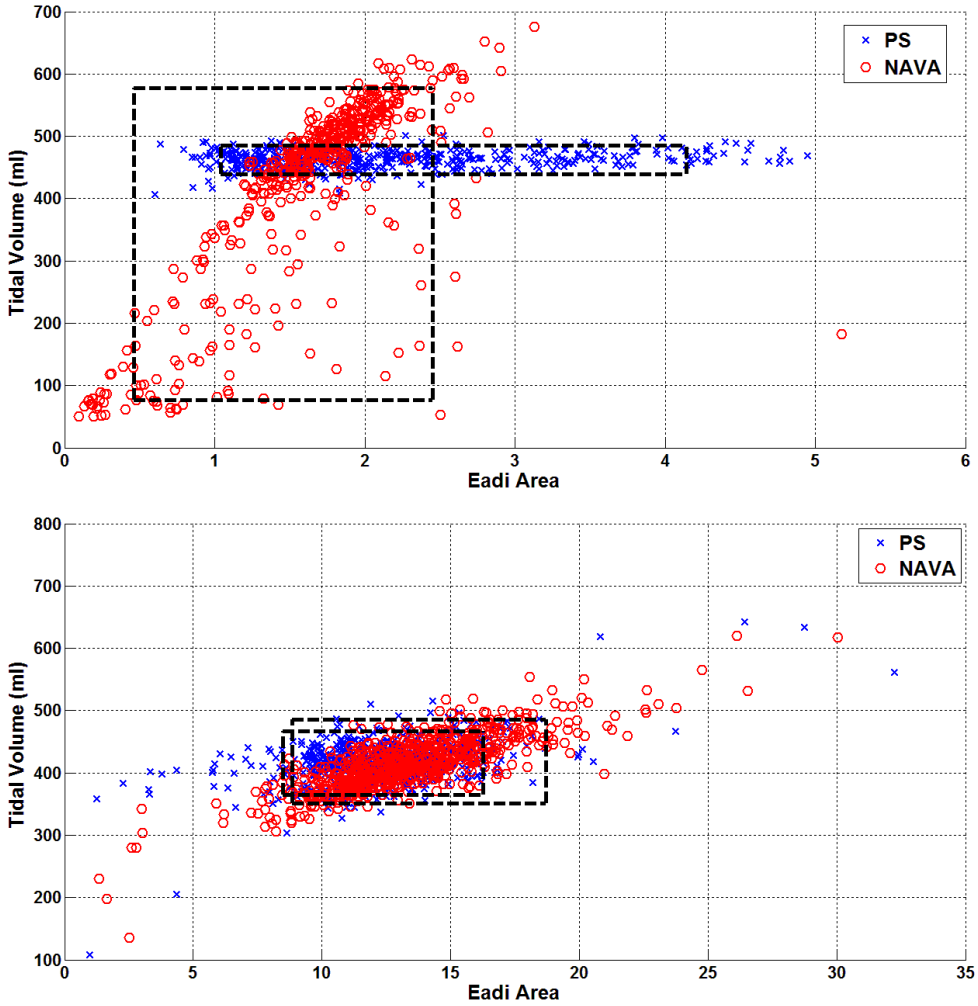

Figure 6.5: *Vt-∫Eadi* plots for NAVA and PS. (Top) Patient 3 with PS/NAVA ratio = 1.51. (Bottom) Patient 4 with PS/NAVA ratio = 1.24. The dashed lines around the data capture the middle 90% of the data for both *∫Eadi* and *Vt* for each mode. In both patients, the outcome tidal volume range for the middle 90% of breaths is 50-100 *ml* wide for PS and much wider for NAVA, despite similar input ranges of *∫Eadi*. The smaller ratio of width over height of the box between modes is similar to having a smaller Range90.

Examining the ratio of Range90 for PS/NAVA (Table 6.5), the median [IQR; 5^{th}-95^{th} percentile] of this ratio is 1.72 [IQR: 1.39-3.14; 0.97-7.18], showing that NAVA consistently had much smaller values than PS. The lower quartile of this Range90 ratio is [0.68-1.39], where only 1 patient had a value less than 1.0, at 0.68. These results show that 21 of 22 patients had better matching of *Vt* and *∫Eadi* for NAVA

than for PS. 4 patients had values greater than, but near to, 1.0, indicating relatively comparable matching of *Vt* and ∫*Eadi* between NAVA and PS.

Range90 values were significantly smaller in NAVA than in PS ($p < 0.005$). Of 22 patients, 21 had lower Range90 with NAVA, and only 1 showed a higher ratio with a better match of ∫*Eadi* and *Vt* by PS. Equally, the comparison of Range90 values showed that 4 of the 5 patients comprising the lowest quartile had values near to 1.0 with the 25^{th} percentile value showing the match of *Vt* and ∫*Eadi* was 1.40x better for NAVA than for PS in Range90 value. Hence, ventilation under NAVA is probably more physiological and adapted to the patient's inspiratory demand than under PS.

The importance of normalizing *Vt* variability to its ∫*Eadi* variability is highlighted when it is observed that although there is no significant difference in ∫*Eadi* variability over the population in Table 6.2 and Table 6.3. ∫*Eadi* can be substantially different between PS and NAVA on a patient-specific basis. Hence, the patient-specific comparisons of Range90 are particularly relevant, and, equally, account for all breaths directly rather than via a grouped statistic.

Correlation analysis was performed between Range90 with CVRs in ∫*Eadi* and *Vt*. For PS, correlation of coefficient R was 0.71 for ∫*Eadi*, and 0.67 for *Vt*, compared to NAVA, R = 0.16 for ∫*Eadi*, and 0.02 for *Vt*. These results indicated that Range90 is an alternate analysis different from variability analysis, and thus a higher variability does not necessarily mean better 'matching'.

The Range90 metric is very simple. Hence, the ventilator *Vt* in response to (not necessarily equally) patient's inspiratory demand can be calculated in real-time. Thus, it could be used to monitor response to ventilator settings and possibly (in future) adapt ventilator settings.

Overall, the results show that PS does not adapt or respond to $\int Eadi$ variation, as it provided relatively constant tidal volumes regardless of the magnitude of $\int Eadi$. This point is illustrated in Figure 6.4. In both cases of Figure 6.4, the range of tidal volumes seen is very narrow for PS, particularly relative to the $\int Eadi$ range. Thus, PS was unable to match *Vt* to the $\int Eadi$.

6.5 Limitations

6.5.1 Data Processing and Filtering

One possible limitation of this study is the definition of a minimum tidal volume that defines a breath versus an artefact, where those breaths with $Vt < 50$ *ml* were ignored. The selection was made through post hoc analysis of the *Vt* distribution indicating a bi-modal distribution, one mode representing physiological respiratory activity and a small mode ($Vt < 50ml$) likely corresponding to artefacts in *Eadi*. This statement is based on the observation that there was no significant ventilator pressurisation associated with *Vt* lower than 50 *ml*. A re-analysis of the data with a limit of 100 *ml* showed no change in the overall results, wherein NAVA provided a better match to patient variability in $\int Eadi$ for 21 of 22 patients, and the lower quartile still had a PS/NAVA ratio of 1.40. Thus, the analysis presented is robust to this choice of excluding breaths with $Vt < 50$ *ml*.

Range90 only considers the matching of *Vt* magnitude of a 'known' breathing cycle towards the corresponding ∫*Eadi*. Thus, if *Vt* > 50*ml* and ∫*Eadi* exist, it is used, and any asynchrony is seen as a mismatch of the *Vt* and ∫*Eadi* magnitude. If *Vt* < 50 *ml* and ∫*Eadi* exist, this information is not included. However, 300~500 'known' breathing cycles are analysed for every patient in each ventilation mode. An average of only 30 breaths of ~500 per patient (6%) was discarded in each phase. Thus, the loss of this potential data, assuming they are true breaths, is negligible.

6.5.2 Application of Range90

It is important to note that, while Range90 shows better matching in NAVA than PS, it is yet to be applied as a bedside monitoring tool. Range90 in this study used 20 minutes of breathing pattern of a patient in each ventilation mode, and the total duration for the study is not clinically feasible. In addition, the availability of *Eadi* signal for Range90 analysis is dependent on the availability of NAVA nasogastric tube. This study is a proof of concept and patient respiratory adaptation time to different ventilation mode was taken into consideration (Viale et al., 1998). Thus, the results indicate that the use of Range90 as a bedside monitoring tool warrants further investigation with shorter monitoring time.

6.5.3 Setting NAVA Gain 'Similar' to Pressure Support

Another limitation is that setting NAVA gain to obtain similar peak pressure as PS, is an approximation based on the built in previsualisation system and only one NAVA gain value is used to compare with PS. The amplitude of delivered pressure during NAVA is variable, as it is proportional to *Eadi* signal. Therefore, it is possible that the

delivered peak pressure may be higher or lower in different patients when comparing PS and NAVA. However, it was found that there was no significant difference between peak pressure between these two ventilation modes ($p > 0.005$) as shown in Table 6.3. Thus, for this cohort of 22 patients, the peak pressure in both modes can be considered as 'similar'.

6.6 Summary

Compared to PS, NAVA allowed better match between *Vt* and *Eadi* as well as higher variability in *Vt*. As higher variability has been associated with improved oxygenation and as higher variability is present in healthier systems, the ability of NAVA in not reducing patient's intrinsic variability could be of potential clinical interest. Studies on comparing patient-ventilator interaction on this cohort, mainly time asynchronies between PS and NAVA was also carried out and published elsewhere (Piquilloud et al., 2011b). Future work is needed to explore if there was a potential effect of this maintained variability obtained with NAVA on patients' outcome.

In this study, only one NAVA level and one PS level was tested and the influence of increasing NAVA level towards *Vt/Eadi* was not determined. The effect of *Vt* and *Eadi* related to increase in NAVA level have been extensively described by Passath et al. (Passath et al., 2010). Based on the results, we can assume that increasing NAVA level will result in a consecutive decrease in *Eadi* and in a small and only initial increase in *Vt*. As a consequence, we can assume that with increased NAVA level, *Vt/Eadi* ratio will also increase. This point is further explored in the next Chapter.

Chapter 7

Application of NAVA for the Noninvasively Ventilated Patients

Ventilation support can be delivered invasively or noninvasively. Non-invasive ventilation (NIV) is ventilator support delivered to the patient without the use of artificial airways such as endotracheal tube (ETT). NIV is widely used in cases of acute respiratory failure (Esteban et al., 2004) and for patients who are considered at risk of post-extubation respiratory failure (Ferrer et al., 2006). NIV is usually delivered in pressure support (PS) mode despite the poor synchronization observed in intensive care unit (ICU) patients (Vignaux et al., 2009). Neurally adjusted ventilatory assist (NAVA) has been shown to improve patient-ventilator interaction in comparison to PS both during invasive and non-invasive ventilation (Piquilloud et al., 2011b, Schmidt et al., 2012, Spahija et al., 2010, Colombo et al., 2008), and increases respiratory variability in comparison to PS (Schmidt et al., 2010), as seen in Chapter 6.

7.1 The NAVA Level Setting

NAVA triggers and cycles the ventilator based on the patient's diaphragmatic electrical activity (*Eadi*). The amount of pressure delivered by the ventilator is proportional to the *Eadi* amplitude (Sinderby et al., 1999). Clinicians can adapt the amount of assist delivered with NAVA by selecting a NAVA level corresponding to a

proportionality factor between instantaneously recorded *Eadi* and delivered pressure. However, common to all forms of PEEP and pressure selection, there is limited information on how to correctly set patient-specific NAVA level (Rozé et al., 2011, Brander et al., 2009, Barwing et al., 2011, Lecomte et al., 2009, Ververidis et al., 2011). Additionally, implementing the best described method at the bedside (Brander et al., 2009) is difficult, potentially limiting the daily use of NAVA. The best way to adapt NAVA level on a day-to-day basis for individual patients is also unknown. Moreover, it is likely that each patient responds differently to various NAVA levels, complicating NAVA selection even further, and creating a patient-specific problem subject to significant inter- and intra- patient variability.

The aims of this study were three-fold. The first goal was to study the matching analysis (Range90) for PS and NAVA during NIV similar to that for the invasive cases in Chapter 6. Second, is to assess the matching between patient-specific inspiratory demand (*Eadi*) with ventilatory supply, tidal volume (*Vt*) at different NAVA levels during NIV. And lastly, is to develop of a new physiological approach for titrating NAVA level settings to the individual patients in a consistent fashion.

7.2 Methodology

This study analyses *Eadi*-time, flow-time signal and derived parameters during NIV at three different NAVA levels. This study was conducted at the University hospital of Liege (Liege, Belgium) and Cliniques Universitaires Saint-Luc (Brussels, Belgium). Ethics Committees of University Hospital of Liege (Comité d'éthique du centre hospitalier universitaire de Liège) and the Ethics Committee of Cliniques

Universitaires Saint-Luc (Commission d'Ethique Biomédicale Hospitalo-Facultaire, Université catholique de Louvain, Faculté de Médecine) have approved the study protocol and use of the data.

7.2.1 Patients

The study cohort consisted of 13 noninvasively ventilated ICU patients (6 males and 7 females). Patients were included in the study if they required NIV because of acute respiratory failure or were at risk of developing respiratory failure after extubation. The specific exclusion criteria were: 1) Severe hypoxemia requiring $FiO_2 > 0.7$; 2) Hemodynamic instability; 3) Patient with a hiatal hernia or other oesophageal problem; upper gastrointestinal bleeding or any other contraindication to the insertion of a nasogastric tube; 4) Poor short term prognosis; and 5) Age < 18 years old. A summary of the patient demographic, clinical diagnosis and the detail ventilator settings for each patient is shown in Table 7.1 (Piquilloud et al., 2012).

7.2.2 Ventilator and Delivered Ventilation

All patients were ventilated with Servo-I ventilators (Maquet, Solna, Sweden) equipped with a commercially available NAVA module and software version 5.0. NIV was delivered though oronasal facemasks (Vygon SA, Ecouen, France) tightly attached to the patient in order to minimise the leaks.

Table 7.1: Patient demographic and ventilator settings

Patients	Gender	Age (years)	BMI	SAPSII Score*	Clinical Diagnosis	FiO_2	PEEP (cmH_2O)	Inspiratory Trigger	P Slope* (ms)	PS Level* (cmH_2O)	ETS* (%)	NAVA Level (uV/cmH_2O)
1	F	62	20.27	33	Exacerbation of COPD*	0.25	5	Flow	150	9	40	0.2
2	F	69	36.73	26	Pneumonia	0.30	7	Flow	150	10	30	0.6
3	F	70	22.48	31	Acute bronchospasm	0.30	7	Flow	150	8	55	0.2
4	F	56	16.7	33	Exacerbation of COPD	0.30	5	Flow	150	12	45	0.2
5	M	64	22.49	54	Acute renal failure	0.50	5	Pressure/ Flow	150	12	30	0.8
6	F	68	23.44	33	Asthma	0.25	9	Flow	150	9	30	0.4
7	M	75	26.12	34	Sepsis	0.40	6	Flow	150	10	30	0.6
8	M	87	23.67	28	Exacerbation of COPD	0.23	5	Flow	150	12	30	0.8
9	M	72	40.04	29	Exacerbation of COPD	0.30	7	Flow	2000	12	50	0.4
10	M	87	27.68	30	Exacerbation of COPD	0.21	6	Flow	50	11	45	0.4
11	F	64	29.14	29	Cardiogenic pulmonary edema	0.40	5	Flow	200	5	50	1.0
12	F	79	27.97	30	Pneumonia	0.70	5	Flow	200	10	50	1.0
13	M	78	27.70	34	Drug intoxication	0.40	5	Flow	350	10	25	0.5
Median		70	26.12	31		0.30	5		150	10	40	0.5
25^{th}		64	22.49	29		0.25	5		150	9	30	0.4
75^{th}		78	28.26	33		0.40	7		200	12	50	0.8

* SAPSII - Simplified acute physiology score, P Slope - Pressurization slope, PS Level - Pressure support level, ETS - Expiratory Trigger Sensitivity, COPD - Chronic obstruct pulmonary disease, SIRS - Systematic inflammation response syndrome

7.2.3 Study Protocol and Recordings

The clinical protocol consisted of two phases. Phase 1 compares the Range90 matching between PS and NAVA during NIV. Phase 2 investigates the effect of NAVA levels to patient's Range90 matching and specific response to each level. Both protocols record the patient's *Eadi* and airway pressure and flow signals using the Servo-I ventilator, sampled at 100Hz using Servo-tracker V4.0 software (Maquet, Solna, Sweden). Positive end-expiratory pressure (PEEP), FiO_2 and inspiratory trigger settings were maintained constant across PS and each NAVA level for a given patient.

7.2.3.1 Phase 1 - PS and NAVA

After written informed consent was obtained, the patient's standard nasogastric tube was replaced by NAVA tube. For each patient, 20 minutes of continuous recording (~300-500 breaths) was carried out at PS. After PS, the ventilation mode was changed to NAVA for further 20 minutes. This NAVA level was set to have similar peak airway pressure (*PIP*) as in PS mode using the previsualization system included with the ventilator.

7.2.3.2 Phase 2 - Various NAVA Levels

The NAVA level set to have similar peak airway pressure as PS is denoted NAVA100. Two additional NAVA levels after NAVA100, denoted NAVA50 and NAVA150, that modified the initial NAVA level by ±50% were also used. Each additional NAVA level was maintained for additional 15 minutes of breathing and continuous recordings. NAVA50 was set by adjusting the NAVA100 level by -50% and NAVA150 was set by +50% of NAVA100 level. The order of NAVA50 and

NAVA150 recording were not standardised. While changing PS to NAVA, the initial NAVA level during NAVA100 can be either very low or high. Thus, a change of ±50% is used rather than a specific change of an absolute value. The exact changes are thus patient-specific. Patient 3 was excluded from Phase 2 trial. After Phase 1 trial, Patient 3 was intubated due to worsening of respiratory failure and thus was excluded from Phase 2 trial.

7.2.4 Data Analysis

Studies comparing patient-ventilator interaction for these patients assessing time asynchrony between PS and NAVA during NIV is presented elsewhere (Piquilloud et al., 2012).

7.2.4.1 Statistical and Correlation Analysis

Inspiratory demand, $\int Eadi$, ventilator tidal volume, Vt, neural inspiratory time, $Ti_{\_Neural}$, inspiratory time, Ti and peak inspiratory pressure, PIP are calculated for every breath during PS and at each NAVA level. Breaths with $Vt < 50\ ml$ were discarded from analysis based on post hoc analysis of the Vt distribution suggesting that breaths with $Vt < 50\ ml$ likely corresponded to measurement artefacts (Moorhead et al., 2012).

The median value of the distributions of $\int Eadi$, Vt, $Ti_{\_Neural}$, Ti and PIP at PS and 3 different NAVA levels were compared using the non-parametric Wilcoxon rank-sum test as they were not normally distributed. A Pearson's correlation analysis was carried out for Vt with $\int Eadi$ at different NAVA levels. Non-parametric Robust

coefficient of variation (CVR = median absolute deviation/ median) was calculated to assess and compare variability analysis in each parameter.

7.2.4.2 Range90 Matching and Patient-Specific Comparison

The 5^{th}-95^{th} range of $Vt/\int Eadi$ (Neuroventilatory efficiency (Passath et al., 2010)), Range90 is calculated for each patient in both PS and every NAVA level for comparison. A smaller value of Range90 indicates consistently better matching of *Vt* to $\int Eadi$. Patients with larger values of Range90 have a higher incidence of inconsistent $Vt/\int Eadi$ breaths, which is a lesser ability to match *Vt* and $\int Eadi$, regardless of the patient-specific $\int Eadi$. The detail description of Range90 can be found in Chapter 6 and Appendix 02.

Thus, the ratio of $Vt/\int Eadi$ for each breath and the analysis of its distribution (Range90) over a given NAVA settings for a single patient enable a fair comparison between different NAVA levels. This simple metric can be readily calculated in real-time to monitor patient-specific response to different NAVA levels. Hence, it may provide a simple solution to titrate NAVA level.

7.3 Results and Discussion

7.3.1 Phase 1 - Ventilation Matching in PS and NAVA

The NIV patients' $\int Eadi$, *Vt*, $Ti_{\_Neural}$, *Ti* and *PIP* at each NAVA and summary are presented in Table 7.2 and Table 7.3. Similar to the findings for invasive ventilation in Chapter 6, there is no significance difference in medians of $\int Eadi$, *Vt*, $Ti_{\_Neural}$, *Ti*

and *PIP* between PS and NAVA. While there is no significant difference in median values, individual patients had very different, patient-specific outcomes comparing NAVA and PS.

Table 7.2: $\int Eadi$, *Vt*, $Ti_{\_Neural}$, *Ti* and peak pressure of the 13 NIV patients

Patients		$\int Eadi(\mu Vs)$	*Vt (ml)*	$Ti_{\_Neural}$ *(s)*	*Ti (s)*	$PIP(cmH_2O)$
1	**PS**	21.3 [18.5-24.2]	433 [401-468]	0.50 [0.43-0.56]	0.64 [0.60-0.68]	15.4 [15.3-15.5]
	NAVA	23.7 [21.2-26.5]	444 [404-490]	0.62 [0.56-0.65]	0.72 [0.70-0.78]	16.4 [15.3-17.9]
2	**PS**	9.6 [7.0-11.9]	495 [460-523]	0.49 [0.45-0.53]	0.65 [0.63-0.68]	18.7 [18.6-18.8]
	NAVA	9.9 [7.8-11.7]	471 [389-544]	0.62 [0.57-0.68]	0.78 [0.72-0.84]	21.3 [18.9-24.3]
3	**PS**	12.2 [11.1-12.9]	406 [391-422]	0.50 [0.46-0.54]	0.57 [0.55-0.58]	15.8 [15.8-15.8]
	NAVA	15.9 [14.2-17.6]	394 [372-418]	0.55 [0.49-0.60]	0.69 [0.65-0.74]	15.3 [14.7-16.1]
4	**PS**	24.0 [20.2-28.9]	394 [343-448]	0.52 [0.46-0.59]	0.63 [0.56-0.70]	17.9 [17.8-18.0]
	NAVA	22.7 [19.5-25.7]	372 [339-406]	0.52 [0.48-0.59]	0.69 [0.63-0.73]	17.3 [16.2-18.5]
5	**PS**	8.4 [4.0-13.5]	714 [689-759]	0.75 [0.71-0.80]	0.95 [0.89-1.02]	18.5 [18.4-18.6]
	NAVA	8.0 [6.5-10.4]	738 [671-810]	0.72 [0.68-0.77]	0.84 [0.80-0.89]	19.8 [17.2-22.6]
6	**PS**	17.4 [15.6-19.2]	545 [532-561]	0.29 [0.26-0.33]	0.53 [0.52-0.54]	19.6 [19.5-19.7]
	NAVA	13.9 [10.4-16.1]	631 [594-675]	0.40 [0.36-0.44]	0.54 [0.50-0.57]	27.3 [25.1-29.5]
7	**PS**	9.7 [8.8-10.7]	644 [630-663]	0.46 [0.43-0.49]	0.60 [0.59-0.61]	17.9 [17.7-18.1]
	NAVA	9.8 [8.9-10.7]	688 [657-718]	0.51 [0.47-0.55]	0.65 [0.62-0.67]	23.2 [21.9-24.5]
8	**PS**	14.1 [10.2-17.7]	732 [671-818]	0.71 [0.60-0.78]	0.94 [0.89-1.00]	18.5 [18.3-20.4]
	NAVA	15.0 [13.1-17.4]	741 [653-833]	0.81 [0.72-0.88]	0.98 [0.91-1.05]	25.0 [22.2-27.9]
9	**PS**	17.7 [14.2-20.8]	496 [455-537]	0.72 [0.62-0.86]	0.73 [0.65-0.86]	19.6 [19.4-19.8]
	NAVA	41.1 [31.2-51.3]	646 [451-862]	1.65 [1.33-1.91]	1.89 [1.60-2.10]	22.5 [19.9-24.9]
10	**PS**	15.9 [12.8-18.6]	614 [558-672]	0.41 [0.35-0.46]	0.53 [0.48-0.58]	18.6 [18.4-18.8]
	NAVA	13.5 [9.5-18.8]	531 [404-657]	0.51 [0.41-0.65]	0.67 [0.55-0.80]	21.5 [17.5-24.0]
11	**PS**	21.4 [4.0-48.1]	341 [112-720]	0.61 [0.29-1.01]	0.95 [0.46-1.35]	10.6 [9.9-11.1]
	NAVA	24.3 [7.6-39.9]	487 [244-908]	0.92 [0.53-1.23]	1.15 [0.74-1.44]	13.2 [11.8-14.4]
12	**PS**	4.6 [2.6-6.4]	528 [489-560]	0.69 [0.60-0.74]	0.71 [0.66-0.76]	14.9 [14.5-15.1]
	NAVA	10.1 [7.5-13.4]	653 [585-726]	0.90 [0.80-1.00]	1.08 [0.98-1.15]	22.3 [18.7-25.9]
13	**PS**	6.3 [3.9-9.4]	630 [475-794]	0.52 [0.37-0.70]	1.37 [0.86-1.96]	13.4 [12.5-14.1]
	NAVA	6.7 [3.3-10.7]	457 [250-613]	0.64 [0.50-0.82]	0.87 [0.69-1.05]	8.1 [6.7-9.5]

Table 7.3: Summary of $\int Eadi$, *Vt*, $Ti_{\_Neural}$, *Ti* and peak pressure median [IQR]

		$\int Eadi(\mu Vs)$	*Vt (ml)*	$Ti_{\_Neural}$ *(s)*	*Ti (s)*	$PIP(cmH_2O)$
Median of Medians [IQR]	**PS**	14.1 [9.3-18.6]	528 [426-634]	0.52 [0.48-0.70]	0.65 [0.59-0.94]	17.9 [15.3-18.6]
	NAVA	13.9 [9.9-23.0]	531 [454-662]	0.62 [0.52-0.83]	0.78 [0.69-1.01]	21.3 [16.1-22.7]
p-value		> 0.005	> 0.005	> 0.005	> 0.005	> 0.005

Table 7.4 shows the Range90 for these 13 NIV patients during PS and NAVA. Overall, 11 of the 13 patients included in the study showed better matching (Lower

Range90) during NAVA than in PS. Patient 4 and Patient 6 had PS/ NAVA Range90 ratios of < 1.00 suggesting that both these patients have lesser matching during NAVA. Equally, Patient 3 has Range90 ratio 1.21, and will not benefit much in terms of matching supply and demand matching when changing from PS to NAVA, so performance is effectively equivalent.

Table 7.4: PS and NAVA Range90 (*ml/µVs*) for all 13 NIV patients

Patients	PS	NAVA	Range90 Ratio PS/NAVA
1	15.3	8.5	1.80
2	129.5	38.4	3.37
3	14.5	12.0	1.21
4	9.3	16.0	0.58*
5	239.0	110.9	2.16
6	24.3	84.0	0.29*
7	34.6	22.9	1.51
8	123.4	24.9	4.96
9	35.0	12.4	2.82
10	42.4	19.9	2.13
11	354.5	47.2	7.51
12	549.3	97.7	5.62
13	445.8	141.8	3.14
Median [IQR]	42.4 [22.1-267.9]	24.9 [15.1-87.43]	2.15 [1.44-3.77]

*Lower Range90 in PS than in NAVA

Similar to results observed in invasively ventilated patients in Chapter 6, NAVA consistently showed lower Range90 (better matching) than PS. Range90 results from IV and NIV patients (Table 6.5 and Table 7.4) for both PS and NAVA are summarised in Figure 7.1. Patient markers below the 1:1 ratio trend line showed better matching during NAVA ventilation. Only 3 of 35 patients from the two different cohorts (IV Patient 21, NIV Patient 4 and NIV Patient 6) had better matching during PS, as shown in Figure 7.1.

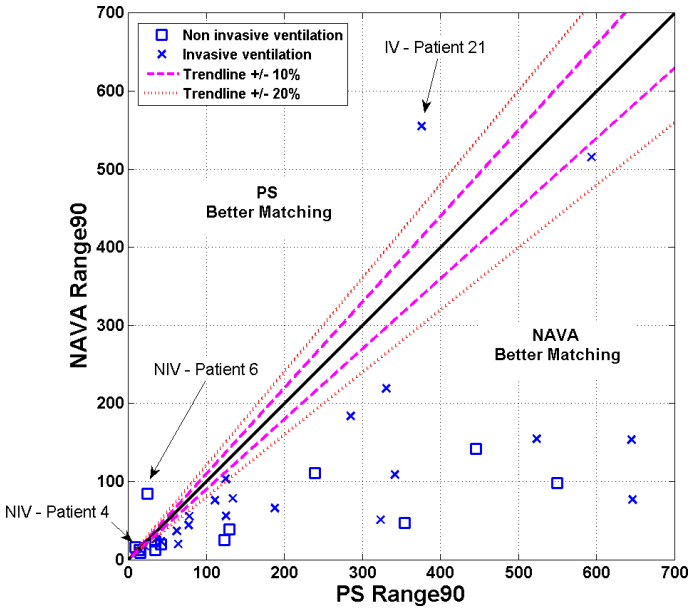

Figure 7.1: Comparing Range90 in PS and NAVA for 22 patients during invasive ventilation and 13 patients during non-invasive ventilation.

It is important to note that the underlying ∫*Eadi* can be very different for every patient. The magnitude of the *Eadi* signal is dependent on the position of the NAVA tube resulting in variable range of *Eadi*. This difference indirectly affects *Vt*/∫*Eadi* ratio. Therefore, inter-patient comparison may not be completely suitable. However, the trends comparing PS and NAVA are clear. Equally, while small difference may not be significant, larger ones show a clear result when comparing patients.

The NAVA level was set to ensure the maximum *PIP* is similar to the *PIP* during PS. However, it was found that some patients still had significantly different *PIP* from NAVA than during PS, suggesting that shifting PS to NAVA may affect patients underlying *Eadi*, resulting in different support expected from NAVA. This finding further verified the limitation pointed out in Chapter 6, questioning the comparison between the 'correct NAVA level' to the associated PS setting. Thus, setting the optimal pressure support remains debatable, and the 'simplest' method of NAVA

level setting is using the previsualisation software (Moorhead et al., 2012). Thus, the previsualisation method is currently, the only method of comparing PS and NAVA setting. Titration of an optimal NAVA pressure level thus warrants further investigation (Brander et al., 2009) as is the cases for almost all forms of PEEP and pressure support.

7.3.2 Phase 2 - Various NAVA Levels

7.3.2.1 Effect of NAVA Levels towards Patients

In this section, NIV patients' ∫*Eadi*, *Vt*, $Ti_{\_Neural}$, *Ti*, *PIP* and duty cycles (*Ti/Ttot = inspiratory time / total time for inspiratory and expiratory*) during different NAVA levels are compared (Tables 7.5-7.10). The summary of these parameters is presented in Table 7.11. Note that Patient 3 is excluded for the NAVA level comparison in Tables 7.5-7.10 for clinical reasons. Patient 3 did not complete the study due to worsening of respiratory failure.

Table 7.5: Patient's inspiratory demand (∫*Eadi*)

Patient	∫*Eadi* (*uVs*), Median [IQR]		
	NAVA50	NAVA100	NAVA150
1	24.5 [21.2-27.6]	23.7 [21.2-26.5]	19.1 [16.4-22.4]*+
2	11.3 [8.1-13.9]	9.9 [7.8-11.7]*	6.9 [5.1-9.0]*+
4	22.6 [17.1-25.6]	22.7 [19.5-25.7]	21.2 [18.3-23.8]+
5	10.1 [8.7-11.5]	8.0 [6.5-10.4]*	8.6 [5.6-10.3]*
6	15.8 [14.5-17.7]	13.9 [10.4-16.1]*	15.2 [12.9-17.3]*+
7	10.5 [9.8-11.4]	9.8 [8.9-10.7]*	9.0 [8.1-9.8]*+
8	23.3 [19.8-25.9]	15.0 [13.1-17.4]*	9.9 [8.3-11.7]*+
9	31.5 [26.3-36.3]	41.1 [31.2-51.3]*	16.6 [14.0-19.1]*+
10	21.1 [15.9-28.6]	13.5 [9.5-18.8]*	13.7 [9.3-18.9]*
11	50.9 [31.5-61.9]	24.3 [7.6-39.9]*	54.9 [36.0-62.9]+
12	8.3 [5.2-11.6]	10.1 [7.5-13.4]*	5.9 [4.0-8.7]*+
13	4.2 [2.4-7.7]	6.7 [3.3-10.7]*	5.3 [2.6-8.5]+
Median of Medians [IQR]	18.5 [10.3-23.9]	13.7 [9.9-23.2]	11.8 [7.8-17.9]

** p<0.005 compared to NAVA50, + p<0.005 compared to NAVA100*

Table 7.6: Ventilatory tidal volume (*Vt*)

Patient	*Vt* (*ml*), Median [IQR]		
	NAVA50	**NAVA100**	**NAVA150**
1	526 [435-564]	444 [404-490]*	474 [424-541]*+
2	450 [379-524]	471 [389-544]	481 [399-586]*
4	324 [294-345]	372 [339-406]*	416 [379-450]*+
5	654 [597-698]	738 [671-810]*	788 [584-895]*
6	549 [525-578]	631 [594-675]*	727 [679-764]*+
7	596 [574-621]	688 [657-718]*	763 [725-802]*+
8	608 [518-689]	741 [653-833]*	715 [605-836]*
9	522 [468-559]	646 [451-862]*	621 [544-696]*
10	523 [411-660]	531 [404-657]	664 [466-854]*+
11	496 [343-705]	487 [244-908]	485 [354-689]
12	543 [486-610]	653 [585-726]*	638 [553-688]*+
13	270 [179-391]	457 [250-613]*	413 [208-708]*
Median of Medians [IQR]	525 [473-573]	581 [464-671]	630 [478-721]

* *p<0.005 compared to NAVA50, + p<0.005 compared to NAVA100*

Table 7.7: Neural inspiratory time (*Ti*)

Patient	*Ti_Neural* (second), Median [IQR]		
	NAVA50	**NAVA100**	**NAVA150**
1	0.68 [0.61-0.75]	0.62 [0.56-0.65]*	0.61 [0.54-0.65]*+
2	0.64 [0.58-0.68]	0.62 [0.57-0.68]	0.59 [0.53-0.66]*+
4	0.54 [0.48-0.59]	0.52 [0.48-0.59]	0.53 [0.49-0.60]
5	0.78 [0.74-0.82]	0.72 [0.68-0.77]*	0.74 [0.62-0.82]*
6	0.40 [0.36-0.43]	0.40 [0.36-0.44]	0.40 [0.36-0.44]
7	0.52 [0.48-0.56]	0.51 [0.47-0.55]*	0.50 [0.46-0.56]*
8	0.94 [0.85-1.04]	0.81 [0.72-0.88]*	0.77 [0.66-0.85]*+
9	1.63 [1.39-1.76]	1.65 [1.33-1.91]	1.25 [1.08-1.48]*+
10	0.58 [0.48-0.73]	0.51 [0.41-0.65]*	0.49 [0.40-0.64]*
11	1.32 [0.98-1.52]	0.92 [0.53-1.23]*	1.27 [1.03-1.49]+
12	0.86 [0.78-0.92]	0.90 [0.80-1.00]*	0.90 [0.80-0.98]*
13	0.77 [0.59-0.93]	0.64 [0.50-0.82]*	0.70 [0.53-0.89]+
Median of Medians [IQR]	0.73 [0.56-0.90]	0.63 [0.52-0.86]	0.66 [0.52-0.84]

* *p<0.005 compared to NAVA50, + p<0.005 compared to NAVA100*

Table 7.8: Inspiratory time (*Ti*)

Patient	*Ti* (second), Median [IQR]		
	NAVA50	**NAVA100**	**NAVA150**
1	0.86 [0.77-0.95]	0.72 [0.70-0.78]*	0.73 [0.69-0.77]*
2	0.78 [0.73-0.83]	0.78 [0.72-0.84]	0.74 [0.68-0.81]*+
4	0.70 [0.64-0.74]	0.69 [0.63-0.73]	0.70 [0.65-0.75]
5	0.90 [0.87-0.94]	0.84 [0.80-0.89]*	0.87 [0.77-0.96]*
6	0.55 [0.51-0.57]	0.54 [0.50-0.57]	0.55 [0.51-0.57]
7	0.65 [0.63-0.67]	0.65 [0.62-0.67]	0.65 [0.62-0.67]
8	1.10 [1.00-1.20]	0.98 [0.91-1.05]*	0.96 [0.86-1.02]*
9	1.78 [1.58-1.94]	1.89 [1.60-2.10]	1.57 [1.35-1.80]*+
10	0.73 [0.63-0.89]	0.67 [0.55-0.80]*	0.62 [0.53-0.81]*
11	1.55 [1.35-1.71]	1.15 [0.74-1.44]*	1.55 [1.28-1.71]+
12	1.01 [0.94-1.06]	1.08 [0.98-1.15]*	1.06 [0.99-1.12]*
13	0.98 [0.82-1.12]	0.87 [0.69-1.05]*	0.93 [0.75-1.15]+
Median of Medians [IQR]	0.88 [0.72-1.06]	0.81 [0.68-1.03]	0.81 [0.68-1.01]

** p<0.005 compared to NAVA50, + p<0.005 compared to NAVA100*

Table 7.9: Peak inspiratory pressure (*PIP*)

Patient	Peak Pressure (cmH_2O), Median [IQR]		
	NAVA50	**NAVA100**	**NAVA150**
1	11.5 [10.6-12.6]	16.4 [15.3-17.9]*	18.7 [17.2-20.7]*+
2	17.1 [14.9-19.2]	21.3 [18.9-24.3]*	23.3 [19.8-27.0]*+
4	12.1 [11.4-12.9]	17.3 [16.2-18.5]*	21.6 [20.2-23.4]*+
5	14.4 [13.1-15.4]	19.8 [17.2-22.6]*	25.4 [20.7-28.6]*+
6	20.1 [19.1-21.1]	27.3 [25.1-29.5]*	35.2 [33.4-35.7]*+
7	16.9 [16.1-17.9]	23.2 [21.9-24.5]*	28.1 [26.3-30.3]*+
8	20.2 [17.4-23.3]	25.0 [22.2-27.9]*	26.4 [21.1-31.0]*+
9	16.2 [14.7-17.0]	22.5 [19.9-24.9]*	21.8 [20.4-24.7]*
10	18.1 [15.9-19.9]	21.5 [17.5-24.0]*	28.4 [22.4-33.0]*+
11	13.2 [12.9-13.8]	13.2 [11.8-14.4]	11.5 [10.7-11.8]*+
12	15.5 [12.9-18.9]	22.3 [18.7-25.9]*	20.6 [17.1-25.8]*+
13	5.9 [5.6-6.6]	8.1 [6.7-9.5]*	7.1 [5.9-8.3]*+
Median of Medians [IQR]	15.9 [12.7-17.6]	21.4 [16.9-22.9]*	22.6 [19.7-27.3]*

** p<0.005 compared to NAVA50, + p<0.005 compared to NAVA100*

Table 7.10: Duty cycle (*Ti/Ttot*)

Patient	Duty Cycle (Ti/Ttot), Median [IQR]		
	NAVA50	**NAVA100**	**NAVA150**
1	0.35 [0.27-0.48]	0.35 [0.33-0.37]	0.34 [0.30-0.36]*+
2	0.41 [0.39-0.44]	0.40 [0.38-0.43]*	0.39 [0.36-0.41]*+
4	0.32 [0.30-0.37]	0.31 [0.29-0.34]*	0.30 [0.29-0.33]*+
5	0.42 [0.40-0.43]	0.40 [0.39-0.42]*	0.42 [0.40-0.71]+
6	0.29 [0.28-0.31]	0.29 [0.27-0.31]*	0.31 [0.29-0.32]*+
7	0.40 [0.38-0.41]	0.36 [0.35-0.38]*	0.37 [0.35-0.38]*+
8	0.40 [0.36-0.52]	0.41 [0.36-0.59]	0.36 [0.32-0.59]*+
9	0.40 [0.37-0.46]	0.39 [0.35-0.45]	0.37 [0.32-0.41]*+
10	0.37 [0.29-0.43]	0.38 [0.31-0.43]	0.38 [0.33-0.42]
11	0.35 [0.31-0.48]	0.41 [0.31-0.70]	0.33 [0.30-0.41]*+
12	0.40 [0.38-0.43]	0.39 [0.37-0.41]*	0.39 [0.37-0.42]*
13	0.43 [0.32-0.96]	0.33 [0.25-0.77]*	0.33 [0.26-0.77]*
Median of Medians [IQR]	0.40 [0.35-0.41]	0.39 [0.34-0.40]	0.37 [0.33-0.39]

** p<0.005 compared to NAVA50, + p<0.005 compared to NAVA100*

Table 7.11: Summary of *∫Eadi*), *Vt*, *Ti_Neural*, *Ti*, *PIP* and *Ti/Ttot*

	Median of Medians [IQR]		
	NAVA50	**NAVA100**	**NAVA150**
***∫Eadi* (μVs)**	18.5 [10.3-23.9]	13.7 [9.9-23.2]	11.8 [7.8-17.9]
***Vt* (*ml*)**	525 [473-573]	581 [464-671]	630 [478-721]
***Ti_Neural* (second)**	0.73 [0.56-0.90]	0.63 [0.52-0.86]	0.66 [0.52-0.84]
***Ti* (second)**	0.88 [0.72-1.06]	0.81 [0.68-1.03]	0.81 [0.68-1.01]
***PIP* (cmH_2O)**	15.9 [12.7-17.6]	21.4 [16.9-22.9]*	22.6 [19.7-27.3]*

** p<0.005 compared to NAVA50, + p<0.005 compared to NAVA100*

Overall, it is observed that NAVA50 had higher $\int Eadi$ = 18.5 μVs [IQR: 10.4-23.6] with lower tidal volume, Vt = 525 ml [IQR: 485-561] corresponding to PIP = 16.20 cmH_2O [IQR: 12.7-17.6]. In contrast, NAVA150 had slightly lower $\int Eadi$ (11.8 μVs [IQR: 8.2-17.2]) and higher Vt (630 ml [IQR: 479-718]) with PIP = 22.6cmH_2O [20.1-26.8]. However, only PIP was found with significant difference ($p < 0.005$), given the low number of patient and comparing the medians. The effect of NAVA levels towards Vt and $\int Eadi$ distribution is further illustrated in Figure 7.2 (Top and middle panel). The boxed areas in Figure 7.2 showed the 5^{th}-95^{th} range of patients corresponding Vt and $\int Eadi$. These two panels showed examples of a NAVA50 Vt-$\int Eadi$ plot having overall lowest Vt and highest $\int Eadi$, NAVA150 had overall higher Vt and lower $\int Eadi$, and NAVA100 is located in between. These results clearly show the effect of NAVA level towards patient $\int Eadi$, while maintaining Vt variability.

Median inspiratory time for NAVA50 is slightly higher at 0.88 s [IQR: 0.72-1.03] ($p < 0.005$ for 7 patients in NAVA100 and 7 patients in NAVA150, when compared to NAVA50). The patients neural inspiratory time is also higher during NAVA50 with 0.73 s [0.56-0.90] compared to other NAVA levels ($p < 0.005$ for 8 patients in NAVA100 and 8 patients in NAVA150, when compared to NAVA50). There was no significant difference between the medians of these data. However, individually, more than half of the patients included in the study had shown significant difference in each tested parameters.

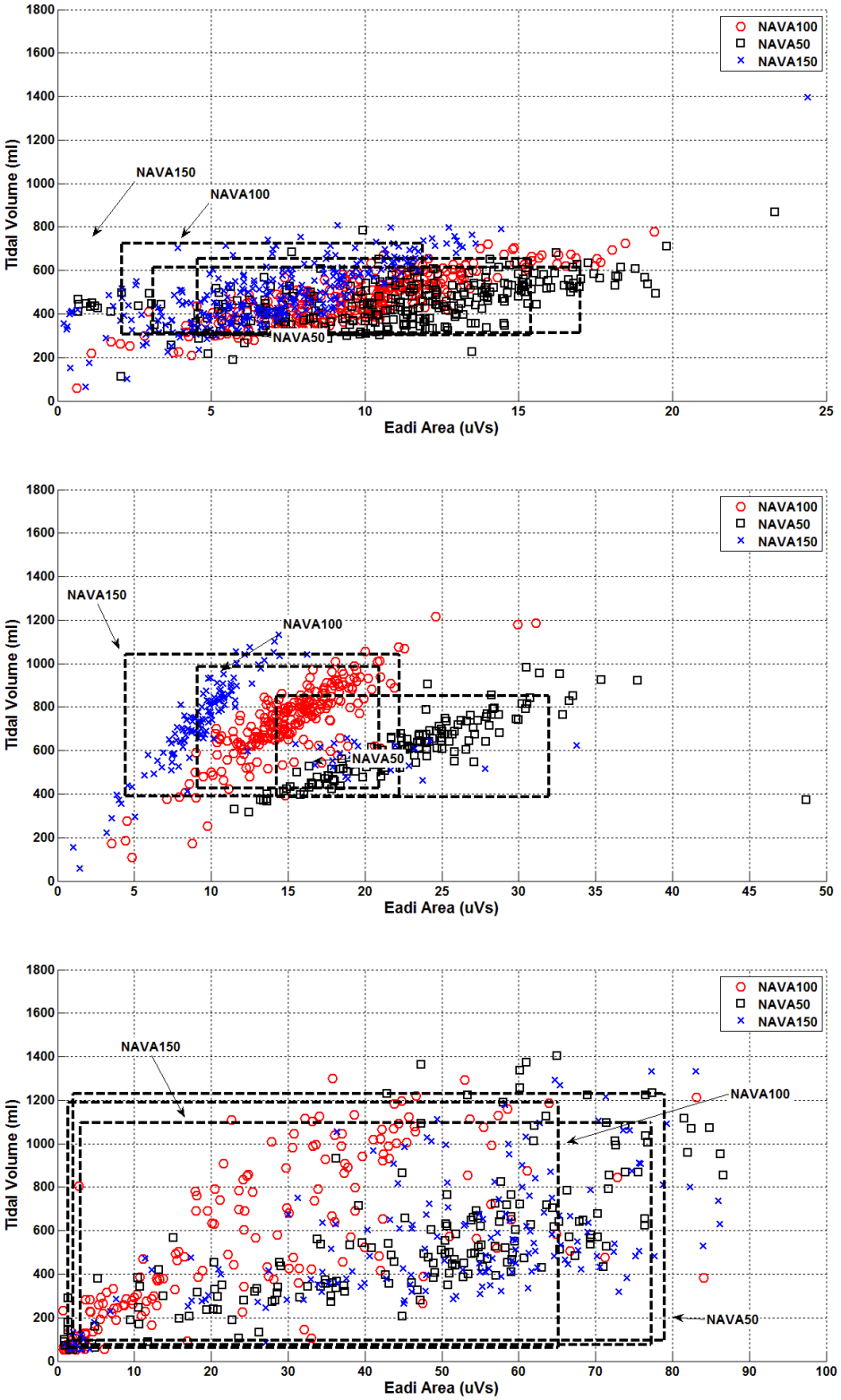

Figure 7.2: Distribution of *Vt-∫Eadi* for patients at different NAVA level. (Top) Patient 2, (Middle) Patient 8, (Bottom) Patient 11. The boxed areas show the breaths included in the 5-95th range.

Overall, the results show that patients behaved, in general, as expected from other studies (Brander et al., 2009, Colombo et al., 2008, Lecomte et al., 2009, Sinderby et al., 2007, Patroniti et al., 2012). More importantly, they also show that NAVA level is highly patient-specific due to significant inter-patient variability. Schmidt et al (Schmidt et al., 2010) showed that higher NAVA level resulted in lower *Eadi* magnitude with higher tidal volume. Higher NAVA level delivers higher, pressure proportional to the level settings, resulting in possible higher ventilator supply, *Vt*, and thus, that the *Eadi* signal that represents the patient-specific demand may possibly decrease. Hence, the overall results in this study match the trend in other published results (Brander et al., 2009, Colombo et al., 2008, Lecomte et al., 2009, Sinderby et al., 2007, Patroniti et al., 2012).

The difference between this study and previous studies is that previous study analyse the effect of specific absolute NAVA level towards $\int Eadi$, *Vt*, $Ti_{\_Neural}$, *Ti*, *PIP* and other related parameters, whereas this study focused on patient-specific response towards relative changes (±50%) of NAVA level. Thus, it is a more physiologically relevant comparison to assess NAVA level titration.

7.3.2.2 Effect of NAVA Level towards Range90 Matching

Table 7.12 presents the initial NAVA values and Range90 values for NAVA100, NAVA50 and NAVA150. The results show that NAVA levels influence the matching between a patient's demand and the delivered *Vt*. Overall, NAVA level set as proposed by the manufacturer (NAVA100), to match the same peak inspiratory pressure as the pressure set under PS; did not give the best matching/ Lowest Range90.

More specifically, comparing Range90 in different NAVA levels as shown in Table 7.12, the Range90 for the entire cohort is the smallest for NAVA50, with median = 26.6 [IQR: 15.8-59.5]. This result shows that NAVA50 had better matching for the cohort, in general, compared to Range90 in NAVA100 = 31.7 [IQR: 18.9-87.4] and Range90 in NAVA150 = 36.4 [IQR 19.7-95.3].

Table 7.12: Patients' Range90 in different NAVA Level

Patient	Initial NAVA Level, (uV/cmH_2O)	Range 90 ($Vt/\int Eadi$)		
		NAVA50	NAVA100	NAVA150
1	0.2	14.7	8.5	14.0
2	0.6	93.7	38.4	138.6
3	0.2	-	12.0	-
4	0.2	36.3	16.0	17.1
5	0.8	48.6	110.9	80.9
6	0.4	20.5	84.0	40.2
7	0.6	20.5	22.9	32.5
8	0.8	7.2	24.9	68.0
9	0.4	10.8	12.4	17.4
10	0.4	16.1	19.9	20.4
11	1.0	30.7	47.2	30.5
12	1.0	277.9	97.7	207.2
13	0.5	92.2	141.8	211.9
Median [IQR]	0.5 [0.4-0.8]	25.6 [15.4-70.4]	31.7 [18.0-90.9]	36.4 [18.9-109.8]
			24.9 [15.1-87.4]#	

 # Include Patient 3

However, cohort results can be misleading for specific patients, and they have better matching at different NAVA levels. More specifically, Patient 11 has minimum Range90 at NAVA150 and 4 patients have a minimum at NAVA100 (Patients 1-2, 4, 12). Thus, only 7 patients (Patients 5-10, 13) had the overall lowest median in NAVA50. These results show the clear inter-patient variability, and also the clinical potential to use $Vt/\int Eadi$ and Range90 to titrate patient-specific NAVA level over a heterogeneous patient cohort.

More specifically, it is less suitable to make Range90 comparison in a cohort. Practically, such an approach could be used in real-time for specific patient if it was implemented in the ventilator in order to choose the best NAVA level for a given patient at a given time. Using regular titration, it could be a new and useful approach to adapt NAVA level over time and especially during weaning from MV, a topic for which only very few data are available (Rozé et al., 2011).

It is observed that several patients have very similar Range90 in two different NAVA levels, with only ±10% difference (Patient 4: NAVA100 and NAVA150, Patient 7: NAVA50 and NAVA150 and Patient 11: NAVA50 and NAVA150). These results show that, the effect of these two different NAVA levels are less significant in the matching of ventilator supply and patient demand. This finding also indicates that supply and demand matching does not necessarily correspond linearly to NAVA level.

Figures 7.3 show $Vt/\int Eadi$ cumulative distributions for Patients 2, 8 and 11 with Range90 values at each NAVA level. These cases each have a minimum Range90 value (best matching) at different NAVA levels. The corresponding Vt and $\int Eadi$ at different NAVA levels were also highlighted earlier in Figure 7.2. More specifically, Range90 suggests that Patient 2 should be ventilated at the original NAVA100 level, Patient 8 could have the original NAVA level of 0.80 can be reduced by 50% for better matching (NAVA50), and Patient 11 would be better matched at the higher NAVA150 level.

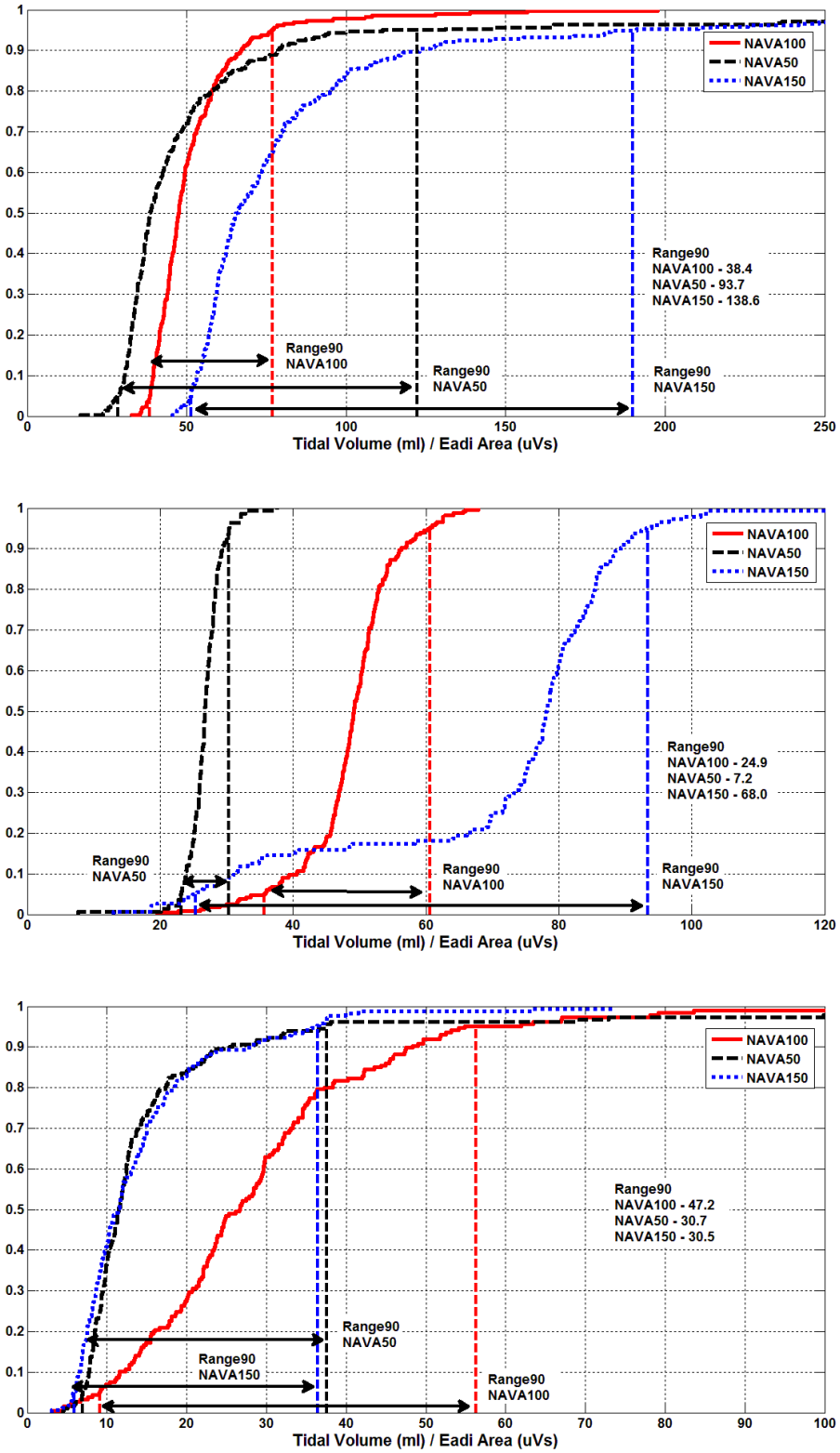

Figure 7.3: Cumulative distribution for $Vt/\int Eadi$ in Range90 analysis. (TOP) Patient 2 - NAVA100 has smaller Range90, (Middle) Patient 8 - NAVA 50 has smaller Range90, (Bottom) Patient 11 – NAVA150 and NAVA50 have a similar Range90, with NAVA150 smaller.

Correlation coefficients in Table 7.13 facilitate examination of the relationship between *Vt* with ∫*Eadi*, independent of the effects of NAVA level on the magnitude of *Eadi* signals. The correlation coefficient between *Vt* and ∫*Eadi* may potentially be another metric to aid in titrating NAVA level. Comparing Pearson's correlation between PS and other NAVA levels, it is clear that NAVA provides better *Vt* and ∫*Eadi* correlation ($p < 0.005$) suggesting better matching of supply and demand.

Table 7.13: Pearson's correlation coefficient, *R*

Patients	**Pearson's Correlation Coefficient (*Vt*-∫*Eadi*)**			
	PS	**NAVA50**	**NAVA100**	**NAVA150**
1	0.51	0.79	0.81	0.81
2	0.44	0.50	0.83	0.76
3	0.19	-	0.74	-
4	0.80	0.73	0.81	0.83
5	0.13	0.53	0.79	0.88
6	0.28	0.72	0.71	0.77
7	0.45	0.72	0.76	0.86
8	0.42	0.77	0.87	0.17
9	0.54	0.88	0.84	0.93
10	0.55	0.91	0.95	0.96
11	0.39	0.77	0.78	0.62
12	0.36	0.50	0.72	0.67
13	0.18	0.84	0.69	0.68
Median [IQR]		0.75 [0.63-0.82]	0.80 [0.74-0.84]	0.79 [0.68-0.87]
	0.42 [0.26-0.52]#		0.79 [0.74-0.83]#	

 # Includes Patient 3

The correlation coefficients for different NAVA levels in this study were similar, indicating that NAVA was able to consistently match supply with demand at different levels. However, individual patients showed otherwise. For example, Patient 2 (NAVA50), Patient 4 (NAVA50), Patient 7 (NAVA150) and Patient 11 (NAVA50), showed significantly lower *R* values compared to other NAVA levels, indicating significant supply and demand mismatch at a patient-specific level. Equally, the small

changes in the value of *R* between NAVA levels may not be clinically significant, indicating that correlation coefficient was not as sensitive to changes in NAVA level as the Range90 metric. The Range90 metric consistently identified *Vt*/∫*Eadi* mismatch between NAVA levels compared to Pearson's correlation, yielding a potentially more sensitive metric. Hence, clinically, large difference would indicate the need for the clinician to look deeper or change their approach to patient treatment.

7.4 Limitations

Several potential limitations of this study should be pointed out. First, NAVA100 was defined to match the value of peak airway pressure during PS as set by clinicians for the specific patients care. However, there was no standardisation of PS settings beyond clinical practice, and thus the appropriate level of assistance may not be optimal at NAVA100. This point clearly shows the variability in the field over this issue.

This study was conducted during NIV ventilation. During NIV, leaks can occur at the patient-mask interface and can influence delivered *Vt* which could affect the results. However, for this study, the mask was tightly attached to the patient by an experienced therapist to minimize the chance of leaks. Additionally, the therapist remained at the bedside during the whole recording to adapt the mask if necessary. These precautions made major leaks at the patient mask interface very unlikely. Additional results and discussion on volume leak can be found in Appendix 03.

Only 3 levels of NAVA were explored for each patient, separated by ±50% from the original NAVA level. At ±50%, the absolute changes of NAVA level can be very small or large depending on the initial clinically selected NAVA level. One consequence of such widely spaced NAVA levels is that, potentially, none of the 3 tested NAVA levels in the trials were optimal. Thus, a more refined set of NAVA levels might well show a better result with this metric at a different NAVA level. However, such refinement in testing is burdensome to the patient and the results clearly showed that clinically set values may not remain optimal.

Finally, it is important to note that while the Range90 metric showed better matching for specific NAVA levels, the advantage of using Range90 to titrate NAVA level is not yet clinically proven. Prior work has shown better matching of *Vt* to *∫Eadi* demand results in less asynchrony in comparing NAVA and PS (Piquilloud et al., 2012). However, the use of Range90 to titrate NAVA levels for better physiological outcome remains to be prospectively tested. The results here show only Range90 sensitivity to different NAVA levels and level of inter-patient variability that can be encountered, thus, demonstrating its clinical potential.

7.5 Summary

Patients who suffered from acute respiratory failure may benefit from the NAVA ventilation mode during NIV, which can better match patient-specific demand with ventilator supply compared to PS. Based on matching and correlation analysis, it was found that each patient reacted differently to different NAVA levels. This finding indicates significant inter-patient variability and patient-specific response. Using the

proposed concept of supply and demand ratios (Range90), more optimal NAVA levels can be found and titrated for each patient based on the simple Range90 metric. This approach can later be used in real-time to adapt NAVA levels if included in software.

Chapter 8

Respiratory Mechanics Estimation for Spontaneously Breathing Patients

8.1 Respiratory Mechanics in Spontaneously Breathing Patient

For fully sedated MV patients, the breathing effort, or work of breathing is fully taken over by the ventilator (Robert J. Mason et al., 2010, Hasan, 2010). Thus, patient-specific respiratory system elastance can be easily determined during the inspiration cycle (Bates and Lauzon, 1992, Baconnier et al., 1995, Avanzolini et al., 1997, Eberhard et al., 2003, Chiew et al., 2011, Brochard et al., 2012). In contrast, spontaneous breathing (SB) patients have individual breathing effort aside from the support given by the ventilator. Thus, additional information on the patient-induced pressure change in the pleural space of these SB patients is required to determine the true respiratory mechanics (Kallet et al., 2007, Grinnan and Truwit, 2005).

Measuring the pressure change in the pleural space (pleural pressure, P_{pl}) requires an invasive manoeuvre. A pressure sensor called a balloon catheter is inserted into the oesophageal to measure the pressure change during breathing (Benditt, 2005). This oesophageal pressure (P_{oe}) is used as a surrogate of pleural pressure and has been suggested as a metric that could be used to guide PEEP titration (Lorino et al., 1981, Lorino et al., 1982, Buscher et al., 2000, Benditt, 2005, Talmor et al., 2006, Talmor et

al., 2008). However, the measuring equipment for oesophageal pressure, the balloon catheter and data acquisition software are not normally available in many conventional ventilators.

In addition, oesophageal pressure measurements are questionable due to their dependency on the location of the balloon catheter inserted into the oesophagus (Talmor et al., 2006, Guérin and Richard, 2012). These uncertainties and invasiveness preclude its regular bedside application in most ICUs, aside from use in specialized research studies (Zaccheo et al., 2010, Stenqvist et al., 2012). Thus, estimating respiratory mechanics to guide MV is currently limited to patients who are fully sedated and is often less reliable when the patient is awake or breathing spontaneously (Iotti et al., 1995, Talmor et al., 2006, Talmor et al., 2008, Mulqueeny et al., 2010, Brochard et al., 2012). This issue significantly limits the use of model-based methods based on estimating respiratory dynamics.

Furthermore, conventional methods estimate linear respiratory elastance components using 2 point measurements ($\Delta P/\Delta V$) from the measured pneumatic signals to obtain the chest wall elastance or lung elastance, (Grinnan and Truwit, 2005). Other approaches use multiple linear regression (Lorino et al., 1981, Muramatsu et al., 2001, Khirani et al., 2010) using the measured pneumatic signals. These methods only provide a single average elastance measurement and do not show the time-varying or dynamic aspects of the true lung mechanics within a breathing cycle, which also contain useful clinical information (Guttmann et al., 1994, Chiew et al., 2011, Zhao et al., 2012a).

In this chapter, a non-invasive model-based method to estimate respiratory mechanics in SB patients is presented. More specifically, the compartment model that describes the respiratory system is extended to provide more in-depth and specific understanding to existing lung physiology. Respiratory mechanics captured during SB potentially provide useful patient and clinical insight in guiding therapy. Such a capability, without invasive oesophageal pressure measurement (Benditt, 2005, Talmor et al., 2008, Khirani et al., 2010, Terzi et al., 2012); would encourage and dramatically extend the application of respiratory mechanics to titrate care in SB patients.

8.2 Methodology

8.2.1 Spontaneously Breathing Respiratory Model

The 'standard' equation of motion for a single compartment linear lung model used to monitor patient-specific respiratory mechanics in sedated patients without the influence of offset pressure is defined (see also Chapters 4 and 5) (Iotti et al., 1995, Bates, 2009a):

$$P_{aw}(t) = R_{rs} \times Q(t) + E_{rs} \times V(t) \quad (8.1)$$

$$P_{aw}(t) = P_{tp}(t) + P_{pl}(t) \quad (8.2)$$

$$P_{tp}(t) = R_{lung} \times Q(t) + E_{lung} \times V(t) \quad (8.3)$$

$$P_{pl}(t) = R_{cw} \times Q(t) + E_{cw} \times V(t) \quad (8.4)$$

Equation 8.1 is derived from combining the influence of pleural pressure (P_{pl}) to the transpulmonary pressure (P_{tp}) (Bates, 2009a). These equations can be used to

separately estimate the components of elastance, resistance and work of breathing (Polese et al., 1991, Coussa et al., 1993). The variables in Equation 8.1-8.4 are defined in Table 8.1.

In a sedated patient, who is fully dependant on MV for work of breathing, it can be assumed that the patient does not have any individual breathing effort. Thus, the pressure changes in the pleural space (chest wall) can be assumed to be zero or constant ($P_{pl} \cong 0$). This assumption yields:

$$P_{aw}(t) - P_{pl}(t) = R_{lung} \times Q(t) + E_{lung} \times V(t) \quad (8.5)$$

$$P_{aw}(t) = R_{lung} \times Q(t) + E_{lung} \times V(t) \quad (8.6)$$

Where Equations (8.5)-(8.6) are used in Chapters 4 and 5.

Table 8.1: List of abbreviation

	Units	**Physiological Meaning**
P_{aw}	cmH_2O	Airway pressure
P_{tp}	cmH_2O	Transpulmonary pressure
P_{pl}	cmH_2O	Pleural pressure (Often measured as oesophageal pressure)
E_{rs}	cmH_2O/l	Respiratory system elastance, also the total of E_{lung} and E_{cw}
E_{lung}	cmH_2O/l	Lung elastance
E_{cw}	cmH_2O/l	Chest wall elastance
R_{rs}	cmH_2Os/l	Respiratory system , also the total of R_{lung} and R_{cw}
R_{lung}	cmH_2Os/l	Lung resistance
R_{cw}	cmH_2Os/l	Chest wall resistance

The respiratory mechanics estimated from Equation 8.6 and measured data thus precludes the effect of the chest wall elastance during inspiration. The previous analysis presented in Chapters 4 and 5 had similar assumptions and only focused on the change of lung elastance, E_{lung}. Physiologically and clinically, in this situation,

E_{lung} is more directly related to alveoli recruitment or overdistension during inspiration.

SB patients have time-variant P_{pl}, and this time-varying P_{pl} follows a specific wave form (Khirani et al., 2010) that is influenced by PEEP. These variables limit the use of the single compartment model in SB patients. As a result, a true lung elastance is not able to be estimated in SB patients without the aid of invasive oesophageal pressure measurement, which is used to estimate the contribution of the chest wall elastance.

In this study, the respiratory elastance for a SB patient is redefined, similar to Chapter 5, as time-varying respiratory elastance (E_{drs}). In addition, E_{drs} defined as a combination of 3 elastance components, instead of just two comprising E_{lung} and E_{cw}, as described in conventional compartment models (Bates, 2009a). These three components are the cage elastance (E_{cage}), demand elastance (E_{demand}) and the lung elastance (E_{lung}) as shown in Equation 8.7.

$$E_{drs}(t) = E_{cage}(t) + E_{demand}(t) + E_{lung}(t) \tag{8.7}$$

Where the demand elastance (E_{demand}), captures time-varying effect of patient-specific and breath-specific demand that aids breathing.

Substituting the $E_{drs}(t)$ into conventional single compartment model thus yields,

$$P_{aw}(t) = (E_{cage}(t) + E_{demand}(t) + E_{lung}(t))\, V(t) + R_{rs} \times Q(t) \tag{8.8}$$

$$P_{aw}(t) = P_{cage}(t) + P_{demand}(t) + P_{lung}(t) + P_{rs}(t) \quad (8.9)$$

A schematic representation of Equations 8.8-8.9 is shown in Figure 8.1.

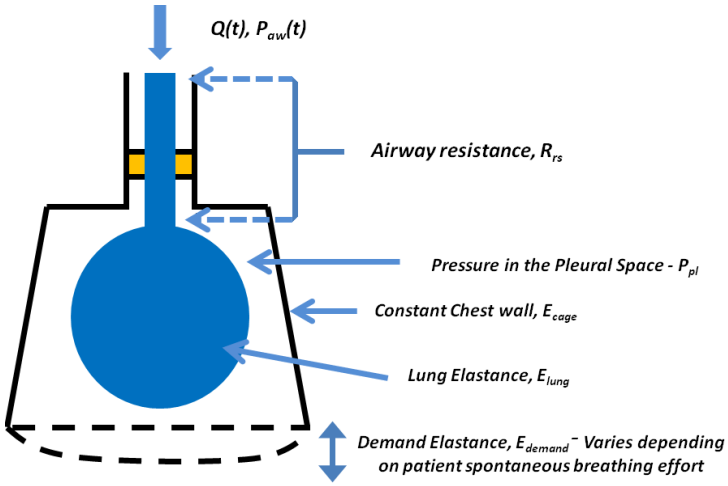

Figure 8.1: The measured airway pressure consists of 3 pressure components: 1) Pressure drop due to airway resistance (P_{rs}), 2) pressure change in the pleural space ($P_{pl} = P_{cage} + P_{demand}$) and 3) pressure in the lung compartment (P_{lung}).

More specifically, these elastance terms define:

- The patient-specific $E_{lung}(t)$ is similar to the description used earlier in Chapter 5, where E_{lung} is time-varying, a measure of the lung condition and injury within a MV supported breathing cycle.
- Cage elastance (E_{cage}) describes the constant elastic properties for the chest wall elastance. The elastance of the patient rib cage, intercostal muscles are assumed not to vary with disease-state and are thus a patient-specific constant (Chiumello et al., 2008).
- Demand elastance (E_{demand}) represents the patient-specific demand. This $E_{demand}(t)$ varies depending on patient-specific and breath-specific effort in SB patients.

P_{cage} and P_{demand} are the pressure components generated from E_{cage} and E_{demand}. Combining these pressure components will thus give information on pleural pressure (P_{pl}). P_{lung} is the pressure in the lung during MV and P_{rs} is the pressure drop due to the airway resistance and endotracheal tube (ETT).

E_{lung} is a measure of lung condition and response to given MV. Thus, $E_{lung}(t)$ is always above zero. Next, assuming $E_{cage}(t)$ as a patient-specific constant, the impact of this parameter in monitoring E_{drs} trends is less significant as it only generates a constant offset. On the other hand, $E_{demand}(t)$ varies within a patient who is spontaneously breathing. Equally, the change of pressure in the pleural space is negative due to the combined movement of the diaphragm and chest cavity. This negative pressure will thus result in 'negative' values for E_{demand} ($E_{demand} < 0$), as patient demand aids breathing effort and thus reduce effective elastance as seen at the airway. Thus, in any given breathing cycle, the time-varying E_{drs} will capture all three elastance components together.

For a fully sedated patient, the time-varying E_{drs} values were found to be positive ($E_{drs} > 0$) and had similar elastance to ARDS patients (Suarez-Sipmann et al., 2007, Carvalho et al., 2008, Chiew et al., 2011). In particular, combined positive E_{lung} and E_{cage}, and no patient demand ($E_{demand} = 0$), result in a positive $E_{drs} > 0$ value. Equally, if the patient has an inspiratory effort, $E_{demand} < 0$. $E_{demand} < 0$ lowers the overall E_{drs} towards 0 or to $E_{drs} < 0$. More specifically, $E_{drs} < 0$ will occur when patient demand is high at the beginning of inspiration and gradually decrease in magnitude as patient demand decreases, during the breath.

8.2.2 Data Analysis

For this study, time-varying E_{drs} are estimated for SB patients. More specifically, data from the SB cohort presented in Chapters 6 and 7 are used. These patients are ventilated using pressure support (PS) and neurally adjusted ventilatory assist (NAVA) ventilation modes. Patients ventilated invasively in Chapter 6 are denoted as IV patients, and, patients ventilated non-invasively in Chapter 7 are denoted as NIV patients. Patient-specific airway pressure and flow profiles are used to estimate time-varying $E_{drs}(t)$ using Equation 8.8. In this study, the airway resistance is set as constant (5 cmH_2Os/l) based on realistic physiological range (Guttmann et al., 1993, Mols et al., 2001, Chiew et al., 2011).

8.2.3 Assessing E_{drs} Trends

During PS or NAVA, time-varying E_{drs} varies depending on patient inspiratory effort. In addition, the inspiratory time for every breathing cycle is different, and demand is patient-specific and breath-specific. To allow fair comparison for all E_{drs} trajectories, the inspiratory time (Ti) is normalised to its maximum value for each breath, and data are interpolated to a new inspiratory time frame (nTi = 1 second). Then, the E_{drs} for each patient is presented as the 5^{th}, 25^{th}, 50^{th}, 75^{th} and 95^{th} percentile across all breathing cycles, which in this case, consist of ~300-500 breaths per ventilation mode (PS and NAVA) in each patient. The E_{drs} trends allow patients response to ventilation mode to be investigated. More specifically, the patient-specific response to ventilator pressure profile can be examined.

8.2.4 Assessing Positive Average E_{drs}

For every E_{drs} trend (the 5^{th}, 25^{th}, 50^{th}, 75^{th} and 95^{th} percentile), an average E_{drs} is calculated. The average E_{drs} is defined as the mean of E_{drs} >0 values after 0.3 second of inspiration. Thus, in general, when:

- $E_{drs} < 0$ - indicates significant patient demand with negative E_{demand}. Similarly, when $E_{drs} < 0$, there is effectively 'no harm' done to the patient, by pressure or flow applied, because it is due to a patient's initial state or demand.
- $E_{drs} > 0$ - implies positive pressure ventilation contributes to the patient-specific lung elastance. Therefore, $E_{drs} > 0$, is a measure of patient lung condition and response to MV, and only $E_{drs} > 0$ may be considered as a potentially 'harmful' state to the lung, depending on level and trend through the breath.

Fundamentally, this extended model is thus general over SB and sedated MV patients, and implies that negative pressure ventilation will generate $E_{drs} < 0$, and positive mechanical ventilation will result in $E_{drs} > 0$. Thus, the average E_{drs} can be used as an indicator to assess patients-specific disease state and response to MV.

For each patient and the cohort, the E_{drs} trends and average E_{drs} over all breaths between modes (PS and NAVA) and NAVA levels (NAVA100, NAVA50 and NAVA150) are compared using non-parametric Wilcoxon rank-sum test, because as they may not be normally distributed, as indicated in Chapters 6 and 7.

8.3 Results and Discussion

8.3.1 E_{drs} Trends and Average E_{drs} for PS and NAVA in IV Patients

In this study, it was found that E_{drs} trajectories and trends for patients ventilated with PS are significantly different from NAVA ($p < 0.005$ for 15/ 22 patients). The result indicates that different MV modes, or more specifically, different pressure delivery will result in different E_{drs} trajectories. An example of inspiratory E_{drs}, pressure, volume, and *Eadi* curves during PS and NAVA is shown in Figure 8.2 for Patient IV9.

At the beginning of an inspiratory cycle, $E_{drs} < 0$. Negative E_{drs} occurs when air flow enters the lung with negative pressure generated inside the patient's pleural space. As the lung volume increases with positive pressure ventilation, E_{drs} increases above 0, as expected from the model definition. Equally, as patient inspiratory demand is met, the magnitude of the E_{demand} component of E_{drs} reduces toward zero and E_{drs} becomes more positive.

During PS, E_{drs} increased from a negative value to patient-specific maximum before decreasing, as shown in Figure 8.2. This result suggests that during PS, the ventilator is triggered by the change of airway pressure or flow. As pleural pressure decreases with the patient's inspiratory demand, the airway pressure or flow changes. When the ventilator detects this change, it provides the full, specified pressure support. This instantaneous step pressure support, known as the pressurisation slope, stretches the lung at the start of ventilation. As the air enters the lung and distributes evenly, the value of E_{drs} drops. If a supported breath overstretches the lung, the overall E_{drs} will increase until the end of the inspiration of a breathing cycle.

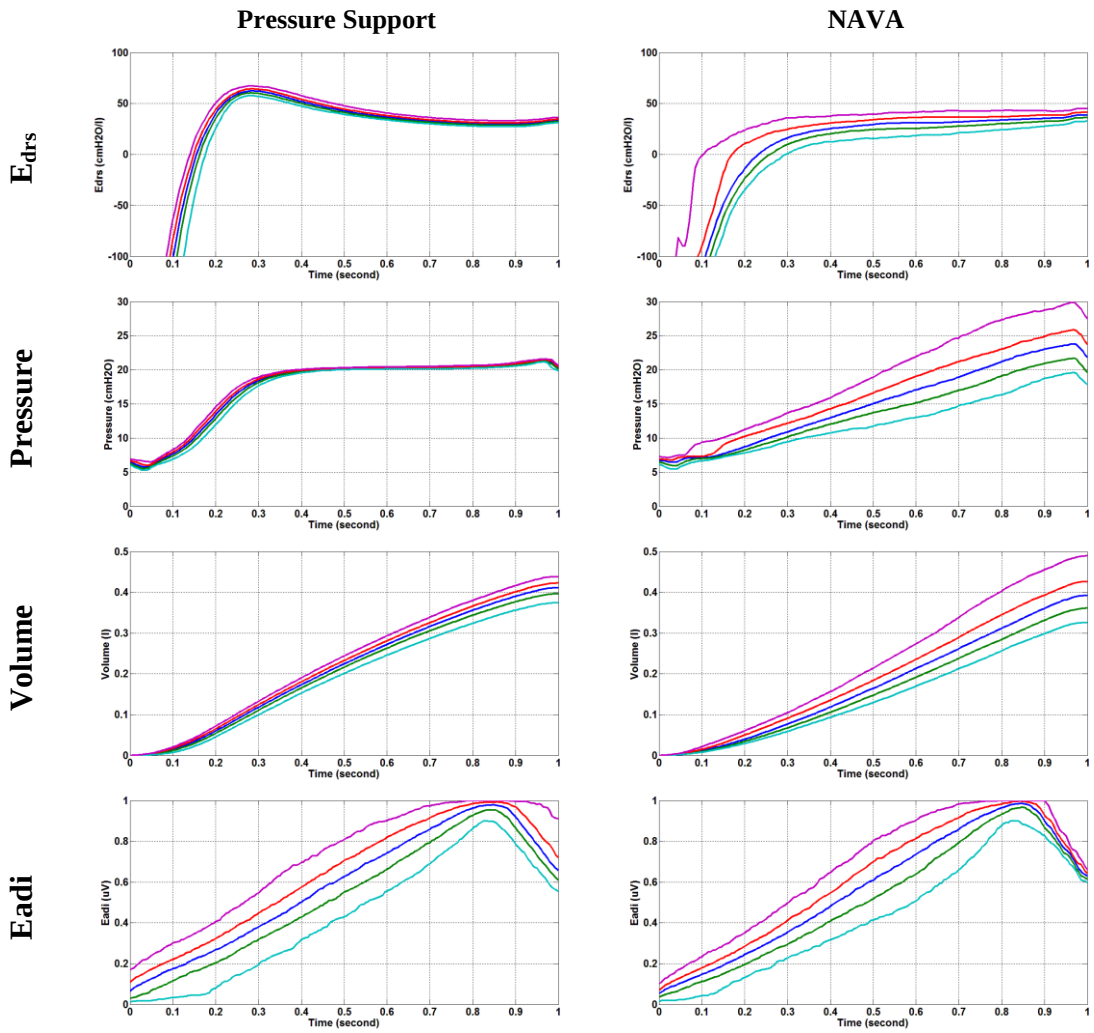

Figure 8.2: Time-varying E_{drs}, pressure, volume and *Eadi* curve for Patient IV 9 during PS (left) and NAVA (Right). The lines indicate the 5th, 25th, 50th, 75th and 95th percentile of all breathing cycles.

During NAVA, E_{drs} begins as negative but the specific maximum E_{drs} is not observed at the beginning of inspiration. It was found that E_{drs} only reaches maximum at near peak inspiratory pressure (*PIP*). This result occurs because NAVA delivers pressure proportional to the measured electrical diaphragm activity (*Eadi*). Thus, the pressure delivered during NAVA only reaches a maximum near the end of inspiratory cycle and in most cases, E_{drs} reaches its peak at peak inspiratory pressure.

Table 8.2 shows the average E_{drs} for the 22 IV patients during PS and NAVA. Comparing Average E_{drs} between PS and NAVA for invasively ventilated patients, it was found that the overall average E_{drs} for the 5^{th}, 25^{th}, 50^{th}, 75^{th} and 95^{th} percentile in PS is higher than NAVA. This result suggested that the NAVA level selected based on similar peak pressure during PS is able to avoid over assistance that may overstretch the lung due to the variable pressure assist during NAVA.

In this cohort, it was found that 18 of 22 patients in NAVA had the 5^{th}-95^{th} range of average E_{drs} wider than in PS. The 5^{th}-95^{th} range is typically wider for NAVA. This result was as expected from Chapters 6 and 7, due to a more variable pressure delivery in NAVA compared to PS.

It was found that 20 patients in PS and 15 patients in NAVA had their 95^{th} percentile average E_{drs} above 25 cmH_2O/l. ARDS patients were noted to have high respiratory system elastance with $E_{rs} \geq 25$ cmH_2O/l (The ARDS Definition Task Force, 2012). This result shows that, in most cases, the proposed average E_{drs} is able to capture the similar mechanics of an ARDS patient measured during full sedation. For patients with average $E_{drs} < 25$ cmH_2O/l, it is suggested that the patient lung is more compliant compared to an ARDS patient.

Table 8.2: Average E_{drs} (5^{th}, 25^{th}, 50^{th}, 75^{th}, 95^{th} percentile) comparing PS and NAVA for the 22 intubated patients in Chapter 6

Patient	Average E_{drs} (*cmH2O/l*)										
	PS						NAVA				
	5th	**25th**	**50th**	**75th**	**95th**		**5th**	**25th**	**50th**	**75th**	**95th**
IV1	27.5	28.8	29.8	30.9	32.8	+	11.3	14.0	16.4	18.8	23.7
IV2	6.3	9.0	10.5	12.2	17.4	+	-	3.7	4.2	8.5	17.0
IV3	52.0	53.8	55.2	56.6	58.9		27.0	31.9	41.4	51.5	68.4
IV4	23.1	28.1	31.6	35.9	41.3	+	14.2	15.9	18.3	21.5	26.3
IV5	38.2	40.8	43.1	45.4	48.7	+	16.1	19.7	22.2	25.0	29.1
IV6	55.6	61.1	64.9	69.4	78.8	+	28.4	44.5	53.9	63.3	80.6
IV7	22.7	25.1	26.7	28.4	32.6	+	5.24	9.9	12.2	14.3	17.4
IV8	23.5	26.0	27.6	30.0	34.5	+	14.8	18.1	19.9	22.2	26.0
IV9	36.8	38.5	40.0	41.5	44.7	+	19.7	25.2	28.9	32.3	38.5
IV10	6.2	7.5	8.14	9.0	10.6	+	-	1.8	2.5	2.6	4.7
IV11	37.2	39.1	40.1	41.2	43.1		29.2	34.9	39.7	44.5	50.3
IV12	22.5	25.5	28.1	33.1	48.8	+	5.7	8.2	10.6	15.7	28.3
IV13	32.8	39.3	43.9	48.4	56.9		15.4	28.4	39.6	51.9	69.7
IV14	31.1	37.3	41.7	48.1	61.1	+	14.7	19.0	23.1	28.7	46.6
IV15	36.8	42.4	45.6	49.3	56.1		32.7	42.7	48.8	55.3	73.7
IV16	24.4	26.5	27.9	29.4	31.6	+	8.7	10.5	12.0	13.8	18.0
IV17	20.5	25.0	28.2	31.1	35.4	+	8.1	12.6	15.4	18.7	24.4
IV18	44.0	48.7	50.4	52.2	56.3		27.4	37.2	43.7	51.6	67.3
IV19	32.3	40.0	45.3	54.4	78.1		46.0	62.2	71.9	81.3	96.8
IV20	34.4	38.1	40.3	42.7	47.1	+	23.7	29.6	33.1	36.9	43.1
IV21	5.1	6.3	9.3	55.8	66.1	+	2.1	6.3	9.1	11.7	16.7
IV22	23.8	34.5	38.7	41.1	44.2		31.4	41.7	48.0	56.7	69.1
Median	29.3	35.9	39.4	41.4	45.9		15.8	19.4	22.7	26.9	33.8
25^{th} prct*	22.7	25.5	27.9	30.9	34.5		10.0	10.5	12.2	15.7	23.7
75^{th} prct*	36.8	40.0	43.9	49.3	56.9		27.9	34.9	41.4	51.6	68.4

*prct – percentile, + $p<0.005$ when compared to NAVA E_{drs} trends

The estimation of average E_{drs} for spontaneous breathing patients is dependent on the initial pleural pressure or the magnitude of negative $E_{demand.}$ Thus, a lower average E_{drs} may also indicate that the patients have comparatively higher individual breathing effort than others, and obviously more than a sedated patient in Chapter 5. In general, SB patients are healthier than sedated patients who require full MV, and the average E_{drs} was able to capture this unique information without the need of oesophageal pressure.

Of note, the estimation of E_{drs} is also dependent on the airway resistance. A higher resistance assumed would downshift the E_{drs} trends whereas a lower assumed resistance would upshift the E_{drs} curves. An example of the influence of different values of R_{rs} (R_{rs} = 1, 5, 10 cmH_2Os/l) in the resulting E_{drs} is shown in Figure 8.3. It was found that E_{drs} increases when R_{rs} is reduced and E_{drs} decreases when R_{rs} is increased. Thus, the impact of R_{rs} towards intra-patient comparison is little or can be neglected, as it only provides a bias but does not change trends. Using a population constant thus ensures equal comparison.

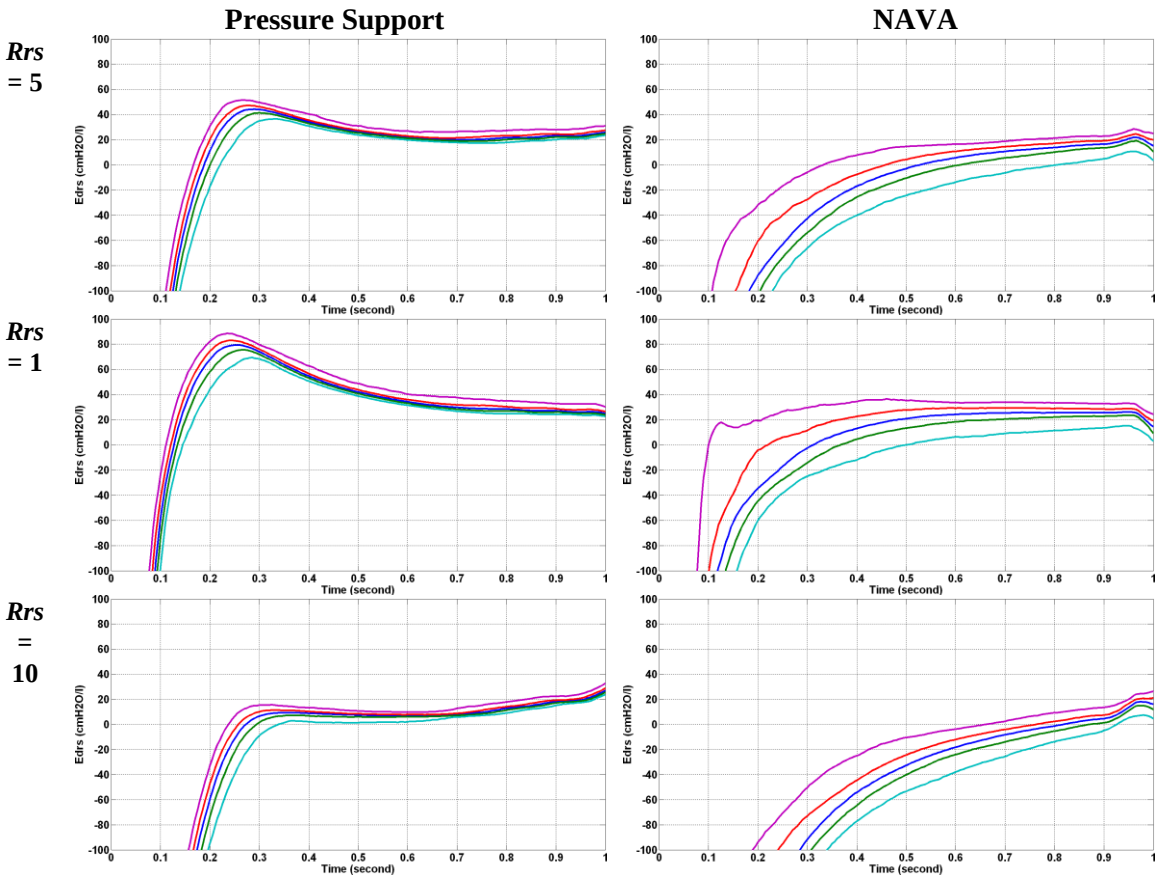

Figure 8.3: Time-varying E_{drs} for Patient IV 7 during PS (left) and NAVA (Right) at different airway resistance. The lines indicate the 5th, 25th, 50th, 75th and 95th percentile of all breathing cycles.

8.3.2 E_{drs} Trends and Average E_{drs} for PS and Various NAVA Levels in NIV Patients

Table 8.3 shows average E_{drs} for the 13 NIV patients under PS and NAVA and Table 8.4 shows the average E_{drs} for additional 2 NAVA levels (NAVA50 and NAVA150). 11 of 13 patients had E_{drs} trends during PS different from NAVA ($p < 0.005$). Similarly, different NAVA levels also results in different E_{drs} trends. It was found that 7 of 12 patients in NAVA50, and all patients in NAVA150 had different E_{drs} trends compared to NAVA100.

Table 8.3: Average E_{drs} (5^{th}, 25^{th}, 50^{th}, 75^{th}, 95^{th} percentile) for PS and NAVA for NIV patients in Chapter 7

Patient	Average E_{drs} (*cmH2O/l*)										
	PS						NAVA100				
	5th	25th	50th	75th	95th		5th	25th	50th	75th	95th
NIV1	10.5	13.3	16.0	17.7	20.0		7.8	9.8	12.2	14.6	18.1
NIV2	12.5	15.8	17.7	19.9	25.6	+	11.5	14.8	17.4	22.8	35.0
NIV3	13.8	15.4	16.5	17.4	18.4	+	8.3	10.1	11.6	12.8	14.4
NIV4	21.1	25.1	28.2	31.9	38.4	+	10.8	16.5	19.2	21.9	25.8
NIV5	11.0	17.2	20.4	22.7	27.3		3.6	6.1	8.1	10.6	14.4
NIV6	6.3	6.9	7.2	7.5	8.1	+	4.1	8.7	10.3	12.2	30.5
NIV7	6.1	6.6	7.1	7.5	7.9	+	8.8	9.6	10.1	10.9	11.9
NIV8	11.9	15.1	17.7	19.8	23.1	+	11.2	14.2	16.9	20.3	30.2
NIV9	16.1	19.1	21.8	24.7	29.7	+	11.0	14.6	18.6	24.9	37.5
NIV10	4.9	6.8	8.7	10.5	13.6	+	8.6	11.2	12.7	13.8	15.6
NIV11	1.4	2.4	1.6	11.4	46.5	+	2.5	1.9	7.8	21.4	46.7
NIV12	3.3	8.5	9.5	10.6	13.5	+	5.8	11.3	15.2	19.4	25.1
NIV13	2.6	5.0	6.8	9.6	42.8	+	0.8	2.4	3.0	3.0	6.3
Median	10.5	13.3	16.0	17.4	23.1		8.3	10.1	12.2	14.6	25.1
25^{th} 75^{th} prct*	4.5 12.8	6.8 16.2	7.2 18.4	10.3 20.6	13.6 31.9		4.0 10.9	8.1 14.3	9.6 17.0	11.9 21.5	14.4 31.6

*prct – percentile, +p<0.005 when compared NAVA100 E_{drs} trends

Similar to the result of the IV patient analysis in Section 8.3.1, a lower median average E_{drs} is observed during NAVA. The lower average E_{drs} during NAVA for both IV and NIV cohorts suggested that during NAVA ventilation, patients had higher negative E_{demand} magnitude. The higher E_{demand}, indirectly suggested that NAVA

patients are more variable and potentially participate more actively in breathing when compared to PS.

Table 8.4: Average E_{drs} (5^{th}, 25^{th}, 50^{th}, 75^{th}, 95^{th} percentile) for NAVA50 and NAVA150 for NIV patients in Chapter 7

Patient	Average E_{drs} (*cmH2O/l*)											
	NAVA50						NAVA150					
	5th	25th	50th	75th	95th		5th	25th	50th	75th	95th	
NIV1	2.9	3.9	4.9	5.3	8.0	+	8.2	12.4	15.5	18.3	22.4	+#
NIV2	5.2	9.0	9.6	10.5	15.7		8.5	15.8	20.7	28.3	44.9	+#
NIV3	-	-	-	-	-		-	-	-	-	-	
NIV4	6.1	7.0	7.7	9.1	11.0	+	13.4	23.6	27.7	30.8	36.1	+#
NIV5	3.4	3.7	4.2	5.5	9.0		7.4	11.2	15.1	20.8	30.6	+#
NIV6	2.9	3.7	4.9	6.8	7.8		13.5	16.4	22.9	32.1	46.3	+#
NIV7	5.2	5.9	6.4	6.9	7.4	+	10.4	12.3	13.4	14.7	16.2	+#
NIV8	10.1	12.7	16.7	21.7	31.6	+	16.1	22.6	27.3	32.9	42.1	+#
NIV9	6.3	7.8	9.9	12.0	16.2	+	19.9	23.8	26.5	30.9	40.6	+#
NIV10	6.7	7.7	8.9	10.0	11.7		10.6	14.0	16.4	18.7	21.3	+#
NIV11	2.4	16.9	27.5	37.4	62.1	+	1.8	8.6	17.6	24.9	34.8	+#
NIV12	3.1	5.8	7.6	10.0	14.7		5.2	9.0	14.1	20.7	27.5	+#
NIV13	-	1.1	1.8	2.5	2.1	+	-	2.4	3.0	3.2	4.9	+#
Median	5.2	6.5	7.7	9.6	11.4		10.4	13.2	17.0	22.9	32.7	
25^{th}	3.0	3.8	4.9	6.2	7.9		7.6	10.1	14.6	18.5	21.9	
75^{th} prct*	6.3	8.4	9.8	11.3	16.0		13.5	19.5	24.7	30.9	41.4	

Note: Patient NIV3 did not undergo ventilation with different NAVA levels *prct – percentile,
+ p<0.005 when compared to NAVA100 E_{drs} trends, # p<0.005 when compared to NAVA50 E_{drs} trends

In most cases, comparing different NAVA gain, NAVA50 had overall lower average E_{drs} as expected due to the lower 'pressure support' provided by lower NAVA levels. Similarly, NAVA150 had the highest average E_{drs}. These results should be expected. However, it is interesting to note that, in some cases, this outcome is not necessarily the case. Figure 8.4 shows an example of E_{drs} trend for Patient NIV12 during NAVA100 and NAVA150. This patient had different E_{drs} trends during NAVA100 when compared to NAVA150. However, the average E_{drs} were almost similar, indicating that perhaps a different NAVA gain may have been more or equally appropriate based on this metric

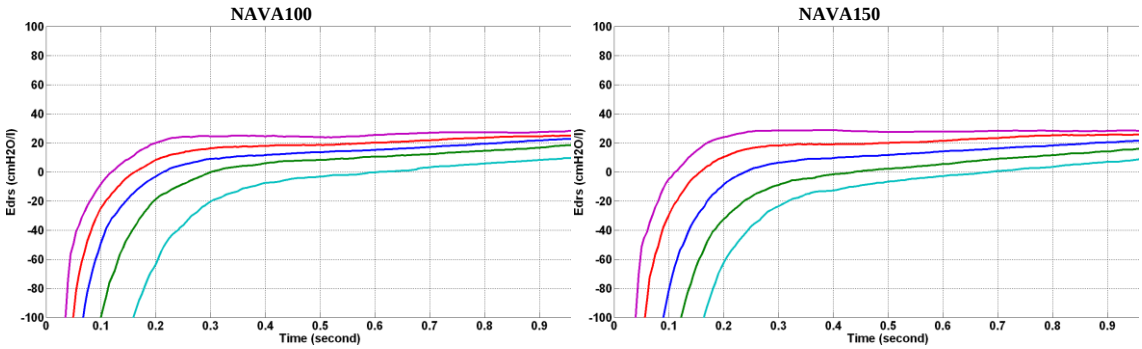

Average E_{drs} (*cmH2O/l*)					Average E_{drs} (*cmH2O/l*)				
5th	**25th**	**50th**	**75th**	**95th**	**5th**	**25th**	**50th**	**75th**	**95th**
5.8	11.3	15.2	19.4	25.1	5.2	9.0	14.1	20.7	27.5

Figure 8.4: E_{drs} trends and average E_{drs} in patients during NAVA100 and NAVA150 for Patient NIV12.

The pressure assist provided by NAVA150 is higher than during NAVA100. Therefore, the resulting E_{drs} trend during NAVA150 is higher. However, the amount of pressure support also influences the underlying *Eadi*, resulting in a lowering of overall patient-specific *Eadi* during NAVA150 (Brander et al., 2009, Colombo et al., 2008, Lecomte et al., 2009, Sinderby et al., 2007, Patroniti et al., 2012). The reduced *Eadi* during NAVA150 thus provides lower NAVA pressure assist, resulting in similar average E_{drs} as NAVA100 as shown in Figure 8.4. Hence, the trade off at NAVA gain and E_{drs} is nonlinear and not necessarily a simple compromise.

Existing methods in titrating care for the mechanically ventilated patient often focus on only one specific pneumatic element, pressure or volume. These methods either optimise the ventilation tidal volume (Brochard et al., 1998, Slutsky, 1999, Gajic et al., 2004, Bonetto et al., 2005, Malhotra, 2007, Meade et al., 2008, Putensen et al., 2009) or the pressure support (Slutsky, 1993, Bernard et al., 1994a, Barberis et al., 2003, Gattinoni et al., 2003, Slutsky and Hudson, 2006, Grasso et al., 2007, Albert et al.,

2009, Gattinoni et al., 2010). While these approaches have shown improvement in patient mortality and in preventing further lung injury, none of these methods investigates the influence of both pneumatic elements simultaneously, which is catered to obtaining recruitment (volume) without damage (pressure).

Time-varying E_{drs} is a measure of patient-specific response towards the ventilator (Chiew et al., 2011). Titrating care using this unique and physiologically relevant parameter can potentially optimise both pneumatic settings of the ventilator (pressure and volume) simultaneously. Equally, the average E_{drs} is able to capture unique parameter in SB patient that is directly relevant to respiratory mechanics without the use of oesophageal pressure. The application of E_{drs} can potentially be used to guide PEEP selection, optimal pressure support and NAVA level in SB patients, which is currently not available without additional invasive manoeuvre. This proof of concept should thus open up new options in selecting the proper SB modes, and its associated PEEP or level of pressure support.

8.4 Limitations

8.4.1 Respiratory Mechanics during Non-invasive Ventilation

Respiratory mechanics estimated in non-invasive ventilation can be erroneous (Peslin et al., 1992, Navajas et al., 2000, Mulqueeny et al., 2010). This error is mainly due to tidal volume leak. However, this leak can be minimised through careful conduct during experimental trials. Equally, during intra-patient analysis, such as changing PS mode to NAVA, or comparing different NAVA levels, the effect of volume leak can be assumed to be similar between modes. In addition, the normalisation time-varying

$E_{drs}(t)$ in spontaneously breathing patients significantly reduces the impact of volume leaks.

8.4.2 Time-varying Elastance

8.4.2.1 Negative and Positive Time-varying Elastance

Time-varying Edrs is not normally calculated in MV patients who are either fully sedated or spontaneously breathing. It provides unique information to monitor patient-specific disease state and response to MV. When applied in SB patients, the negative E_{drs} only corresponds to the negative pressure generated in the pleural space to inflate the lung. Existing data on time-varying E_{drs} or compliance in sedated patients has been shown to be positive (Chiew et al., 2011, Zhao et al., 2012a). Thus, $E_{drs} < 0$ is only possible for patients who are breathing spontaneously. The validity of the estimated negative values of E_{drs} in SB patients thus warrants further investigation as a measure of patient-specific demand similar to the use of oesophageal pressure.

8.4.2.2 Average Time-varying Elastance

The average E_{drs} was calculated as the mean of $E_{drs}>0$ after 0.3 second time frame. The 0.3 second time frame was selected after post-hoc analysis of the volume-time curves, where most cases had inspiratory lung volumes of 50~100 *ml* after 0.3 second. The average E_{drs} were recalculated using different time frames such as 0.2 second, 0.4 second and 0.5 second to test the robustness of this assumption. It was found that there was no significant difference in the overall results ($p < 0.005$), and had Pearson's correlation of coefficient, $R > 0.95$ in every tested time frames. This result shows that average E_{drs} calculated after 0.3 second remains valid for all cases.

Average E_{drs} can also be calculated through setting tidal volume threshold of 50~100 *ml* instead of using an inspiratory time threshold (In this study, the threshold time frame is 0.3 second). However, SB patients have variable breathing cycles (with different *Ti*, *Vt*, flow and pressure). Using normalised inspiratory time as the threshold for calculating average E_{drs} after the time frame of >0.3 have similar effects when reference to threshold tidal volume. Thus, using the proposed method to quantify average E_{drs} for SB patients remains valid and robust to other approaches, and can be applied continuously in MV patients without interrupting care.

8.5 Summary

In summary, a new model that defines conventional respiratory elastance into 3 separate components is presented. The proposed model was able to capture unique dynamic respiratory mechanics for spontaneously breathing patients during PS and NAVA ventilation at different NAVA levels, which is otherwise not possible in conventional models or methods. The work presented here is the first of its kind to monitor time-varying E_{drs} in SB patients without additional measuring equipment or interrupt care. Thus, revealing a model that fits all ventilation condition and the potential to' standardise' MV treatment in a consistent fashion.

Chapter 9

Conclusions

This thesis presents model-based methods to aid clinicians in guiding mechanical ventilation (MV) for the critically ill. Four unique models and metrics are developed, and each model is tested in the experimental or clinical trials developed for the purpose. These models are capable of capturing physiologically relevant parameters that describe patient-specific condition and potential specific response to MV settings.

In Chapter 3, an experiment study that investigates the respiratory mechanics of healthy and oleic acid induced ARDS animal was presented. This experimental study provides a unique platform for the studies of model-based methods. The first model that used this experimental study is the minimal recruitment model. The model is able to capture the physiological condition of both the anesthetised healthy and the oleic acid induced ARDS lung, thus, showing its specificity in differentiating disease and healthy conditions. In addition, a disease state grouping metric (DSG) is developed based on model-based estimated threshold opening pressure (TOP) and standard deviation (SD). Using this metric, the patient condition in both healthy and ARDS scenarios can be monitored and aid clinicians to select the optimal ventilation mode that best suits the patient's specific condition. The results and findings further validate and encourage the application of this minimal model to guide therapy in regular clinical use or a specifically designed randomised clinical trial.

Chapter 4 focused on monitoring respiratory mechanics of the experimental animals using a single compartment linear lung model. Similar to the minimal model, the parameter estimation for the single compartment model provides unique insight to patient condition and its evolution. More specifically, the model was able to capture varying respiratory mechanics with disease progression and the change of MV settings. The model was also able to continuously monitor the respiratory mechanics during disease progression without addition invasive tests or protocols. This model has shown higher resolution in terms of monitoring than the minimal recruitment model, which requires multiple PEEP changes to distinguish subject-specific condition. The single compartment model thus allows an in-depth understanding on the subject-specific disease state, response to PEEP, and evolution over time. Hence, it offers significant potential to guide PEEP titration in regular clinical use.

Chapter 5 extends the single compartment model to capture time-varying dynamic respiratory elastance (E_{drs}) within a breathing cycle. E_{drs} describes patient-specific lung response to ventilator assisted pressure within each breathing cycle, enabling the understanding of overall patient lung recruitment status and overdistension within every breathing cycle. Thus, where single constant elastance might not see overdistension in a breath, E_{drs} can capture this behaviour and recommend a different mode of MV. Equally, it clearly captures and highlights for clinician the presence and impact of COPD and auto-PEEP. To test this model, PV data from ARDS patients who underwent a clinical protocol were used. The model is able to uniquely describe patient respiratory mechanics breath-by-breath, at different PEEP levels. The model

can be applied to titrate patient-specific optimal PEEP based on a metric that balance ventilation risk and rewards, both for care and by ventilation mode.

Patients who are spontaneously breathing are ventilated in partially assisted ventilation modes. These assisted ventilation modes provide partial ventilation support to the patients to reduce their work of breathing and aid them in recovery. In this thesis, the comparison between widely used pressure support ventilation (PS) and a state of the art ventilation mode, neurally adjusted ventilatory assist (NAVA) is presented. A metric (Range90) is developed to analyse the matching of patient demand and respective support provided by the ventilator. The results have concluded that NAVA was able to provide better matching than PS during invasive (Chapter 6) and non-invasive ventilation (Chapter 7), thus showing the need for patient-specific ventilation in this cohort.

In particular, the Range90 metric can also be used in titrating patient-specific NAVA level based on the concept of supply and demand matching. The results have shown that patient-specific response to NAVA level is different, even in these cohorts, and thus concluded that the existing method (NAVA previsualisation) is not appropriate. Hence, patient-specific optimal NAVA level remains a huge area of interest with no conclusive findings. Titrating NAVA level with Range90 provides a simple and unique initial solution for this problem.

Finally, the single compartment model with time-varying E_{drs} is extended in spontaneously breathing patient (SB). Respiratory mechanics estimation in SB

patients cannot currently be carried out without additional invasive and costly measuring tools. Thus, respiratory mechanics monitoring for SB patients remains a research tool and cannot be used to titrate MV in real time. The single compartment model is extended to capture clinically useful respiratory mechanics using non-invasive model-based method and can thus estimate SB patient time-varying elastance without compromising patient-model physiological relevance. A metric (average E_{drs}) that defines spontaneously breathing patient's disease sate response to MV is also presented and validated on extensive clinical data. This metric is shown to be capable of providing unique information to guide MV for spontaneously breathing patients. More critically, it extends the single compartment model-based approach to cover all form of MV and MV patients - a single tool to guide MV.

In conclusion, this thesis has presented several unique and physiologically relevant models that can capture patient-specific condition and response to MV settings. The models have been tested in experimental ARDS animal model and ICU patients. Results from the studies have shown the models can be used to guide MV decision making in the heterogeneous ICU population. Thus, revealing a path to standardise patient-specific MV in a consistent fashion.

Chapter 10

Future Work

The models and metrics developed in this thesis have shown good clinical viability. However, the application of these models to guide MV in real-time as a standard part of ICU care warrants further investigation in a clinical environment to ensure its robustness and validity. In particular, there is a need to show that a proven model can improve overall patient outcome; to prove its level of impact. Several potential future works that extend the existing research are presented.

10.1 Simulating Actual Clinical Condition in ARDS Animal

Experimental ARDS animal models are easily recruitable with PEEP at the early stage of ARDS (Ballard-Croft et al., 2012). However, it is possible that the actual ARDS patients are exposed to long term lung injury, resulting in consolidated lung regions and are not responsive to PEEP changes. These patients are known as non-recruiters, and their response to PEEP or recruitability are low (Gattinoni et al., 2006a, Caironi et al., 2010). The models ability in capturing these patients' respiratory mechanics needs to be investigated. These symptoms can be modelled with by exposing the animal model to long term injury. This prolonged lung injury will result in lung consolidation (swelling and hardening of the infected lung regions) (Gattinoni et al., 1998), which mimic the lung physiology of non-recruiters ARDS patients.

10.2 Different ARDS Animal Models

Animal models of ARDS provide a rapid, consistent means of clinical testing compared to human clinical trials, which is crucial in early model developing and before testing on humans to mitigate risk. Respiratory mechanics of 9 piglets during healthy state and ARDS state were studied. Only 3 of 9 piglets successfully developed ARDS after oleic acid injection. Given the low ARDS animal sample, the result was not conclusive with statistical significance. Additional experimental animal trials can be carried out to investigate the statistical significance of the thesis finding. However, the oleic acid animal model is variable and difficult to achieve. Different ARDS animal models, such as the lavage model, endotoxin model or smoke models can be used (Rosenthal et al., 1998, Matute-Bello et al., 2008, Ware, 2008, Ballard-Croft et al., 2012). Different ARDS animal models will also simulate different ARDS pathologics, and thus provide a unique platform to investigate the models robustness.

10.3 Comparison of PS and Variable NAVA Levels

Compared to PS, it was found that NAVA significantly improved patient-ventilator interaction, allowing better matching and improves patient overall gas exchange and prevent over assistance. However, there is no conclusive result on which ventilation mode is better (Terzi et al., 2012). Questions arise from all studies, such as: 1) is the comparison between PS and NAVA a fair comparison? And 2) What is the optimal NAVA setting?. These questions need to be addressed. The Range90 supply and demand matching proposed in this thesis potentially offers a unique approach to determine optimal NAVA level. However, utilising this method warrants further study

and more specifically, comparison with other of NAVA level titration method (Brander et al., 2009) needs to be carried out.

10.4 Validation of Model Findings with Additional Monitoring Tools

The aim of model-based methods is to guide MV using model derived patient-specific parameters from measured data. One of the major concerns of the derived parameters is their clinical relevance and validity to actual physiological condition. Thus, it is important to compare the model findings with additional monitoring tool. In particular, this outcome can be achieved with the use of non-invasive lung imaging methods, such as the electrical impedance tomography (EIT) (Denai et al., 2010, Zhao et al., 2010a) and lung ultrasound (Bouhemad et al., 2007, Peris et al., 2010). These monitoring tools enable the recruitment of collapsed and dependent lung regions to be observed in real time. Combining the results obtained from model-based methods and monitoring tools will thus validate their respective findings.

The time-varying dynamic E_{drs} provides unique insight to patient-specific respiratory mechanics with time and response to MV. However, the current findings warrants further investigation. In particular, the combination of time-varying patients demand (E_{demand}), and constant chest wall elastance (E_{cage}) are the primary contribution to the change of pressure in pleural space. This assumption can be confirmed with oesophageal pressure measurements in sedated and/or spontaneously breathing patients. These measurements will further validate the model's definition and assumptions, and thus encourage the model's application to guide MV throughout a

patient stay without interrupting therapy, which can have negative consequences on outcome and patient-centered quality of care.

10.5 Standard Clinical Protocol and Data Collection

One of the major issues with ARDS studies is that there is always a lack of patient samples in a specific cohort. Thus, recruiting more ARDS patients for clinical trials remains the primary focus for model-based studies. This thesis has outlined a non-invasive clinical protocol that is suitable for data collection (Chapter 5). This protocol has several unique features that are designed for this purpose. First, a staircase recruitment manoeuvre is carried out to study patient-specific response to PEEP. Second, low tidal volume setting and limiting the peak airway pressure thus provide a conditional protective lung ventilation strategy. And lastly, recording arterial blood gases thus provides information on the effect of recruitment manoeuvre towards patient gas exchange. Patients admitted to the ICU, requiring MV can undergo this specific protocol allowing patient data to be recorded in a consistent fashion. The protocol standardisation will not only improve data sample size, the significant data samples can indirectly lead to a development of a virtual patient database. This database will lead to more comprehensive study in model-based MV.

10.6 Randomised Controlled Trials

One important research study that must be carried out in future is a randomised controlled trial (RCT). Randomised controlled trials include several patient cohorts and provides a platform to evaluate the impact of the model-based methods on patient outcome (Esteban et al., 2008, Jadad et al., 1996). In particular, one patient cohort

undergoes non-intervention, standard treatment as decided by the attending clinicians. The second matched patient cohort would undergo the proposed clinical protocol, in which the PEEP will be selected based on mode-based methods. These 2 cohorts analyses their respective patients outcome such as desaturation events (measured as oxygen saturation, $SpO_2 < 90\%$), improved gas exchange (measured by arterial blood gases), length of mechanical ventilation and importantly, the mortality rates. These patient outcomes and physiologically relevant markers will provide a fair comparison between non-interventional MV and model-based MV, assessing the performance, efficacy, and overall impact of model-based MV application in clinical settings. It is the last step and answer required to take these, or any, model-based method into regular clinical usage.

References:

ABBOUD, S., BARNEA, O., GUBER, A., NARKISS, N. & BRUDERMAN, I. 1995. Maximum expiratory flow-volume curve: mathematical model and experimental results. *Medical Engineering & Physics,* 17**,** 332-336.

ABOAB, J., LOUIS, B., JONSON, B. & BROCHARD, L. 2006. Relation between PaO_2/F_IO_2 ratio and F_IO_2: a mathematical description. *Intensive Care Medicine,* 32**,** 1494-1497.

ADLER, A., SHINOZUKA, N., BERTHIAUME, Y., GUARDO, R. & BATES, J. H. T. 1998. Electrical impedance tomography can monitor dynamic hyperinflation in dogs. *J Appl Physiol,* 84**,** 726-732.

ALBAICETA, G., GARCIA, E. & TABOADA, F. 2007. Comparative study of four sigmoid models of pressure-volume curve in acute lung injury. *BioMedical Engineering OnLine,* 6**,** 7.

ALBAICETA, G. M., BLANCH, L. & LUCANGELO, U. 2008. Static pressure-volume curves of the respiratory system: were they just a passing fad? *Current Opinion in Critical Care,* 14**,** 80-86.

ALBAICETA, G. M., LUYANDO, L. H., PARRA, D., MENENDEZ, R., CALVO, J., PEDREIRA, P. R. & TABOADA, F. 2005. Inspiratory vs. expiratory pressure-volume curves to set end-expiratory pressure in acute lung injury. *Intensive Care Med,* 31**,** 1370 - 8.

ALBAICETA, G. M., TABOADA, F., PARRA, D., LUYANDO, L. H., CALVO, J., MENENDEZ, R. & OTERO, J. 2004. Tomographic study of the inflection points of the pressure-volume curve in acute lung injury. *Am J Respir Crit Care Med,* 170**,** 1066 - 72.

ALBERT, S. P., DIROCCO, J., ALLEN, G. B., BATES, J. H. T., LAFOLLETTE, R., KUBIAK, B. D., FISCHER, J., MARONEY, S. & NIEMAN, G. F. 2009. The role of time and pressure on alveolar recruitment. *Journal of Applied Physiology,* 106**,** 757-765.

ALLARDET-SERVENT, J., FOREL, J.-M., ROCH, A., GUERVILLY, C., CHICHE, L., CASTANIER, M., EMBRIACO, N., GAINNIER, M. & PAPAZIAN, L. 2009. Fio2 and acute respiratory distress syndrome definition during lung protective ventilation *. *Critical Care Medicine,* 37**,** 202-e6 10.1097/CCM.0b013e31819261db.

AMATO, M. B. P., BARBAS, C. S. V., MEDEIROS, D. M., MAGALDI, R. B., SCHETTINO, G. P., LORENZI-FILHO, G., KAIRALLA, R. A., DEHEINZELIN, D., MUNOZ, C., OLIVEIRA, R., TAKAGAKI, T. Y. & CARVALHO, C. R. R. 1998. Effect of a Protective-Ventilation Strategy on Mortality in the Acute Respiratory Distress Syndrome. *N Engl J Med,* 338**,** 347-354.

ANDREASSEN, S., STEIMLE, K. L., MOGENSEN, M. L., SERNA, J. B. D. L., REES, S. & KARBING, D. S. 2010. The effect of tissue elastic properties and surfactant on alveolar stability. *Journal of Applied Physiology,* 109**,** 1369-1377.

ASHBAUGH, D., BOYD BIGELOW, D., PETTY, T. & LEVINE, B. 1967. ACUTE RESPIRATORY DISTRESS IN ADULTS. *The Lancet,* 290**,** 319-323.

AVANZOLINI, G., BARBINI, P., CAPPELLO, A., CEVENINI, G. & CHIARI, L. 1997. A new approach for tracking respiratory mechanical parameters in real-time. *Annals of Biomedical Engineering,* 25**,** 154-163.

BACONNIER, P. F., CARRY, P.-Y., EBERHARD, A., PERDRIX, J.-P. & FARGNOLI, J.-M. 1995. A computer program for automatic measurement of respiratory mechanics in artificially ventilated patients. *Computer Methods and Programs in Biomedicine,* 47**,** 205-220.

BADET, M., BAYLE, F., RIQUE, RICHARD, J.-C., GU & RIN, C. 2009. Comparison of Optimal Positive End-Expiratory Pressure and Recruitment Maneuvers During Lung-

Protective Mechanical Ventilation in Patients With Acute Lung Injury/Acute Respiratory Distress Syndrome. *Respiratory Care,* 54**,** 847-854.

BAEHRENDTZ, S. 1985. THE INFLUENCE OF AN END-INSPIRATORY PAUSE ON GAS EXCHANGE AND CENTRAL HAEMODYNAMICS IN PATIENTS WITH ACUTE RESPIRATORY FAILURE. *Clinical Physiology,* 5**,** 93-98.

BALLARD-CROFT, C., WANG, D., SUMPTER, L. R., ZHOU, X. & ZWISCHENBERGER, J. B. 2012. Large-Animal Models of Acute Respiratory Distress Syndrome. *The Annals of Thoracic Surgery,* 93**,** 1331-1339.

BARBAS, C. S. L. V., DE MATOS, G. F. J., PINCELLI, M. P., DA ROSA BORGES, E., ANTUNES, T., DE BARROS, J. M., OKAMOTO, V., BORGES, J. O. B., AMATO, M. B. P. & RIBEIRO DE CARVALHO, C. R. 2005. Mechanical ventilation in acute respiratory failure: recruitment and high positive end-expiratory pressure are necessary. *Current Opinion in Critical Care,* 11**,** 18-28.

BARBERIS, L., MANNO, E. & GU RIN, C. 2003. Effect of end-inspiratory pause duration on plateau pressure in mechanically ventilated patients. *Intensive Care Medicine,* 29**,** 130-134.

BARWING, J., LINDEN, N., AMBOLD, M., QUINTEL, M. & MOERER, O. 2011. Neurally adjusted ventilatory assist vs. pressure support ventilation in critically ill patients: an observational study. *Acta Anaesthesiologica Scandinavica,* 55**,** 1261-1271.

BASTARACHE, J. A. & BLACKWELL, T. S. 2009. Development of animal models for the acute respiratory distress syndrome. *Disease Models & Mechanisms,* 2**,** 218-223.

BATES, J. H. T. 2009a. *Lung Mechanics: An Inverse Modeling Approach*, Cambridge University Press.

BATES, J. H. T. Year. Pulmonary mechanics: A system identification perspective. *In:* Engineering in Medicine and Biology Society, 2009. EMBC 2009. Annual International Conference of the IEEE, 3-6 Sept. 2009 2009b. 170-172.

BATES, J. H. T. & LAUZON, A. M. 1992. A nonstatistical approach to estimating confidence intervals about model parameters: application to respiratory mechanics. *Biomedical Engineering, IEEE Transactions on,* 39**,** 94-100.

BEN-TAL, A. 2006. Simplified models for gas exchange in the human lungs. *Journal of Theoretical Biology,* 238**,** 474-495.

BENDITT, J. O. 2005. Esophageal and Gastric Pressure Measurements. *Respiratory Care,* 50**,** 68-77.

BERNARD, G. R., ARTIGAS, A., BRIGHAM, K. L., CARLET, J., FALKE, K., HUDSON, L., LAMY, M., LEGALL, J. R., MORRIS, A. & SPRAGG, R. 1994a. The American-European Consensus Conference on ARDS. Definitions, mechanisms, relevant outcomes, and clinical trial coordination. *Am J Respir Crit Care Med,* 149**,** 818 - 24.

BERNARD, G. R., ARTIGAS, A., BRIGHAM, K. L., CARLET, J., FALKE, K., HUDSON, L., LAMY, M., LEGALL, J. R., MORRIS, A. & SPRAGG, R. 1994b. Report of the American-European consensus conference on ARDS: Definitions, mechanisms, relevant outcomes and clinical trial coordination. *Intensive Care Medicine,* 20**,** 225-232.

BERSTEN, A. D. 1998. Measurement of overinflation by multiple linear regression analysis in patients with acute lung injury. *Eur Respir J,* 12**,** 526-532.

BODENSTEIN, M., DAVID, M. & MARKSTALLER, K. 2009. Principles of electrical impedance tomography and its clinical application. *Crit Care Med,* 37**,** 713-724.

BOKER, A., HABERMAN, C. J., GIRLING, L., GUZMAN, R. P., LOURIDAS, G., TANNER, J. R., CHEANG, M., MAYCHER, B. W., BELL, D. D. & DOAK, G. J. 2004. Variable Ventilation Improves Perioperative Lung Function in Patients Undergoing Abdominal Aortic Aneurysmectomy. *Anesthesiology,* 100**,** 608-616.

BONETTO, C., TERRAGNI, P. & RANIERI, V. M. 2005. Does high tidal volume generate ALI/ARDS in healthy lungs? *Intensive Care Medicine,* 31**,** 893-895.

BORGES, J. B., OKAMOTO, V. N., MATOS, G. F., CARAMEZ, M. P., ARANTES, P. R., BARROS, F., SOUZA, C. E., VICTORINO, J. A., KACMAREK, R. M., BARBAS, C. S., CARVALHO, C. R. & AMATO, M. B. 2006. Reversibility of lung collapse and hypoxemia in early acute respiratory distress syndrome. *Am J Respir Crit Care Med,* 174**,** 268 - 278.

BORGES SOBRINHO, J. B., DE CARVALHO, C. R. R. & AMATO, M. B. P. 2006. Is Maximal Lung Recruitment Worth It? *American Journal of Respiratory and Critical Care Medicine,* 174**,** 1159a.

BOUHEMAD, B., ZHANG, M., LU, Q. & ROUBY, J.-J. 2007. Clinical review: Bedside lung ultrasound in critical care practice. *Critical Care,* 11**,** 205.

BRANDER, L., LEONG-POI, H., BECK, J., BRUNET, F., HUTCHISON, S. J., SLUTSKY, A. S. & SINDERBY, C. 2009. Titration and Implementation of Neurally Adjusted Ventilatory Assist in Critically Ill Patients. *Chest,* 135**,** 695-703.

BRANDER, L. & SLUTSKY, A. 2006. Assisted spontaneous breathing during early acute lung injury. *Critical Care,* 10**,** 102.

BRANSON, R. D. & JOHANNIGMAN, J. A. 2009. Innovations in Mechanical Ventilation. *Respiratory Care,* 54**,** 933-947.

BRENNER, D. J. & HALL, E. J. 2007. Computed Tomography - An Increasing Source of Radiation Exposure. *N Engl J Med,* 357**,** 2277-2284.

BRIEL M, M. M. M. A. & ET AL. 2010. Higher vs lower positive end-expiratory pressure in patients with acute lung injury and acute respiratory distress syndrome: Systematic review and meta-analysis. *JAMA: The Journal of the American Medical Association,* 303**,** 865-873.

BROCHARD, L., MARTIN, G., BLANCH, L., PELOSI, P., BELDA, F. J., JUBRAN, A., GATTINONI, L., MANCEBO, J., RANIERI, V. M., RICHARD, J.-C., GOMMERS, D., VIEILLARD-BARON, A., PESENTI, A., JABER, S., STENQVIST, O. & VINCENT, J.-L. 2012. Clinical review: Respiratory monitoring in the ICU - a consensus of 16. *Critical Care,* 16**,** 219.

BROCHARD, L., ROUDOT-THORAVAL, F., ROUPIE, E., DELCLAUX, C., CHASTRE, J., FERNANDEX-MONDEJAR, E., CLEMENTI, E., MANCEBO, J., FACTOR, P., MATAMIS, D., RANIERI, M., BLANCH, L., RODI, G., MENTEC, H., DREYFUSS, D., FERRER, M., BRUN-BUISSON, C., TOBIN, M. & LEMAIRE, F. 1998. Tidal Volume Reduction for Prevention of Ventilator-induced Lung Injury in Acute Respiratory Distress Syndrome. *Am J Respir Crit Care Med,* 158**,** 1831-1838.

BROCHARD, L., RUA, F., LORINO, H., LEMAIRE, F. & HARF, A. 1991. Inspiratory Pressure Support Compensates for the Additional Work of Breathing Caused by the Endotracheal Tube. *Anesthesiology,* 75**,** 739-745.

BROWER, R. G., LANKEN, P. N., MACINTYRE, N., MATTHAY, M. A., MORRIS, A., ANCUKIEWICZ, M., SCHOENFELD, D. & THOMPSON, B. T. 2004. Higher versus Lower Positive End-Expiratory Pressures in Patients with the Acute Respiratory Distress Syndrome. *N Engl J Med,* 351**,** 327-336.

BRUNET, F., JEANBOURQUIN, D., MONCHI, M., MIRA, J. P., FIEROBE, L., ARMAGANIDIS, A., RENAUD, B., BELGHITH, M., NOUIRA, S. & DHAINAUT, J. F. 1995. Should mechanical ventilation be optimized to blood gases, lung mechanics, or thoracic CT scan? *American Journal of Respiratory and Critical Care Medicine,* 152**,** 524-30.

BURCHARDI, H. 2004. Aims of sedation/analgesia. *Minerva Anestesiol,* 70**,** 137 - 143.

BURLESON, B. S. & MAKI, E. D. 2005. Acute Respiratory Distress Syndrome. *Journal of Pharmacy Practice,* 18**,** 118-131.

BURROWES, K. S., CLARK, A. R., MARCINKOWSKI, A., WILSHER, M. L., MILNE, D. G. & TAWHAI, M. H. 2011. Pulmonary embolism: predicting disease severity. *Philosophical Transactions of the Royal Society A: Mathematical, Physical and Engineering Sciences,* 369**,** 4255-4277.

BURROWES, K. S., HUNTER, P. J. & TAWHAI, M. H. 2005. Anatomically based finite element models of the human pulmonary arterial and venous trees including supernumerary vessels. *J Appl Physiol,* 99**,** 731-738.

BURROWES, K. S., SWAN, A. J., WARREN, N. J. & TAWHAI, M. H. 2008. Towards a virtual lung: multi-scale, multi-physics modelling of the pulmonary system. *Philosophical Transactions of the Royal Society A: Mathematical, Physical and Engineering Sciences,* 366**,** 3247-3263.

BUSCHER, H., VALTA, P., SYDOW, M., THIES, K. & BURCHARDI, H. 2000. Pressure signal transmission of five commercially available oesophageal balloon catheters. *Intensive Care Med,* 26**,** 462-465.

BUSSO, T. & ROBBINS, P. A. 1997. Evaluation of estimates of alveolar gas exchange by using a tidally ventilated nonhomogenous lung model. *Journal of Applied Physiology,* 82**,** 1963-1971.

CABELLO, B. & MANCEBO, J. 2006. Work of breathing. *Intensive Care Medicine,* 32**,** 1311-1314.

CAGIDO, V. R. & ZIN, W. A. 2007. The pressure-volume curve. *In:* GULLO, A. (ed.) *Anaesthesia, Pain, Intensive Care and Emergency A.P.I.C.E.* Springer Milan.

CAIRONI, P., CRESSONI, M., CHIUMELLO, D., RANIERI, M., QUINTEL, M., RUSSO, S. G., CORNEJO, R., BUGEDO, G., CARLESSO, E., RUSSO, R., CASPANI, L. & GATTINONI, L. 2010. Lung Opening and Closing during Ventilation of Acute Respiratory Distress Syndrome. *American Journal of Respiratory and Critical Care Medicine,* 181**,** 578-586.

CAIRONI, P. & GATTINONI, L. 2007. How to monitor lung recruitment in patients with acute lung injury. *Current Opinion in Critical Care,* 13**,** 338-343 10.1097/MCC.0b013e32814db80c.

CARNEY, D., DIROCCO, J. & NIEMAN, G. 2005. Dynamic alveolar mechanics and ventilator-induced lung injury. *Crit Care Med,* 33**,** S122-S128.

CARNEY, D. E., BREDENBERG, C. E., SCHILLER, H. J., PICONE, A. L., MCCANN, U. G., GATTO, L. A., BAILEY, G., FILLINGER, M. & NIEMAN, G. F. 1999. The Mechanism of Lung Volume Change during Mechanical Ventilation. *American Journal of Respiratory and Critical Care Medicine,* 160**,** 1697-1702.

CARVALHO, A., JANDRE, F., PINO, A., BOZZA, F., SALLUH, J., RODRIGUES, R., ASCOLI, F. & GIANNELLA-NETO, A. 2007. Positive end-expiratory pressure at minimal respiratory elastance represents the best compromise between mechanical stress and lung aeration in oleic acid induced lung injury. *Critical Care,* 11**,** R86.

CARVALHO, A., JANDRE, F., PINO, A., BOZZA, F., SALLUH, J., RODRIGUES, R., SOARES, J. & GIANNELLA-NETO, A. 2006. Effects of descending positive end-expiratory pressure on lung mechanics and aeration in healthy anaesthetized piglets. *Critical Care,* 10**,** R122.

CARVALHO, A., SPIETH, P., PELOSI, P., VIDAL MELO, M., KOCH, T., JANDRE, F., GIANNELLA-NETO, A. & DE ABREU, M. 2008. Ability of dynamic airway pressure curve profile and elastance for positive end-expiratory pressure titration. *Intensive Care Medicine,* 34**,** 2291-2299.

CARVALHO, N. C., G LDNER, A., BEDA, A., SPIETH, P., RENTZSCH, I. & DE ABREU, G. M. 2011. Effects of different levels of spontaneous breathing activity during biphasic positive

airway pressure ventilation on lung function and pro‐inflammatory response in an experimental model of acute lung injury: 5AP4‐9. *European Journal of Anaesthesiology (EJA),* 28**,** 79.

CHAO, D. C. & SCHEINHORN, D. J. 1996. Barotrauma vs Volutrauma. *CHEST Journal,* 109**,** 1127-1128.

CHASE, J. G., LE COMPTE, A., PREISER, J.-C., SHAW, G., PENNING, S. & DESAIVE, T. 2011. Physiological modeling, tight glycemic control, and the ICU clinician: what are models and how can they affect practice? *Annals of Intensive Care,* 1:11.

CHASE, J. G., YUTA, T., MULLIGAN, K., SHAW, G. & HORN, B. 2006. A novel mechanical lung model of pulmonary diseases to assist with teaching and training. *BMC Pulmonary Medicine,* 6**,** 21.

CHENG, W., DELONG, D. S., FRANZ, G. N., PETSONK, E. L. & FRAZER, D. G. 1995. Contribution of opening and closing of lung units to lung hysteresis. *Respiration Physiology,* 102**,** 205-215.

CHEVALIER, P. A., RODARTE, J. R. & HARRIS, L. D. 1978. Regional lung expansion at total lung capacity in intact vs. excised canine lungs. *Journal of Applied Physiology,* 45**,** 363-369.

CHIEW, Y. S., CHASE, J. G., LAMBERMONT, B., JANSSEN, N., SCHRANZ, C., MOELLER, K., SHAW, G. & DESAIVE, T. 2012a. Physiological relevance and performance of a minimal lung model -- an experimental study in healthy and acute respiratory distress syndrome model piglets. *BMC Pulmonary Medicine,* 12**,** 59.

CHIEW, Y. S., CHASE, J. G., SHAW, G., SUNDARESAN, A. & DESAIVE, T. 2011. Model-based PEEP Optimisation in Mechanical Ventilation. *BioMedical Engineering OnLine,* 10**,** 111.

CHIEW, Y. S., CHASE, J. G., SHAW, G. M. & DESAIVE, T. 2012b. Respiratory system elastance monitoring during PEEP titration. *Critical Care,* 16**,** P103.

CHIEW, Y. S., DESAIVE, T., LAMBERMONT, B., JANSSEN, N., SHAW, G. M., SCHRANZ, C., MISHRA, A., DAMANHURI, N. & CHASE, J. Year. Performance of lung recruitment model in healthy anesthetized pigs. *In:* 2012 World Congress of Medical Physics and Biomedical Engineering, May 26-31, 2012c Beijing, China. 1-page.

CHIEW, Y. S., PIQUILLOUD, L., DESAIVE, T., LAMBERMONT, B., ROESELER, J., REVELLY, J., BIALAIS, E., TASSAUX, D., JOLLIET, P. & CHASE, J. Year. Range90 as indicator for ventilator output versus patients demand: NAVA and pressure support for non-invasively ventilated patients. *In:* 2012 World Congress of Medical Physics and Biomedical Engineering, May 26-31 2012d Beijing, China. 1-page.

CHIUMELLO, D., CARLESSO, E., CADRINGHER, P., CAIRONI, P., VALENZA, F., POLLI, F., TALLARINI, F., COZZI, P., CRESSONI, M., COLOMBO, A., MARINI, J. J. & GATTINONI, L. 2008. Lung Stress and Strain during Mechanical Ventilation for Acute Respiratory Distress Syndrome. *Am J Respir Crit Care Med,* 178**,** 346-355.

CHOI, J., XIA, G., TAWHAI, M., HOFFMAN, E. & LIN, C.-L. 2010. Numerical Study of High-Frequency Oscillatory Air Flow and Convective Mixing in a CT-Based Human Airway Model. *Annals of Biomedical Engineering,* 38**,** 3550-3571.

CLARK, A., BURROWES, K. & TAWHAI, M. 2011. Blood flow redistribution and ventilation-perfusion mismatch during embolic pulmonary arterial occlusion. *Pulmonary Circulation,* 1**,** 365-376.

COLOMBO, D., CAMMAROTA, G., BERGAMASCHI, V., DE LUCIA, M., CORTE, F. & NAVALESI, P. 2008. Physiologic response to varying levels of pressure support and neurally adjusted ventilatory assist in patients with acute respiratory failure. *Intensive Care Medicine,* 34**,** 2010-2018.

COOPER, A. B., FERGUSON, N. D. & HANLY, P. J. 1999. Long-term follow-up of survivors of acute lung injury: lack of effect of a ventilation strategy to prevent barotrauma. *Crit. Care Med.,* 27**,** 2616.

CORREA, T. D., PASSOS, R. H., KANDA, S., TANIGUCHI, C., HOELZ, C., BASTOS, J., MATOS, G. F. J., MEYER, E. C. & BARBAS, C. S. V. 2007. Flow or pressure triggering during pressure support ventilation? *Critical Care,* 11**,** P65.

COSTA, E. L. V., GONZALEZ LIMA, R. & AMATO, M. B. P. 2009. Electrical Impedance Tomography. *In:* VINCENT, J.-L. (ed.) *Yearbook of Intensive Care and Emergency Medicine.* Springer Berlin Heidelberg.

COUSSA, M. L., GUERIN, C., EISSA, N. T., CORBEIL, C., CHASSE, M., BRAIDY, J., MATAR, N. & MILIC-EMILI, J. 1993. Partitioning of work of breathing in mechanically ventilated COPD patients. *Journal of Applied Physiology,* 75**,** 1711-1719.

CROTTI, S., MASCHERONI, D., CAIRONI, P., PELOSI, P., RONZONI, G., MONDINO, M., MARINI, J. J. & GATTINONI, L. 2001. Recruitment and Derecruitment during Acute Respiratory Failure . A Clinical Study. *Am J Respir Crit Care Med,* 164**,** 131-140.

DASTA, J. F., MCLAUGHLIN, T. P., MODY, S. H. & PIECH, C. T. 2005. Daily cost of an intensive care unit day: The contribution of mechanical ventilation. *Crit Care Med,* 33**,** 1266-1271.

DE MATOS, G., STANZANI, F., PASSOS, R., FONTANA, M., ALBALADEJO, R., CASERTA, R., SANTOS, D., BORGES, J., AMATO, M. & BARBAS, C. 2012. How large is the lung recruitability in early acute respiratory distress syndrome: a prospective case series of patients monitored by computed tomography. *Critical Care,* 16**,** R4.

DE RYK, J., THIESSE, J., NAMATI, E. & MCLENNAN, G. 2007. Stress distribution in a three dimensional, geometric alveolar sac under normal and emphysematous conditions. *International Journal of Chronic Obstructive Pulmonary Disease,* 2(1)**,** 81-91.

DELLAMONICA, J., LEROLLE, N., SARGENTINI, C., BEDUNEAU, G., DI MARCO, F., MERCAT, A., RICHARD, J., DIEHL, J., MANCEBO, J., ROUBY, J., LU, Q., BERNARDIN, G. & BROCHARD, L. 2011. PEEP-induced changes in lung volume in acute respiratory distress syndrome. Two methods to estimate alveolar recruitment. *Intensive Care Medicine,* 37**,** 1595-1604.

DENAI, M. A., MAHFOUF, M., MOHAMAD-SAMURI, S., PANOUTSOS, G., BROWN, B. H. & MILLS, G. H. 2010. Absolute Electrical Impedance Tomography (aEIT) Guided Ventilation Therapy in Critical Care Patients: Simulations and Future Trends. *Information Technology in Biomedicine, IEEE Transactions on,* 14**,** 641-649.

DESAI, A. & DEEP, A. 2006. Ventilatory strategies and adjunctive therapy in ARDS. *Indian Journal of Pediatrics,* 73**,** 661-668.

DESAIVE, T., CHASE, J. G., SUNDARESAN, A., HANN, C. E., MORIMONT, P., LAMBERMONT, B. & SHAW, G. M. 2009. Model based assessment of Dynamic FRC (dFRC). *21st European Society of Intensive Care Medicine (ESICM) Annual Congress.* Vienna, Austria.

DEVAQUET, J., JONSON, B., NIKLASON, L., SI LARBI, A.-G., UTTMAN, L., ABOAB, J. & BROCHARD, L. 2008. Effects of inspiratory pause on CO2 elimination and arterial Pco2 in acute lung injury. *Journal of Applied Physiology,* 105**,** 1944-1949.

DICARLO, S. E. 2008. Teaching alveolar ventilation with simple, inexpensive models. *Advances in Physiology Education,* 32**,** 185-191.

DONG, G., BAYFORD, R. H., GAO, S., SATIO, Y. & YERWORTH, R. J. 2003. The application of the generalised vector pattern matching method for EIT image reconstruction. *Physiol. Meas.,* 24**,** 449.

DONOVAN, G. M. 2011. Multiscale mathematical models of airway constriction and disease. *Pulmonary Pharmacology & Therapeutics,* 24**,** 533-539.

DREYFUSS, D. & SAUMON, G. 1992. Barotrauma is volutrauma, but which volume is the one responsible? [editorial]. *Intensive Care Med.,* 18**,** 139.

EBERHARD, A., CARRY, P.-Y., PERDRIX, J.-P., FARGNOLI, J.-M., BIOT, L. C. & BACONNIER, P. F. 2003. A program based on a 'selective' least-squares method for respiratory mechanics monitoring in ventilated patients. *Computer Methods and Programs in Biomedicine,* 71**,** 39-61.

ESTEBAN, A., ALIA, I., TOBIN, MARTIN J., GIL, A., GORDO, F., VALLVERDU, I., BLANCH, L., BONET, A., VAZQUEZ, A., DE PABLO, R., TORRES, A., DE LA CAL, MIGUEL A. & MACIAS, S. 1999. Effect of Spontaneous Breathing Trial Duration on Outcome of Attempts to Discontinue Mechanical Ventilation. *Am. J. Respir. Crit. Care Med.,* 159**,** 512-518.

ESTEBAN, A., ANZUETO, A., ALIA, I., GORDO, F., APEZTEGUIA, C., PALIZAS, F., CIDE, D., GOLDWASER, R., SOTO, L., BUGEDO, G., RODRIGO, C., PIMENTEL, J., RAIMONDI, G. & TOBIN, M. J. 2000. How Is Mechanical Ventilation Employed in the Intensive Care Unit? . An International Utilization Review. *Am. J. Respir. Crit. Care Med.,* 161**,** 1450-1458.

ESTEBAN, A., ANZUETO, A., FRUTOS, F., ALIA, I., BROCHARD, L., STEWART, T., BENITO, S., EPSTEIN, S., APEZTEGUIA, S., NIGHTINGALE, P., ARROLIGA, A. & TOBIN, M. 2002. Characteristics and outcomes in adult patients receiving mechanical ventilation: a 28-day international study. *Jama,* 287**,** 345-355.

ESTEBAN, A., COOK, D. J., ANZUETO, A., GATTINONI, L., CHIUMELLO, D. & VAGGINELLI, F. 2005. Management of Patients with Respiratory Failure: An Evidence-based Approach. *In:* VINCENT, J.-L. (ed.) *Evidence-Based Management of Patients with Respiratory Failure.* Springer Berlin Heidelberg.

ESTEBAN, A., FERGUSON, N. D., MEADE, M. O., FRUTOS-VIVAR, F., APEZTEGUIA, C., BROCHARD, L., RAYMONDOS, K., NIN, N., HURTADO, J., TOMICIC, V., GONZALEZ, M., ELIZALDE, J., NIGHTINGALE, P., ABROUG, F., PELOSI, P., ARABI, Y., MORENO, R., JIBAJA, M., D'EMPAIRE, G., SANDI, F., MATAMIS, D., MONTANEZ, A. M., ANZUETO, A. & FOR THE, V. G. 2008. Evolution of Mechanical Ventilation in Response to Clinical Research. *Am. J. Respir. Crit. Care Med.,* 177**,** 170-177.

ESTEBAN, A., FRUTOS-VIVAR, F., FERGUSON, N. D., ARABI, Y., APEZTEGU A, C., GONZ LEZ, M., EPSTEIN, S. K., HILL, N. S., NAVA, S., SOARES, M.-A., D'EMPAIRE, G., AL A, I. & ANZUETO, A. 2004. Noninvasive Positive-Pressure Ventilation for Respiratory Failure after Extubation. *New England Journal of Medicine,* 350**,** 2452-2460.

FAGERBERG, A., S NDERGAARD, S., KARASON, S. & ANEMAN, A. 2009. Electrical impedence tomography and heterogeneity of pulmonary perfusion and ventilation in porcine acute lung injury. *Acta anaesthesiologica Scandinavica,* 53**,** 1300 - 1309.

FALKE KONRAD, J. 2003. The introduction of positive endexpiratory pressure into mechanical ventilation: a retrospective. *Intensive Care Medicine,* 29**,** 1233-1236.

FARRE, R., FERRER, M., ROTGER, M., TORRES, A. & NAVAJAS, D. 1998. Respiratory mechanics in ventilated COPD patients: forced oscillation versus occlusion techniques. *European Respiratory Journal,* 12**,** 170-176.

FERGUSON, N. D., FRUTOS-VIVAR, F., ESTEBAN, A., ANZUETO, A., ALIA, I., BROWER, R. G., STEWART, T. E., APEZTEGUIA, C., GONZALEZ, M., SOTO, L., ABROUG, F. & BROCHARD, L. 2005. Airway pressures, tidal volumes, and mortality in patients with acute respiratory distress syndrome. *Crit Care Med,* 33**,** 21-30.

FERNANDES, C. R. 2006. A importância da pressão pleural na avaliação da mecânica respiratória. *Revista Brasileira de Anestesiologia,* 56**,** 287-303.

FERRER, M., VALENCIA, M., NICOLAS, J. M., BERNADICH, O., BADIA, J. R. & TORRES, A. 2006. Early Noninvasive Ventilation Averts Extubation Failure in Patients at Risk. *American Journal of Respiratory and Critical Care Medicine,* 173**,** 164-170.

FERRING, M. & VINCENT, J. L. 1997. Is outcome from ARDS related to the severity of respiratory failure? *European Respiratory Journal,* 10**,** 1297-1300.

FRAWLEY, P. M. & HABASHI, N. M. 2001. Airway Pressure Release Ventilation: Theory and Practice. *AACN Advanced Critical Care,* 12**,** 234-246.

FRERICHS, I. 2000. Electrical impedance tomography (EIT) in applications related to lung and ventilation: a review of experimental and clinical activities. *Physiological Measurement,* 21**,** R1.

FULEIHAN, S. F., WILSON, R. S. & PONTOPPIDAN, H. 1976. Effect of Mechanical Ventilation with End‐inspiratory Pause on Blood‐Gas Exchange. *Anesthesia & Analgesia,* 55**,** 122-130.

G NTHER, A., SCHMIDT, R., HARODT, J., SCHMEHL, T., WALMRATH, D., RUPPERT, C., GRIMMINGER, F. & SEEGER, W. 2002. Bronchoscopic administration of bovine natural surfactant in ARDS and septic shock: impact on biophysical and biochemical surfactant properties. *European Respiratory Journal,* 19**,** 797-804.

GAJIC, O., DARA, S. I., MENDEZ, J. L., ADESANYA, A. O., FESTIC, E., CAPLES, S. M., RANA, R., ST. SAUVER, J. L., LYMP, J. F., AFESSA, B. & HUBMAYR, R. D. 2004. Ventilator-associated lung injury in patients without acute lung injury at the onset of mechanical ventilation *. *Critical Care Medicine,* 32**,** 1817-1824.

GAMA DE ABREU, M., SPIETH, P. M. & PELOSI, P. 2009. Variable Mechanical Ventilation: Breaking the Monotony. *In:* VINCENT, J.-L. (ed.) *Intensive Care Medicine.* Springer New York.

GAMA DE ABREU, M., SPIETH, P. M., PELOSI, P., CARVALHO, A. R., WALTER, C., SCHREIBER-FERSTL, A., AIKELE, P., NEYKOVA, B., H BLER, M. & KOCH, T. 2008. Noisy pressure support ventilation: A pilot study on a new assisted ventilation mode in experimental lung injury *. *Critical Care Medicine,* 36**,** 818-827 10.1097/01.CCM.0000299736.55039.3A.

GANZERT, S., MOLLER, K., STEINMANN, D., SCHUMANN, S. & GUTTMANN, J. 2009. Pressure-dependent stress relaxation in acute respiratory distress syndrome and healthy lungs: an investigation based on a viscoelastic model. *Crit Care.,* 13**,** R199.

GARCIA, C. S. N. B., ROCCO, P. R. M. & ZIN, W. A. 2006. Understanding the Mechanism of Ventilator-Induced Lung Injury Perioperative and Critical Care Medicine. *In:* GULLO, A. & BERLOT, G. (eds.). Springer Milan.

GATTINONI, L. 2011a. Counterpoint: Is Low Tidal Volume Mechanical Ventilation Preferred for All Patients on Ventilation? NoLow Tidal Volume Mechanical Ventilation Counterpoint. *CHEST Journal,* 140**,** 11-13.

GATTINONI, L. 2011b. Rebuttal From Dr Gattinoni. *CHEST Journal,* 140**,** 15-15.

GATTINONI, L. & CAIRONI, P. 2008. Refining Ventilatory Treatment for Acute Lung Injury and Acute Respiratory Distress Syndrome. *JAMA,* 299**,** 691-693.

GATTINONI, L., CAIRONI, P., CRESSONI, M., CHIUMELLO, D., RANIERI, V. M., QUINTEL, M., RUSSO, S., PATRONITI, N., CORNEJO, R. & BUGEDO, G. 2006a. Lung Recruitment in Patients with the Acute Respiratory Distress Syndrome. *N Engl J Med,* 354**,** 1775-1786.

GATTINONI, L., CAIRONI, P., PELOSI, P. & GOODMAN, L. R. 2001. What Has Computed Tomography Taught Us about the Acute Respiratory Distress Syndrome? *Am J Respir Crit Care Med,* 164**,** 1701-1711.

GATTINONI, L., CAIRONI, P., VALENZA, F. & CARLESSO, E. 2006b. The role of CT-scan studies for the diagnosis and therapy of acute respiratory distress syndrome. *Clin Chest Med,* 27**,** 559 - 570.

GATTINONI, L., CARLESSO, E., BRAZZI, L. & CAIRONI, P. 2010. Positive end-expiratory pressure. *Current Opinion in Critical Care,* 16**,** 39-44.

GATTINONI, L., CARLESSO, E., CADRINGHER, P., VALENZA, F., VAGGINELLI, F. & CHIUMELLO, D. 2003. Physical and biological triggers of ventilator-induced lung injury and its prevention. *Eur Respir J,* 22**,** 15s-25.

GATTINONI, L., PELOSI, P., SUTER, P. M., PEDOTO, A., VERCESI, P. & LISSONI, A. 1998. Acute Respiratory Distress Syndrome Caused by Pulmonary and Extrapulmonary Disease . Different Syndromes? *Am J Respir Crit Care Med,* 158**,** 3-11.

GIRARD, T. D. & BERNARD, G. R. 2007. Mechanical Ventilation in ARDS. *Chest,* 131**,** 921-929.

GOSS, C. H., BROWER, R. G., HUDSON, L. D., RUBENFELD, G. D. & FOR THE, A. N. 2003. Incidence of acute lung injury in the United States*. *Critical Care Medicine,* 31**,** 1607-1611 10.1097/01.CCM.0000063475.65751.1D.

GOULET, R., HESS, D. & KACMAREK, R. M. 1997. Pressure vs Flow Triggering During Pressure Support Ventilation. *CHEST Journal,* 111**,** 1649-1653.

GRANT, C. A., FRASER, J. F., DUNSTER, K. R. & SCHIBLER, A. 2009. The assessment of regional lung mechanics with electrical impedance tomography: a pilot study during recruitment manoeuvres. *Intensive Care Med,* 35**,** 166 - 170.

GRASSO, S., STRIPOLI, T., DE MICHELE, M., BRUNO, F., MOSCHETTA, M., ANGELELLI, G., MUNNO, I., RUGGIERO, V., ANACLERIO, R., CAFARELLI, A., DRIESSEN, B. & FIORE, T. 2007. ARDSnet Ventilatory Protocol and Alveolar Hyperinflation: Role of Positive End-Expiratory Pressure. *Am J Respir Crit Care Med,* 176**,** 761-767.

GRINNAN, D. & TRUWIT, J. 2005. Clinical review: Respiratory mechanics in spontaneous and assisted ventilation. *Critical Care,* 9**,** 472 - 484.

GROTJOHAN, H. P., VAN DER HEIJDE, R. M. J. L., JANSEN, J. R. C., WAGENVOORT, C. A. & VERSPRILLE, A. 1996. A stable model of respiratory distress by small injections of oleic acid in pigs. *Intensive Care Medicine,* 22**,** 336-344.

GU RIN, C., FOURNIER, G. & MILIC-EMILI, J. 2001. Effects of PEEP on inspiratory resistance in mechanically ventilated COPD patients. *European Respiratory Journal,* 18**,** 491-498.

GU RIN, C. & RICHARD, J.-C. 2012. Comparison of 2 Correction Methods for Absolute Values of Esophageal Pressure in Subjects With Acute Hypoxemic Respiratory Failure, Mechanically Ventilated in the ICU. *Respiratory Care,* 57**,** 2045-2051.

GUERIN, C. 2008. Questions on the Reversibility of Lung Collapse in Early Acute ARDS. *American Journal of Respiratory and Critical Care Medicine,* 177**,** 555.

GULLO, A., BERLOT, G., GARCIA, C. S. N. B., ROCCO, P. R. M. & ZIN, W. A. 2006. Understanding the Mechanism of Ventilator-Induced Lung Injury. *Perioperative and Critical Care Medicine.* Springer Milan.

GUTTMANN, J., EBERHARD, L., FABRY, B., BERTSCHMANN, W. & WOLFF, G. 1993. Continuous calculation of intratracheal pressure in tracheally intubated patients. *Anesthesiology,* 79**,** 503 - 513.

GUTTMANN, J., EBERHARD, L., FABRY, B., ZAPPE, D., BERNHARD, H., LICHTWARCK-ASCHOFF, M., ADOLPH, M. & WOLFF, G. 1994. Determination of volume-dependent respiratory system mechanics in mechanically ventilated patients using the new SLICE method. *Technol Health Care,* 2**,** 175 - 191.

HAGER, D. N., KRISHNAN, J. A., HAYDEN, D. L. & BROWER, R. G. 2005. Tidal volume reduction in patients with acute lung injury when plateau pressures are not high. *Am J Respir Crit Care Med,* 172**,** 1241 - 5.

HALTER, J. M., STEINBERG, J. M., SCHILLER, H. J., DASILVA, M., GATTO, L. A., LANDAS, S. & NIEMAN, G. F. 2003. Positive End-Expiratory Pressure after a Recruitment Maneuver Prevents Both Alveolar Collapse and Recruitment/Derecruitment. *Am J Respir Crit Care Med,* 167**,** 1620-1626.

HANN, C. E., CHASE, J. G., LIN, J., LOTZ, T., DORAN, C. V. & SHAW, G. M. 2005. Integral-based parameter identification for long-term dynamic verification of a glucose-insulin system model. *Computer Methods and Programs in Biomedicine,* 77**,** 259-270.

HARDMAN, J. G. & AITKENHEAD, A. R. 2003. Validation of an Original Mathematical Model of CO2 Elimination and Dead Space Ventilation. *Anesthesia & Analgesia,* 97**,** 1840-1845.

HARRIS, R. S., HESS, D. R. & VENEGAS, J. G. 2000. An objective analysis of the pressure-volume curve in the acute respiratory distress syndrome. *Am J Respir Crit Care Med,* 161**,** 432 - 9.

HASAN, A. 2010. *Understanding Mechanical Ventilation: A Practical Handbook*, Springer.

HELLER, H., BRANDT, S. & SCHUSTER, K. D. 2002. Development of an algorithm for improving the description of the pulmonary pressure-volume curve. *J Appl Physiol,* 92**,** 1770.

HENZLER, D., ORFAO, S., ROSSAINT, R. & KUHLEN, R. 2003. Modification of a sigmoidal equation for the pulmonary pressure-volume curve for asymmetric data. *J Appl Physiol,* 95**,** 2183 - 4.

HICKLING, KEITH G. 1998. The Pressure-Volume Curve Is Greatly Modified by Recruitment . A Mathematical Model of ARDS Lungs. *Am. J. Respir. Crit. Care Med.,* 158**,** 194-202.

HICKLING, K. G. 2002. Reinterpreting the pressure-volume curve in patients with acute respiratory distress syndrome. *Curr Opin Crit Care,* 8**,** 32 - 8.

HOARE, Z. & LIM, W. S. 2006. Pneumonia: update on diagnosis and management. *BMJ,* 332**,** 1077-1079.

HODGSON, C., TUXEN, D., DAVIES, A., BAILEY, M., HIGGINS, A., HOLLAND, A., KEATING, J., PILCHER, D., WESTBROOK, A., COOPER, D. & NICHOL, A. 2011a. A randomised controlled trial of an open lung strategy with staircase recruitment, titrated PEEP and targeted low airway pressures in patients with acute respiratory distress syndrome. *Critical Care,* 15**,** R133.

HODGSON, C. L., TUXEN, D. V., BAILEY, M. J., HOLLAND, A. E., KEATING, J. L., PILCHER, D., THOMSON, K. R. & VARMA, D. 2011b. A Positive Response to a Recruitment Maneuver With PEEP Titration in Patients With ARDS, Regardless of Transient Oxygen Desaturation During the Maneuver. *Journal of Intensive Care Medicine,* 26**,** 41-49.

HOLDER, D. S., RAO, A. & HANQUAN, Y. 1996. Imaging of physiologically evoked responses by EIT tomography with cortical electrodes in the anaesthetised rabbit. *Physiol. Meas.,* 17**,** 179.

HUBMAYR, R. D. 2011a. Point: Is Low Tidal Volume Mechanical Ventilation Preferred for All Patients on Ventilation? YesLow Tidal Volume Mechanical Ventilation Point. *CHEST Journal,* 140**,** 9-11.

HUBMAYR, R. D. 2011b. Rebuttal From Dr Hubmayr. *CHEST Journal,* 140**,** 14-15.

HUH, J., JUNG, H., CHOI, H., HONG, S.-B., LIM, C.-M. & KOH, Y. 2009. Efficacy of positive end-expiratory pressure titration after the alveolar recruitment manoeuvre in patients with acute respiratory distress syndrome. *Critical Care,* 13**,** R22.

INGELSTEDT, S., JONSON, B., NORDSTR M, L. & OLSSON, S.-G. 1972. A Servo-Controlled Ventilator Measuring Expired Minute Volume, Airway Flow and Pressure. *Acta Anaesthesiologica Scandinavica,* 16**,** 7-27.

IOTTI, G. A., BRASCHI, A., BRUNNER, J. X., SMITS, T., OLIVEI, M., PALO, A. & VERONESI, R. 1995. Respiratory mechanics by least squares fitting in mechanically ventilated patients: Applications during paralysis and during pressure support ventilation. *Intensive Care Medicine,* 21**,** 406-413.

JABER, S., DELAY, J.-M., MATECKI, S., SEBBANE, M., ELEDJAM, J.-J. & BROCHARD, L. 2005. Volume-guaranteed pressure-support ventilation facing acute changes in ventilatory demand. *Intensive Care Medicine,* 31**,** 1181-1188.

JADAD, A. R., MOORE, R. A., CARROLL, D., JENKINSON, C., REYNOLDS, D. J., GAVAGHAN, D. J. & MCQUAY, H. J. 1996. Assessing the quality of reports of randomized clinical trials: is blinding necessary? *Control Clin Trials,* 17**,** 1 - 12.

JANNEY, C. D. 1959. Super-syringe. *Anesthesiology,* 20**,** 709-711.

JONSON, B., RICHARD, J. C., STRAUS, C., MANCEBO, J., LEMAIRE, F. & BROCHARD, L. 1999. Pressure-Volume Curves and Compliance in Acute Lung Injury . Evidence of Recruitment Above the Lower Inflection Point. *Am J Respir Crit Care Med,* 159**,** 1172-1178.

JONSON, B. & SVANTESSON, C. 1999. Elastic pressure-volume curves: what information do they convey? *Thorax,* 54**,** 82-87.

JULIEN, M., HOEFFEL, J. M. & FLICK, M. R. 1986. Oleic acid lung injury in sheep. *Journal of Applied Physiology,* 60**,** 433-440.

KALLET, R. H. & BRANSON, R. D. 2007. Do the NIH ARDS Clinical Trials Network PEEP/FIO2 Tables Provide the Best Evidence-Based Guide to Balancing PEEP and FIO2 Settings in Adults? *Respiratory Care,* 52**,** 461-477.

KALLET, R. H., HEMPHILL, J. C., DICKER, R. A., ALONSO, J. A., CAMPBELL, A. R., MACKERSIE, R. C. & KATZ, J. A. 2007. The Spontaneous Breathing Pattern and Work of Breathing of Patients With Acute Respiratory Distress Syndrome and Acute Lung Injury. *Respiratory Care,* 52**,** 989-995.

KARASON, S., KARLSEN, K. L., LUNDIN, S. & STENQVIST, O. 1999. A simplified method for separate measurements of lung and chest wall mechanics in ventilator-treated patients. *Acta Anaesthesiologica Scandinavica,* 43**,** 308-315.

KARASON, S., SONDERGAARD, S., LUNDIN, S. & STENQVIST, O. 2001. Continuous on-line measurements of respiratory system, lung and chest wall mechanics during mechanic ventilation. *Intensive Care Medicine,* 27**,** 1328-1339.

KARASON, S., SONDERGAARD, S., LUNDIN, S., WIKLUND, J. & STENQVIST, O. 2000a. Evaluation of pressure/volume loops based on intratracheal pressure measurements during dynamic conditions. *Acta Anaesthesiologica Scandinavica,* 44**,** 571-577.

KARASON, S., SONDERGAARD, S., LUNDIN, S., WIKLUND, J. & STENQVIST, O. 2000b. A new method for non-invasive, manoeuvre-free determination of “static” pressure–volume curves during dynamic/therapeutic mechanical ventilation. *Acta Anaesthesiologica Scandinavica,* 44**,** 578-585.

KHIRANI, S., POLESE, G., ALIVERTI, A., APPENDINI, L., NUCCI, G., PEDOTTI, A., COLLEDAN, M., LUCIANETTI, A., BACONNIER, P. & ROSSI, A. 2010. On-line monitoring of lung mechanics during spontaneous breathing: a physiological study. *Respiratory Medicine,* 104**,** 463-471.

KITAOKA, H., NIEMAN, G. F., FUJINO, Y., CARNEY, D., DIROCCO, J. & KAWASE, I. 2007. A 4-Dimensional Model of the Alveolar Structure. *The Journal of Physiological Sciences,* 57**,** 175-185.

KOGLER, V. M. 2009. Advantage of spontaneous breathing in patients with respiratory failure. *SIGNA VITAE,* 4.

KOLLEF, M. H. & SCHUSTER, D. P. 1995. The Acute Respiratory Distress Syndrome. *New England Journal of Medicine,* 332**,** 27-37.

KONDILI, E., PRINIANAKIS, G., HOEING, S., CHATZAKIS, G. & GEORGOPOULOS, D. 2000. Low flow inflation pressure-time curve in patients with acute respiratory distress syndrome. *Intensive Care Medicine,* 26**,** 1756-1763.

KOSTIC, P., ZANNIN, E., ANDERSSON OLERUD, M., POMPILIO, P., HEDENSTIERNA, G., PEDOTTI, A., LARSSON, A., FRYKHOLM, P. & DELLACA, R. 2011. Positive end-expiratory pressure optimization with forced oscillation technique reduces ventilator induced lung injury: a controlled experimental study in pigs with saline lavage lung injury. *Critical Care,* 15**,** R126.

KRESS, J. P., POHLMAN, A. S. & HALL, J. B. 2002. Sedation and Analgesia in the Intensive Care Unit. *Am. J. Respir. Crit. Care Med.,* 166**,** 1024-1028.

KUEBLER, W. M., MERTENS, M. & PRIES, A. R. 2007. A two-component simulation model to teach respiratory mechanics. *Advances in Physiology Education,* 31**,** 218-222.

KUHLEN, R. & PUTENSEN, C. 1999. Maintaining spontaneous breathing efforts during mechanical ventilatory support. *Intensive Care Medicine,* 25**,** 1203-1205.

KUNST, P. W. A., B HM, S. H., DE ANDA, G. V., AMATO, M. B. P., LACHMANN, B., POSTMUS, P. E. & DE VRIES, P. M. J. M. 2000a. Regional pressure volume curves by electrical impedance tomography in a model of acute lung injury. *Crit Care Med,* 28**,** 178-183.

KUNST, P. W. A., DE ANDA, G. V., B HM, S. H., FAES, T. J. C., LACHMANN, B., POSTMUS, P. E. & DE VRIES, P. M. J. M. 2000b. Monitoring of recruitment and derecruitment by electrical impedance tomography in a model of acute lung injury. *Critical Care Medicine,* 28**,** 3891-3895.

LACHMANN, B. 1992. Open up the lung and keep the lung open. *Intensive Care Med,* 18**,** 319 - 321.

LAMBERMONT, B., GHUYSEN, A., JANSSEN, N., MORIMONT, P., HARTSTEIN, G., GERARD, P. & D'ORIO, V. 2008. Comparison of functional residual capacity and static compliance of the respiratory system during a positive end-expiratory pressure (PEEP) ramp procedure in an experimental model of acute respiratory distress syndrome. *Critical Care,* 12**,** R91.

LAUZON, A. M. & BATES, J. H. 1991. Estimation of time-varying respiratory mechanical parameters by recursive least squares. *Journal of Applied Physiology,* 71**,** 1159-1165.

LECOMTE, F., BRANDER, L., JALDE, F., BECK, J., QUI, H., ELIE, C., SLUTSKY, A. S., BRUNET, F. & SINDERBY, C. 2009. Physiological response to increasing levels of neurally adjusted ventilatory assist (NAVA). *Respiratory Physiology & Neurobiology,* 166**,** 117-124.

LEE, W. L., STEWART, T. E., MACDONALD, R., LAPINSKY, S., BANAYAN, D., HALLETT, D. & MEHTA, S. 2002. Safety of Pressure-Volume Curve Measurement in Acute Lung Injury and ARDS Using a Syringe Technique*. *Chest,* 121**,** 1595-1601.

LEVITZKY, M. G. 2007. *Pulmonary physiology,* New York, McGraw-Hill Medical.

LEVY, M. M. 2002. Optimal PEEP in ARDS: Changing concepts and current controversies. *Critical Care Clinics,* 18**,** 15-33.

LEWANDOWSKI, K., METZ, J. & DEUTSCHMANN, C. 1995. Incidence, severity, and mortality of acute respiratory failure in Berlin, Germany. *Am. J. Respir. Crit. Care Med.,* 151**,** 1121.

LICHTWARCK-ASCHOFF, M., HEDLUND, A. J., NORDGREN, K. A., WEGENIUS, G. A., MARKSTROM, A. M., GUTTMANN, J. & SJOSTRAND, U. H. 1999. Variables used to set PEEP in the lung lavage model are poorly related. *Br J Anaesth,* 83**,** 890-897.

LICHTWARCK-ASCHOFF, M., KESSLER, V., SJOSTRAND, U. H., HEDLUND, A., MOLS, G., RUBERTSSON, S., MARKSTROM, A. M. & GUTTMANN, J. 2000. Static versus dynamic respiratory mechanics for setting the ventilator. *Br J Anaesth,* 85**,** 577-586.

LINDAHL, S. 1979. Influence of an end inspiratory pause on pulmonary ventilation, gas distribution, and lung perfusion during artificial ventilation. *Critical Care Medicine,* 7(12)**,** 540-546.

LIONHEART, W. R. B. 2004. Review: developments in EIT reconstruction algorithms: pitfalls, challenges and recent developments. *Physiol. Meas.,* 25**,** 125.

LORINO, H., LORINO, A.-M., HARF, A., ATLAN, G. & LAURENT, D. 1982. Linear modeling of ventilatory mechanics during spontaneous breathing. *Computers and Biomedical Research,* 15**,** 129-144.

LORINO, H., LORINO, A. M., HARF, A. M., ATLAN, G. & LAURENT, D. 1981. Mathematical modeling of ventilatory mechanics during spontaneous breathing. *Proc Annu Symp Comput Appl Med Care***,** 440-444.

LU, Q., MALBOUISSON, L. M., MOURGEON, E., GOLDSTEIN, I., CORIAT, P. & ROUBY, J. J. 2001. Assessment of PEEP-induced reopening of collapsed lung regions in acute lung injury: are one or three CT sections representative of the entire lung? *Intensive Care Medicine,* 27**,** 1504-1510.

LU, Q. & ROUBY, J.-J. 2000. Measurement of pressure-volume curves in patients on mechanical ventilation: methods and significance. *Critical Care,* 4**,** 91 - 100.

LUCANGELO, U., BERNAB , F. & BLANCH, L. 2007. Lung mechanics at the bedside: make it simple. *Current Opinion in Critical Care,* 13**,** 64-72

LUCANGELO, U., PELOSI, P., ZIN, W., ALIVERTI, A., CRIMI, E., SORBO, L. & RANIERI, V. M. 2008. Ventilator-Associated Lung Injury. *Respiratory System and Artificial Ventilation.* Springer Milan.

LUECKE, T., CORRADI, F. & PELOSI, P. 2012. Lung imaging for titration of mechanical ventilation. *Current Opinion in Anesthesiology,* 25**,** 131-140 10.1097/ACO.0b013e32835003fb.

LUHR, O. R., ANTONSEN, K. & KARLSSON, M. 1999. Incidence and mortality after acute respiratory failure and acute respiratory distress syndrome in Sweden, Denmark, and Iceland. *Am. J. Respir. Crit. Care Med.,* 159**,** 1849.

MA, B. & BATES, J. 2010. Modeling the Complex Dynamics of Derecruitment in the Lung. *Annals of Biomedical Engineering,* 38**,** 3466-3477.

MACINTYRE, N., NISHIMURA, M., USADA, Y., TOKIOKA, H., TAKEZAWA, J. & SHIMADA, Y. 1990. The Nagoya conference on system design and patient-ventilator interactions during pressure support ventilation. *Chest,* 97**,** 1463-1466.

MACINTYRE, N. R. 1986. Respiratory function during pressure support ventilation. *Chest,* 89**,** 677-683.

MACINTYRE, N. R. 2008. Is There a Best Way to Set Positive Expiratory-End Pressure for Mechanical Ventilatory Support in Acute Lung Injury? *Clinics in chest medicine,* 29**,** 233-239.

MAGGIORE, S. M., RICHARD, J. C. & BROCHARD, L. 2003. What has been learnt from P/V curves in patients with acute lung injury/acute respiratory distress syndrome. *Eur Respir J,* 22**,** 22s-26.

MAISCH, S., BOEHM, S., WEISMANN, D., REISSMANN, H., BECKMANN, M., FUELLEKRUG, B., MEYER, A. & SCHULTE AM ESCH, J. 2007. Determination of functional residual capacity by oxygen washin-washout: a validation study. *Intensive Care Medicine,* 33**,** 912-916.

MALBOUISSON, L. M., MULLER, J.-C., CONSTANTIN, J.-M., LU, Q. I. N., PUYBASSET, L., ROUBY, J.-J. & THE, C. T. S. A. S. G. 2001. Computed Tomography Assessment of Positive End-expiratory Pressure-induced Alveolar Recruitment in Patients with Acute Respiratory Distress Syndrome. *Am. J. Respir. Crit. Care Med.,* 163**,** 1444-1450.

MALHOTRA, A. 2007. Low-Tidal-Volume Ventilation in the Acute Respiratory Distress Syndrome. *N Engl J Med,* 357**,** 1113-1120.

MARINI, J. J. 1992. What derived variables should be monitored during mechanical ventilation? *Respiratory Care,* 37**,** 1097-1107.

MARINI, J. J. 2011. Spontaneously regulated vs. controlled ventilation of acute lung injury/acute respiratory distress syndrome. *Current Opinion in Critical Care,* 17**,** 24-29 10.1097/MCC.0b013e328342726e.

MARINI, J. J., CAPPS, J. S. & CULVER, B. H. 1985. The inspiratory work of breathing during assisted mechanical ventilation. *Chest,* 87**,** 612-618.

MARINI, J. J. & GATTINONI, L. 2004. Ventilatory management of acute respiratory distress syndrome: a consensus of two. *Crit Care Med,* 32**,** 250 - 255.

MARKHORST, D., GENDERINGEN, H. & VUGHT, A. 2004. Static pressure-volume curve characteristics are moderate estimators of optimal airway pressures in a mathematical model of (primary/pulmonary) acute respiratory distress syndrome. *Intensive Care Medicine,* 30**,** 2086-2093.

MARKHORST, D., KNEYBER, M. & VAN HEERDE, M. 2008. The quest for optimal positive end-expiratory pressure continues. *Critical Care,* 12**,** 408.

MASSA, C. B., ALLEN, G. B. & BATES, J. H. T. 2008. Modeling the dynamics of recruitment and derecruitment in mice with acute lung injury. *Journal of Applied Physiology,* 105**,** 1813-1821.

MATUTE-BELLO, G., FREVERT, C. W. & MARTIN, T. R. 2008. Animal models of acute lung injury. *American Journal of Physiology - Lung Cellular and Molecular Physiology,* 295**,** L379-L399.

MEAD, J. & WHITTENBERGER, J. L. 1953. Physical Properties of Human Lungs Measured During Spontaneous Respiration. *Journal of Applied Physiology,* 5**,** 779-796.

MEADE, M. O., COOK, D. J., GUYATT, G. H., SLUTSKY, A. S., ARABI, Y. M., COOPER, D. J., DAVIES, A. R., HAND, L. E., ZHOU, Q., THABANE, L., AUSTIN, P., LAPINSKY, S., BAXTER, A., RUSSELL, J., SKROBIK, Y., RONCO, J. J., STEWART, T. E. & FOR THE LUNG OPEN VENTILATION STUDY, I. 2008. Ventilation Strategy Using Low Tidal Volumes, Recruitment Maneuvers, and High Positive End-Expiratory Pressure for Acute Lung Injury and Acute Respiratory Distress Syndrome: A Randomized Controlled Trial. *JAMA,* 299**,** 637-645.

MERCAT, A., RICHARD, J.-C. M., VIELLE, B., JABER, S., OSMAN, D., DIEHL, J.-L., LEFRANT, J.-Y., PRAT, G., RICHECOEUR, J., NIESZKOWSKA, A., GERVAIS, C., BAUDOT, J., BOUADMA, L., BROCHARD, L. & FOR THE EXPIRATORY PRESSURE STUDY, G. 2008. Positive End-Expiratory Pressure Setting in Adults With Acute Lung Injury and Acute Respiratory Distress Syndrome: A Randomized Controlled Trial. *JAMA,* 299**,** 646-655.

MERGONI, M., VOLPI, A., BRICCHI, C. & ROSSI, A. 2001. Lower inflection point and recruitment with PEEP in ventilated patients with acute respiratory failure. *J Appl Physiol,* 91**,** 441-450.

MERTENS, M., TABUCHI, A., MEISSNER, S., KRUEGER, A., SCHIRRMANN, K., KERTZSCHER, U., PRIES, A. R., SLUTSKY, A. S., KOCH, E. & KUEBLER, W. M. 2009. Alveolar dynamics in acute lung injury: Heterogeneous distension rather than cyclic opening and collapse *. *Critical Care Medicine,* 37**,** 2604-2611.

MIRELES-CABODEVILA, E., DIAZ-GUZMAN, E., HERESI, G. A. & CHATBURN, R. L. 2009. Alternative modes of mechanical ventilation: A review for the hospitalist. *Cleveland Clinic Journal of Medicine,* 76**,** 417-430.

MODRYKAMIEN, A., CHATBURN, R. L. & ASHTON, R. W. 2011. Airway pressure release ventilation: An alternative mode of mechanical ventilation in acute respiratory distress syndrome. *Cleveland Clinic Journal of Medicine,* 78**,** 101-110.

MOGENSEN, M. L., STEIMLE, K. S., KARBING, D. S. & ANDREASSEN, S. 2011. A model of perfusion of the healthy human lung. *Computer Methods and Programs in Biomedicine,* 101**,** 156-165.

MOLS, G., KESSLER, V., BENZING, A., LICHTWARCK‐ASCHOFF, M., GEIGER, K. & GUTTMANN, J. 2001. Is pulmonary resistance constant, within the range of tidal volume ventilation, in patients with ARDS? *British Journal of Anaesthesia,* 86**,** 176-182.

MONTGOMERY, A. B., STAGER, M. A., CARRICO, C. J. & HUDSON, L. D. 1985. Causes of mortality in patients with the adult respiratory distress syndrome. *Am. Rev. Respir. Dis.,* 132**,** 485.

MOORHEAD, K., PIQUILLOUD, L., LAMBERMONT, B., ROESELER, J., CHIEW, Y. S., CHASE, J. G., REVELLY, J.-P., BIALAIS, E., TASSAUX, D., LATERRE, P.-F., JOLLIET, P., SOTTIAUX, T. & DESAIVE, T. 2012. NAVA enhances tidal volume and diaphragmatic electro-myographic activity matching: a Range90 analysis of supply and demand. *Journal of Clinical Monitoring and Computing***,** 1-10.

MORTELLITI, M. P. & MANNING, H. L. 2002. Acute respiratory distress syndrome. *American Family Physician,* 65**,** 1823-1830.

MUDERS, T., LUEPSCHEN, H. & PUTENSEN, C. 2010. Impedance tomography as a new monitoring technique. *Current Opinion in Critical Care,* 16**,** 269-275.

MULQUEENY, Q., TASSAUX, D., VIGNAUX, L., JOLLIET, P., SCHINDHELM, K., REDMOND, S. & LOVELL, N. H. Year. Online estimation of respiratory mechanics in non-invasive pressure support ventilation: A bench model study. *In:* Engineering in Medicine and Biology Society (EMBC), 2010 Annual International Conference of the IEEE, Aug. 31 2010-Sept. 4 2010 2010. 2489-2492.

MURAMATSU, K., YUKITAKE, K., NAKAMURA, M., MATSUMOTO, I. & MOTOHIRO, Y. 2001. Monitoring of nonlinear respiratory elastance using a multiple linear regression analysis. *European Respiratory Journal,* 17**,** 1158-1166.

MURRAY, J. F., MATTHAY, M. A., LUCE, J. M. & FLICK, M. R. 1988. An Expanded Definition of the Adult Respiratory Distress Syndrome. *American Journal of Respiratory and Critical Care Medicine,* 138**,** 720-723.

NAVAJAS, D., ALCARAZ, J., PESLIN, R., ROCA, J. & FARRE, R. 2000. Evaluation of a method for assessing respiratory mechanics during noninvasive ventilation. *European Respiratory Journal,* 16**,** 704-709.

NÈVE, V., DE LA ROQUE, E. D., LECLERC, F., LETEURTRE, S., DORKENOO, A., SADIK, A., CREMER, R. & LOGIER, R. 2000. Ventilator-induced Overdistension in Children. *American Journal of Respiratory and Critical Care Medicine,* 162**,** 139-147.

NIESZKOWSKA, A., LU, Q., VIEIRA, S., ELMAN, M., FETITA, C. & ROUBY, J. 2004. Incidence and regional distribution of lung overinflation during mechanical ventilation with positive end-expiratory pressure. *Crit Care Med,* 32**,** 1496 - 1503.

OLEGARD, C., SONDERGAARD, S., PALSSON, J., LUNDIN, S. & STENQVIST, O. 2010. Validation and clinical feasibility of nitrogen washin/washout functional residual capacity measurements in children. *Acta Anaesthesiologica Scandinavica,* 54**,** 370-376.

OOSTVEEN, E., MACLEOD, D., LORINO, H., FARR , R., HANTOS, Z., DESAGER, K., MARCHAL, F. & MEASUREMENTS, O. B. O. T. E. T. F. O. R. I. 2003. The forced oscillation technique

in clinical practice: methodology, recommendations and future developments. *European Respiratory Journal,* 22**,** 1026-1041.

OTIS, A. B., FENN, W. O. & RAHN, H. 1950. Mechanics of Breathing in Man. *Journal of Applied Physiology,* 2**,** 592-607.

PAPPERT, D., ROSSAINT, R. & SLAMA, K. 1994. Influence of positioning on ventilation-perfusion relationships in severe adult respiratory distress syndrome. *Chest,* 106**,** 1511.

PASSATH, C., TAKALA, J., TUCHSCHERER, D., JAKOB, S. M., SINDERBY, C. & BRANDER, L. 2010. Physiologic Response to Changing Positive End-Expiratory Pressure During Neurally Adjusted Ventilatory Assist in Sedated, Critically Ill Adults. *Chest,* 138**,** 578-587.

PATRONITI, N., BELLANI, G., SACCAVINO, E., ZANELLA, A., GRASSELLI, G., ISGR , S., MILAN, M., FOTI, G. & PESENTI, A. 2012. Respiratory pattern during neurally adjusted ventilatory assist in acute respiratory failure patients. *Intensive Care Medicine,* 38**,** 230-239.

PAVONE, L., ALBERT, S., CARNEY, D., GATTO, L., HALTER, J. & NIEMAN, G. 2007. Injurious mechanical ventilation in the normal lung causes a progressive pathologic change in dynamic alveolar mechanics. *Critical Care,* 11**,** R64.

PELOSI, P., GOLDNER, M., MCKIBBEN, A., ADAMS, A., ECCHER, G., CAIRONI, P., LOSAPPIO, S., GATTINONI, L. & MARINI, J. J. 2001. Recruitment and derecruitment during acute respiratory failure: an experimental study. *Am J Respir Crit Care Med,* 164**,** 122 - 30.

PERIS, A., ZAGLI, G., BARBANI, F., TUTINO, L., BIONDI, S., DI VALVASONE, S., BATACCHI, S., BONIZZOLI, M., SPINA, R., MINIATI, M., PAPPAGALLO, S., GIOVANNINI, V. & GENSINI, G. F. 2010. The value of lung ultrasound monitoring in H1N1 acute respiratory distress syndrome. *Anaesthesia,* 65**,** 294-297.

PESENTI, A., TAGLIABUE, P., PATRONITI, N. & FUMAGALLI, R. 2001. Computerised tomography scan imaging in acute respiratory distress syndrome. *Intensive Care Med,* 27**,** 631 - 639.

PESLIN, R., DA SILVA, J. F., CHABOT, F. & DUVIVIER, C. 1992. Respiratory mechanics studied by multiple linear regression in unsedated ventilated patients. *Eur Respir J,* 5**,** 871-878.

PESTA A, D., HERN NDEZ-GANCEDO, C., ROYO, C., P REZ-CHRZANOWSKA, H. & CRIADO, A. 2005. Pressure–volume curve variations after a recruitment manoeuvre in acute lung injury/ARDS patients: implications for the understanding of the inflection points of the curve. *European Journal of Anaesthesiology,* 22**,** 175-180.

PETTY, T. L. & ASHBAUGH, D. G. 1971. The adult respiratory distress syndrome: clinical features, factors influencing prognosis and principles of management. *Chest,* 60**,** 233.

PHUA, J., BADIA, J. R., ADHIKARI, N. K. J., FRIEDRICH, J. O., FOWLER, R. A., SINGH, J. M., SCALES, D. C., STATHER, D. R., LI, A., JONES, A., GATTAS, D. J., HALLETT, D., TOMLINSON, G., STEWART, T. E. & FERGUSON, N. D. 2009. Has Mortality from Acute Respiratory Distress Syndrome Decreased over Time?: A Systematic Review. *Am J Respir Crit Care Med,* 179**,** 220-227.

PILLET, O., CHOUKROUN, M. L. & CASTAING, Y. 1993. Effects of inspiratory flow rate alterations on gas exchange during mechanical ventilation in normal lungs. Efficiency of end-inspiratory pause. *CHEST Journal,* 103**,** 1161-1165.

PIQUILLOUD, L., CHIEW, Y. S., BIALAIS, E., LAMBERMONT, B., ROESELER, J., CHASE, J. G., DESAIVE, T., SOTTIAUX, T., TASSAUX, D., JOLLIET, P. & REVELLY, J. Year. Neurally Adjusted Ventilatory Assist (NAVA) improves the matching of diaphragmatic electrical activity and tidal volume in comparison to pressure support (PS). *In:* 24th

Annual Congress of the European Society of Intensive Care Medicine (ESICM 2011), October 1-5 2011a Berlin, Germany. 1-page.

PIQUILLOUD, L., TASSAUX, D., BIALAIS, E., LAMBERMONT, B., SOTTIAUX, T., ROESELER, J., LATERRE, P.-F., JOLLIET, P. & REVELLY, J.-P. 2012. Neurally adjusted ventilatory assist (NAVA) improves patient–ventilator interaction during non-invasive ventilation delivered by face mask. *Intensive Care Medicine*, 1-8.

PIQUILLOUD, L., VIGNAUX, L., BIALAIS, E., ROESELER, J., SOTTIAUX, T., LATERRE, P.-F., JOLLIET, P. & TASSAUX, D. 2011b. Neurally adjusted ventilatory assist improves patient–ventilator interaction. *Intensive Care Medicine,* 37, 263-271.

POLESE, G., ROSSI, A., APPENDINI, L., BRANDI, G., BATES, J. H. & BRANDOLESE, R. 1991. Partitioning of respiratory mechanics in mechanically ventilated patients. *Journal of Applied Physiology,* 71, 2425-2433.

PULLETZ, S., ADLER, A., KOTT, M., ELKE, G., GAWELCZYK, B., SCH DLER, D., ZICK, G., WEILER, N. & FRERICHS, I. 2012. Regional lung opening and closing pressures in patients with acute lung injury. *Journal of critical care,* 27, 323.e11-323.e18.

PUTENSEN, C., MUTZ, NORBERT J., PUTENSEN-HIMMER, G. & ZINSERLING, J. 1999. Spontaneous Breathing During Ventilatory Support Improves Ventilation-Perfusion Distributions in Patients with Acute Respiratory Distress Syndrome. *Am. J. Respir. Crit. Care Med.,* 159, 1241-1248.

PUTENSEN, C., THEUERKAUF, N., ZINSERLING, J. R., WRIGGE, H. & PELOSI, P. 2009. Meta-analysis: Ventilation Strategies and Outcomes of the Acute Respiratory Distress Syndrome and Acute Lung Injury. *Annals of Internal Medicine,* 151, 566-576.

PUTENSEN, C. & WRIGGE, H. 2004. Clinical review: Biphasic positive airway pressure and airway pressure release ventilation. *Critical Care,* 8, 492 - 497.

PUTENSEN, C., ZECH, S., WRIGGE, H., ZINSERLING, J., STUBER, F., VON SPIEGEL, T. & MUTZ, N. 2001. Long-Term Effects of Spontaneous Breathing During Ventilatory Support in Patients with Acute Lung Injury. *Am. J. Respir. Crit. Care Med.,* 164, 43-49.

QUAGLINI, S., BARAHONA, P., ANDREASSEN, S., REES, S., ALLER D, C., KJ RGAARD, S., TOFT, E. & THORGAARD, P. 2001. Diagnosing Patient State in Intensive Care Patients Using the Intelligent Ventilator (INVENT) System. *Artificial Intelligence in Medicine.* Springer Berlin / Heidelberg.

RAMSEY, C. D., FUNK, D., MILLER, R. R. I. & KUMAR, A. 2010. Ventilator management for hypoxemic respiratory failure attributable to H1N1 novel swine origin influenza virus. *Critical Care Medicine,* 38, e58-e65.

RANIERI, V. M., GIULIANI, R., FIORE, T., DAMBROSIO, M. & MILIC-EMILI, J. 1994. Volume-pressure curve of the respiratory system predicts effects of PEEP in ARDS: "occlusion" versus "constant flow" technique. *American Journal of Respiratory and Critical Care Medicine,* 149, 19-27.

RANIERI, V. M., GIUNTA, F., SUTER, P. M. & SLUTSKY, A. S. 2000a. Mechanical ventilation as a mediator of multisystem organ failure in acute respiratory distress syndrome. *JAMA,* 284, 43 - 44.

RANIERI, V. M., ZHANG, H., MASCIA, L., AUBIN, M., LIN, C.-Y., MULLEN, J. B., GRASSO, S., BINNIE, M., VOLGYESI, G. A., ENG, P. & SLUTSKY, A. S. 2000b. Pressure–Time Curve Predicts Minimally Injurious Ventilatory Strategy in an Isolated Rat Lung Model. *Anesthesiology,* 93, 1320-1328.

RAO, A., GIBSON, A. & HOLDER, D. S. 1997. EIT images of electrically induced epileptic activity in anaesthetised rabbits. *Med. Biol. Eng. Comput.,* 35, 327.

REDDY, P. I., AL-JUMAILY, A. M. & BOLD, G. T. 2011. Dynamic surface tension of natural surfactant extract under superimposed oscillations. *Journal of Biomechanics,* 44**,** 156-163.

REES, S. E., KJ RGAARD, S., THORGAARD, P., MALCZYNSKI, J., TOFT, E. & ANDREASSEN, S. 2002. The Automatic Lung Parameter Estimator (ALPE) System: Non-Invasive Estimation of Pulmonary Gas Exchange Parameters in 10-15 Minutes. *Journal of Clinical Monitoring and Computing,* 17**,** 43-52.

REYNOLDS, H. N., MCCUNN, M., BORG, U., HABASHI, N., COTTINGHAM, C. & BAR-LAVI, Y. 1998. Acute respiratory distress syndrome: estimated incidence and mortality rate in a 5 million-person population base. *Critical Care,* 2**,** 29–34.

RICARD, J. D., DREYFUSS, D. & SAUMON, G. 2003. Ventilator-induced lung injury. *Eur Respir J,* 22**,** 2s-9.

RICHARD, J.-C., JANIER, M., LAVENNE, F., TOURVIEILLE, C., LE BARS, D., COSTES, N., GIMENEZ, G. & GUERIN, C. 2005. Quantitative Assessment of Regional Alveolar Ventilation and Gas Volume Using 13N-N2 Washout and PET. *Journal of Nuclear Medicine,* 46**,** 1375-1383.

ROBERT J. MASON, V. COURTNEY BROADDUS, THOMAS R. MARTIN, TALMADGE E. KING, DEAN E. SCHRAUFNAGEL, JOHN F. MURRAY & NADEL, J. A. 2010. *MURRAY AND NADEL'S TEXTBOOK OF RESPIRATORY MEDICINE*.

ROSE, L. & HAWKINS, M. 2008. Airway pressure release ventilation and biphasic positive airway pressure: a systematic review of definitional criteria. *Intensive Care Medicine,* 34**,** 1766-1773.

ROSE, L., PRESNEILL, J. J., JOHNSTON, L., NELSON, S. & CADE, J. F. 2009. Ventilation and weaning practices in Australia and New Zealand. *Anaesthesia And Intensive Care,* 37**,** 99-107.

ROSENTHAL, C., CARONIA, C., QUINN, C., LUGO, N. & SAGY, M. 1998. A comparison among animal models of acute lung injury. *Critical Care Medicine,* 26**,** 912-916.

ROSSI, A., POLESE, G., BRANDI, G. & CONTI, G. 1995. Intrinsic positive end-expiratory pressure ($PEEP_i$). *Intensive Care Medicine,* 21**,** 522-536.

ROSSI, F. S., MASCARETTI, R. S., HADDAD, L. B., FREDDI, N. A., MAUAD, T. & REBELLO, C. M. 2008. Utilization of the lower inflection point of the pressure-volume curve results in protective conventional ventilation comparable to high frequency oscillatory ventilation in an animal model of acute respiratory distress syndrome. *Clinics,* 63**,** 237-244.

ROUBY, J. J., CONTANTIN, J. M., GIRARDI, C., ZHANG, M. & QIN, L. 2004. Mechanical Ventilation in patients with acute respiratory distress syndrome. *Anesthesiology,* 101**,** 228 - 234.

ROUBY, J. J., LHERM, T. & MARTIN DE LASSALE, E. 1993. Histologic aspects of pulmonary barotrauma in critically ill patients with acute respiratory failure. *Intensive Care Med.,* 19**,** 383.

ROUSSELOT, J. M., PESLIN, R. & DUVIVIER, C. 1992. Evaluation of the Multiple Linear-Regression Method to Monitor Respiratory Mechanics in Ventilated Neonates and Young-Children. *Pediatric Pulmonology,* 13**,** 161-168.

ROZ , H., LAFRIKH, A., PERRIER, V., GERMAIN, A., DEWITTE, A., GOMEZ, F., JANVIER, G. & OUATTARA, A. 2011. Daily titration of neurally adjusted ventilatory assist using the diaphragm electrical activity. *Intensive Care Medicine,* 37**,** 1087-1094.

RUSCA, M., PROIETTI, S., SCHNYDER, P., FRASCAROLO, P., HEDENSTIERNA, G., SPAHN, D. R. & MAGNUSSON, L. 2003. Prevention of Atelectasis Formation During Induction of General Anesthesia. *Anesthesia & Analgesia,* 97**,** 1835-1839.

SCHILLER, H. J., STEINBERG, J., HALTER, J., MCCANN, U., DASILVA, M., GATTO, L. A., CARNEY, D. & NIEMAN, G. 2003. Alveolar inflation during generation of a quasi-static pressure/volume curve in the acutely injured lung. *Critical Care Medicine,* 31**,** 1126-1133 10.1097/01.CCM.0000059997.90832.29.

SCHIRRMANN, K., MERTENS, M., KERTZSCHER, U., KUEBLER, W. M. & AFFELD, K. 2010. Theoretical modeling of the interaction between alveoli during inflation and deflation in normal and diseased lungs. *Journal of Biomechanics,* 43**,** 1202-1207.

SCHLESINGER, A. E., WHITE, D. K., MALLORY, G. B., HILDEBOLDT, C. F. & HUDDLESTON, C. B. 1995. Estimation of total lung capacity from chest radiography and chest CT in children: comparison with body plethysmography. *American Journal of Roentgenology,* 165**,** 151-4.

SCHMIDT, M., DEMOULE, A., CRACCO, C., GHARBI, A., FIAMMA, M.-N., STRAUS, C., DUGUET, A., GOTTFRIED, S. B. & SIMILOWSKI, T. 2010. Neurally Adjusted Ventilatory Assist Increases Respiratory Variability and Complexity in Acute Respiratory Failure. *Anesthesiology,* 112**,** 670-681 10.1097/ALN.0b013e3181cea375.

SCHMIDT, M., DRES, M., RAUX, M., DESLANDES-BOUTMY, E., KINDLER, F., MAYAUX, J., SIMILOWSKI, T. & DEMOULE, A. 2012. Neurally adjusted ventilatory assist improves patient–ventilator interaction during postextubation prophylactic noninvasive ventilation*. *Critical Care Medicine,* 40**,** 1738-1744 10.1097/CCM.0b013e3182451f77.

SCHRANZ, C., DOCHERTY, P. D., CHIEW, Y. S., CHASE, J. G., X00F & LLER, K. 2012. Structural Identifiability and Practical Applicability of an Alveolar Recruitment Model for ARDS Patients. *Biomedical Engineering, IEEE Transactions on,* 59**,** 3396-3404.

SCHRANZ, C., GUTTMANN, J. & MOLLER, K. 2010. An Approach towards Parameter Identification in Hierarchical Models of Respiratory Mechanics. *Biomed Tech.,* 55 (Suppl. 1).

SCHRANZ, C., KNOBEL, C., KRETSCHMER, J., ZHAO, Z. & MOLLER, K. 2011. Hierarchical Parameter Identification in Models of Respiratory Mechanics. *IEEE Trans Biomed Eng*.

SCHUESSLER, T. F., GOTTFRIED, S. B. & BATES, J. H. T. 1997. A model of the spontaneously breathing patient: applications to intrinsic PEEP and work of breathing. *Journal of Applied Physiology,* 82**,** 1694-1703.

SCHULTZ, M., HAITSMA, J., SLUTSKY, A. & GAJIC, O. 2007. What tidal volumes should be used in patients with acute lung injury? *Anesthesiology,* 106**,** 1085 - 1087.

SCHUSTER, D. P. 1994. ARDS: clinical lessons from the oleic acid model of acute lung injury. *Am J Respir Crit Care Med,* 149**,** 245 - 260.

SEBEL, P. 1985. *Respiration, the breath of life,* New York, Torstar Books.

SERVILLO, G., DE ROBERTIS, E., MAGGIORE, S., LEMAIRE, F., BROCHARD, L. & TUFANO, R. 2002. The upper inflection point of the pressure-volume curve. *Intensive Care Medicine,* 28**,** 842-849.

SERVILLO, G., SVANTESSON, C., BEYDON, L., ROUPIE, E., BROCHARD, L., LEMAIRE, F. & JONSON, B. 1997. Pressure-volume curves in acute respiratory failure: automated low flow inflation versus occlusion. *American Journal of Respiratory and Critical Care Medicine,* 155**,** 1629-36.

SHARAN, M., SINGH, M. P. & SINGH, B. 1988. A mathematical model for the process of gas exchange in lung capillaries using nth order one-step kinetics of oxygen uptake by haemoglobin. *The ANZIAM Journal,* 30**,** 203-213.

SHIU, K. K. & ROSEN, M. J. 2006. Is There a Safe Plateau Pressure Threshold for Patients with Acute Lung Injury and Acute Respiratory Distress Syndrome? *American Journal of Respiratory and Critical Care Medicine,* 173**,** 686.

SINDERBY, C. 2002. Neurally adjusted ventilatory assist (NAVA). *Minerva Anestesiologica* 68**,** 378-380.

SINDERBY, C., BECK, J., SPAHIJA, J., DE MARCHIE, M., LACROIX, J., NAVALESI, P. & SLUTSKY, A. S. 2007. Inspiratory Muscle Unloading by Neurally Adjusted Ventilatory Assist During Maximal Inspiratory Efforts in Healthy Subjects*. *Chest,* 131**,** 711-717.

SINDERBY, C., NAVALESI, P., BECK, J., SKROBIK, Y., COMTOIS, N., FRIBERG, S., GOTTFRIED, S. B. & LINDSTROM, L. 1999. Neural control of mechanical ventilation in respiratory failure. *Nat Med,* 5**,** 1433-1436.

SLUTSKY, A. 1993. Mechanical Ventilation. American College of Chest Physicians' Consensus Conference. *Chest,* 104(6)**,** 1833-1859.

SLUTSKY, A., BROCHARD, L., SINDERBY, C., SPAHIJA, J. & BECK, J. 2005a. Neurally-adjusted Ventilatory Assist. *Mechanical Ventilation.* Springer Berlin Heidelberg.

SLUTSKY, A. S. 1999. Lung Injury Caused by Mechanical Ventilation*. *Chest,* 116**,** 9S-15S.

SLUTSKY, A. S., BROCHARD, L., PUTENSEN, C., HERING, R. & WRIGGE, H. 2005b. Spontaneous Breathing During Ventilatory Support in Patients with ARDS. *In:* VINCENT, J.-L. (ed.) *Mechanical Ventilation.* Springer Berlin Heidelberg.

SLUTSKY, A. S. & HUDSON, L. D. 2006. PEEP or No PEEP -- Lung Recruitment May Be the Solution. *N Engl J Med,* 354**,** 1839-1841.

SLUTSKY, A. S. & TREMBLAY, L. N. 1998. Multiple system organ failure. Is mechanical ventilation a contributing factor? *Am J Respir Crit Care Med,* 157**,** 1721 - 1725.

SONDERGAARD, S., KARASON, S., WIKLUND, J., LUNDIN, S. & STENQVIST, O. 2003. Alveolar pressure monitoring: an evaluation in a lung model and in patients with acute lung injury. *Intensive Care Medicine,* 29**,** 955-962.

SPAHIJA, J., DE MARCHIE, M., ALBERT, M., BELLEMARE, P., DELISLE, S., BECK, J. & SINDERBY, C. 2010. Patient-ventilator interaction during pressure support ventilation and neurally adjusted ventilatory assist *. *Critical Care Medicine,* 38**,** 518-526 10.1097/CCM.0b013e3181cb0d7b.

SPIETH, P. & GAMA DE ABREU, M. 2012. Lung recruitment in ARDS: We are still confused, but on a higher PEEP level. *Critical Care,* 16**,** 108.

SPIETH, P. M., CARVALHO, A. R., G LDNER, A., PELOSI, P., KIRICHUK, O., KOCH, T. & DE ABREU, M. G. 2009a. Effects of Different Levels of Pressure Support Variability in Experimental Lung Injury. *Anesthesiology,* 110**,** 342-350 10.1097/ALN.0b013e318194d06e.

SPIETH, P. M., CARVALHO, A. R., PELOSI, P., HOEHN, C., MEISSNER, C., KASPER, M., HUBLER, M., VON NEINDORFF, M., DASSOW, C., BARRENSCHEE, M., UHLIG, S., KOCH, T. & DE ABREU, M. G. 2009b. Variable Tidal Volumes Improve Lung Protective Ventilation Strategies in Experimental Lung Injury. *Am. J. Respir. Crit. Care Med.,* 179**,** 684-693.

STEIMLE, K. L., MOGENSEN, M. L., KARBING, D. S., BERNARDINO DE LA SERNA, J. & ANDREASSEN, S. 2011. A model of ventilation of the healthy human lung. *Computer Methods and Programs in Biomedicine,* 101**,** 144-155.

STENQVIST, O. 2003. Practical assessment of respiratory mechanics. *British Journal of Anaesthesia,* 91**,** 92-105.

STENQVIST, O., GRIVANS, C., ANDERSSON, B. & LUNDIN, S. 2012. Lung elastance and transpulmonary pressure can be determined without using oesophageal pressure measurements. *Acta Anaesthesiologica Scandinavica***,** n/a-n/a.

STEWART, T. E., MEADE, M. O., COOK, D. J., GRANTON, J. T., HODDER, R. V., LAPINSKY, S. E., MAZER, C. D., MCLEAN, R. F., ROGOVEIN, T. S., SCHOUTEN, B. D., TODD, T. R. J., SLUTSKY, A. S. & THE PRESSURE- AND VOLUME-LIMITED VENTILATION STRATEGY GROUP 1998. Evaluation of a Ventilation Strategy to Prevent Barotrauma in Patients at High Risk for Acute Respiratory Distress Syndrome. *N Engl J Med,* 338**,** 355-361.

STOCK, M. C., DOWNS, J. B. & FROLICHER, D. A. 1987. Airway pressure release ventilation. *Crit Care Med,* 15**,** 462 - 466.

STORSTEIN, O., FIELD, A. S. J., MASSUMI, R. & GRAY, F. D. J. 1959. Airway Resistance and Lung Compliance. *Yale Journal of Biology and Medicine,* 31(6)**,** 387-396.

SUAREZ-SIPMANN, F. & BOHM, S. 2009. Recruit the lung before titrating the right positive end-expiratory pressure to protect it. *Critical Care,* 13**,** 134.

SUAREZ-SIPMANN, F., BOHM, S. H., TUSMAN, G., PESCH, T., THAMM, O., REISSMANN, H., RESKE, A., MAGNUSSON, A. & HEDENSTIERNA, G. 2007. Use of dynamic compliance for open lung positive end-expiratory pressure titration in an experimental study. *Crit Care Med,* 35**,** 214 - 221.

SUH, G. Y., KWON, O. J., YOON, J. W., PARK, S. J., HAM, H. S., KANG, S. J., KOH, W.-J., CHUNG, M. P. & KIM, H. J. 2003. A Practical Protocol for Titrating "Optimal" PEEP in Acute Lung Injury: Recruitment Maneuver and PEEP Decrement. *J Korean Med Sci,* 18**,** 349-354.

SUNDARESAN, A., CHASE, J., SHAW, G., CHIEW, Y. S. & DESAIVE, T. 2011a. Model-based optimal PEEP in mechanically ventilated ARDS patients in the Intensive Care Unit. *BioMedical Engineering OnLine,* 10**,** 64.

SUNDARESAN, A. & CHASE, J. G. 2011. Positive end expiratory pressure in patients with acute respiratory distress syndrome - The past, present and future. *Biomedical Signal Processing and Control,* 7**,** 93-103.

SUNDARESAN, A., GEOFFREY CHASE, J., HANN, C. E. & SHAW, G. M. 2011b. Dynamic functional residual capacity can be estimated using a stress-strain approach. *Computer Methods and Programs in Biomedicine,* 101**,** 135-143.

SUNDARESAN, A., YUTA, T., HANN, C. E., GEOFFREY CHASE, J. & SHAW, G. M. 2009. A minimal model of lung mechanics and model-based markers for optimizing ventilator treatment in ARDS patients. *Computer Methods and Programs in Biomedicine,* 95**,** 166-180.

SUTER, P., FAIRLEY, B. & ISENBERG, M. 1975. Optimum End-Expiratory Airway Pressure in Patients with Acute Pulmonary Failure. *N Engl J Med,* 292**,** 284-289.

SWAN, A. J., CLARK, A. R. & TAWHAI, M. H. 2012. A computational model of the topographic distribution of ventilation in healthy human lungs. *Journal of Theoretical Biology,* 300**,** 222-231.

TAKEUCHI, M., GODDON, S., DOLHNIKOFF, M., SHIMAOKA, M., HESS, D., AMATO, M. B. P. & KACMAREK, R. M. 2002. Set Positive End-expiratory Pressure during Protective Ventilation Affects Lung Injury. *Anesthesiology,* 97**,** 682-692.

TAKEUCHI, M., IMANAKA, H., TACHIBANA, K., OGINO, H., ANDO, M. & NISHIMURA, M. 2005. Recruitment maneuver and high positive end-expiratory pressure improve hypoxemia in patients after pulmonary thromboendarterectomy for chronic pulmonary thromboembolism *. *Critical Care Medicine,* 33**,** 2010-2014 10.1097/01.CCM.0000178174.53373.DA.

TALMOR, D., SARGE, T., MALHOTRA, A., O'DONNELL, C. R., RITZ, R., LISBON, A., NOVACK, V. & LORING, S. H. 2008. Mechanical Ventilation Guided by Esophageal Pressure in Acute Lung Injury. *New England Journal of Medicine,* 359**,** 2095-2104.

TALMOR, D., SARGE, T., O'DONNELL, C. R., RITZ, R., MALHOTRA, A., LISBON, A. & LORING, S. H. 2006. Esophageal and transpulmonary pressures in acute respiratory failure. *Crit Care Med,* 34**,** 1389 - 1394.

TASSAUX, D., GAINNIER, M., BATTISTI, A. & JOLLIET, P. 2005. Impact of Expiratory Trigger Setting on Delayed Cycling and Inspiratory Muscle Workload. *American Journal of Respiratory and Critical Care Medicine,* 172**,** 1283-1289.

TASSAUX, D., MICHOTTE, J.-B., GAINNIER, M., GRATADOUR, P., FONSECA, S. & JOLLIET, P. 2004. Expiratory trigger setting in pressure support ventilation: From mathematical model to bedside. *Critical Care Medicine,* 32**,** 1844-1850 10.1097/01.CCM.0000138561.11634.6F.

TAWHAI, M. H. & BATES, J. H. T. 2011. Multi-scale lung modeling. *Journal of Applied Physiology,* 110**,** 1466-1472.

TAWHAI, M. H., HOFFMAN, E. A. & LIN, C.-L. 2009. The lung physiome: merging imaging-based measures with predictive computational models. *Wiley Interdisciplinary Reviews: Systems Biology and Medicine,* 1**,** 61-72.

TAWHAI, M. H., HUNTER, P., TSCHIRREN, J., REINHARDT, J., MCLENNAN, G. & HOFFMAN, E. A. 2004. CT-based geometry analysis and finite element models of the human and ovine bronchial tree. *J Appl Physiol,* 97**,** 2310-2321.

TERZI, N., PELIEU, I., GUITTET, L., RAMAKERS, M., SEGUIN, A., DAUBIN, C., CHARBONNEAU, P., DU CHEYRON, D. & LOFASO, F. 2010. Neurally adjusted ventilatory assist in patients recovering spontaneous breathing after acute respiratory distress syndrome: Physiological evaluation *. *Critical Care Medicine,* 38**,** 1830-1837 10.1097/CCM.0b013e3181eb3c51.

TERZI, N., PIQUILLOUD, L., ROZE, H., MERCAT, A., LOFASO, F., DELISLE, S., JOLLIET, P., SOTTIAUX, T., TASSAUX, D., ROESLER, J., DEMOULE, A., JABER, S., MANCEBO, J., BROCHARD, L. & RICHARD, J.-C. 2012. Clinical review: Update on neurally adjusted ventilatory assist - report of a round-table conference. *Critical Care,* 16**,** 225.

THE ACUTE RESPIRATORY DISTRESS SYNDROME NETWORK 2000. Ventilation with Lower Tidal Volumes as Compared with Traditional Tidal Volumes for Acute Lung Injury and the Acute Respiratory Distress Syndrome. *N Engl J Med,* 342**,** 1301-1308.

THE ARDS DEFINITION TASK FORCE, A. 2012. Acute respiratory distress syndrome: The berlin definition. *JAMA: The Journal of the American Medical Association,* 307**,** 2526-2533.

TUBIANA, M., NAGATAKI, S., FEINENDEGEN, L. E., DIMITROYANNIS, D. A., FRUSH, D. P., GOSKE, M. J., HERNANZ-SCHULMAN, M., SOYER, P., VARNHOLT, H., BRENNER, D. J. & HALL, E. J. 2008. Computed Tomography and Radiation Exposure. *N Engl J Med,* 358**,** 850-853.

TUSMAN, G., B HM, S. H., VAZQUEZ DE ANDA, G. F., DO CAMPO, J. L. & LACHMANN, B. 1999. 'Alveolar recruitment strategy' improves arterial oxygenation during general anaesthesia. *British Journal of Anaesthesia,* 82**,** 8-13.

TUSMAN, G., B HM, S. H., WARNER, D. O. & SPRUNG, J. 2012. Atelectasis and perioperative pulmonary complications in high-risk patients. *Current Opinion in Anesthesiology,* 25**,** 1-10.

TUTUNCU, A. S., CAKAR, N., CAMCI, E., ESEN, F., TELCI, L. & AKPIR, K. 1997. Comparison of pressure- and flow-triggered pressure-support ventilation on weaning parameters in patients recovering from acute respiratory failure. *Critical Care Medicine,* 25**,** 756-760.

VALTA, P., UUSARO, A., NUNES, S., RUOKONEN, E. & TAKALA, J. 1999. Acute respiratory distress syndrome: Frequency, clinical course, and costs of care. *Critical Care Medicine,* 27**,** 2367-2374.

VARPULA, T., VALTA, P., NIEMI, R., TAKKUNEN, O., HYNYNEN, M. & PETTIL , V. 2004. Airway pressure release ventilation as a primary ventilatory mode in acute respiratory distress syndrome. *Acta Anaesthesiologica Scandinavica,* 48**,** 722-731.

VENEGAS, J. G., HARRIS, R. S. & SIMON, B. A. 1998. A comprehensive equation for the pulmonary pressure-volume curve. *J Appl Physiol,* 84**,** 389 - 95.

VERVERIDIS, D., VAN GILS, M., PASSATH, C., TAKALA, J. & BRANDER, L. 2011. Identification of Adequate Neurally Adjusted Ventilatory Assist (NAVA) During Systematic Increases in the NAVA Level. *Biomedical Engineering, IEEE Transactions on,* 58**,** 2598-2606.

VIALE, J. P., DUPERRET, S., MAHUL, P., DELAFOSSE, B., DELPUECH, C., WEISMANN, D. & ANNAT, G. U. Y. 1998. Time Course Evolution of Ventilatory Responses to Inspiratory Unloading in Patients. *American Journal of Respiratory and Critical Care Medicine,* 157**,** 428-434.

VICTORINO, J. A., BORGES, J. B., OKAMOTO, V. N., MATOS, G. F., TUCCI, M. R., CARAMEZ, M. P., TANAKA, H., SIPMANN, F. S., SANTOS, D. C., BARBAS, C. S., CARVALHO, C. R. & AMATO, M. B. 2004. Imbalances in regional lung ventilation: a validation study on electrical impedance tomography. *Am J Respir Crit Care Med,* 169**,** 791 - 800.

VIEIRA, SILVIA R. R., PUYBASSET, L., RICHECOEUR, J., LU, Q. I. N., CLUZEL, P., GUSMAN, PABLO B., CORIAT, P. & ROUBY, J.-J. 1998. A Lung Computed Tomographic Assessment of Positive End-Expiratory Pressure-induced Lung Overdistension. *Am. J. Respir. Crit. Care Med.,* 158**,** 1571-1577.

VIGNAUX, L., VARGAS, F., ROESELER, J., TASSAUX, D., THILLE, A., KOSSOWSKY, M., BROCHARD, L. & JOLLIET, P. 2009. Patient–ventilator asynchrony during non-invasive ventilation for acute respiratory failure: a multicenter study. *Intensive Care Medicine,* 35**,** 840-846.

VILLAR, J., KACMAREK, R., PEREZ-MENDEZ, L. & AGUIRRE-JAIME, A. 2006. A high positive end-expiratory pressure, low tidal volume ventilatory strategy improves outcome in persistent acute respiratory distress syndrome: A randomized, controlled trial. *Crit Care Med,* 34**,** 1311 - 1318.

WARD, N. S., LIN, D. Y., NELSON, D. L., HOUTCHENS, J., SCHWARTZ, W. A., KLINGER, J. R., HILL, N. S. & LEVY, M. M. 2002. Successful determination of lower inflection point and maximal compliance in a population of patients with acute respiratory distress syndrome. *Crit Care Med,* 30**,** 963 - 968.

WARE, L. B. 2008. Modeling human lung disease in animals. *American Journal of Physiology - Lung Cellular and Molecular Physiology,* 294**,** L149-L150.

WARE, L. B. & MATTHAY, M. A. 2000. The Acute Respiratory Distress Syndrome. *N Engl J Med,* 342**,** 1334-1349.

WEINACKER, A. B. & VASZAR, L. T. 2001. ACUTE RESPIRATORY DISTRESS SYNDROME: Physiology and New Management Strategies. *Annual Review of Medicine,* 52**,** 221-237.

WEISMANN, D., REI MANN, H., MAISCH, S., F LLEKRUG, B. & SCHULTE, J. 2006. Monitoring of Functional Residual Capacity by an Oxygen Washin/Washout; Technical Description and Evaluation. *Journal of Clinical Monitoring and Computing,* 20**,** 251-260.

WERNER, R., EHRHARDT, J., SCHMIDT, R. & HANDELS, H. 2009. Patient-specific finite element modeling of respiratory lung motion using 4D CT image data. *Medical Physics,* 36**,** 1500-1511.

WRIGGE, H., ZINSERLING, J., NEUMANN, P., MUDERS, T., MAGNUSSON, A., PUTENSEN, C. & HEDENSTIERNA, G. 2005. Spontaneous breathing with airway pressure release ventilation favors ventilation in dependent lung regions and counters cyclic alveolar

collapse in oleic-acid-induced lung injury: a randomized controlled computed tomography trial. *Crit Care,* 9**,** R780 - R789.

WYSOCKI, M., CRACCO, C., TEIXEIRA, A., MERCAT, A., DIEHL, J.-L., LEFORT, Y., DERENNE, J.-P. & SIMILOWSKI, T. 2006. Reduced breathing variability as a predictor of unsuccessful patient separation from mechanical ventilation *. *Critical Care Medicine,* 34**,** 2076-2083 10.1097/01.CCM.0000227175.83575.E9.

XIA, G., TAWHAI, M., HOFFMAN, E. & LIN, C.-L. 2010. Airway Wall Stiffening Increases Peak Wall Shear Stress: A Fluid–Structure Interaction Study in Rigid and Compliant Airways. *Annals of Biomedical Engineering,* 38**,** 1836-1853.

YOUNES, M. 1992. Proportional Assist Ventilation, a New Approach to Ventilatory Support: Theory. *Am. J. Respir. Crit. Care Med.,* 145**,** 114-120.

ZACCHEO, M., MILBRANDT, E. & BOUJOUKOS, A. 2010. The esophagus ... not just for food anymore? *Critical Care,* 14**,** 326.

ZAMBON, M. & VINCENT, J.-L. 2008. Mortality Rates for Patients With Acute Lung Injury/ARDS Have Decreased Over Time*. *Chest,* 133**,** 1120-1127.

ZANNIN, E., DELLACA, R., KOSTIC, P., POMPILIO, P., LARSSON, A., PEDOTTI, A., HEDENSTIERNA, G. & FRYKHOLM, P. 2012. Optimizing positive end-expiratory pressure by oscillatory mechanics minimizes tidal recruitment and distension: an experimental study in a lavage model of lung injury. *Critical Care,* 16**,** R217.

ZHAO, Z., GUTTMANN, J. & MOLLER, K. 2012a. Adaptive Slice Method: A new method to determine volume dependent dynamic respiratory system mechanics. *Physiol Meas.,* 33**,** 51-64.

ZHAO, Z., JOSEF, G. & KNUT, M. 2012b. Assessment of a volume-dependent dynamic respiratory system compliance in ALI/ARDS by pooling breathing cycles. *Physiological Measurement,* 33**,** N61.

ZHAO, Z., MOLLER, K., STEINMANN, D., FRERICHS, I. & GUTTMANN, J. 2009. Evaluation of an electrical impedance tomography-based Global Inhomogeneity Index for pulmonary ventilation distribution. . *Intensive Care Med.,* 35**,** 1900-6.

ZHAO, Z., STEINMANN, D., FRERICHS, I., GUTTMANN, J. & MOLLER, K. 2010a. PEEP titration guided by ventilation homogeneity: a feasibility study using electrical impedance tomography. *Crit Care,* 14**,** R8.

ZHAO, Z., STEINMANN, D., FRERICHS, I., GUTTMANN, J. & MOLLER, K. 2010b. Ventilation inhomogeneity is one criterion among many in multidimensional PEEP titration. *Critical Care,* 14**,** 424.

ZILBERBERG, M. D., LUIPPOLD, R. S., SULSKY, S. & SHORR, A. F. 2008. Prolonged acute mechanical ventilation, hospital resource utilization, and mortality in the United States. *Critical Care Medicine,* 36**,** 724-730 10.1097/CCM.0B013E31816536F7.

Appendix 01:

Trend comparison between E_{Static} and E_{rsIB}, R_{Static} and R_{rsIB} for all 3 Animal Subjects

The Figure 01.1 shows the trend comparison between E_{Static} and E_{rsIB}, R_{Static} and R_{rsIB} for all cases as presented in Chapter 4.

Subject 5

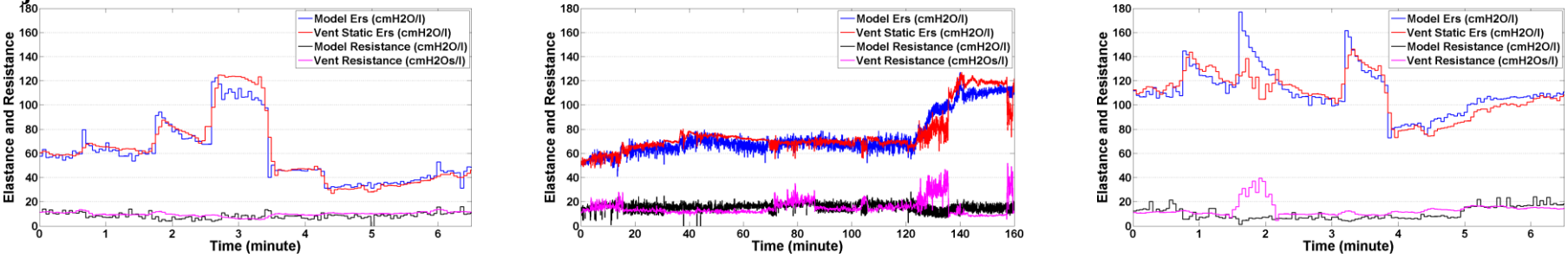

Subject 6

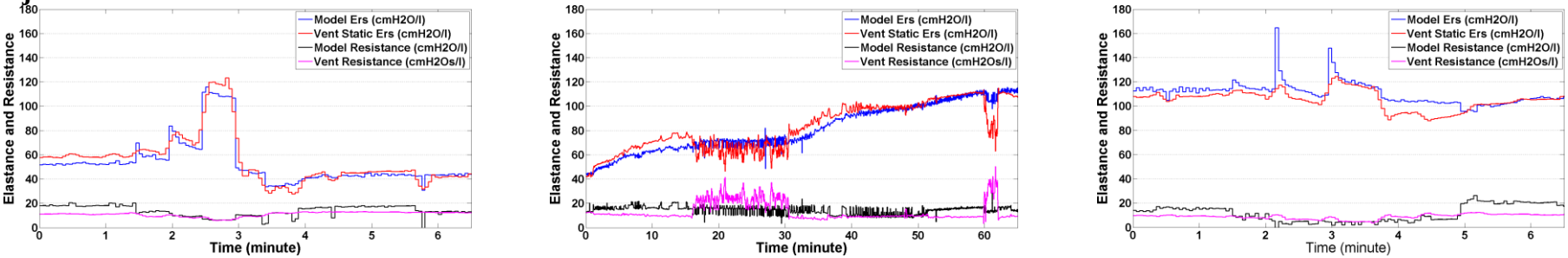

Subject 9

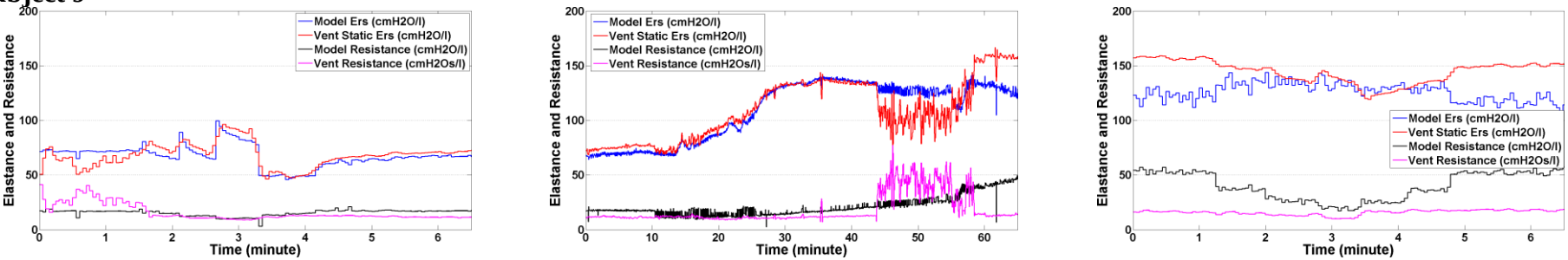

Phase 1 (Healthy) **Phase 2 (Progression)** **Phase 3 (ARDS)**

Figure A01.1: E_{Static}, E_{rsIB}, R_{Static} and R_{rsIB} for Subject 5 (Top), 6 (Middle), and 9 (Bottom). (From Left to Right) Phase 1, Phase 2 and Phase 3. Blue line indicate E_{rsIB}, red line indicates E_{Static}, black line indicate R_{Static}, pink line indicate R_{Static}. E_{Static} and R_{Static} are calculated using the automated end of inspiratory pause feature in provided in the ventilator.

Appendix 02:

Case Examples and Range90 Calculation

This additional document shows the step-by-step method for Range90 calculation for this given patient. An example of patient flow and respective *Eadi* signal is shown in Figure 02.1 and 02.2.

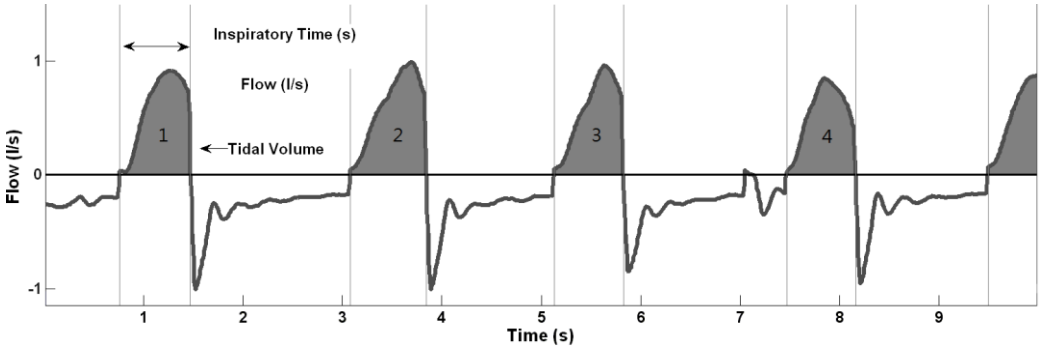

Figure 02.1: Example of a patient's flow-time curve. The shaded area is the ventilator supply (Tidal volume, *Vt*)

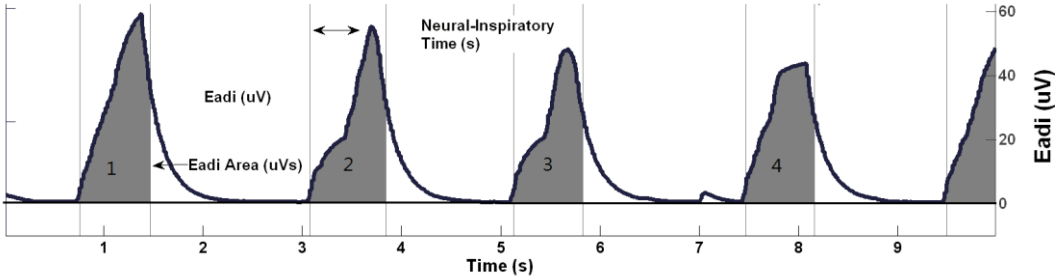

Figure 02.2: Example of a patient's *Eadi*-time curve. The shaded area is the patient's demand (∫*Eadi*)

1. Obtain tidal volume (*Vt*) and ∫*Eadi* for each breathing cycle as shown in Figure 02.1 and 02.1.
2. The Neuroventilatory efficiency (*Vt*/∫*Eadi* ratio) for each breathing cycle is calculated.

(Example: $Vt_1/\int Eadi_1$, $Vt_2/\int Eadi_2$, $Vt_3/\int Eadi_3$, $Vt_4/\int Eadi_4$ …, $Vt_n/\int Eadi_n$).

3. The 5^{th} percentile of every $Vt/\int Eadi$ ratio is determined (5^{th} $Vt/\int Eadi$).
4. The 95^{th} percentile of every $Vt/\int Eadi$ ratio is determined (95^{th} $Vt/\int Eadi$).
5. Range90 = 95^{th} $Vt/\int Eadi$ - 5^{th} $Vt/\int Eadi$
6. For a patient who has consistent $Vt/\int Eadi$ ratio, Range90 will be smaller.
7. For a patient who has variable $Vt/\int Eadi$ ratio, Range90 will be higher.

Case examples comparing better and less matching

Example: Vt = 1.0 and $\int Eadi$ = 1.0 for baseline value

Case A - Patient with better matching

$\int Eadi$ = 1.0, Vt = 1.0, $Vt/\int Eadi$ = 1.0 (Moderate demand, Moderate supply)

$\int Eadi$ = 2.0, Vt = 2.0, $Vt/\int Eadi$ = 1.0 (High demand, High supply)

$\int Eadi$ = 0.5, Vt = 0.5, $Vt/\int Eadi$ = 1.0 (Low demand, Low supply)

…

95^{th} -5^{th} of all $Vt/\int Eadi$ for Case A will be small resulting in smaller Range90 value.

Case B - Patient with less matching

$\int Eadi$ = 1.0, Vt = 2.0, $Vt/\int Eadi$ = 2.0 (Moderate demand, High supply)

$\int Eadi$ = 2.0, Vt = 1.0, $Vt/\int Eadi$ = 0.5 (High demand, Moderate supply)

$\int Eadi$ = 0.5, Vt = 1.0, $Vt/\int Eadi$ = 1.0 (Low demand, Moderate supply)

…

Thus, 95^{th} -5^{th} of all $Vt/\int Eadi$ for Case B will be higher, with larger Range90 value compared to Case A

Appendix 03:

Additional Findings for Chapter 7:

Application of NAVA for the Noninvasively Ventilated Patients

Table 03.1-03.5 present patients' robust coefficient of variation (CVR) on inspiratory demand $\int Eadi$, peak inspiratory pressure (P_{in}), ventilatory tidal volume (Vt) and inspiratory time (Ti) at each NAVA level, as summarised in the manuscript. Wilcoxon rank sum test for significance was carried out in every patient to compare the effect of different NAVA level. The summary of coefficients of variation (CVR) in $\int Eadi$, Vt, Ti_{Neural}, Ti, and PIP are shown in Table 03.6-03.7.

Volume leaks (V_leaks) for using NIV face mask are calculated and result is presented in Table 03.8. This leak is calculated as the difference between inspiratory tidal volume (Vt) and expiration tidal volume (Vte) ($V\_leaks = Vt - Vte$). Inspiratory and expiratory tidal volume is obtained through flow integration. However, during, flow integration, the near zero flow value during expiratory cycle will cause a volume drift. This drift is often corrected for each breath for better comparison in a standard ventilator. During spontaneous breathing, patient will have variable breath, with variable Vt and variable Vte. This variability will thus affect the calculation of leaks.

However, if the drift is assumed to be constant for each breath, this will allow a fair comparison of intra patient volume leaks, and not for inter patient comparison.

Table 03.1: CVR for patient's inspiratory demand (∫*Eadi*)

Patient	PS	NAVA50	NAVA100	NAVA150
1	0.14	0.13	0.11	0.16
2	0.25	0.24	0.20	0.29
3	0.08	-	0.11	-
4	0.18	0.18	0.14	0.12
5	0.54	0.13	0.26	0.27
6	0.11	0.10	0.19	0.15
7	0.10	0.08	0.09	0.09
8	0.26	0.14	0.14	0.17
9	0.19	0.16	0.25	0.15
10	0.18	0.36	0.33	0.35
11	0.87	0.29	0.68	0.21
12	0.42	0.39	0.30	0.38
13	0.46	0.52	0.54	0.55
Median [IQR]		0.17 [0.13-0.33]	0.23 [0.14-0.32]	0.19 [0.15-0.32]
	0.19 [0.13-0.43]#		0.20 [0.13-0.31]#	

 # Include Patient 3

Table 03.2: CVR for Ventilatory tidal volume (*Vt*)

Patient	PS	NAVA50	NAVA100	NAVA150
1	0.08	0.12	0.09	0.12
2	0.06	0.16	0.17	0.19
3	0.04	-	0.06	-
4	0.13	0.09	0.09	0.09
5	0.05	0.07	0.09	0.17
6	0.02	0.05	0.07	0.06
7	0.03	0.04	0.05	0.05
8	0.09	0.14	0.12	0.16
9	0.08	0.09	0.32	0.12
10	0.09	0.23	0.24	0.30
11	0.72	0.34	0.63	0.34
12	0.07	0.12	0.11	0.10
13	0.26	0.35	0.39	0.54
Median [IQR]		0.12 [0.08-0.20]	0.12 [0.09-0.28]	0.14 [0.10-0.25]
	0.08 [0.05-0.10]#		0.11 [0.09-0.26]#	

 # Include Patient 3

Table 03.3: CVR for Neural Inspiratory Time ($Ti_{\_Neural}$)

Patient	PS	NAVA50	NAVA100	NAVA150
1	0.14	0.10	0.05	0.08
2	0.08	0.08	0.10	0.10
3	0.08	-	0.11	-
4	0.13	0.09	0.10	0.09
5	0.06	0.05	0.06	0.14
6	0.10	0.10	0.10	0.10
7	0.07	0.08	0.07	0.10
8	0.13	0.10	0.10	0.13
9	0.17	0.10	0.18	0.17
10	0.15	0.21	0.24	0.22
11	0.57	0.19	0.38	0.17
12	0.09	0.08	0.11	0.10
13	0.32	0.21	0.25	0.26
Median [IQR]		0.10 [0.08-0.15]	0.10 [0.09-0.21]	0.12 [0.10-0.17]
	0.08 [0.05-0.10]#		0.10 [0.09-0.20]#	

 # Include Patient 3

Table 03.4: CVR for Inspiratory Time (*Ti*)

Patient	PS	NAVA50	NAVA100	NAVA150
1	0.06	0.10	0.04	0.05
2	0.05	0.06	0.08	0.09
3	0.04	-	0.06	-
4	0.11	0.07	0.07	0.07
5	0.06	0.04	0.05	0.10
6	0.02	0.05	0.06	0.05
7	0.02	0.03	0.03	0.03
8	0.05	0.09	0.07	0.08
9	0.15	0.10	0.12	0.15
10	0.09	0.17	0.19	0.18
11	0.48	0.12	0.32	0.13
12	0.07	0.06	0.08	0.07
13	0.38	0.16	0.21	0.20
Median [IQR]		0.08 [0.06-0.11]	0.08 [0.06-0.16]	0.09 [0.06-0.14]
	0.06 [0.05-0.12]#		0.07 [0.06-0.14]#	

 # Include Patient 3

Table 03.5: CVR for Peak Inspiratory Pressure (P_{in})

Patient	PS	NAVA50	NAVA100	NAVA150
1	0.09	0.09	0.08	0.09
2	<0.01	0.13	0.12	0.16
3	<0.01	-	0.05	-
4	<0.01	0.06	0.07	0.08
5	0.01	0.08	0.13	0.16
6	<0.01	0.05	0.08	0.01
7	0.01	0.05	0.06	0.07
8	0.02	0.15	0.11	0.19
9	0.01	0.08	0.10	0.09
10	0.01	0.11	0.14	0.18
11	0.05	0.03	0.10	0.03
12	0.02	0.19	0.16	0.23
13	0.06	0.08	0.17	0.17
Median [IQR]		0.08 [0.06-0.12]	0.11 [0.08-0.14]	0.13 [0.08-0.17]
	0.01 [0-0.03]#		0.07 [0.06-0.14]#	

 # Include Patient 3

Table 03.6: Robust Coefficient of Variation (CVR) in *Vt*, *∫Eadi*, *Ti_Neural*, *Ti* and *PIP* (Median [IQR]). (NAVA with Patient 3)

	Median [IQR]	
	PS	**NAVA**
∫Eadi	0.19 [0.13-0.43]	0.20 [0.13-0.31]
Vt	0.08 [0.05-0.10]	0.11 [0.09-0.26]
Ti_Neural	0.08 [0.05-0.10]	0.10 [0.09-0.20]
Ti	0.06 [0.05-0.12]	0.07 [0.06-0.14]
PIP	0.01 [0.00-0.03]*	0.07 [0.06-0.14]*

* p-value <0.005

Table 03.7: Summary CVR *∫Eadi*, *Vt*, *Ti_Neural*, *Ti*, *PIP* (Median [IQR]). (NAVA100 without Patient 3)

	CVR, Median [IQR]		
	NAVA50	**NAVA100**	**NAVA150**
∫Eadi	0.17 [0.13-0.31]	0.22 [0.14-0.31]	0.19 [0.15-0.32]
Vt	0.12 [0.08-0.19]	0.12 [0.09-0.28]	0.14 [0.09-0.24]
Ti_Neural	0.10 [0.08-0.15]	0.10 [0.09-0.21]	0.12 [0.10-0.17]
Ti	0.08 [0.06-0.11]	0.07 [0.05-0.16]	0.09 [0.06-0.14]
PIP	0.08 [0.06-0.12]	0.11 [0.08-0.14]	0.12 [0.07-0.18]

** P>0.05 for every parameter*

Table 03.8: Leaks (*Vt_leak*)

Patient	*Vt_leak* (*ml*), Median [IQR]			
	PS	**NAVA50**	**NAVA100**	**NAVA150**
1	43 [23-67]	112 [48-211]	56 [29-97]*	65 [35-116]*+
2	71 [55-96]	55 [37-76]	75 [49-109]*	66 [42-89]*+
3	22 [11-34]	-	25 [12-52]	-
4	44 [21-82]	50 [28-130]	44 [22-73]*	44 [24-78]*
5	215 [182-290]	201 [161-258]	217 [182-270]*	346 [242-455]*
6	79 [68-91]	84 [71-101]	79 [59-100]*	100 [79-120]*+
7	24 [10-38]	28 [13-45]	38 [25-51]*	43 [29-59]*+
8	66 [31-139]	66 [34-173]	94 [49-284]*	103 [40-305]*
9	27 [11-55]	35 [18-72]	135 [66-231]*	57 [20-93]+
10	99 [57-157]	49 [22-88]	45 [22-83]	81 [37-147]*+
11	274 [96-614]	141 [54-273]	177 [61-312]	95 [43-178]*+
12	40 [15-244]	43 [18-126]	40 [16-85]	49 [23-86]+
13	232 [96-536]	134 [34-274]	181 [78-407]*	197 [83-509]*
Median of Medians [IQR]		61 [46-123]	77 [45-156]	74 [53-102]
	66 [37-128]#		75 [43-146]#	

** P<0.05 compare to NAVA50*
+ P<0.05 compare to NAVA100
 # Include Patient 3